BULLETIN

OF THE

CHEMICAL SOCIETY OF JAPAN

Vol. 34 No. 2 February 1961

OHIO STATE UNIVERSITY APR 27 1961

CONTENTS

General and Physical

Solvent Shift of Methyl Proton Nuclear Magnetic Resonance . N. NAKAGAWA and S. FUJIWARA 143

The Mechanical Behavior of Swollen Polystyrene. Poly-*p*-chlorostyrene and their Copolymers in Benzene. II. Stress Relaxation under Constant Strain . . . . . K. OGINO 153

The Chemical Reaction in Silent Electric Discharge. I. . . . . K. MORINAGA and M. SUZUKI 157

Studies on Tritium Labeled Compounds. IV. Preparation of Tritium Labeled Alanine by Means of Electric Discharge . . . . . Y. SATO and T. TAKAHASHI 169

Visco-elastic Behaviors of Aluminum Soap-Hydrocarbon Systems. I. Aluminum Stearate in Nujol . . . . . S. SHIBA 194

Visco-elastic Behaviors of Aluminum Soap-Hydrocarbon Systems. II. Aluminum Soaps in Nujol . . . . . S. SHIBA 198

Infrared Studies of the Librations of Water Molecules in the Solid Matrices at 20°K. T. MIYAZAWA 202

Studies on Mass Spectra and Appearance Potentials of Acetic Acid and Deuteroacetic Acid CD_3COOH. . . . . K. HIROTA, K. NAGOSHI and M. HATADA 226

Theoretical Reactivity Index of Addition in the "Frontier Electron Theory" . . . . . K. FUKUI, C. NAGATA, T. YONEZAWA and K. MOROKUMA 230

Diamagnetic Behavior of Some Aliphatic Molecules in Crystals . . . . . A. MOOKHERJI, S. N. MOOKHERJI and D. NEOGY 233

The Surface Tension and the Critical Micelle Concentration in Aqueous Solution of β-D-Alkyl Glucosides and their Mixtures. . . . . K. SHINODA, T. YAMAGUCHI and R. HORI 237

The Resonance Effect of Amide Group on the Polymerizability of Lactam Derivatives. I. The Infrared Spectrum of *N*-Methyl Lactams . . . . . N. OGATA 245

The Resonance Effect of Amide Group on the Polymerizability of Lactam Derivatives. II. The Basicity of Amide Group of Lactams. . . . . N. OGATA 248

Über die Kupfer-salze der ω-Aminosäure. I. Zur Kenntnis des Kupfer-Glycins. . . K. TOMITA 280

Über die Kupfer-salze der ω-Aminosäure. II. Über die Kristallstruktur des Kupfer-Glycin- Monohydrates. . . . . K. TOMITA und I. NITTA 286

Analytical and Inorganic

A Study on Anion Exchange and Amine Extraction of Rare Earth Elements in Nitric Acid . . . . . F. ICHIKAWA 183

Spectrophotometric Determination of Submicrogram Quantities of Orthophosphate in Natural Waters. . . . . K. SUGAWARA and S. KANAMORI 258

Organic and Biological

Syntheses of Benzo[b]tropothiazine and its Derivatives . . . . . T. NOZOE, T. ASAO and K. TAKAHASHI 146

On Pyrazino[d, d']ditropone and its Derivatives. . . . . T. ASAO 151

Dehydrogenation of Secondary Alcohols with Reduced Copper. III. Catalytic Dehydrogenation of Isopropyl Alcohol. (Part 1) . . . . . K. KAWAMOTO 161

Studies on Tritium Labeled Compounds. II. Preparation of Tritium Labeled Stearic Acid. . . . . Y. SATO, T. MESHI and T. TAKAHASHI 167

(Continued on inside cover)

Published by the Chemical Society of Japan

THE CHEMICAL SOCIETY OF JAPAN
(NIPPON KAGAKUKAI)

Founded in 1948

Successor to the former Chemical Society of Japan founded in 1878 and to the Society of Chemical Industry, Japan founded in 1898.

OFFICERS

Shoichiro NAGAI, *President*, Nihon University, Tokyo
Eiichi IWASE, *Vice-President*, Institute of Physical and Chemical Research, Tokyo
Wasaburo KIMURA, *Vice-President*, Nagoya University
Sojiro OKA, *Vice-President*, The University of Tokyo
Ichiro SAKURADA, *Vice-President*, Kyoto University
Hiroshi SOBUE, *Vice-President*, The University of Tokyo

BULLETIN OF THE CHEMICAL SOCIETY OF JAPAN

Editor: Yoshiyuki URUSHIBARA, The University of Tokyo, Tokyo
Assistant Editor: Saburo NAGAKURA, The University of Tokyo, Tokyo
Editorial Board:

Toshio ANDO	Ichiro MIYAGAWA	Tadashi SUEHIRO
Yoshié BANSHO	Masazumi NAKAGAWA	Kenzi TAMARU
Hidehiro GOTÔ	Koji NAKANISHI	Takeo WATASE
Yoshimasa HIRATA	Shigeo OKUMURA	Iwao YASUMORI
Kenichi HONDA	Kazuo SAITO	Tsuneo YOSHINO
Sunao IMANISHI	Naoyasu SATA	Koshiro YOSHIOKA

(Continued from outside cover)

Studies on Dehydroalanine Derivatives. IV. Synthesis of *N*-phthaloyl-Dehydroalanine by Thermal Decomposition of Cysteine and Serine in the Presence of Phthalic Anhydride. S. SAKAKIBARA 171

Studies on Dehydroalanine Derivatives. V. Radical Polymerization of *N*-Carboxy-dehydroalanine Anhydride and of *N*-Phthaloyl-dehydroalanine. Synthesis of a New Amphoteric Polymer. . . . . S. SAKAKIBARA 174

The Acid Product obtained in the Synthesis of 2-Phenyltropone Derivatives from 2-Phenylsuberone . . . . . T. MUROI 178

Vinyl Polymerization. XLVIII. Polymerization of Methylstyrenes and the Effect of Dimethylaniline on their Polymerization. . . . . K. IMOTO, K. TAKEMOTO and Y. IIKUBO 186

Studies on Dehydroalanine Derivatives. III. Formation of Amino Acids from Poly-dehydroalanine . . . . . S. SAKAKIBARA 205

The Beckmann Rearrangement of the Geometrical Isomers of Cyclohexyl Phenyl Ketoxime in Liquid Sulfur Dioxide. . . . . R. TADA, Y. MASUBUCHI and N. TOKURA 209

Some Copper Complexes of Diazoaminobenzene Derivatives and their Properties . . . . . H. YAMADA, H. OHTA, M. YAMAGUCHI and T. TSUMAKI 241

Studies on Heavy-Nitrogen Labeled Compounds. III. Preparation of ^{15}N-Labeled α-Hydroximino-propionic Acid. . . . . Y. SATO, T. MESHI and N. SUGIMOTO 243

Studies on the Thiocarbamoylthiocarbonates. I. Synthesis of Aryl Thiocarbamoyldithiocarbonates . . . . . A. KAJI 254

Reduction of Organic Compounds with Urushibara Catalysts under High Pressure. VII. Feature of Various Urushibara Catalysts as Revealed in the Reduction of Benzophenone . S. TAIRA 261

Formation of Cyclohexano[*c*] 1, 2, 5-oxadiazole from 1, 2-Cyclohexanedione Dioxime. An Attempted Beckmann Rearrangement with Thionyl Chloride in Liquid Sulfur Dioxide. . . . . N. TOKURA, R. TADA and K. YOKOYAMA 270

A Synthesis of an Octahydrophenanthrene Derivative. . . . . T. MATSUMOTO and A. SUZUKI 274

Applied

On the Reactivity of Various Silicate Minerals toward Acids. . . . . H. MASE 214

Short Communications

Electron Spin Resonance and Electronic Absorption Spectra of the Radical Anions of Pyridine and Acridine . . . . . K. KUWATA, T. OGAWA and K. HIROTA 291

Selectivity in Radiation-Induced Crosslinking and Scission of Polyvinyl Alcohol (PVA) . . . . . Y. HIRANO and A. AMEMIYA 292

A Method for Estimation of the Hydration Numbers of Ions in Ion Exchange Resins. . . . . H. OHTAKI, K. GONDA and H. KAKIHANA 293

The Crystal Structure of $[Cr(NH_3)_6]$ $[CuCl_5]$ . . . . . M. MORI, Y. SAITO and T. WATANABE 295

Solvent Shift of Methyl Proton Nuclear Magnetic Resonance

By Naoya NAKAGAWA and Shizuo FUJIWARA

(Received June 27, 1960)

The solvent effect of high resolution proton magnetic resonance has been investigated by many workers[1-3], recently. We also reported that the HCN, $-C\equiv CH$, and $-CH_3$ protons show quite large solvent shifts[4]. In this paper, we will show the results of the investigations for methyl protons in various compounds.

Chemical shifts of the NMR spectra of methyl protons in a number of organic compounds dissolved in solvents such as benzene, pyridine, dioxane, and carbon tetrachloride were measured by the internal reference method. Each sample consists of solute, solvent, and cyclohexane as the internal reference, with a molar ratio of 1 : 9 : 0.25, and is sealed in a glass tube of 3.5 mm. O. D. The apparatus of the NMR measurement is the one constructed by one of the authors (S. F.), and is operated at 27 Mc. The details of this set-up were reported elsewhere[5]. The chemical shifts of the methyl protons of the samples were measured on the recorded charts as the separations from cyclohexane by taking the separation between toluene CH_3 and cyclohexane as 0.75 p.p.m. This value of the reference was determined by the side-band technique[6].

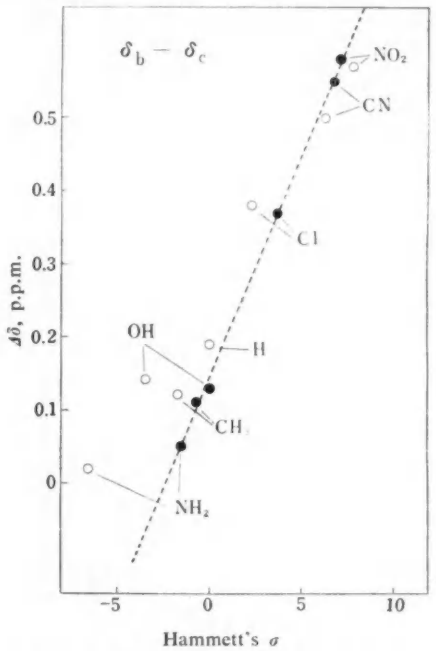

Fig. 1. Solvent shifts and Hammett's σ of substituted toluenes.

● meta ○ para

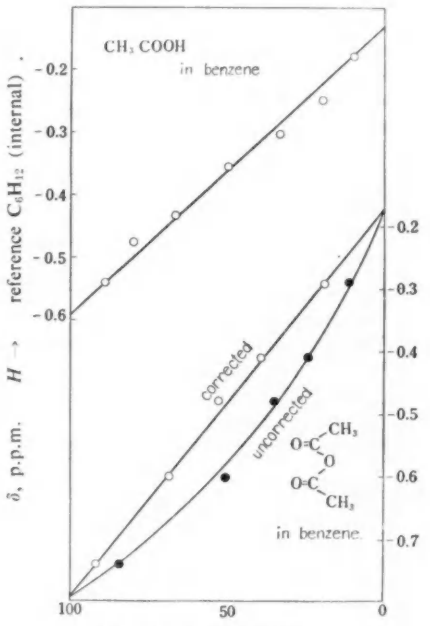

Fig. 2. Chemical shifts of CH_3 protons

1) As to the references of this effect before 1958, see, J. A. Pople, W. G. Schneider and H. J. Bernstein, "High-Resolution Nuclear Magnetic Resonance", McGraw-Hill, New York (1959), pp. 400–432.

2) E. B. Whipple, J. H. Goldstein, L. Mandell, G. S. Reddy and G. R. McClure, *J. Am. Chem. Soc.*, **81**, 1321 (1959).

3) R. E. Glick, D. F. Kates and S. J. Ehrenson, *J. Chem. Phys.*, **31**, 567 (1959).

4) N. Nakagawa and S. Fujiwara, to be published in *J. Org. Chem.*

5) S. Fujiwara and H. Shimizu, in press in *J. Chem. Phys.*

6) J. T. Arnold and M. G. Packard, *J. Chem. Phys.*, **19**, 1608 (1951).

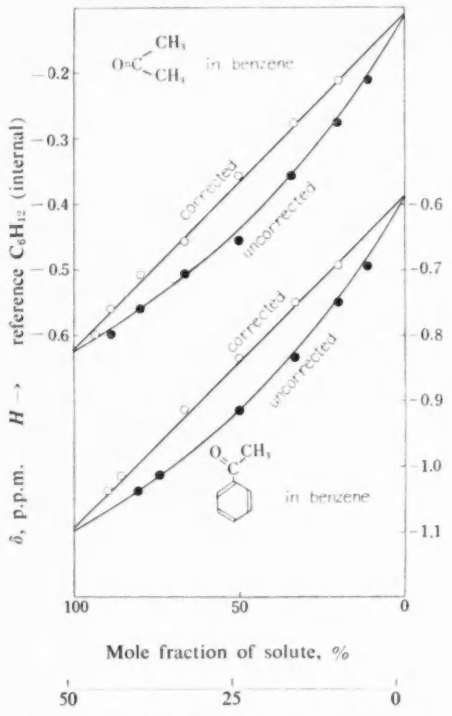

Fig. 3. Chemical shifts of CH_3 protons.

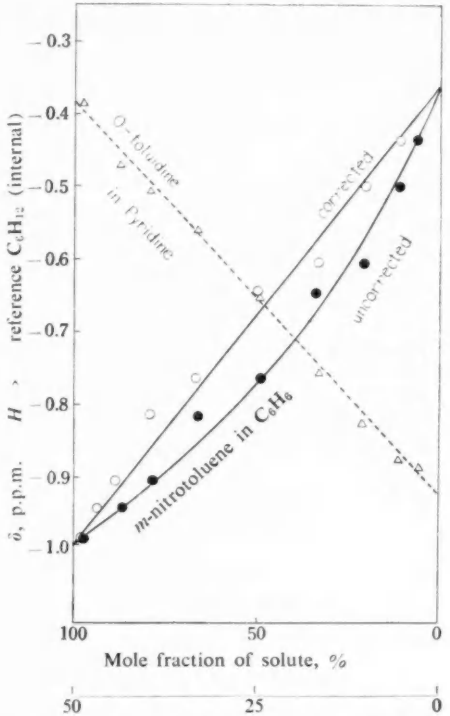

Fig. 4. Chemical shifts of CH_3 protons.

TABLE I. CHEMICAL SHIFTS OF METHYL PROTONS

Temperature: 11~12°C
Concentration: solute: solvent: cyclohexane = 1 : 9 : 0.25 (mol.)
Unit of chemical shift: p.p.m. from cyclohexane

Solute	Without solvent $-\delta_0$	In C_6H_6 $-\delta_b$	In C_5H_5N $-\delta_p$	In dioxane $-\delta_d$	In CCl_4 $-\delta_c$
Toluene	0.75	0.71	0.81	0.89	0.90
p-Nitrotoluene	—	0.50	0.90	1.01	1.07
p-Tolunitrile	0.90	0.50	0.87	0.97	1.00
p-Chlorotoluene	0.65	0.50	0.75	0.85	0.88
p-Xylene	0.71	0.72	0.83	0.79	0.84
p-Cresol*	0.70	0.66	0.91	0.77	0.80
p-Toluidine	—	0.73	0.82	0.70	0.76
m-Nitrotoluene*	0.99	0.48	0.93	1.03	1.06
m-Tolunitrile	0.87	0.42	0.82	0.93	0.97
m-Chlorotoluene	0.64	0.48	0.77	0.85	0.84
m-Xylene*	0.71	0.75	0.86	0.83	0.86
m-Cresol*	0.66	0.67	0.89	0.83	0.80
m-Toluidine	0.66	0.72	0.83	0.75	0.76

TABLE I (Continued)

o-Nitrotoluene	1.09	0.80	1.14	1.18	1.16
o-Tolunitrile	0.99	0.73	1.02	1.12	1.11
o-Chlorotoluene	0.78	0.71	0.85	0.91	0.93
o-Xylene	0.61	0.61	0.74	0.77	0.81
o-Cresol*	0.76	0.69	1.11	0.74	0.77
o-Toluidine	0.37	0.39	0.88	0.61	0.58
γ-Picoline	0.75	0.41	0.79	0.87	0.93
β-Picoline	0.76	0.46	0.81	0.87	0.88
α-Picoline	1.09	1.03	1.17	1.08	1.11
Acetone	0.65	0.24	0.66	0.62	0.67
Acetophenone	1.07	0.72	1.12	1.07	1.12
Acetic acid	0.60	0.17	0.80	0.52	0.62
Acetic anhydride	0.74	0.25	0.78	0.73	0.74
Methyl iodide	0.74	0.09	—	0.70	0.72
Acetonitrile	0.52	−0.43	0.52	0.51	0.53
Nitromethane	2.87	1.75	3.00	2.88	2.88

* Measurements for the compounds with asterisks were made at 17°C.

TABLE II. "SOLVENT SHIFTS" $\Delta\delta$ OF METHYL PROTONS

Temperature: 11~12°C
Concentration: solute : solvent : cyclohexane = 1 : 9 : 0.25 (mol.)
Unit: p.p.m. ±0.03 p.p.m.

Solute	$\Delta\delta \equiv \delta_b - \delta_p$	$\delta_b - \delta_d$	$\delta_b - \delta_e$	$\delta_p - \delta_d$	$\delta_p - \delta_e$	$\delta_d - \delta_e$
Toluene	0.17	0.18	0.19	0.01	0.02	0.02
p-Nitrotoluene	0.40	0.51	0.57	0.11	0.17	0.06
p-Tolunitrile	0.37	0.47	0.50	0.10	0.13	0.03
p-Chlorotoluene	0.25	0.35	0.38	0.09	0.13	0.04
p-Xylene	0.11	0.07	0.12	−0.04	0.01	0.05
p-Cresol*	0.25	0.11	0.14	−0.14	−0.11	0.03
p-Toluidine	0.08	−0.03	0.02	−0.11	−0.06	0.05
m-Nitrotoluene*	0.45	0.55	0.58	0.09	0.13	0.03
m-Tolunitrile	0.40	0.51	0.55	0.11	0.15	0.04
m-Chlorotoluene	0.29	0.38	0.37	0.08	0.07	−0.01
m-Xylene*	0.11	0.08	0.11	−0.04	0.00	0.03
m-Cresol*	0.23	0.17	0.13	−0.06	−0.09	−0.03
m-Toluidine	0.11	0.04	0.05	−0.07	−0.06	0.01
o-Nitrotoluene	0.33	0.37	0.35	0.04	0.02	−0.02
o-Tolunitrile	0.30	0.40	0.39	0.10	0.09	−0.01
o-Chlorotoluene	0.14	0.20	0.22	0.06	0.08	0.02
o-Xylene	0.13	0.16	0.19	0.03	0.07	0.03
o-Cresol*	0.42	0.05	0.07	−0.37	−0.35	0.02
o-Toluidine	0.49	0.22	0.20	−0.27	−0.30	−0.03
γ-Picoline	0.38	0.46	0.52	0.08	0.14	0.06
β-Picoline	0.34	0.41	0.41	0.06	0.07	0.01
α-Picoline	0.14	0.05	0.08	−0.10	−0.07	0.03
Acetone	0.42	0.38	0.43	−0.04	0.01	0.05
Acetophenone	0.40	0.35	0.40	−0.06	0.00	0.06
Acetic acid	0.64	0.35	0.45	−0.29	−0.19	0.10
Acetic anhydride	0.53	0.48	0.49	−0.05	−0.04	0.01
Methyl iodide	—	0.62	0.63	—	—	0.02
Acetonitrile	0.95	0.94	0.97	−0.01	0.01	0.02
Nitromethane	1.26	1.13	1.13	−0.13	−0.13	0.02

* Values for the compounds with asterisks are for 17°C.

The results of measurements are summarized as shown in Table I. In meta- and para-substituted toluenes, the solvent shifts of the methyl protons, $\Delta\delta$, which are defined as the difference between the chemical shifts in any two solutions of different solvents, are linearly correlated with Hammett's sigma values as shown in Fig. 1. If we assume that the solvent shift of cyclohexane is constant, and if this is also the case with respect to the samples listed in the same column of Table II, the observed values of $\Delta\delta$ will mainly refer to the solvent shifts of the methyl protons.

In the results of Tables I and II, we notice that the magnitudes of the solvent shifts of the methyl protons are increased with the acidity of the methyl protons of the solute molecule. For example, the $\Delta\delta$ value of *p*-nitrotoluene for the benzene-CCl_4 system is 0.57 p.p.m. and that of *p*-toluidine is 0.02 p.p.m. This result coincides with the behavior of the solute parameter x_1 of the medium effect defined by Bothner-By[7].

According to the results of the measurements, we can conclude that the chemical shift of methyl proton in acetic acid is a linear function of the mole fraction solute (Fig. 2), as in the cases of nitromethane and of acetonitrile[5]. In acetic anhydride, or in acetone, the linear relation is not obtained with the simple mole fraction of the solute, but a fine linearity is obtained by taking the corrected mole fraction as abscissa, where one methyl group of the solute is taken into account as one solute molecule (cf. Figs. 2 and 3). In the cases of acetophenone and *m*-nitrotoluene, similar corrections are also necessary, and we have used the corrected mole fractions as shown in Figs. 3 and 4, where the number of the phenyl groups of the solute has been taken into account for the calculation as well as the solvent benzene.

In the case of *o*-toluidine, the chemical shifts of the methyl protons linearly depend on the simple mole fraction of the solvent (cf. Fig. 4) and, moreover, the magnitudes of the solvent shifts are anomalously large (cf. Table II). Similar results are observed with *o*-cresole.

The authors' thanks are due to Mr. Hiroshi Shimizu of the University of Tokyo and Professor Hajime Kashiwagi of Nagoya University for valuable discussions.

University of Electro-communications
Chofu, Tokyo (N. N.)

Department of Chemistry
Faculty of Science
The University of Tokyo
Hongo, Tokyo (S. F.)

7) A. A. Bothner-By: Private communication. The present authors are very grateful to Dr. Bothner-By for sending them the reprint.

Syntheses of Benzo[b]tropothiazine and its Derivatives

By Tetsuo NOZOE, Toyonobu ASAO and Kazuko TAKAHASHI

(Received July 22, 1960)

The preparation of oxime and arylhydrazones of quinoxalotropone (I) by the condensation of 5-nitroso- or 5-arylazo-tropolones and *o*-phenylenediamine was reported earlier in this laboratory[1]. A parent compound II, named benzo[b]tropazine, was obtained also by condensation of 2-halo- or 2-methoxy-tropone, or 3-carboxy-tropolone and *o*-phenylenediamine[2]. In the present series of this work, several compounds having a new ring system IV containing sulfur and nitrogen atoms were synthesized and examinations were made on their properties.

A mixture of 2-halotropone (III) and *o*-aminothiophenol in methanol was allowed to stand at room temperature and red plates IV, m.p. 87°C, $C_{13}H_9NS$, were obtained. IV is stable to heating with alkali or hydrochloric acid, is easily soluble in various organic solvents and in dilute acid to form a deep red solution, and easily gives some molecular compounds such as picrate. The ultraviolet absorption spectrum of IV (Fig. 1) in hydrochloric acid solution shows a shift to a longer wavelength region compared with that in methanol.

Attempted catalytic hydrogenation of IV in

1) T. Nozoe, M. Sato and T. Matsuda, *Sci. Repts. Tohoku Univ., First Ser.*, **37**, 407 (1953); T. Nozoe, S. Ito, S. Suzuki and K. Hiraga, *Proc. Japan Acad.*, **32**, 344 (1956); S. Ito, *Sci. Repts. Tohoku Univ., First Ser.*, **42**, 236 (1958).

2) T. Nozoe, Y. Kitahara, K. Takase and M. Sasaki, *Proc. Japan Acad.*, **32**, 349 (1956).

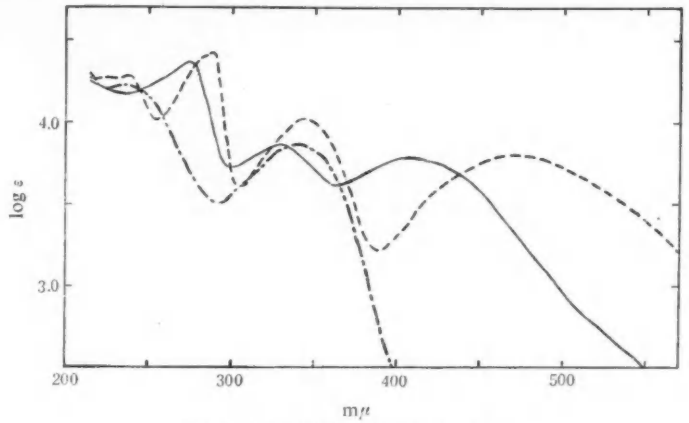

Fig. 1. Ultraviolet absorption spectra.
—·—· II (in methanol), —— IV (in methanol), ---- IV (in 0.1 N HCl).

the presence of palladium-carbon or Adams catalyst was unsuccessful with no hydrogen uptake and the complete recovery of the

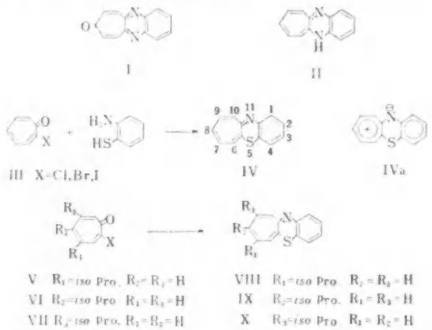

original compound IV. The reaction of IV with methyl iodide did not give methiodide, but gave hydroiodide of IV. Hydrobromide of IV was also formed by treatment of IV with hydrobromic acid.

From these properties, the course of preparation, and the analytical values of IV and its several derivatives, the structure of IV could be proved to be cyclohepta[b]benzo-[e]-1,4-thiazine, for which the name of benzo[b]-tropothiazine is proposed.

It is interesting to compare compound IV with compound II. The latter compound II forms colorless prisms with poor solubility, and is unstable toward acids, reducible with palladium-carbon to 2,3-pentamethylene-quinoxaline. Also the ultraviolet spectrum of compound II is quite different from that of compound IV as shown in Fig. 1. These results would indicate that IV is stabilized by the resonance between IV and IVa.

Three kinds of isopropyl-2-halotropones (V, VI and VII)[3,4] were also reacted with *o*-aminothiophenol, easily affording 7-, 8- and 9-isopropylbenzo[b]tropothiazines (VIII, IX and X) as red oils. These isopropyl compounds have properties similar to those of the compound IV. In view of the fact that the abnormal nucleophilic substitution, which is frequently observed in troponoid chemistry*, does not occur in the reaction of 2-halotropone derivatives and methylmercaptane[5], it is considered that the same normal substitution occurs in the reaction of 2-halotropone derivatives and *o*-aminothiophenol; therefore it is assumed that the structure of VIII-X is correct.

2-Bromo-7-methoxytropone (XI)[6] gave a red oil XII, $C_{14}H_{11}ONS$, by the condensation with *o*-aminothiophenol. The compound XII, like IV, is soluble in dilute acid and gives molecular compounds such as picrate. Hydrolysis of XII with hydrochloric acid gave red needles XIII, m.p. 169°C, which were identical with a compound obtained by the reaction of 3-bromo-2-methoxytropone (XIV)[6]

3) S. Seto, *Sci. Repts. Tohoku Univ., First Ser.*, **37**, 286 (1953).
4) W. v. E. Doering and L. H. Knox, *J. Am. Chem. Soc.*, **75**, 297 (1953).
* It has been known that in the nucleophilic substitution reaction of 2-halotropones various reagents do not attack at the carbon-2 but at the carbon-7 in the majority of cases.

Cf. T. Nozoe, S. Seto and T. Sato, *Proc. Japan Acad.*, **30**, 473 (1954); T. Nozoe, "Non-Benzenoid Aromatic Compounds", Edited by D. Ginsburg, Interscience Publishers, Inc., New York (1959), p. 339.
5) K. Matsui, This Bulletin, **33**, 1448 (1960).
6) T. Nozoe, Y. Kitahara and S. Masamune, *Proc. Japan Acad.*, **27**, 649 (1951).

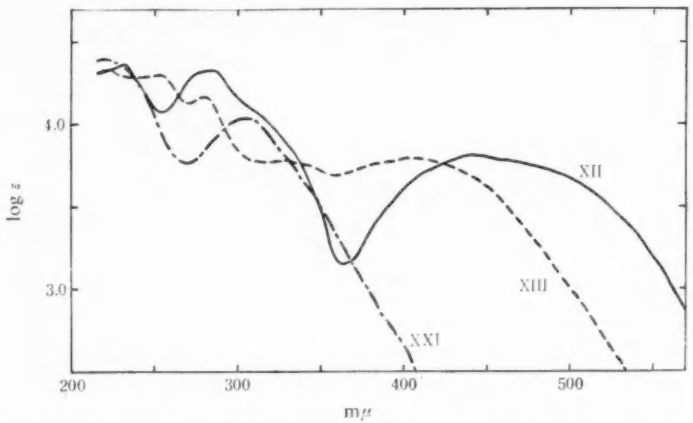

Fig. 2. Ultraviolet absorption spectra of XII, XIII and XXI in methanol.

and *o*-aminothiophenol. XIII was also obtained from 2-bromotropolone (XV) in good yield. From these results, it is assumed that the structure of XII is 10-methoxybenzo[b]tropothiazine and of XIII is 10-hydroxybenzo[b]-tropothiazine.

Attempted substitution of methoxyl in XII with amino or substituted amino group was not successful. The original compound XII was recovered unchanged.

2-Bromo-5-isopropyl-7-methoxytropone (XVI)[7] gave 7-isopropyl-10-methoxybenzo[b]tropothiazine (XVII) by the reaction with *o*-aminothiophenol. Hydrolysis of XVII with hydrochloric acid afforded 7-isopropyl-10-hydroxybenzo[b]-tropothiazine (XVIII). This was also obtained by the reaction of 3-bromo-6-isopropyl-2-methoxytropone (XIX)[7] or 7-bromohinokitiol (3-bromo-6-isopropyltropolone) (XX) with *o*-aminothiophenol. XIII and XVIII do not dissolve in dilute acids. XIII does not give molecular compounds such as picrate, but XVIII gives them.

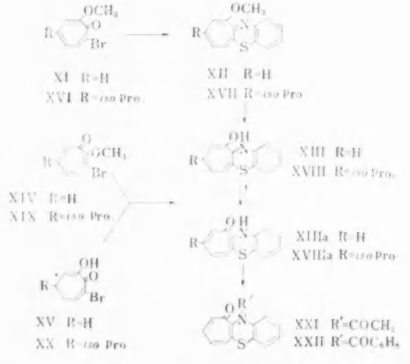

It is considered that compounds XIII and XVIII could exist in two tautomeric forms respectively, i.e. 10-hydroxy derivatives of benzo[b]tropothiazine (XIII and XVIII) and benzothiazinotropone derivatives (XIIIa and XVIIIa). Information on this problem comes from the following data: 1) The ultraviolet spectrum of XII is similar to IV rather than to XIII as shown in Fig. 2. 2) The infrared spectrum of XIII shows ν_{NH} at 3218 cm^{-1} and $\nu_{C=O}$ at 1607 cm^{-1} (small peak). 3) XIII did not react with diazomethane, but gave yellow acetate XXI with acetic anhydride and orange benzoate XXII with benzoyl chloride in poor yield. The hydrolysis of these acyl derivatives converts them into XIII. $\nu_{C=O}$ at 1673 cm^{-1} in infrared spectrum of XXI indicates that XXI is *N*-acetyl derivative. Remarkable shifts to a shorter wavelength region in the ultraviolet spectra of XXI and XXII (Fig. 2) seem to indicate that a conjugation of seven membered ring and benzene nucleus in XIII is broken by the introduction of the acyl group in the *N*-atom, as an additional reason for the decrease of the coplanarity of these nuclei is also considered.

From consideration of the above results, it seems reasonable to conclude that XIII would exist not as 10-hydroxybenzo[b]tropothiazine, but as its keto form, benzo-1,4-thiazino[3,2-b]-tropone (XIIIa). XVIII would be named 8-isopropylbenzo-1,4-thiazino[3,2-b]tropone (XVIIIa).

It is supposed that *N*-alkylation of the compound XII is possible as in the case of phenothiazine, but the attempted alkylations were not actually successful. Further experiments in this field will be reported in near future.

7) S. Seto, *Sci. Repts. Tohoku Univ., First Ser.*, **37**, 298 (1953).

Experimental**

Benzo[b]tropothiazine (IV). — A solution of 2 g. of 2-chlorotropone and 2 g. of *o*-aminothiophenol in 20 ml. of methanol was allowed to stand at room temperature for 3 hr. The solvent was distilled off and 100 ml. of water added to the residue, and the insoluble portion was filtered off. The filtrate was extracted with two 10 ml. portions of benzene. The mother liquor left after benzene extraction was adjusted to make it slightly alkaline with sodium carbonate solution, then was extracted with five 10 ml. portions of benzene. The latter benzene extract was dried over sodium sulfate and the benzene was distilled off, affording 2.4 g. of deep red crystals. Recrystallization of the crude crystals from petroleum (b. p. 60~70°C) gave 2.2 g. of IV as red plates, m. p. 86~87°C.

The reaction of 2-bromo- or 2-iodo-tropone with *o*-aminothiophenol gave the same compound IV.

Found: C, 74.05; H, 4.20; N, 6.61. Calcd. for $C_{13}H_9NS$: C, 73.92; H, 4.30; N, 6.63%.

λ_{max}^{MeOH} mμ (log ε): 275 (4.37), 330 (3.86), 405 (3.79). $\lambda_{max}^{0.1N\ HCl}$ mμ (log ε): 224 (4.27), 238 (4.28), 289 (4.44), 343 (4.02), 470 (3.81).

Picrate; dark brown needles, m. p. 188~189°C (decomp.).

Found: C, 51.75; H, 3.16; N, 12.73. Calcd. for $C_{19}H_{12}O_7N_4S$: C, 51.82; H, 2.75; N, 12.72%.

Styphnate; dark brown needles, m. p. 204~205°C (decomp.).

Found: C, 50.09; H, 2.75; N, 12.10. Calcd. for $C_{19}H_{12}O_9N_4S$: C, 50.00; H, 2.65; N, 12.10%.

Hydriodide; black violet needles, m. p. 194~195.5°C, 210~220°C (decomp.).

Found: C, 46.35; H, 3.42; N, 4.51. Calcd. for $C_{13}H_{10}NSI$: C, 46.00; H, 2.97; N, 4.13%.

Hydrobromide; black violet needles, m. p. 207°C (decomp.).

Found: C, 51.95; H, 3.37; N, 4.28. Calcd. for $C_{13}H_{10}NSBr$: C, 53.42; H, 3.45; N, 4.79%.

7-Isopropylbenzo[b]tropothiazine (VIII). — Reaction of 150 mg. of 2-chloro-4-isopropyltropone (V) with 100 mg. of *o*-aminothiophenol in methanol afforded 150 mg. of VIII as red oil.

Picrate; violet needles, m.p. 172~173°C (decomp.).

Found: C, 54.62; H, 3.68; N, 11.59. Calcd. for $C_{22}H_{15}O_7N_4S$: C, 54.77; H, 3.76; N, 11.62%.

Styphnate; dark violet needles, m.p. 169~170°C (decomp.).

Found: C, 53.15; H, 3.53; N, 11.22. Calcd. for $C_{22}H_{18}O_9N_4S$: C, 53.01; H, 3.63; N, 11.24%.

8-Isopropylbenzo[b]tropothiazine (IX). — IX as red oil was obtained from 2-halo-5-isopropyltropone (VI) and *o*-aminothiophenol.

Picrate; violet needles, m. p. 176~177°C.

Found: C, 54.74; H, 3.79; N, 11.52%.

Styphnate; violet needles, m.p. 176.5~177.5°C.

Found: C, 52.74; H, 3.42; N, 11.23%.

9-Isopropylbenzo[b]tropothiazine (X). — X as red oil was obtained from 2-halo-6-isopropyltropone (VII) and *o*-aminothiophenol.

Picrate; violet plates, m. p. 198~199°C (decomp.).

Found: C, 54.39; H, 3.27; N, 11.64%.

Styphnate; violet prisms, m. p. 191~192°C (decomp.).

Found: C, 53.19; H, 3.77; N, 10.97%.

10-Methoxybenzo[b]tropothiazine (XII). — A solution of 215 mg. of 2-bromo-7-methoxytropone (XI) and 130 mg. of *o*-aminothiophenol in 3 ml. of methanol was warmed for twenty minutes. After allowing it to stand at room temperature for 10 min., the solvent was distilled off, and 20 ml. of water was added and extracted with two 5 ml. portions of benzene. The water layer left after the benzene extraction was adjusted to slightly alkaline with sodium carbonate and was extracted with benzene. The latter benzene extract was dried over sodium sulfate and the solvent was removed, affording 150 mg. of XII as red oil, and was purified by chromatogram, using an alumina.

λ_{max}^{MeOH} mμ (log ε): 222 (4.33), 253 (4.28), 280 (4.15), 328 (3.78), 408~410 (3.78).

Picrate; dark brown needles, m. p. 184~185°C.

Found: C, 51.01; H, 2.83; N, 11.76. Calcd. for $C_{21}H_{14}O_8N_4S$: C, 51.07; H, 3.00; N, 11.91%.

Styphnate; dark brown needles, m. p. 173~174°C.

Found: C, 49.55; H, 2.78; N, 11.25. Calcd. for $C_{21}H_{14}O_9N_4S$: C, 49.39; H, 2.90; N, 11.52%.

Benzo-1, 4-thiazino[3, 2-b]tropone (XIII). — a) A solution of 3 g. of 3-bromotropolone (XV) and 2 g. of *o*-aminothiophenol in 20 ml. of methanol was refluxed for 2 hr. The red needles which separated out by cooling thoroughly were collected by filtration and recrystallization from ethanol or acetic acid, giving 2.6 g. of XIII as red needles, m. p. 168~169°C.

Found: C, 68.84; H, 3.76; N, 6.11. Calcd. for $C_{13}H_9ONS$: C, 68.72; H, 3.99; N, 6.17%.

λ_{max}^{MeOH} mμ (log ε): 233 (4.36), 285 (4.33), 440 (3.82). $\lambda_{max}^{0.1N\ HCl}$ mμ (log ε): 230 (4.37), 285 (4.35), 450 (3.81).

b) After allowing a solution of 215 mg. of 3-bromo-2-methoxytropone (XIV) and 130 mg. of *o*-aminothiophenol in 2 ml. of a methanol to stand under cooling, 220 mg. of XIII was obtained.

c) A solution of 50 mg. of XII in 3 ml. of 2N hydrochloric acid was refluxed for 5 hr., and the crystals which separated out were recrystallized from ethanol, affording 30 mg. of XIII.

10-Methoxy-8-isopropylbenzo[b]tropothiazine (XVII). — A solution of 520 mg. of 2-methoxy-4-isopropyl-7-bromotropone (XVI) and 250 mg. of *o*-aminothiophenol in 2 ml. of methanol was refluxed for thirty minutes. The solvent was distilled off and 7 ml. of water was added to the residue and the solution was extracted with benzene. The mother liquor left after the benzene extraction was adjusted to slightly alkaline with sodium carbonate and was extracted with benzene. The latter benzene extract was dried and the removal of the solvent left 270 mg. of red oil. The oil was crystallized with methanol and the recrystallization from methanol gave XVII as orange prisms, m. p. 123~124°C.

** All the melting points were uncorrected. The microanalyses were carried out by Mr. S. Azumi and Miss A. Iwanaga, and I. R. spectra were measured with Perkin-Elmer Model 112 by the member of Professor Kinumaki's laboratory, Research Institute, Chemistry of Non-Aqueous Solution, Tohoku Univ., to whom the authors' sincere acknowledgements are hereby extended.

Found: C, 71.70; H, 5.84; N, 4.93. Calcd. for $C_{17}H_{17}ONS$: C, 72.06; H, 6.05; N, 4.94%.

λ_{max}^{MeOH} mμ (log ε): 225 (4.41), 255 (4.24 sh), 280 (4.14 sh), 333 (3.74), 408~410 (3.78).

Picrate: brown needles, m.p. 160~161°C.

Found: C, 53.99; H, 3.93; N, 10.85. Calcd. for $C_{23}H_{20}O_8N_4S$: C, 53.91; H, 3.93; N, 10.93%.

Styphnate: brown needles, m.p. 145~146°C.

Found: C, 52.74; H, 3.75; N, 10.60. Calcd. for $C_{23}H_{20}O_8N_4S$: C, 52.25; H, 3.81; N, 10.61%.

8-Isopropylbenzo-1, 4-thiazino[3, 2-b]tropone (XVIII).—a) A solution of 500 mg. of 7-bromohinokitiol (3-bromo-6-isopropyltropolone) (XX) and 250 mg. of *o*-aminothiophenol in 3 ml. of methanol was refluxed for an hour, the solvent was distilled off and 20 ml. of water was added to the residue, and then extracted six times with 3 ml. each of benzene. The benzene solution was dried over sodium sulfate, passed through an alumina column, and 440 mg. of oily substance was obtained after removal of the solvent from the effluent. The oil crystallized with cyclohexane and the recrystallization from cyclohexane afforded XVIII as red needles, m.p. 94~95°C.

Found: C, 71.01; H, 5.50; N, 5.27. Calcd. for $C_{16}H_{15}ONS$: C, 71.36; H, 5.61; N, 5.20%.

λ_{max}^{MeOH} mμ (log ε): 237 (4.31), 277 (4.23), 430 (3.65).

Picrate: brownish violet plates, m.p. 141~142°C.

Found: C, 53.70; H, 3.98; N, 11.19. Calcd. for $C_{22}H_{18}O_9N_4S$: C, 53.01; H, 3.64; N, 11.24%.

Styphnate: brownish violet plates, m.p. 170~171°C.

Found: C, 51.47; H, 3.47; N, 10.39. Calcd. for $C_{22}H_{18}O_9N_4S$: C, 51.36; H, 3.53; N, 10.89%.

b) A solution of 260 mg. of 2-methoxy-3-bromo-6-isopropyltropone (XIX) and 130 mg. of *o*-aminothiophenol in 3 ml. of methanol was allowed to stand for an hour. 300 mg. of red crystals was obtained after treatment using the same method as (a). These crystals showed no depression of melting point on admixture with a specimen obtained in (a).

c) After refluxing a solution of 50 mg. of XVII in 3 ml. of 2 N hydrochloric acid for 5 hr., the solution was extracted with benzene and the benzene extract was passed through an alumina column, affording 30 mg. of red needles, m.p. 92~93°C. The crystals showed no depression of melting point on admixture with XVIII.

Acetate (XXI) of XIII.—One hundred mg. of XIII were dissolved in 0.5 ml. of acetic anhydride, to which one drop of concentrated sulfuric acid was added, and then the mixture was allowed to stand at room temperature. After removing the acetic anhydride, the residue was dissolved in benzene and the benzene solution was passed through an alumina layer. The first elution gave unreacted XIII, but the second effluent afforded yellow prisms. Recrystallization of the latter crystals from methanol gave XXI as yellow prisms, m.p. 169.5~170.5°C.

Found: C, 66.62; H, 3.71; N, 5.36. Calcd. for $C_{15}H_{11}O_2NS$: C, 66.91; H, 4.12; N, 5.20%.

λ_{max}^{MeOH} mμ (log ε): 220 (4.39), 303 (4.04).

Benzoate (XXII) of XIII.—To a solution of 100 mg. of XIII in 1 ml. of pyridine, 0.2 ml. of benzoylchloride was added and heated for 20 min. The crystals separated out by adding water were dissolved into benzene and the insoluble portion was recrystallized from methanol, affording XXII as orange prisms, m.p. 193~194°C.

Found: C, 72.39; H, 3.71; N, 4.38. Calcd. for $C_{20}H_{13}O_2NS$: C, 72.50; H, 3.96; N, 4.23%.

λ_{max}^{MeOH} mμ (log ε): 220 (4.49), 308 (4.01).

The authors wish to take this opportunity to express their gratitude for the donation of the Grant in Aid for Scientific Research from the Ministry of Education and for financial assistance from the Sankyô Co., Ltd.

Department of Chemistry
Faculty of Science
Tohoku University
Katahira-cho, Sendai

On Pyrazino[d, d']ditropone and its Derivatives

By Toyonobu Asao

(Received July 22, 1960)

It is already known that 2, 5-diaminotroponimine reacts with formic acid and nitrous acid forming 1, 3-diazaazulene or 1,2,3-triazaazulene derivatives respectively[1-2].

If one considers the facile condensation of 5-nitrosotropolone with 1, 2-diamine to form a troponeoxime with the heterocyclic system[3-6], it is expected that the formation of a new 7-6-7 hetrocyclic system in which N-atoms are located in a six-membered ring by application of 2, 5-diaminotroponimine, will make a tautomer of 4,5-diaminotroponimine.

An account of the attempt to synthesize such a 7-6-7 membered ring system is reported herein.

Heating of 5-nitrosotropolone (I)[7] in methanol afforded brown crystals, m. p. over 300°C, $C_{14}H_{11}ON_5Cl$, very easily with dihydrochloride of 2, 5-diaminotroponimine (II)[1]. Neutralization of the aqueous solution of these crystals with sodium hydrogencarbonate gave brown powder III, m. p. over 300°C, $C_{11}H_{10}ON_4$, indicating the former crystals to be monohydrochloride of III. III is insoluble in various organic solvents and recrystallized with difficulty. Ultraviolet spectra of III in acidic and alkaline media show a little shift to longer wavelength region compared with that in methanol.

The structural confirmation of III came from alkaline permanganate oxidation, in which pyrazine tetracarboxylic acid dihydrate, m. p. 205°C[8], was obtained. Its tetramethyl ester obtained by the reaction with diazomethane showed no depression of melting point on admixture with authentic tetramethyl pyrazinetetracarboxylate, m. p. 182°C, obtained by methylation of pyrazinetetracarboxylic acid, the latter being synthesized by oxidation of quinoxalotroponeoxime[5]. Therefore, together with its analytical value and the following reactions, it is clear that III is pyrazino[d, d']-ditroponemonoiminemonooxime.

Attempted acetylation of III with acetic anhydride led to the formation of a black substance. However, acetate V was obtained by the reaction of acetate IV[3] of 5-nitrosotropolone with II.

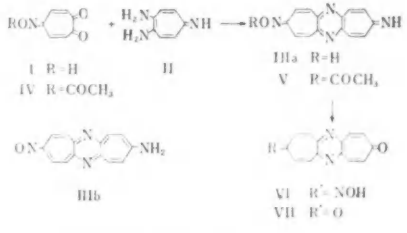

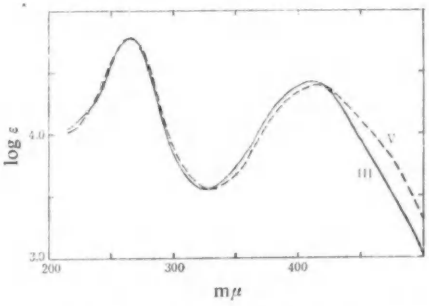

Fig. 1. Ultraviolet absorption spectra of III and V in methanol.

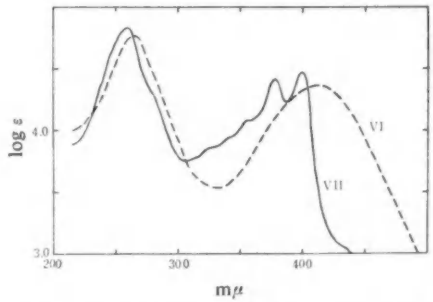

Fig. 2. Ultraviolet absorption spectra of VI and VII in methanol.

1) T. Nozoe, M. Sato, S. Ito, K. Matsui and T. Matsuda, *Proc. Japan Acad.*, **29**, 565 (1953).
2) T. Nozoe, S. Ito and K. Matsui, ibid., **30**, 313 (1954).
3) T. Nozoe, M. Sato and T. Matsuda, *Sci. Repts. Tohoku Univ., First Ser.*, **37**, 407 (1953).
4) T. Nozoe, S. Ito, S. Suzuki and K. Hiraga, *Proc. Japan Acad.*, **32**, 344 (1956).
5) S. Ito, *Sci. Repts. Tohoku Univ., First Ser.*, **42**, 236 (1958).
6) S. Ito, ibid., **43**, 247 (1959).
7) T. Nozoe, S. Seto, H. Takeda and T. Sato, ibid., **35**, 274 (1952).
8) F. D. Chattaway and W. G. Humphrey, *J. Chem. Soc.*, **1929**, 645.

From the similarity of the ultraviolet spectra of III and V shown in Fig. 1, compound III is assumed to have the structure IIIa rather than its tautomeric form IIIb.

Although III and V are easily soluble in aqueous alkali, acidification of these solutions with acetic acid afforded not the original substance but the same needles VI, m. p. 266°C, $C_{14}H_9O_2N_3$, from both III and V. The infrared spectrum of VI shows peaks at 3250 (O-H), at 1627 (C=O) and at 1585 cm^{-1} (C=C). VI gives carbonyl derivatives such as oxime and 2, 4-dinitrophenylhydrazone. These results indicate VI to be pyrazino[d, d']ditroponemonoxime, which is produced by hydrolysis of the acetyl group and or imino group in V or III.

The reaction of benzoate[7] of 5-nitrosotropolone and II afforded dark brown crystals. Although these crystals were unstable for further purification, VI was obtained by treatment of these crystals with alkaline.

Heating of III or VI in formic acid in the presence of copper carbonate[5,9] gave pyrazino-[d, d']ditropone (VII), peaks of infrared spectrum at 1635 (C=O) and at 1598 cm^{-1} (C=C), in poor yield. The ultraviolet spectrum of VII (Fig. 2) exhibits the characteristic fine structure compared with III and VI. This kind of fine structure has been observed in the case of quinoxalotropone or pyrazinotropone[5,6]. While being stable to acid, VII is unstable to alkali and gradually turns to brown in alkaline solution.

Experimental*

Pyrazino[d, d']ditroponemonoiminemonoxime (III.)—A solution of 900 mg. of I and 1.1 g. of dihydrochloride of II dissolved in 40 ml. of methanol was refluxed for twenty minutes and brownish orange crystals separated out. After cooling, 1.3 g. of the crystals, m. p. over 300°C, were obtained by filtration. These crystals are positive to the halogen test and are insoluble in various organic solvents. Recrystallization of the crystals was carried out from a large amount of dilute hydrochloric acid.

Found: C, 58.55; H, 3.66; N, 18.93. Calcd. for $C_{14}H_{10}ON_4 \cdot HCl$: C, 58.64; H, 3.88; N, 19.54%.

Neutralization of these crystals dissolved in a large amount of water with aqueous sodium hydrogencarbonate gave brown powder III, m. p. over 300°C. Attempted recrystallization of III from various solvents was in vain.

Found: C, 66.98; H, 4.10; N, 22.10. Calcd. for $C_{14}H_{10}ON_4$: C, 67.19; H, 4.03; N, 22.39%.

Picrate; red needles, m. p. over 300°C, turn to black from about 225°C.

Found: C, 50.21; H, 3.00; N, 20.50. Calcd. for $C_{20}H_{13}O_8N_7$: C, 50.11; H, 2.73; N, 20.45%.

Oxidation of III.—To a solution of 500 mg. of III and 400 mg. of potassium hydroxide dissolved in 40 ml. of water, a solution of 5g. of potassium permanganate dissolved in 250 ml. of water was added at 80°C in a period of 6 hr. The excess of potassium permanganate was killed by a few drops of methanol and the resulting manganese dioxide was filtered. Manganese dioxide was washed with hot water thoroughly, and the combined solution of filtrate and washing was concentrated to about 15 ml., and was acidified with dilute hydrochloric acid affording colorless crystals, 230 mg. Recrystallization of the crystals from hydrochloric acid gave pyrazinetetracarboxylic acid as colorless plates, m. p. 205°C (decomp.).

Found: C, 32.72; H, 2.43; N, 9.81. Calcd. for $C_8H_4O_8N_2 \cdot 2H_2O$: C, 32.89; H, 2.76; N, 9.59%.

By the methylation reaction of 10 mg. of pyrazinetetracarboxylic acid with diazomethane, colorless needles, m. p. 181~182°C (from methanol-benzene) were obtained. This ester showed no depression of melting point on admixture with tetramethyl pyrazinetetracarboxylate obtained by another route.

Found: C, 46.32; H, 3.84; N, 8.92. Calcd. for $C_{12}H_{12}O_8N_2$: C, 46.16; H, 3.87; N, 8.97%.

Acetate V.—A solution of 200 mg. of acetate IV of 5-nitrosotropolone and 200mg. of dihydrochloride of II dissolved in 5 ml. of methanol was refluxed for 10 min., affording 300 mg. of red needles, which turn to black from around 250°C.

Found: C, 58.27; H, 3.77; N, 17.81. Calcd. for $C_{16}H_{12}O_5N_4 \cdot HCl$: C, 58.44; H, 3.98; N, 17.04%.

Neutralization of aqueous solution of the above crystals gave acetate V of III as brown powder, m. p. over 300°C.

Found: C, 65.60; H, 3.99; N, 19.07. Calcd. for $C_{16}H_{12}O_2N_4$: C, 65.75; H, 4.14; N, 19.17%.

Pyrazino[d, d']ditroponemonoxime (VI).—A solution of 100 mg. of hydrochloride of III dissolved in 1.5 ml. of 3 N sodium hydroxide solution was heated gently for 3 min. Ammonia gas evolved during this time. After allowing the solution to stand for 30 min. at room temperature, it was acidified with a few drops of acetic acid. Orange crystals, 70 mg., precipitated out were recrystallized from pyridine yielding, orange needles, m. p. 266°C (carbonize).

Found: C, 66.95; H, 3.77; N, 17.16. Calcd. for $C_{14}H_9O_2N_3$: C, 66.92; H, 3.61; N, 16.73%.

Oxime; red fine crystals (from pyridine), m. p. over 300°C.

Found: C, 63.79; H, 3.84; N, 20.62. Calcd. for $C_{14}H_{10}O_2N_4$: C, 63.15; H, 3.79; N, 21.04%.

2, 4-Dinitrophenylhydrazone; violet crystals, carbonize at about 265°C.

Found: C, 55.31; H, 3.24; N, 22.88. Calcd. for $C_{20}H_{13}O_5N_7$: C, 55.68; H, 3.04; N, 22.77%.

Pyrazino[d, d']ditropone (VII).—a) A mixture of 150 mg. of hydrochloride of III and 150 mg. of copper carbonate in 4.5 ml. of 80% formic acid was

9) R. Robinson, *Nature*, **173**, 541 (1954).

* All the melting points were uncorrected. The microanalyses were carried out by Messrs. S. Oyama, S. Azumi and Miss A. Iwanaga, and I. R. spectra were measured with Perkin-Elmer Model 112 by a member of Professor Kinumaki's laboratory, Research Institute, Chemistry of Non-Aqueous Solution, Tohoku Univ., to whom the author's sincere acknowledgements are hereby extended.

heated at 80°C for 70 hr. The resulting brown precipitates were filtered affording 30 mg. of VI. By neutralization of the filtrate, 20 mg. of precipitates were obtained. Recrystallization from pyridine gave VII as gold-colored needles, m. p. 244~245°C (decomp.).

Found: C, 71.14; H, 3.43; N, 12.38. Calcd. for $C_{14}H_8O_2N_2$: C, 71.18; H, 3.41; N, 11.86%.

b) Three hundred milligrams of VI were heated at 75°C for 120 hr. with 300 mg. of copper carbonate and 10 ml. of 80% formic acid. After cooling, 150 mg. of undissolved VI was obtained. Neutralization of the filtrate with sodium hydrogencarbonate afforded 70 mg. of solid. Recrystallization from pyridine gave gold-colored needles VII, m. p. 244~245°C (decomp.).

The author takes this opportunity to express his sincere gratitude to Professor Tetsuo Nozoe for his kind guidance throughout these experiments, as well as to Assistant Professor Toshio Mukai and Dr. Sho Ito for their kind advice and suggestions.

Department of Chemistry
Faculty of Science
Tohoku University
Katahiracho, Sendai

The Mechanical Behavior of Swollen Polystyrene, Poly-p-chlorostyrene and their Copolymers in Benzene. II. Stress Relaxation under Constant Strain

By Kazuyoshi OGINO

(Received May 2, 1960)

In the previous paper[1], the stress relaxation of swollen polymethylacrylate gels in several organic solvents was studied, and it was shown that the smaller the volume fraction of polymer is, the greater degree of relaxation, and the higher temperature dependency of stress relaxation are observed.

In this paper, the stress relaxation of gel swollen in benzene is studied as a function of intermolecular force which is controlled by changing the content of substituted chlorine atoms in the chain molecules[2].

When a viscoelastic body is strained quickly to a definite extent and kept at this state, the relaxation of stress is observed.

Tobolsky et al. have shown[3] that the relaxation curves at different temperatures can be superposed upon each other when plotted as the reduced stress, g, against the logarithmic time, and that a change in temperature corresponds to a shift of the curve along the logarithmic time scale. (In the present experiment, the stress is arbitrarily reduced to 20°C, and is denoted by g_{20}.)

The existence of this superposition principle of relaxation curves at different temperatures indicates that the relaxation curves for the same polymer at different temperatures are identical if plotted as the reduced stress vs. the logarithm of (Kt) where K is a function of temperature. Or we can express the reduced stress g_{20}, for example, as a function of Kt[3]; i. e.,

$$g_{20} = g_{20}(Kt)$$

It is found that the temperature dependence on K may be expressed by Arrhenius's equation[3]

$$K = A \exp.(-H/RT)$$

The apparent activation energy H can therefore be calculated by plotting the logarithm of the time factor K against the reciprocal of absolute temperature.

Experimental

Samples.—About 4 cc. of styrene (for sample A), *p*-chlorostyrene (for sample D) or their mixtures (for samples B and C) which contains one drop (about 2 mg.) of divinylbenzene and about 10 mg. of benzoyl peroxide was polymerized thermally in bulk in a sealed glass tube. They were swollen in

TABLE I. VOLUMES OF STYRENE AND *p*-CHLOROSTYRENE MONOMER TAKEN INTO POLYMERIZATION

Sample	*p*-Chlorostyrene, cc.	Styrene, cc.
A	0	4
B	1.6	2.4
C	2.4	1.6
D	4	0

1) K. Ogino, This Bulletin, **31**, 580 (1958).
2) K. Ogino, ibid., **32**, 553 (1959).
3) A. V. Tobolsky et al., *J. Polymer Sci.*, **3**, 669 (1948).

benzene to the equilibrium state. Benzene was purified by shaking several times with concentrated sulfuric acid, and with distilled water, and was then dried over calcium chloride and redistilled.

Volumes of *p*-chlorostyrene and styrene monomer before polymerization are shown in Table I.

Apparatus. — The apparatus used to observe the change of stress with time is the same as was described in the previous paper[1], and is shown in Fig. 1; a definite strain (11.2%) is given to the specimen (A) and the stress, measured by the vertical component of the chain length, is recorded on a rotating drum. The chain corresponding to and following the decaying stress at each time is controlled by a balancing motor (E) which is connected to a relay (F) through an amplifier circuit (G).

Results and Discussion

The experimental curves of the reduced stress against logarithmic time for each polymer are shown in Figs. 2, 3, 4 and 5.

The apparent activation energy for the relaxation obtained by plotting the logarithm of the time factor K against the reciprocal temperature is also shown in each figure.

If these curves at different temperatures are superposed with each other by suitable translations along the logarithmic time axis, the master curves shown in Fig. 6 are obtained.

Four parameters in the mechanical model[1]

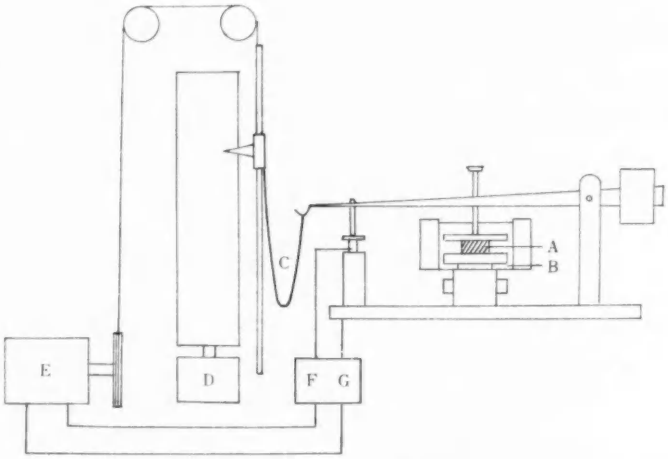

Fig. 1. Chainomatic balance.
(A): Specimen (B): Solvent (C): Chain (D): Rotating drum
(E): Balancing motor (F): Relay (G): Amplifier circuit

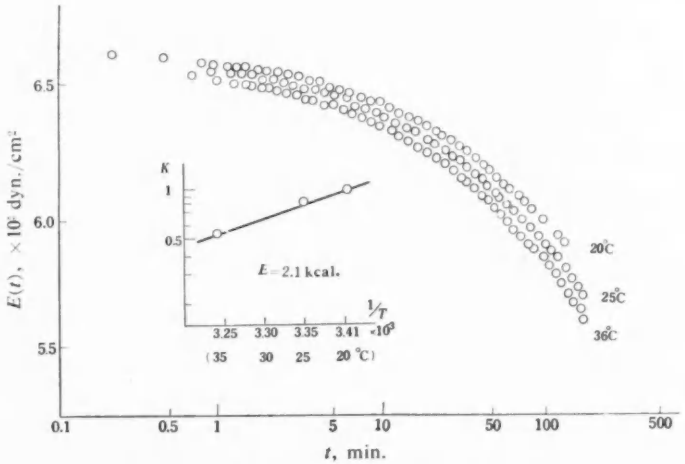

Fig. 2. Stress relaxation curves for sample A, $E=2.1$ kcal.

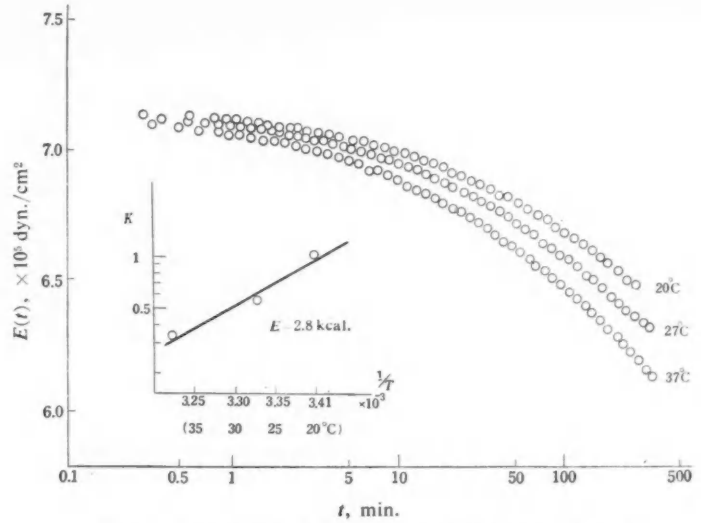

Fig. 3. Stress relaxation curves for sample B, E=2.8 kcal.

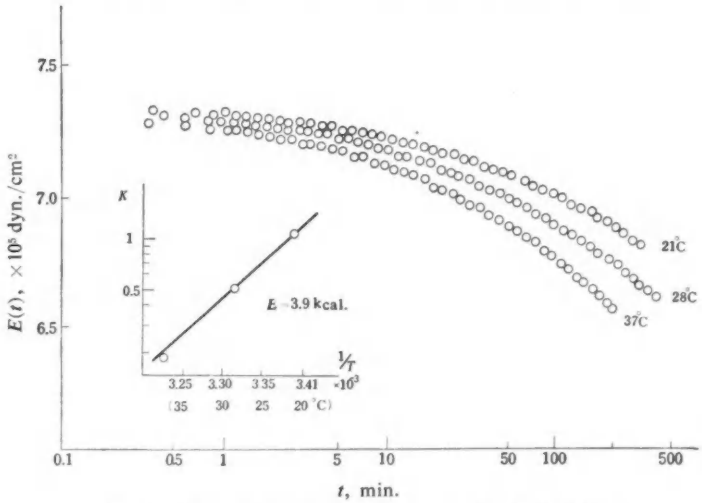

Fig. 4. Stress relaxation curves for sample C, E=3.9 kcal.

to express the curves of Fig. 6 are listed in Table II.

As these gels are cross-linked chemically by divinylbenzene, we can expect that the stress relaxation in the present case arises mainly from the breakage or slippage of some weak bonds such as entanglements or other secondary bonds present between junction points.

The value of G_1, in Table II, increases with the increase of chlorine content. Considering that these gels have nearly equal values of v_r, volume fraction of polymer at swelling equilibrium[4], the fact that the initial Young's modulus G_1 increases with the increase of chlorine content leads to the assumption that the stronger interaction force between chain molecules appears by the presence of chlorine atoms.

As each parameter in the four-element model for the chlorine rich gel, especially η_2 or η_3, is large, we can assume that the contribution of chlorine atoms to the relaxation or viscous

4) K. Ogino, This Bulletin, 31, 577 (1958).

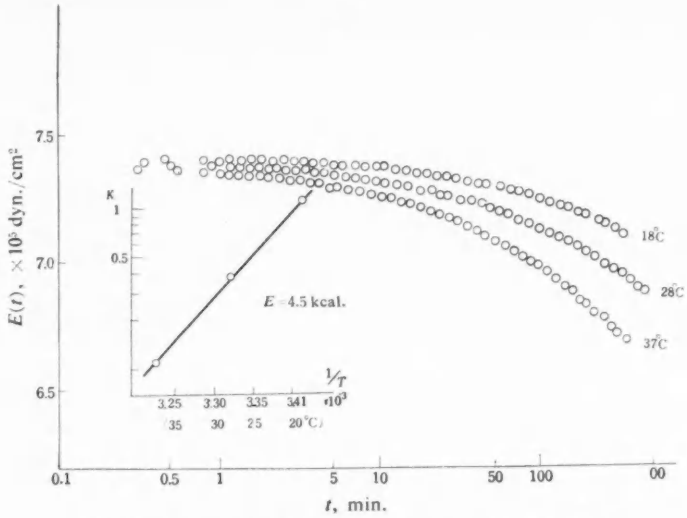

Fig. 5. Stress relaxation curves for sample D, $E=4.5$ kcal.

TABLE II. PARAMETER VALUES IN FOUR-ELEMENT MODEL

Sample	v_r	G_1 dyn./cm²	G_2 dyn./cm²	η_2 (poise)	η_3 (poise)	η_3/G_1, sec.	η_2/G_2, sec.
A	4.3	5.90×10^6	2.54×10^5	3.90×10^5	8.55×10^{11}	1.45×10^5	1.5
B	4.1	6.35×10^6	7.50×10^7	4.70×10^5	3.75×10^{12}	5.95×10^5	6.7
C	4.0	6.54×10^9	1.23×10^9	2.39×10^9	3.35×10^{12}	5.12×10^5	19.4
D	4.4	6.63×10^6	3.00×10^5	2.95×10^9	3.99×10^{12}	6.03×10^5	10

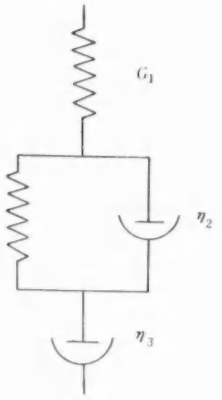

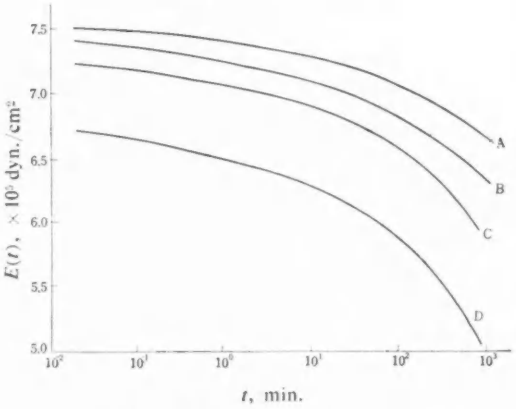

Fig. 6. Relaxation master curves.

property is, primarily, a decisive factor.

When we express these mechanical properties by this four-element model, the value of the retardation time η_2/G_2 can be expected to have a comparable value to the observation time scale, and values of these parameters in Table II can be considered to be reasonable from this point.

Hatfield and Rathmann assumed[5] that for swollen gels viscous flow or molecular slippage is brought about by chemical rupture of primary bonds. For the fact that η_2/G_2 in Table II has the order of about 10^5 sec., the author assumed that the retardation time of this order

5) M. R. Hatfield and G. B. Bathmann, *J. Appl. Phys.*, **25**, 1082 (1951).

may correspond to the slippage of some secondary bonds in polymeric substances.

The values of η_3 in the four-element model for the other polymeric substances are much smaller than that of this gel (about 10^7 poises is expected in the usual case). This parameter may be considered to correspond to a process of a longer retardation time. It will be possible to consider that for swollen gels most of the secondary bonds are set free by solvation, and that the number of bonds which are to slip off or to be liberated per unit time under constant strain are much fewer than those in the dry and undiluted states. The apparent rate of flow will therefore be smaller, and the viscosity will then be much greater (10^{12} poises).

The apparent activation energy for relaxation process is also great when the chlorine content increases. The great activation energy means great temperature dependence. As the contribution of energy term to the elasticity or the value of μ, polymer-solvent interaction parameter[4], increases with the increase of chlorine content[2], we can presume that the cause of the great temperature dependence may be the fact that the breaking of some secondary bonds are favored because the solvent-polymer contacts increase, or that these bonds come to be slipped off more easily as temperature rises. In the case of polystyrene gel, on the other hand, there may be no residual secondary bonds to be released by temperature rise.

These facts can be interpreted by considering the appearance of the interaction force by the introduction of chlorine atoms, as was mentioned here and in the previous paper[2].

In this discussion, the author considered that the nature of the solvent itself has no influence upon the relaxation phenomena of swollen gels, as it may not be affected by the different content of chlorine atoms in the swollen gels.

Acknowledgement is made to Professor H. Akamatu and Assistant Professor T. Nakagawa for their support and advice in this experiment.

Department of Chemistry
Faculty of Science
The University of Tokyo
Hongo, Tokyo

The Chemical Reaction in Silent Electric Discharge. I

By Kihei MORINAGA and Momotaro SUZUKI

(Received June 16, 1960)

In a series of reports[1-3], it was proposed that in regard to the chemical processes in silent electric discharge, more significance should be put on the high frequency pulse current which accompanies the discharge, rather than on the basic current, usually 50 c/s, which sustains the whole discharge process.

In the present work some electrical, as well as geometrical conditions contributing significantly to the ozone formation process, were studied in more detail. This seems to have been helpful in realizing the actual feature of the reaction.

Experimental

The discharge tube used was of the Siemens type with two concentric glass cylinders which served as dielectric electrodes. The whole length and diameter of the discharge tube was 35 cm. and 4 cm. respectively. The outer surface of the outer cylinder was patched with tin foil and the inner tube was filled with brine. The area covered by the foil patches varied from 50 to 200 cm^2 for the purpose of having the desired electrode area. To change the gap distance, several ozonizers of the same type with different gap distance of 1~3 mm. were used. The electrical system was a usual circuit. The current of 50 c/s city source was sent through a voltage regulator to a leakage transformer where the voltage was stepped up to the required value. The discharge current was side circuited by a cathode ray oscillograph (Toshiba ST-1651) for the observation of basic 50 c/s, as well as the high frequency pulse current.

The whole system of the circuit is shown diagrammatically in Fig. 1. A series of shots of each oscillogram were taken using the single sweep system. The time constant of the oscillogram circuit was 5.4×10^{-6} sec.

1) M. Suzuki, *Proc. Japan Acad.*, **26**, 21 (1950).
2) M. Suzuki and Y. Naito, ibid., **28**, 429 (1951).
3) M. Suzuki, S. Okazaki and T. Yamamoto, *J. Am. Chem. Soc., Adv. Chem. Ser.*, **No. 26**, 331 (1957).

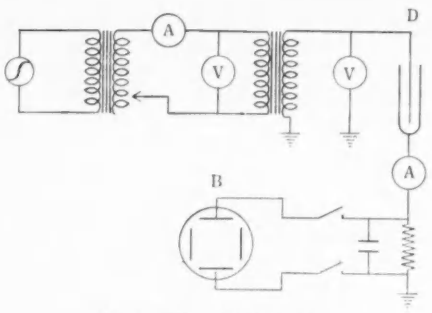

Fig. 1. The circuit system.
D, ozonizer; B, oscillograph

The sum of the height of each pulse current which appears as hairs on the base current diagram in an oscillogram, is due to the total electricity carried through the electric discharge during a cycle of base current which is simply noted here as pulse current[2]. The value of the sum in every run is an arithmetic mean of several successive shots of the oscillogram.

To obtain the yield of ozone in each run the leading glass tube distance from the discharge tube to the ozone absorption bulb was shortened as much as possible. The gas mixture submitted to the discharge was led through the neutral potassium iodide solution in the absorption bulb which was later analyzed by the usual known process. The oxygen, which served as a reactant, was taken from a cylinder and used after drying with calcium chloride.

Results

Variation in ozone concentration in the oxygen gas after leaving the discharge vessel

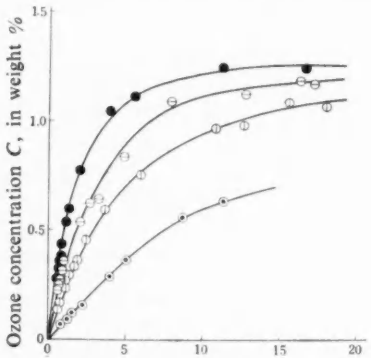

Fig. 2. The relation between the ozone concentration C and the residence time τ. Gap distance 2 mm. electrode area 100 cm².
● Pulse current 184~199 μamp.
⊖ 148~155 μamp.
◐ 87~92 μamp.
⊙ 28~30 μamp.

with apparent residence time τ, is shown in Fig. 2. The ozone concentration increases at first linearly as the time of residence increases, until finally it reaches a saturation value. At a saturation state the rates of the ozone formation and of the ozone destruction by any of the chemical entities existing there have equal values. This leads to the stationary ozone concentration in the exit gas.

The rate value of ozone formation Y (mg./sec.) at $\tau=0$ where presumably hardly any destruction reaction takes place is referred to further in the results. This consideration will simplify the discussion to some extent, because the reaction, in that case, will be restricted simply to the formation of ozone.

The numerical value of the pulse current is obtainable from the comparison of the sum of length of a certain pulse current with an adequate standard current. In Fig. 3, the value of Y (mg./sec. at $\tau=0$) is plotted against the pulse current in μamp. which was obtained through the above procedure. These curves manifest themselves again as a group of straight lines of which the inclination depends solely upon the physical conditions under which the experiments were carried out.

The dependence of ozone yield per unit pulse current Y_1 (mg./sec. μamp.) on A/d, where A (cm²) is the area of the electrode,

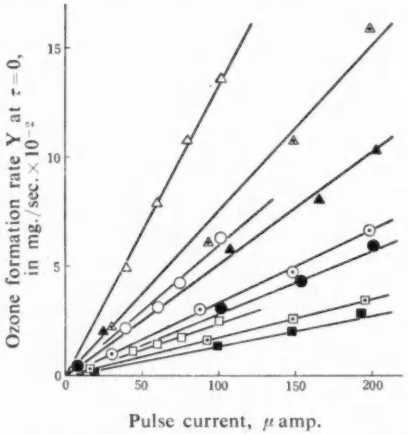

Fig. 3. The relation between the rate of ozone formation at $\tau=0$ in the various shape of ozonizers and the pulse current.
△ Area 200 cm². Gap 1 mm.
○ Area 100 cm². Gap 1 mm.
□ Area 50 cm². Gap 1 mm.
◬ Area 200 cm². Gap 2 mm.
⊙ Area 100 cm². Gap 2 mm.
◙ Area 50 cm². Gap 2 mm.
▲ Area 200 cm². Gap 3 mm.
● Area 100 cm². Gap 3 mm.
■ Area 50 cm². Gap 3 mm.

and d (mm.) is the gap distance between electrodes, is shown in Fig. 4. Y_1 values increase linearly with A/d, no matter how the individual value of A or d varies respectively, nor does it depend upon the total value of the current through the discharge vessel. The inclination of the straight lines has the value of 7.0×10^{-7} (mg./sec. μamp. cm.).

In Figs. 5, 6 and 7, ozone concentration (weight %) at steady state was plotted against pulse current. It will be seen from the figures that the ozone concentration is the highest at a certain optimum value of electrode area, and above or under this value the ozone concentration becomes lower.

Discussion

The behavior of the diagram which manifests itself in Fig. 4 seems to require some explanation from the chemical as well as the electrical viewpoint.

To begin with, under the experimental conditions during which the measurements were made, Paschen's law is applicable with virtual validity[4]. Then, as the pressure throughout the measurements is atmospheric and therefore constant, the sparking potential E_s, which initiates each individual small discharge at certain points on the electrode surface, depends solely on the gap distance d[2]. Further, E_s should increase proportionally with d within our experimental conditions[2].

With increasing E_s, the leaving of electrons from the electrode surface will be more difficult where on the oscillogram the hairs will shift to the upper part of the basic wave form and its placement will be more dense. Keeping ones sight on a certain definite number of electrons from the electrode, and taking into consideration the fact that the spots are distributed fairly uniformly and that the number of electrons issuing from each spot are virtually equal[2], the number of spots from which the individual small discharge starts will accordingly be less and the decrease of the number of spots in a unit area shows that the spots are located more sporadically. Or in our experimental conditions the greater the gap distance is, the greater the sparking potential, the less the number of spots in a unit area where the individual small discharge starts and finally the more the number of electrons which leave each spot, so long as one definite number of electrons which come into reactions are dealt with.

Now electrons leaving the electrode will collide with surrounding chemical molecules initiating some chemical change which leads to a chemical reaction.

Collisions which would cause some chemical reaction would seem to prevail as long the electrons travel along the spark gap distance. But actually the electrons, just after leaving the electrode, only then have sufficient energy to provoke a chemical effect such as dissociation. With the first collision, electron energy is virtually lost. Normally, the electron would regain energy in the electrical field; but, because of the very short mean free path, which is in the order of 10^{-6} cm. at atmospheric pressure[5], the electrons can not acquire sufficient energy to be able to react further chemically. Thus, further collisions between electron and molecule will hardly contribute to the initiation of the ozone formation. Accordingly, after the first collision, the distance traveled by the electron through gap distance may be disregarded in this discussion.

As far the change of Townsend's first coefficient α in relation to the gap distance; α/P is known to be the function of X/P where X is field strength. In this experiment the pressure is constant, α therefore, depends solely on X. As $X=E_s/d$ and E_s increases proportionally with d, the X value is independent of d. Thus the behavior of α along with change of d can likely be neglected in this present case.

In Fig. 4 Y_1 is shown to be proportional to the electrode area A and inversely proportional to the gap distance d. The increase of A, keeping the total electron number constant, leads to the increase of the total spot number in a whole discharge tube, because the increase

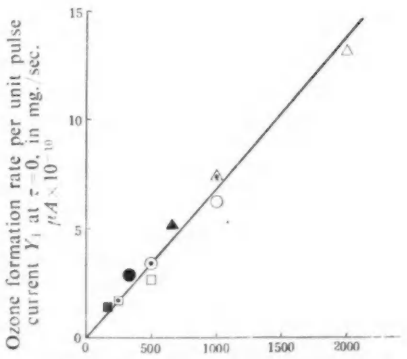

Fig. 4. The rate Y_1 of ozone formation per unit pulse current at various value of A/d.

4) K. S. Fitzsimons, *Phys. Rev.*, **58**, 197 (1940); W. R. Haseltine, ibid., 72, 423 (1947).
5) R. H. Healey and J. W. Reed, "The Behaviour of Slow Electrons", Amalgamated Wireless Press, Sydney (1941).

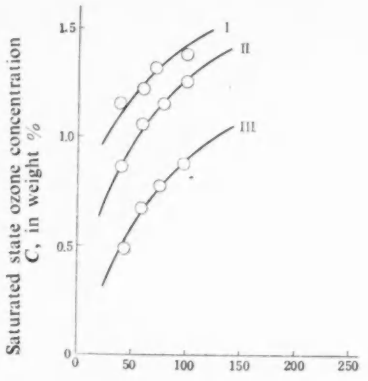

Fig. 5. Saturation ozone concentration against pulse current (Gap distance 1 mm.).
I Electrode area $A=100\,cm^2$; II $A=200\,cm^2$; III $A=50\,cm^2$

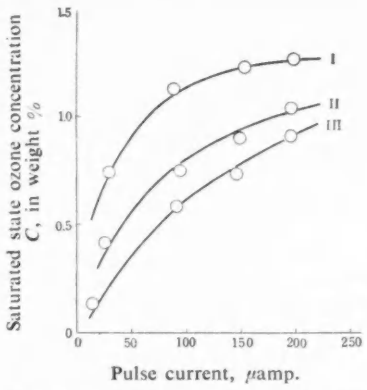

Fig. 6. Saturation ozone concentration against pulse current (Gap distance 2 mm.).
I Electrode area $A=100\,cm^2$; II $A=200\,cm^2$; III $A=50\,cm^2$

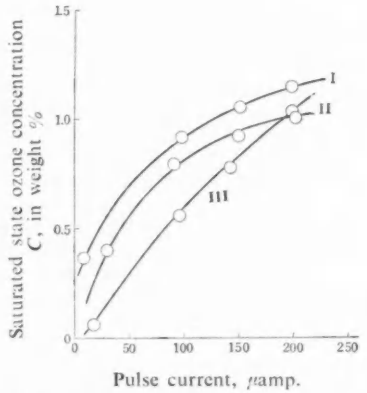

Fig. 7. Saturation ozone concentration against pulse current (Gap distance 3 mm.).
I Electrode area $A=100\,cm^2$; II $A=200\,cm^2$; III $A=50\,cm^2$

of the discharge area implies that the spots come to be distributed more sporadically and more chances are offered for the generation of more new spots. This corresponds to the effect of decreasing gap distance as just stated above. It might be conceivable if Y_1 be inversely proportional to d; then it should be proportional to A.

A tentative explanation of this phenomena is proposed as follows: In the experiment the average value of the pulse current is about 100 μamp., and the number of hairs on the half wave of 50 c/s base current from city source, in an oscillogram, is virtually 30~50. The number of spots involved in a hair, i.e. in one shot of pulse current, is about $10\sim10^2$ [2], thus the number of electrons ejected from a spot has the order of 10^{10}. On the other hand, the area of each spot is $10^{-2}\sim10^{-4}\,cm^2$ [2], and the number of molecules just in front of this area is about 10^{19} or a little less, which means that the above number of gas molecules has almost the same number or a little fewer than those of ejected electrons from a spot.

Now the velocity of electrons, just after they leave the electrode, is estimated at $10^8\sim10^9$ cm./sec.[6] which features, because of the virtually instantaneous time of travel up to the first collision, that the electron beam from each spot might seem to suffer hardly any appreciable conical diversion and hit the molecule target covering almost the same dimension as the spot area.

In this pattern of collision, the more sporadically the spots are located, the more packed is the ejected stream electrons, which lead to the increase of the ineffective collision. The rate of the ineffectiveness will essentially be regarded to be linear to the rate of congestion of the electron stream. Thus the effective collision number for a definite number of electrons of Y_1 is proportional to the number of spots, or in other words, to the electrode area and the reciprocal of the gap distance.

The postulate appears qualitatively to make sense, but from the quantitative point of view further and more detailed investigation may be required.

6) N. E. Bradbury and R. A. Nielson, *Phys. Rev.*, **49**, 338 (1936); **51**, 69 (1937).

Summary

1. The ozone yield Y from oxygen gas in the silent electric discharge in a Siemens ozonizer is proportional to the pulse current which was measured from an oscillogram where Y is referred to $\tau=0$ value. The proportionality is valid independent of the gap distance d between electrodes and the effective area A of electrodes.

2. The above ozone yield Y_1 which is referred to $\tau=0$ and further to unit pulse current is proportional to A/d.

3. The reason of the above relationship is briefly discussed.

Department of Chemistry
Defense Academy
Yokosuka

Dehydrogenation of Secondary Alcohols with Reduced Copper. III[1]. *Catalytic Dehydrogenation of Isopropyl Alcohol (Part 1)**

By Kazuaki KAWAMOTO**

(Received July 16, 1960)

Although there are a large number of patents and are latively small number of reports concerning the vapor phase dehydrogenation of isopropyl alcohol to acetone, the majority deal with the use of copper in some form as the catalysts. Sabatier[2] found that reduced copper heated at 200~300°C is a suitable catalyst for the dehydrogenation of alcohols to aldehydes or ketones with no side reaction, and he showed that isopropyl alcohol, in the presence of reduced copper, is dehydrogenated to acetone slowly at 150°C, and rapidly and smoothly in the whole range of temperatures between 250°C and 430°C without the formation of a large amount of propylene. This method was improved by Bouveault[3], Armstrong[4] and Palmer[5]. A remarkable addition to the knowledge of the contact action of reduced copper was made by Komatsu[6], who found that reduced copper has the property of promoting not only the dehydrogenation but also dehydration of alcohols and that isopropyl alcohol is transformed into acetone and propylene by exposure to high temperature (300°C). Platonow et al.[7] found that in the presence of copper dehydrogenation of isopropyl alcohol at 300°C furnishes 53.2% of the theoretical yield of acetone. Moreover, Katsuno[8] reported the synthesis of acetone from isopropyl alcohol, using copper-active-carbon or copper-kieselguhr as a catalyst. Dunbar and Arnold[9] also used a copper-chromium-oxide catalyst with considerable success in the dehydrogenation of isopropyl alcohol.

The reduced copper is little used at present for the industrial synthesis of ketones from alcohols. However, copper is considered as the most important component in the majority of widely used mixed catalysts. Therefore, the behavior of the reduced copper catalyst will be of special interest for the interpretation of the mechanism of catalysis with mixed copper catalysts.

Earlier, Frolich et al.[10] found that the copper catalyst prepared by precipitation with sodium hydroxide is more active in the decomposition of methanol than that precipitated with ammonia, and Fischer and Meyer[11] studied the influence of the precipitants on the

1) Previous paper, *J. Chem. Soc. Japan, Pure Chem. Sec.* (*Nippon Kagaku Zasshi*), **80**, 681 (1959).

* The major part of this research was presented at the 11th Annual Meeting of the Chemical Society of Japan, Tokyo, April 3, 1958.

** Present address, Institute of Commodities, Faculty of Economics, Kagawa University, Takamatsu Kagawa-ken.

2) P. Sabatier and J. B. Senderens, *Compt. rend.*, **136**, 738, 921, 983 (1903); P. Sabatier and J. B. Senderens, *Bull. soc. chim. France*, (3) **33**, 263 (1905); P. Sabatier, "Die Katalyse in der Organischen Chemie", Akademische Verlagsgesellschaft m. b. H., Leipzig (1927).

3) L. Bouveault, *Bull. soc. chim. France*, (4) **3**, 119 (1908).

4) E. F. Armstrong and T. P. Hilditch, *Proc. Roy. Soc.*, **A97**, 259 (1920).

5) W. G. Palmer, *Proc. Roy. Soc.*, **A98**, 13 (1920); W. G. Palmer, ibid., **A99**, 412 (1921); W. G. Palmer, ibid., **A101**, 175 (1922); W. G. Palmer and F. H. Constable, ibid., **A106**, 250 (1924).

6) S. Komatsu, *Mem. Coll. Sci. Kyoto Imp. Univ.*, **A7**, 85 (1924).

7) M. S. Platonow, S. B. Anissimow and W. M. Krascheninnikowa, *Ber.*, **69**, 1050 (1936).

8) M. Katsuno, *J. Soc. Chem. Ind. Japan*, (*Kogyo Kagaku Zasshi*), **45**, 1026 (1942); M. Katsuno, ibid., **46**, 109 (1943).

9) R. E. Dunbar and M. R. Arnold, *J. Org. Chem.*, **10**, 501 (1945).

10) P. K. Frolich, M. R. Fenske, L. R. Perry and N. L. Hurd, *J. Am. Chem. Soc.*, **51**, 187 (1929).

11) F. Fischer and K. Meyer, *Brennstoff Chem.*, **12**, 225 (1931).

nickel-thoria-kieselguhr catalyst, which is used as a catalyst for the Fischer-Tropsch synthesis. For this catalyst potassium carbonate was the best precipitant and the preparation using sodium hydroxide or potassium hydroxide was virtually inactive. Further, Niwa and Yamaguchi[12] reported that the activity of the copper catalyst prepared with sodium hydroxide is greater than that treated with ammonium carbonate.

As no comparative study of the action of reduced copper catalysts prepared with a number of precipitants upon secondary alcohols has been reported, the present work has been undertaken to discover how the reaction temperature and the precipitant influence the activity and the behavior of the catalysts, and furthermore to find the most suitable condition and the most suitable catalyst for the preparation of acetone from isopropyl alcohol. Experiments were carried out at several temperatures between 185°C and 325°C, and five different precipitants, i. e. sodium hydroxide, potassium hydroxide, potassium carbonate, sodium bicarbonate and potassium bicarbonate, were used.

Experimental

Purification of Isopropyl Alcohol and Acetone.—The isopropyl alcohol used in this research was purified, after being dried with anhydrous potassium carbonate, by fractionation through a Widmer column: b. p. 82~82.5°C, n_D^{25} 1.3753, d_4^{25} 0.7811. Acetone was also purified in an analogous manner: b. p. 56.2~56.3°C, n_D^{25} 1.3564, d_4^{25} 0.7844.

Preparation of Catalysts.—Komatsu and Kurata[13] previously found that the reduced copper catalysts derived from copper sulfate and copper nitrate act to promote both dehydrogenation and dehydration of *l*-menthol. The degree of dehydration, however, was smaller with the catalyst prepared from copper nitrate than with that from copper sulfate under the same conditions. Consequently, the present author used copper nitrate as the starting material to prepare the dehydrogenation catalyst. Copper nitrate was prepared from electrolytic copper and nitric acid, and was purified by recrystallization. The catalysts are classified into Cu I, II, III, IV and V, as shown in Table I. These catalysts were prepared similarly except for the species and amount of the precipitant. For example, Cu I was prepared as follows: A solution of 30 g. of cupric nitrate hexahydrate in 900 ml. of distilled water was kept at 90°C. A sodium hydroxide solution, prepared from 300 ml. of distilled water and 15 g. of sodium hydroxide, was brought to the same temperature and added rapidly to the stirred copper nitrate solution. After the mixture was stirred at this temperature for 30 min., the precipitate was washed by decantation with a copious amount of warm water (at 70°C), collected on a glass filter, dried in an electric oven at 105°C for 10 hr., powdered in an agate mortar and finally stored in a stoppered bottle. It has been reported[14] that the occluded or absorbed impurities (mainly anions) in the preparation of reduced copper influence the activity. Accordingly, to minimize the inclusion of such impurities dilute solutions were used for precipitation and the resulting precipitates were then washed well with distilled water by decantation. The chemicals used were of the purest reagent grade and all vessels were washed with nitric acid and rinsed with distilled water.

TABLE I. PREPARATION OF CATALYSTS

Catalyst	Precipitant	Amount of precipitant g.	Distilled water ml.	Color of catalyst
Cu I	NaOH	15	300	black
Cu II	KOH	24	500	black
Cu III	K_2CO_3	25	500	dark brown
Cu IV	$NaHCO_3$	30	300	yellowish green
Cu V	$KHCO_3$	40	400	yellowish green

Apparatus.—The apparatus, illustrated diagrammatically in Fig. 1, is designed to measure the ratio of dehydrogenation and dehydration by the catalysts. Hydrogen coming from the reservoir (A) was passed through a tube (C) containing heated copper gauze to remove the oxygen present in the hydrogen by converting it into water, and then through a bottle (D) containing a 30% sodium hydroxide solution

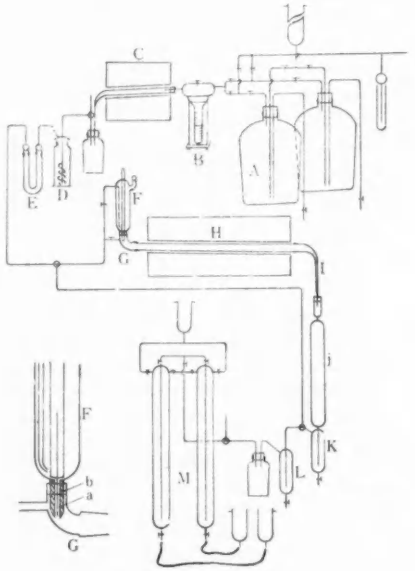

Fig. 1. Apparatus.

12) M. Niwa and M. Yamaguchi, *J. Chem. Soc. Japan, Pure Chem. Sec.* (*Nippon Kagaku Zasshi*), **73**, 159, 162 (1952).
13) S. Komatsu and M. Kurata, *Mem. Coll. Sci. Kyoto Imp. Univ.*, **A8**, 147 (1925).
14) H. Hasegawa, *J. Chem. Soc. Japan, Ind. Chem. Sec.* (*Kogyo Kagaku Zasshi*), **58**, 334 (1955).

and a solid sodium hydroxide tube (E). The hydrogen flow was measured by passing it through a calibrated flowmeter (B). The reaction tube (H) was a hard glass tube of 1 m. length and 18 mm. inside diameter, and was set in a combustion furnace and in this tube 10 g. of the catalyst to be used was spread in a length of approximately 70 cm. This tube was inclined at an angle of about 5° to insure proper drainage of the liquid product and the temperature was measured by a thermometer at a position of 30 cm. from the exit end of the catalyst bed. A rate of flow of the sample can be kept approximately constant by varying the extent of the insertion of the tungsten wire (a) into the capillary (b) (Fig. 1), and connecting the funnel (F) with a receiver (K) to keep the pressure equal. The sample is vaporized through a vaporizer (G) before reaching the catalyst. This vaporizer was made of a hard glass tube filled with glass wool and heated to a desired temperature by a heater. The reaction tube was connected with a condenser (J) by means of an adapter (I). The liquid product condensed was collected in a receiver (K) and uncondensed vapor was absorbed in water in a bottle (L). Noncondensable gas was collected in a gas-holder (M).

Procedure.—The catalyst was placed in the reaction tube and the apparatus was tested for gas-tightness. After the tube was filled with hydrogen, the furnace was heated to the reduction temperature, and was kept at this temperature for the period of reduction. Care was taken during the reduction to avoid the overheating of the catalyst as the reaction is exothermic, and the reduction temperature was always below 185°C. The standard flow rate of hydrogen (measured at room temperature) was 750~900 ml. per hour. The reduction was continued until the color of the catalyst changed from black or yellowish green to reddish purple and then the hydrogen supply was stopped and the resulting catalyst was heated to the operating temperature. Experiments were performed at 185, 250, 305 and 325°C under the ordinary pressure, and in the case of the copper catalyst precipitated with sodium hydroxide, further experiments were carried out at 220°C and 280°C, and during the run which lasted for several hours, the temperature was maintained within about ±5°C of the desired temperature. A definite weight of the alcohol or acetone was supplied from the dropping funnel (F) at the predetermined rate. The vapor coming out from the reaction tube was condensed by passing through a condenser cooled with ice water and the escaped gas from the condenser was passed into ice-cooled distilled water (50 ml.) to catch condensable products completely. The noncondensable gas which came out of the receiver (L) was collected in a gas-holder and its volume was measured from time to time. At the end of the run, the weight of liquid products collected in the receiver, that absorbed by water in the bottle, and the volume of noncondensable gas in the gas-holder were measured. The condensed product and the water solution in the bottle were combined. If an oily product

Table II. Influence of precipitants and temperatures on dehydrogenation of isopropyl alcohol

Exp. no.	Precipitant	Temp. °C	Isopropyl alcohol g.	Velocity g./hr.	Acetone g.	Oily product g.	Gas collected l.	Percentage of conversion* %
1	NaOH	185	39.69	10.82	21.78	0	8.57	57.9
2	KOH	185	38.81	12.25	19.71	0	7.95	54.9
3	K_2CO_3	185	39.04	11.71	18.39	0	7.38	50.7
4	$NaHCO_3$	185	38.83	11.95	19.95	0	8.06	55.7
5	$KHCO_3$	185	39.02	12.01	20.55	0	8.26	56.7
6	NaOH	220	39.49	10.53	20.06	9.26	9.64	65.5
7	NaOH	250	39.59	10.55	18.60	11.53	9.07	61.4
8	KOH	250	38.66	12.21	19.69	9.97	9.91	68.7
9	K_2CO_3	250	39.24	12.07	24.46	5.25	10.87	74.3
10	$NaHCO_3$	250	38.87	11.66	30.92	0	12.35	85.2
11	$KHCO_3$	250	38.78	11.08	30.96	0	12.36	85.5
12	NaOH	280	39.63	10.56	26.98	4.24	11.39	77.0
13	NaOH	305	39.18	11.47	33.55	0	13.63	93.3
14	KOH	305	38.86	11.96	33.51	0	13.63	94.1
15	K_2CO_3	305	39.36	11.52	34.33	0	13.51	92.0
16	$NaHCO_3$	305	38.93	12.29	34.77	0	13.75	94.7
17	$KHCO_3$	305	38.82	11.65	35.11	0	13.89	95.9
18	NaOH	325	38.96	11.40	34.41	0	13.91	95.7
19	KOH	325	38.87	11.96	34.43	0	14.03	96.7
20	K_2CO_3	325	39.32	11.80	35.15	0	13.87	94.6
21	$NaHCO_3$	325	38.91	11.12	35.44	0	14.01	96.6
22	$KHCO_3$	325	38.91	11.39	35.62	0	14.07	97.0

* Calculated from the volume of the gaseous product collected in each experiment on the assumption that original isopropyl alcohol is transformed completely into gases such as hydrogen or propylene.

was formed, this was separated from the water layer and washed with a known volume (20 ml.) of distilled water. If the oily product was not formed, the aqueous solution was analyzed by the method described below.

Analysis of the Products.—The aqueous solution was recognized to consist of acetone and unchanged isopropyl alcohol by the preparation of the 2,4-dinitrophenylhydrazone and the phenylurethan, respectively, and the content of the acetone was determined by the hydroxylamine method[15]. The reliability of this analytical method was checked by titrating a known sample of acetone and the result was found to be correct within experimental errors. The oily product, which was obtained in some of the experiments, was dried with anhydrous sodium sulfate and then fractionally distilled through a Widmer column. Isobutyl methyl ketone was present in a fraction that showed the properties: b. p. 110~125 C, n_D^{25} 1.3963, d_4^{25} 0.7908, and a semicarbazone, m. p. 133~133.5°C and a 2,4-dinitrophenylhydrazone, m. p. 93.5~94°C were obtained and showed no depression of the melting points when mixed with the known derivatives of isobutyl methyl ketone. Diisobutyl ketone was found mainly in a fraction as follows: b. p. 160~170°C, n_D^{25} 1.4115, d_4^{25} 0.8012, and it was identified on the basis of the preparation of the 2,4-dinitrophenylhydrazone, m. p. 92~92.5°C and the semicarbazone, m. p. 122~122.5°C which were shown to be the corresponding derivatives of diisobutyl ketone by the mixed melting point determination. The formation of unsaturated and hydroxy ketones such as mesityl oxide, phorone and diacetone alcohol, was not detected in the oily product.

Results and Discussion

The influence of the precipitants and reaction temperatures on the activity and the selectivity of the copper catalysts is summarized in Table II. Experiments were controlled so as to regulate the reducing condition of the precipitate* with hydrogen as far as possible and further to maintain the constancy of the velocity of the isopropyl alcohol passing over the catalyst. To find the difference in the reaction products on varying the reaction temperature and the optimum temperature for dehydrogenation, the catalytic reaction was performed at 185, 250, 305 and 325°C. Since isopropyl alcohol was not changed in the absence of the catalysts over the range (185~325°C) of temperatures, the changes shown in Table II do not involve the simple pyrolysis of isopropyl alcohol. The yield of acetone shown in Table II does not necessarily represent the maximum yield but is an average of three or four experiments under the constant operating condition. However the fluctuation in the yields of acetone and of the oily product obtained by the repeated experiments was less than 1 per cent, and thus within the limit of experimental error in the determination of acetone.

Influence of the Reaction Temperatures on the Dehydrogenating Activity of Reduced Copper.—The dehydrogenating activity of the various copper catalysts depends upon the temperature at which the reaction is carried out. Using a copper catalyst, the equilibrium constant for the reaction of isopropyl alcohol to form acetone and hydrogen has been measured[16]. Though the results obtained by various workers show little agreement, it is accepted that the equilibrium transfers to the direction of dehydrogenation at the reaction temperature above 220°C. Consequently, at low temperatures the copper catalyst has a poor activity for dehydrogenation. In the present research all catalysts act to promote dehydrogenation of isopropyl alcohol at high temperatures, and at the highest reaction temperature (325°C) the dehydrogenation of isopropyl alcohol to acetone is the highest.

Influence of the Precipitants on the Dehydrogenating Activity of Reduced Copper.—As shown in Table II, the dehydrogenating activity of the copper catalysts varies considerably with the sort of precipitants, and the catalyst prepared by the treatment with potassium bicarbonate showed the largest activity. On the contrary, the catalyst prepared with sodium hydroxide showed the smallest activity. The dehydrogenating activity of the copper catalysts prepared with various precipitants is in the following order: $KHCO_3 > NaHCO_3 > K_2CO_3 > KOH > NaOH$.

The author presumed that the catalysts prepared with alkali bicarbonates possess a capillary or a porous structure on account of the evolution of carbon dioxide at precipitation or the hydrogen treatment, and this is one of the reasons for the large dehydrogenating activity of the catalysts.

The Relation between the Amount of Gas Evolved and that of Acetone Produced.—When the oily product was not formed, the difference between the theoretical yield of acetone and the percentage of conversion was a few per cent. Therefore, the dehydration of isopropyl alcohol to propylene seems to occur little at temperatures below 325°C. Accordingly, the dehydration is not an important factor from the viewpoint of dehydrogenation. When the

15) M. Katsuno, *J. Soc. Chem. Ind. Japan, (Kogyo Kagaku Zasshi)*, **46**, 112 (1943).

* Copper compound prepared from copper nitrate by "precipitant".

16) G. S. Parks and H. M. Huffman, "Free Energies of Some Organic Compounds", Reinhold Pub. Corp., New York (1932), p. 22; H. J. Kolb and R. L. Burwell, Jr., *J. Am. Chem. Soc.*, **67**, 1084 (1945); A. H. Cubberley and M. B. Mueller, ibid., **68**, 1149 (1946).

oily product was not formed, a proportional relation was found between the amount of the gas evolved and that of acetone produced, namely the greater the amount of the evolved gas, the greater the amount of acetone. This is reasonably accounted for by considering that both the gas and acetone result from the dehydrogenation of isopropyl alcohol. Also the amount of the gas collected increased proportionally with the temperature rise.

The Relation between the Amount of Gas Evolved and the Reaction Time.—A test was made by the following method to see whether the catalytic activity is kept constant during the whole reaction time or not. The amount of gas evolved (Table II) was measured at intervals of 15~20 min. and the volumes of the evolved gas reduced to the normal state were plotted against the reaction time in Fig. 2. Since the evolution of the gas is constant during the reaction time as seen in Fig. 2, it is concluded that the sustained activity of the catalyst holds over the period of the operation. Thus the constancy of the activity of the catalyst can be detected by inspecting the amount of the gas evolved.

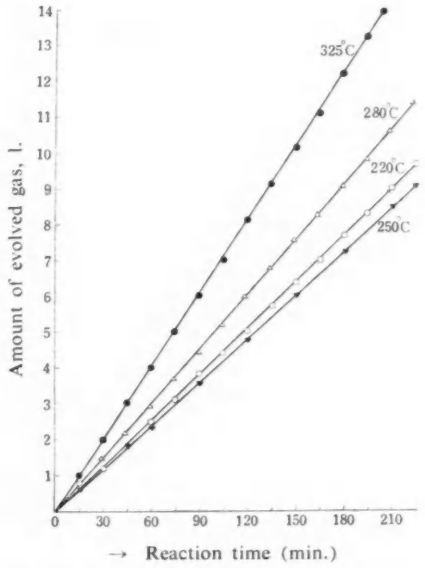

Fig. 2. The amount of evolved gas as a function of the reaction time for various temperatures (precipitant: NaOH)

Two Types of Reduced Copper Catalysts.—It was found that there are two distinct types of reduced copper catalysts. One of them catalyzes the decomposition of isopropyl alcohol to acetone and hydrogen; that is, promotes dehydrogenation. Cu IV and Cu V belong to this type. The other type catalyzes the conversion of isopropyl alcohol into isobutyl methyl ketone and diisobutyl ketone together with acetone and hydrogen, that is, promotes both dehydrogenation and condensation. Cu I, Cu II and Cu III belong to this type. Further, there is a distinct difference in color before reduction between these two types of catalysts. As shown in Table I, the precipitates prepared with sodium hydroxide, potassium hydroxide, and potassium carbonate are black or dark brown in color. On the contrary, those prepared with potassium bicarbonate and sodium bicarbonate have a yellowish green color. Cu I and Cu II were nearly equal in the activity for the production of both the oily product and acetone, and Cu III has a relatively poor activity for the formation of the oily product. Also Cu IV and Cu V were entirely inactive to the production of the oily product. There is thus a marked difference of activity between the copper catalysts prepared with alkali hydroxides and those prepared with alkali bicarbonates with respect to the relative amount of acetone formed. Cu I and Cu II are especially convenient for preparing isobutyl methyl ketone and diisobutyl ketone. The new synthetic process of these ketones, which consists in passing isopropyl alcohol over Cu I or Cu II under the atmospheric pressure at 220~250°C, is now proposed as one which has not yet been observed with a copper catalyst alone.

Mechanism of the Condensation Reaction.—Lassieur[17] found that a mixture of acetone and hydrogen, when it is passed over reduced nickel at 200~300°C, yields mesityl oxide, isobutyl methyl ketone, phorone and diisobutyl ketone. Concerning the mechanism of this reaction he showed that acetone undergoes condensation to give mesityl oxide and phorone, and these unsaturated ketones are then reduced by hydrogen.

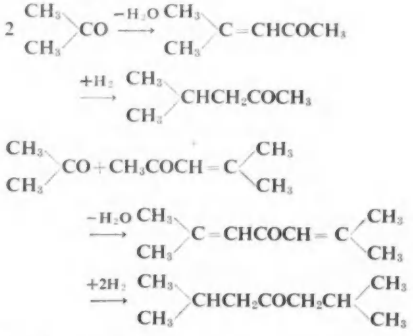

17) M. A. Lassieur, *Compt. rend.*, **156**, 795 (1913).

On the other hand, Ipatieff and Haensel[18] found that in the presence of a copper-alumina or a copper-zinc-oxide-alumina catalyst, a mixture of isopropyl alcohol and acetone is converted into isobutyl methyl ketone and diisobutyl ketone, and that in the absence of isopropyl alcohol, acetone reacts to give only small amounts of mesityl oxide and phorone, and they reported that isobutyl methyl ketone is obtained by a regular ketonic condensation of acetone to diacetone alcohol and then a hydrogen disproportionation between isopropyl alcohol and diacetone alcohol.

$$2\,CH_3COCH_3 \rightleftarrows (CH_3)_2COHCH_2COCH_3$$

$$(CH_3)_2COHCH_2COCH_3 + CH_3CHOHCH_3 \rightarrow (CH_3)_2CHCH_2COCH_3 + CH_3COCH_3 + H_2O$$

In the present research, isobutyl methyl ketone and diisobutyl ketone were obtained from isopropyl alcohol with the copper catalyst prepared with sodium hydroxide or potassium hydroxide, but the formation of mesityl oxide, diacetone alcohol and phorone was not observed. Further, it was confirmed that, when the catalytic reaction is carried out with acetone alone under a condition similar to that in the experiment with isopropyl alcohol, acetone is not changed. It is generally recognized that hydrogen atoms of a methyl group adjacent to a carbonyl group are reactive. From these considerations, the formation of the reaction products obtained by the present author can be illustrated by the following schemes:

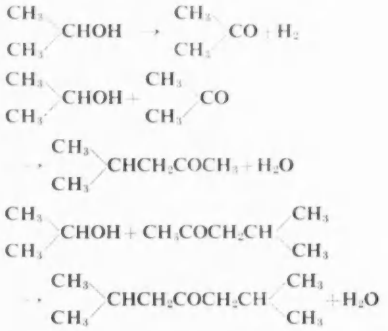

Further, the following results have been obtained by the present author: (1) Alicyclic alcohols (cyclohexanol and *l*-menthol) do not undergo alcohol-ketone condensation under a condition similar to that employed for isopropyl alcohol[1], consequently giving no higher ketones. (2) When *sec*-butyl alcohol is passed over reduced copper, 5-methyl-3-heptanone together with ethyl methyl ketone is formed.* From these results it seems that the condensation reaction takes place when three hydrogen atoms are attached to the alpha carbon atom of a carbonyl group, but is not favored when only two hydrogen atoms are attached. The alcohols which on dehydrogenation can yield ketones containing a methyl group adjacent to the carbonyl group can condense with the ketones produced.

Up to the present, isobutyl methyl ketone has been prepared by the following method: Acetone is first condensed in the presence of bases to give diacetone alcohol, and this diacetone alcohol is dehydrated by heating with an acid such as sulfuric acid to give mesityl oxide, and then the mesityl oxide thus formed is hydrogenated in the presence of a copper catalyst to give isobutyl methyl ketone. It is of interest that isobutyl methyl ketone can be prepared in one step by passing isopropyl alcohol over reduced copper as described above.

Summary

In order to determine whether the dehydrogenating activity of reduced copper is affected by the species of precipitants in the preparation, the dehydrogenation of isopropyl alcohol to acetone was studied by using five different precipitants, i. e. sodium hydroxide, potassium hydroxide, potassium carbonate, sodium bicarbonate and potassium bicarbonate. The dehydrogenation was the highest with no side reaction at 305~325°C, especially when potassium bicarbonate was used as precipitant.

When the copper catalysts, prepared with sodium hydroxide, potassium hydroxide and potassium carbonate, were used, condensation together with dehydrogenation occurred. The formation of higher ketones is explained by the assumption of intermolecular dehydration between acetone and original isopropyl alcohol.

The author wishes to express his hearty thanks to Professor T. Matsuura for his kind guidance and valuable suggestions throughout this work.

Department of Chemistry
Faculty of Science
Hiroshima University
Hiroshima

18) V. N. Ipatieff and V. Haensel, *J. Org. Chem.*, 7, 189 (1942).

* Presented at the 13th Annual Meeting of the Chemical Society of Japan, April, 1960.

Studies on Tritium Labeled Compounds. II.[1] *Preparation of Tritium Labeled Stearic Acid*

By Yoshishige SATO, Teruhiko MESHI and Tadao TAKAHASHI

(Received May 19, 1960)

In an attempt to prepare ^{3}H-labeled stearic acid as a biochemical tracer, we have carried out three different methods; chemical method, electric discharge method and recoil tritium labeling method. Wolfgang, Pratt and Rowland[2] investigated the labeling of organic compounds by a electric discharge in tritium in 0.05 mmHg region on the assumption that accelerated tritium ions will be active transients required for labeling. Dorfman and Wilzbach[3] have recently conducted investigations on the labeling method by means of electric discharge in a 10 mmHg region. We have also studied the labeling method by electric discharge in tritium-hydrogen in 100 mmHg region[1].

Wolfgang and Rowland[4] have developed a ^{3}H-labeling method of organic compounds. According to their reports, the compound to be labeled is mixed with lithium salt and the mixture is irradiated by slow neutrons in a reactor. A considerable fraction of the energetic tritium produced in the ^{6}Li(n, α)T reaction will replace bound hydrogen in the molecules of stopping medium to form a radioactive form of the original hydrogenous molecule.

We have made investigations on the recoil tritium labeling method using a mixture of stearic acid and lithium carbonate in a reactor of the Japan Atomic Research Laboratory (JRR-1).

Experimental and Results

Chemical Method.—*Reduction of Ethyl Linoleate*[5]. —154 mg. of ethyl linoleate, 5 mg. of platinum oxide catalyst and 2 ml. of ethyl acetate are mixed together in a reaction vessel connected with a vacuum apparatus. Then in the apparatus, H^3-labeled ethyl stearate was prepared by catalytic hydrogenation of ethyl linoleate with ^{3}H–H gas liberated by electrolysis of ^{3}HHO. After about 20 min., 23 ml. (theoretical: 22.4 ml.) of ^{3}H–H was absorbed and the uptake of ^{3}H–H has ceased. The catalyst was removed by filtration and after the solvent was evaporated, ^{3}H-labeled ethyl stearate was hydrolyzed by heating under reflux for three hours with potassium hydroxide-methanol solution. The solution was acidified with 10 N-hydrochloric acid, cooled and filtered. Then, deposited ^{3}H-stearic acid was extracted with ether. The yield of ^{3}H-stearic acid was 90% on the basis of ethyl linoleate, with a specific activity of 0.9 μc/mg.

Exchange Method in the Presence of Catalyst.—In an attempt to prepare ^{3}H-stearic acid, exchange method for deuterium labeling of fatty acid developed by Heyninger, Rittenberg and Schoenheimer[6] was employed. In a glass tube, 20 mg. of PtO_2 suspended in 1 ml. of ethyl alcohol was reduced in a hydrogen stream. After alcohol was distilled, 200 mg. of stearic acid, 5 mg. of potassium hydroxide and 0.4 ml. of ^{3}HHO (50 mc./ml.) were added. The mixture was frozen, the tube was sealed and then heated at 135°C for a week. After the period of reaction, the tube was opened and connected with a vacuum apparatus, and the liquid was distilled in vacuo. The dried residue was dissolved in potassium hydroxide-ethyl alcohol solution and filtered, and the filtrate was acidified with hydrochloric acid. The deposited ^{3}H-stearic acid was recrystallized from ether. The yield of ^{3}H-stearic acid was 90% on the basis of stearic acid, with a specific activity of 6.2 μc/mg.

Electric Discharge Method.—Discharge was carried out in a sample cell of approximately 20 ml., with tungsten electrodes (15 mm. apart). A sample to be labeled was placed on the bottom of the glass cell. Discharge was normally run from 20 sec. to 180 sec. in ^{3}H–H mixture gas under a constant pressure of 100 mm Hg. The following is the procedure: A quantity of approximately 20 mg. was placed on the bottom of a glass cell and the cell was degassed. After the degassing was completed, ^{3}H–H gas liberated by electrolysis of tritiated water (30 mc./ml.) was introduced into the cell and the discharge was made to run. In running of the discharge, the electrodes were over-heated. The electrodes were cooled by stopping the discharge. The cell was again degassed and air was introduced into the cell.

The stearic acid was then assayed for tritium in a gas-flow counter. The following table summarize the results.

Table I shows activity levels obtained for stearic acid subjected to the discharge technique. The

1) Y. Sato, T. Meshi, T. Takahashi and N. Sugimoto, *Japanese J. Pharm. and Chem.* (*Yakugaku Kenkyu*), **32**, (5) 317 (1960).

2) R. Wolfgang, T. Pratt and F. S. Rowland, *J. Am. Chem. Soc.*, **78**, 5132 (1956).

3) L. M. Dorfman and K. E. Wilzbach, *J. Phys. Chem.*, **63**, 799 (1959).

4) F. S. Rowland, C. N. Turton and R. Wolfgang, *J. Am. Chem. Soc.*, **78**, 2354 (1956).

5) R. F. Glascock and L. R. Reinius, *Biochem. J.*, **62**, 529 (1956).

6) W. E. Van Heyningen, D. Rittenberg and R. Schoenheimer, *J. Biol. Chem.*, **125**, 495 (1938).

Chart I

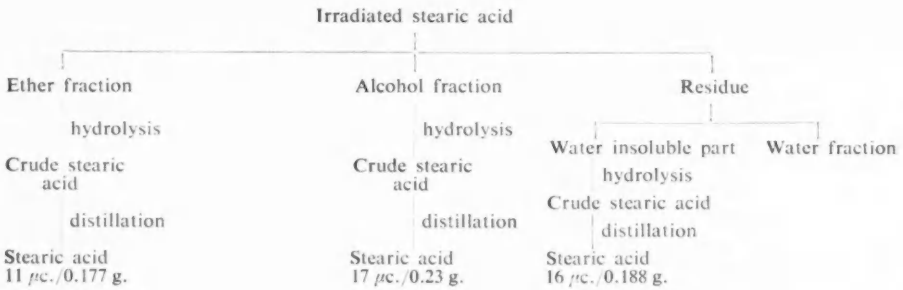

TABLE I. LABELING BY ELECTRIC DISCHARGE IN ^{3}H–H GAS

^{3}H–H Pressure, mm Hg	Discharge Time, sec.	Activity, μc./g.
100	20	1.9
100	40	5.7
100	60	8.6
100	120	23.6
100	180	91.6

tritium content of the product increases approximately with the discharge time.

Recoil Tritium Labeling Method. — A mixture of 2 g. stearic acid and 1 g. lithium carbonate was irradiated with thermal neutrons for 17 hr. at a flux 2.5×10^{11} n/cm^2 sec. The irradiated product was first extracted with anhydrous ether, and then with anhydrous ethyl alcohol. Infrared spectra of the ether fraction, alcohol fraction and the residue are shown in Fig. 1. It was recognized, that ester of fatty acid was produced by irradiation. Hydrolysis of each fraction was carried out by alcoholic potassium hydroxide. The hydrolyzed compounds were identified as stearic acid by infrared spectra, and they all distilled in vacuo (10 mm Hg) at 206~208°C.

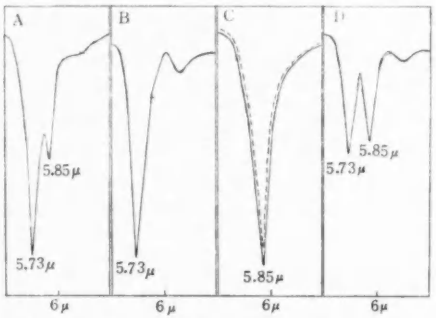

Fig. 1. Infrared absorption spectra of recoil tritiated stearic acid.
A: Residue, B: Alcohol fraction, C: —— Authentic stearic acid, ---- Hydrolyzed specimens of A, B and D, D: Ether fraction.

The stearic acid was assayed for tritium by means of a gas-flow counter. Chart I represents the experimental treatments described above.

The total yield of radio active stearic acid was about 0.6 g. (about 30%). Activity (A) of recoil tritium atoms produced by irradiation was calculated on the basis of the following equation.

$$A = \sigma N f (1 - e^{-0.693/t})$$

σ: Cross section 945 barn, N: Number of Li atom, f: Neutron flux, T: Half-life, t: Irradiation time.

When a mixture of stearic acid and lithium carbonate was irradiated by a 2.5×10^{11} neutron flux, value of A was 832 μc. The tritium content of the obtained stearic acid was therefore about 5% of the theoretical value.

Radioactivity Measurement of Tritium Labeled Stearic Acid. — Tritium activity was counted according to the Jackson and Lampe's method.[7] A windowless gas flow counter was used for radioassay of ^{3}H-stearic acid. The self-absorption characteristics of tritium labeled stearic acid samples are given in Fig. 2.

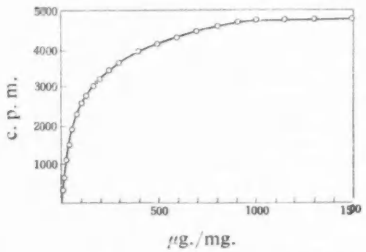

Fig. 2. Self-absorption curve of ^{3}H-stearic acid.

These curves indicate that self-absorption is negligible up to sample weights of about 20 μg. per sq. cm.

7) F. L. Jackson and H. W. Lampe, *Anal. Chem.*, **28**, 1735 (1956).

Discussion

By using tritium gas with higher specific activity than in above chemical process, it is easy to get a much higher specific activity. A higher specific activity can also be obtained using the discharge method when the discharge time is made prolonged and the tritium gas is of a higher specific activity. Tritium labeling in a reactor, on the other hand, is less usable, since this method gives rise to high destruction and lower specific activity. From the infrared absorption spectra of each fraction of irradiated products, it was recognized that the irradiated products contain fatty acid ester, because a 5.73 μ band of these products was identical with the carboxyl band of ethyl stearate.

Summary

Chemical reduction method, exchange method, electric discharge method and recoil tritium labeling method were applied for preparing tritium labeled stearic acid. As the result of the recoil tritium labeling, the irradiated stearic acid was found to contain high destruction products which are mainly composed of esters of fatty acid.

Osaka Research Laboratory
Tanabe Seiyaku Co., Ltd.
Kashima-cho, Higashiyodogawa-ku
Osaka

Studies on Tritium Labeled Compounds. IV. Preparation of Tritium Labeled Alanine by Means of Electric Discharge*

By Yoshishige SATO and Tadao TAKAHASHI

(Received July 4, 1960)

On the assumption that accelerated-tritium ions are the active transients required for labeling, Wolfgang, Pratt and Rowland[1] studied methods for preparing tritium labeled organic compounds using the electric discharge method. On the other hand, Dorfman and Wilzbach[2] investigated the labeling method under electric discharge in a 10 mmHg pressure region and reported that the labeling would be expected to occur as a result of the primary process of ionization, excitation and dissociation of tritium molecules in the gas phase. We recently reported[3] that the labeling would be produced in the same mechanism as that reported by Dorfman and Wilzbach. In this work, we carried out tritium labeling under electric discharge by employing α-hydroximinopropionic acid as the sample and obtained DL-alanine of a high specific activity.

Experimental and Results

About 50 mg. of α-hydroximinopropionic acid was placed in the bottom of a glass cell which has two electrodes of tungsten as shown in Fig. 1. The cell was attached to a vacuum line and degassed. ^{3}H-H gas, which was liberated by electrolysis of tritiated water (130 mc./ml.), was introduced into the cell and electric discharge (8000 V.) was struck at 40 mmHg for 10 min.

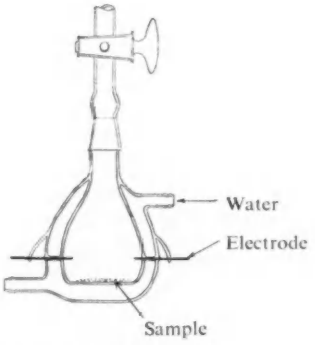

Fig. 1. Discharge cell.

During the discharge, the electrodes were overheated. In order to avoid over-heating, the electrodes were cooled by passing of cold water around the outside of the cell and by stopping further discharge. After the discharge the cell was degassed and air was introduced into the cell. As it was presumed that tritium labeled alanine was produced by this method, the discharged sample was extracted with ether. Almost all α-hydroximinopropionic

* Part III: Y. Sato, T. Meshi and T. Takahashi, This Bulletin, 33, 1146 (1960).

1) R. Wolfgang, T. Pratt and F. S. Rowland, *J. Am. Chem. Soc.*, 78, 5132 (1956).

2) L. M. Dorfman and K. E. Wilzbach, *J. Phys. Chem.*, 63, 799 (1959).

acid being soluble in ether, was removed from the discharged sample by filtration. The amount of residue was about 5 mg. and was assayed for tritium in a gas flow counter. Its specific activity was 0.66 μc./mg.; on the other hand, the specific activity of ether soluble part was 0.71 μc./mg.

Paper chromatography of the residue, using *n*-butanol-acetic acid-water (4 : 1 : 1) as developing solvent, was performed. Owing to the low energy of the β-rays from tritium, the radioactivity from tritium could not be measured directly on the paper chromatogram. The paper was cut into pieces, and the active products were extracted with water. Water was evaporated in stainless steel dishes, and the activity of the extracted products was measured in a gas flow counter. Fig. 2 shows the results of the paper chromatogram and the radioactivity. As a comparison, parallel runs were made with ordinary DL-alanine and α-hydroximinopropionic acid.

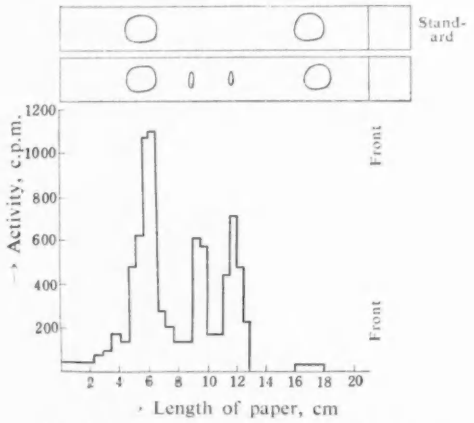

Fig. 2. Paper chromatography and the radioactivity of ether insoluble part. For comparison spots obtained with pure DL-alanine and α-Hydroximinopropionic acid are shown.

Four hundred μg. of ether insoluble part of sample was employed as a sample of paper chromatography. DL-Alanine, the unidentified product A and B and, α-hydroximinopropionic acid were obtained in the amounts and with activity values as shown in Table I.

TABLE I. SPECIFIC ACTIVITY OF THE PRODUCTS SEPARATED BY PAPER CHROMATOGRAPHY

Compound	Activity c. p. m.	Amount μg.	Sp. act. μc./mg.	R_f
DL-Alanine	15600	20*	4.4	0.28
Unidentified product A	4600	2*	12.9	0.36
B	6450	2*	17.2	0.45
α-Hydroximino-propionic acid	100	350**	0.0016	0.80

* Determination by spraying with ninhydrin.
** Determination by spraying with Bromophenyl Blue.

Discussion

In the previous reports[3], it was reported that specific activity of tritium labeled DL-alanine obtained by means of electric discharge was only about 0.02 μc./mg. when DL-alanine was used as the sample. However, in this paper, tritium labeled DL-alanine with specific activity of 4.4 μc./mg. was obtained by using α-hydroximinopropionic acid as the sample. A higher specific activity can be expected by using carrier free tritium gas.

Summary

To obtain tritium labeled alanine of a high specific activity by means of electric discharge, α-hydroximinopropionic acid was employed in place of alanine. After electric discharge, tritium labeled α-hydroximinopropionic acid was removed by ether extraction and the residue was chromatographed. Tritium labeled alanine was obtained with a specific activity of 4.4 μc./mg. which was two hundred times as great as that obtained by the use of alanine.

Osaka Research Laboratory
Tanabe Seiyaku Co., Ltd.
Kashimacho, Higashiyodogawa-ku
Osaka

3) Y. Sato, T. Meshi, T. Takahashi and N. Sugimoto, *Tanabe Seiyaku Kenkyû Nempô*, 5, (1) 57 (1960).

Studies on Dehydroalanine Derivatives. IV. Synthesis of N-Phthaloyl-Dehydroalanine by Thermal Decomposition of Cysteine and Serine in the Presence of Phthalic Anhydride

By Shumpei SAKAKIBARA

(Received July 13, 1960)

Bergmann et al.[1] reported, that in alkaline solution, serine- or cysteine- diketopiperazine (or peptide) was converted to dehydroalanine-diketopiperazine (or peptide). Weygand and Rinno[2] pointed out that *N*-trifluoroacetyl-serine was converted into *N*-trifluoroacetyl dehydroalanine, when it was distilled under high vacuum. In the present investigation, the thermal decomposition of cysteine and of serine in the presence of phthalic anhydride were studied.

Usually α-amino acids are easily *N*-phthaloylated when heated with phthalic anhydride at 180°C for about half an hour[3]. However, cystine has not yet been tested owing to its poor solubility and reactivity. On the contrary, cysteine and serine were both very unstable to heat, and their *N*-phthaloyl derivatives have not been separated from the respective reaction mixtures after the thermal treatment. When a mixture of cysteine and phthalic anhydride was heated at or above 150°C, formation of hydrogen sulfide was detected by its characteristic odor and by using the lead acetate paper test. The thermal decomposition of cysteine at about 180°C was, however, not so great that its complete decomposition might not be expected within a short time. It was found experimentally that an equimolar amount of yellow mercuric oxide greatly accelerated the desulfhydration reaction and the reagent was rapidly converted into mercuric sulfide at 180°C. After purification of the reaction mixture, *N*-phthaloyl dehydroalanine (I) was obtained as colorless prisms (m. p. 171°C). Use of more than twice the molar equivalent of phthalic anhydride resulted in a better yield, because during the reaction, water is formed and the excess phthalic anhydride may compensate for the partial rehydrolysis of the newly-formed phthaloylimino groups.

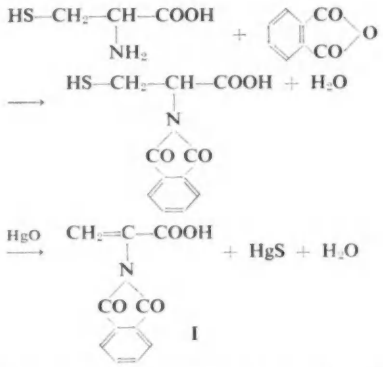

I

When a mixture of serine and phthalic anhydride was heated at 180°C, vigorous evolution of water was observed, and the mixture changed to a dark brown syrup within a short time. At the same time, the formation of pyruvic acid was detected by its order. The purification of the reaction product was very difficult and the yield of substance I was poor. Perhaps part of the serine might have been converted into its *O*-phthalic acid monoester, which was then decomposed to pyruvic acid and ammonia at high temperature before the *N*-phthaloylation reaction occurred. Therefore it was necessary to establish conditions

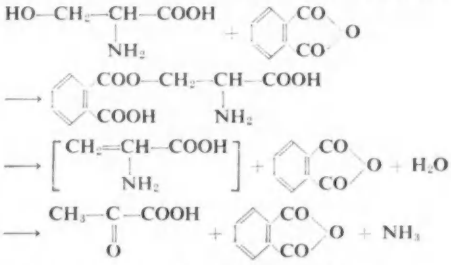

in which the *N*-phthaloylation of serine was complete before such a dehydration reaction could occur. Sheehan et al. have shown[4] that usual amino acids could be *N*-phthaloylated in

1) M. Bergmann and A. Miekeley, *Ann.*, **458**, 40 (1927); B. H. Nicolet, *J. Am. Chem. Soc.*, **53**, 3066 (1931); B. H. Nicolet, *J. Biol. Chem.*, **140**, 685 (1941).
2) F. Weygand and H. Rinno, *Chem. Ber.*, **92**, 517 (1959).
3) J. H. Billman and W. F. Harting, *J. Am. Chem. Soc.*, **70**, 1473 (1948).
4) J. C. Sheehan, M. Goodman and G. P. Hess, ibid., **78**, 1367 (1956).

a gentle reaction in boiling dioxane. However, they did not mention such a reaction for serine. When serine and an equimolar amount of phthalic anhydride were boiled in dioxane for about five hours, a part of the serine remained in suspension, but twice the molar amount of phthalic anhydride readily solubilized the remaining serine in dioxane. Perhaps *O*, *N*-diphthaloylated serine (II) is formed under these conditions.

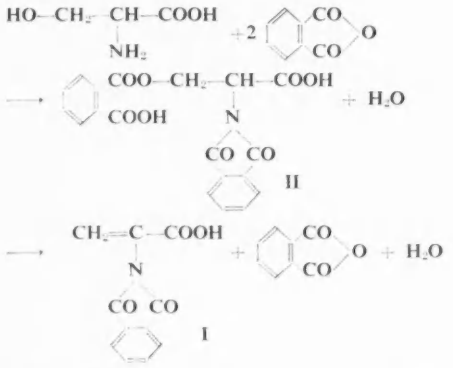

After the solvent had been distilled off, the residual syrup was heated gently in an oil bath at 200°C for about one hour under reduced pressure, and as in the case of cysteine, *N*-phthaloyl dehydroalanine (I) was obtained from the reaction mixture. The melting points of substance I from cysteine and serine were the same (m.p. 171°C), and no depression of the melting point was observed, when equal amounts of product I from cysteine and from serine were mixed. However, the yield of substance I from serine was inferior to that from cysteine. When substance I was recrystallized from dimethylformamide, crystals were obtained which melted at 84~88°C and contained one mole of dimethylformamide as crystallization solvent. Since the dimethylformamide complex was readily crystallizable, this procedure was suitable for purification of the product.

Hydrogenation of substance I gave rise to *N*-phthaloyl-DL-alanine, and lanthionine could also be formed from substance I by an addition reaction with L-cysteine under the conditions described by Schöberl[5].

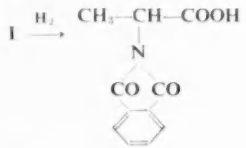

5) A. Schöberl, *Chem Ber.*, **80**, 379 (1947).

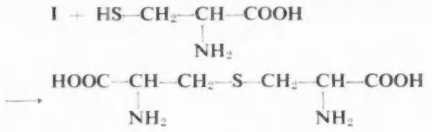

The properties of substance I all supported structure I.

Bergmann[6] first prepared *N*-acetyl dehydroalanine from pyruvic acid and acetamide as follows:

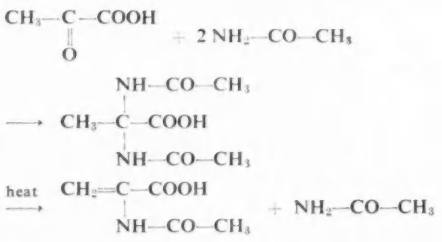

Many investigators utilized this procedure for preparing other *N*-acyl-dehydroalanine derivatives[7]. However, an attempt in the present work to prepare substance I by this procedure failed, because of the poor reactivity of phthalimide with pyruvic acid.

Substance I can polymerize to a vinylidene-type poly-α-phthalimino acrylic acid, which may be converted into poly-α-amino acrylic acid by hydrazinolysis.

Experimental

N-Phthaloyl Dehydroalanine (I) from Cysteine.—A mixture of freshly prepared cysteine (12 g.) and phthalic anhydride (37 g.) was placed in a round bottomed flask (300 ml.) fitted with a distillation adaptor. The flask was heated in an oil bath at 180°C (for about 20 min.) until a clear syrup was obtained, and then the water formed was distilled off under vacuum, using a water pump for about 10 min. more. An intimate mixture of yellow mercuric oxide (20 g.) and phthalic anhydride (22 g.) was added to the reaction mixture in one portion and then the flask was kept under vacuum for about 10~15 min. at 180~190°C. After being cooled to 50~60°C, the reaction mixture was extracted with hot ethyl acetate (300 ml.). The black precipitate was centrifuged off, and extracted three times with 40 ml. each of ethyl acetate. The combined extracts were concentrated to dryness under reduced pressure. The excess phthalic anhydride was separated by sublimation at 140°C in vacuo. The residue was dissolved in ethyl acetate (about 50 ml.) and the resinous products were precipitated by adding ether (about 150~200 ml.). The precipitates were centrifuged off and the supernatant was concentrated to dryness. The

6) M. Bergmann and K. Grafe, *Z. Phys. Chem.*, **187**, 187 (1930).
7) Cf. S. Sakakibara, This Bulletin, **32**, 13 (1959).

residue was recrystallized from toluene (about 30 ml.) to yield light-brown prisms (15 g.), which melt at 150~165°C. The small amount of phthalic anhydride remaining was sublimed out at 140°C in vacuo, and the remaining crystals were recrystallized from ethyl acetate after treatment with a small amount of active charcoal. The yield of slightly colored prisms with a melting point of 164~167°C was 60% (13.2 g.).

For final purification, the product was recrystallized from dimethyl formamide. The dimethyl formamide-complex (plates) formed melted at 84~88°C.

Found: C, 58.70; H, 4.98; N, 9.11. Calcd. for $C_{11}H_7O_4N \cdot C_3H_7ON$: C, 58.00; H, 4.84; N, 9.65%.

The complex was dried at 120°C in vacuo for about 3 hr. and recrystallized from ethyl acetate to yield colorless prisms with m. p. 169~171°C. The over-all yield was about 50~55%.

Found: C, 60.80; H, 3.17; N, 6.37. Calcd. for $C_{11}H_7O_4N$: C, 60.82; H, 3.24; N, 6.46%.

I from Serine.—A mixture of DL-serine (10.5 g.) and phthalic anhydride (37 g.) in dioxane (100 ml.) was refluxed until a clear solution was obtained (for about 5 hr.). The solution was concentrated to dryness in a flask, as shown in Fig. 1, under

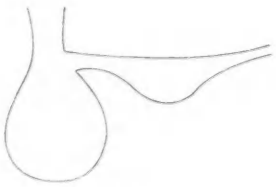

Fig. 1.

reduced pressure, and the residue was heated to 190~200°C under reduced pressure for about 20 min., during which time about 22 g. of phthalic anhydride distilled over. The residue was dissolved in ethyl acetate (50 ml.) and resinous products were precipitated by adding ether (150~200 ml.). The precipitates were centrifuged off, and the supernatant was concentrated to dryness. The residue was heated at 190~200°C for about 20 min. in vacuo and then the same procedures for separating the resinous products formed were repeated. The residue obtained was recrystallized from toluene (30 ml.) to yield light-brown prisms (9 g.) which melted at 150~160°C. The crystals were recrystallized from butanol-toluene (1:1) and then from dimethylformamide. The dimethylformamide complex (8.5 g., m. p. 82~88°C) was dried at 120°C in vacuo for about 3 hr. and recrystallized from ethyl acetate to yield colorless prisms (5 g.) with m. p. 169~171°C. The yield was 23%. The product was identified exactly with that obtained from cysteine by the mixed melting point test.

***N*-Phthaloyl DL-Alanine (II).**—A solution of I (1 g.) in ethanol (30 ml.) was hydrogenated in the presence of silk-palladium catalyst[8] (150 mg.) in an autoclave. The initial hydrogen pressure was 60 atm. The mixture was heated at 40°C for about 3 hr. and then at 70°C for additional 3 hr. After the reaction, the mixture was cooled to room temperature, and the catalyst was filtered off. The filtrate concentrated to dryness under reduced pressure. The residue was recrystallized from water-ethanol, and prisms with m. p. 159~161°C (650 mg.) and with m. p. 157~160°C (280 mg.) were obtained; the total yield was 93%. No depression of the melting point was observed, when the substance with m. p. 159~161°C was mixed with an authentic sample with m. p. 161~161.5°C. The infrared absorption spectrum of the product was also exactly the same as that of an authentic sample.

Lanthionine (III).—Substance I (3.3 g.) and L-cysteine hydrochloride (1.6 g.) were dissolved in aqueous N sodium hydroxide (24 ml.), and the solution was heated at 50°C for 1 hr. and then at 80°C for 2 hr. in an atmosphere of hydrogen. Concentrated hydrochloric acid (30 ml.) was added to the reaction mixture and the solution was boiled for about 6 hr. After colling to room temperature, the phthalic acid formed was filtered off, and the filtrate was concentrated to dryness under reduced pressure. The residue was dissolved in water, and recrystallized by neutralizing the solution with aqueous ammonia. After being kept overnight in a refrigerator, the crystals were filtered off and recrystallized from 6 N hydrochloric acid and aqueous ammonia as described above. The crystals formed were filtered off, washed with water, and alcohol, and dried; wt. 1.8 g., the yield was 86% (calcd. from cysteine).

Found: C, 34.18; H, 6.02; N, 13.44; S, 15.39. Calcd. for $C_6H_{12}O_4N_2S$: C, 34.61; H, 5.81; N, 13.45; S, 15.40%.

Summary

N-Phthaloyl dehydroalanine (I) was synthesized by heating cysteine or serine in the presence of phthalic anhydride. Yellow mercuric oxide greatly accelerated the desulfhydration reaction. The yield of I from serine was inferior to that from cysteine. *N*-Phthaloyl-DL-alanine and lanthionine were derived from I.

The author wishes to express his thanks to Professor Shiro Akabori and Professor Shunsuke Murahashi for their valuable advice and encouragement.

Institute for Protein Research
Osaka University
Kita-ku, Osaka

8) Y. Izumi, This Bulletin, 32, 932 (1959).

Studies on Dehydroalanine Derivatives. V. Radical Polymerization of N-Carboxy-dehydroalanine Anhydride and of N-Phthaloyl-dehydroalanine. Synthesis of a New Amphoteric Polymer

By Shumpei SAKAKIBARA

(Received July 13, 1960)

Dehydroalanine derivatives such as *N*-carboxy-dehydroalanine anhydride (I)[1] and *N*-phthaloyl-dehydroalanine (II)[2] are considered as vinylidene derivatives. In the present communication, radical homo-polymerization and co-polymerization of compounds I and II are described.

As reported previously[3], compound I is readily polymerized to poly-dehydroalanine in pyridine at 100°C with the evolution of carbon dioxide. The polymer obtained is dark brown because of the presence of conjugated double bonds. On the other hand, it was found in this study, that, when this same compound I was heated at 50°C in a dry inert solvent such as ethyl acetate or acetone in the presence of a radical initiator, the solution changed to an opaque jelly within 2 hr. Since, no evolution of carbon dioxide was observed during the polymerization reaction, it was considered that active *N*-carboxy anhydride groups were still present in the polymer obtained. This suggestion was supported by the fact that, when the polymer obtained was dissolved in aqueous ammonia, the solution rapidly turned into a clear gel. Perhaps intermolecular cross-linkages are formed in the solution due to a secondary polymerization reaction of the remaining *N*-carboxy anhydride groups.

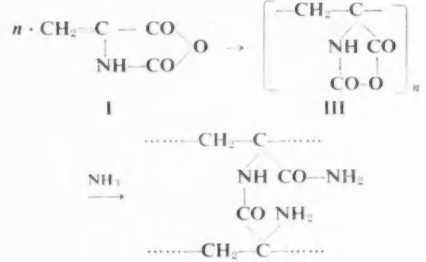

I III

However, separation of analytically pure poly-*N*-carboxy-α-amino acrylic acid anhydride (III) from the reaction mixture was unsuccessful because of the partial hydrolysis and secondary polymerization of the *N*-carboxy anhydride groups during the course of the purification of this compound. Actually, due to air humidity or impurities in the solvents used, analytical data of the polymers obtained from different experiments were between the theoretical values for formula III and those for the completely decarboxylated formula IV. Moreover, it was found that the nitrogen content of the compound gradually increased during storage over phosphorous pentoxide in a desiccator at room temperature. Since the *N*-carboxy anhydride groups should be in juxtaposition in polymer III, they may readily polymerize forming the poly-lactam IV.

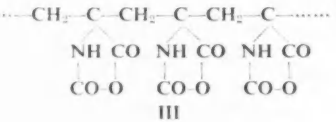

III

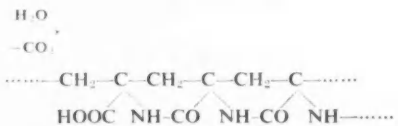

IV

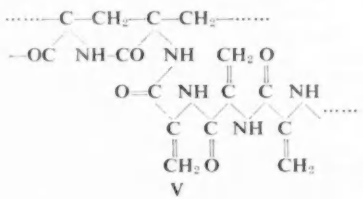

V

Structure V could scarcely be considered because polymerization of *N*-carboxy-dehydroalanine anhydride I to poly-dehydroalanine is very slow as described previously[3]. This is also supported by the color; that is, the polymer obtained was white, not dark brown like poly-dehydroalanine.

Polymer III was soluble in aqueous alkaline solution accompanied with decarboxylation reaction, but not in inert solvents. When the polymer was hydrolyzed with aqueous N potassium hydroxide at 100°C, the greater part of the hydrolyzed polymer was precipitated on acidification of the medium. As shown from

1) S. Sakakibara, This Bulletin, 32, 13 (1959).
2) S. Sakakibara, ibid., 34, 171 (1961).
3) S. Sakakibara, ibid., 32, 814 (1959).

the pH-titration curve of the hydrolyzed polymer (Fig. 1), there were few amino groups and these were far exceeded by the number of carboxyl groups. Perhaps this is due to ureide formation as well as lactam formation, as described below (formula VI).

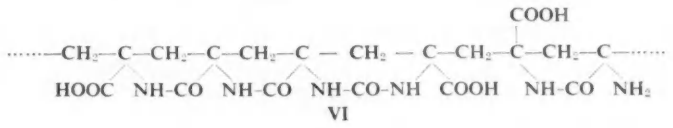

VI

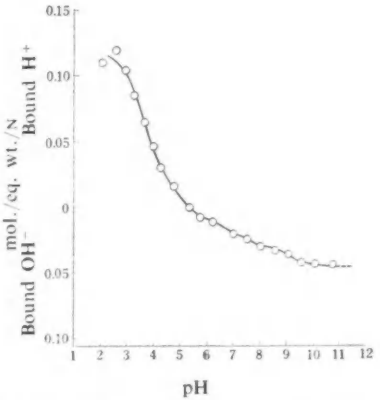

Fig. 1. pH-Titration curve of compound VI.

Frank[4] and Smets et al.[5] indicated that the equilibrium between a five-membered cyclic lactam and its open amino acid, in a polymer chain, tends to the former. Such a ureide-ring may be more stable against hydrolysis than a lactam.

Radical polymerizability of α-phthalimido acrylic acid (II) was rather weak. When the monomer was heated in methanol at 60°C for about 200 hr. in the presence of azobisisobutylonitrile, a polymer(VII) was separated as a methanol-insoluble oil. The polymer was finally obtained as white powder, and it was soluble in dimethylformamide, and in hot acetic acid.

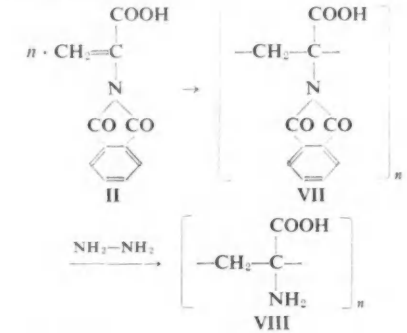

4) H. P. Frank, *J. Polymer Sci.*, **12**, 570 (1954).

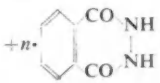

After hydrazinolysis, poly-α-amino acrylic acid (VIII) was obtained in poor yield. To molecular weight of the starting polymer may not have been very high. The poly-α-amino acrylic acid obtained was soluble in water. However, elementary analysis and pH-titration (Fig. 2) indicated that the content of ionizable groups was lower, than the calculated values, for the same reason as explained above.

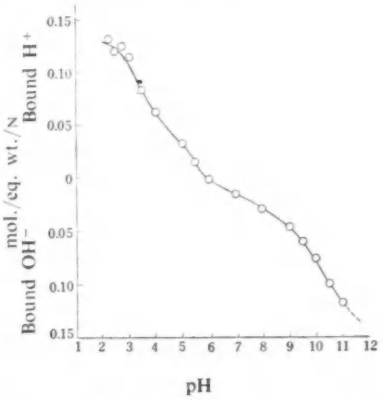

Fig. 2. pH-Titration curve of compound VIII.

Copolymerization of monomer II with vinyl acetate (V. Ac.) in methanol gave a gelatinous precipitate (IX-a). From the mother liquor, a second fraction (IX-b) was precipitated on addition of ether. Elementary analysis indicated that polymer IX-a was about 8 : 5-co-polymer (II : V. Ac.) and polymer IX-b was about 1 : 5-co-polymer (II : V. Ac.). The former was only soluble in dimethyl formamide, but the latter was soluble in pyridine, glacial acetic acid, dimethyl formamide, *m*-cresol, chloroform, hot ethanol, a mixture of methanol and acetone, and of ethyl acetate and acetone. Polymer IX-b was sparingly soluble in methanol, ethyl acetate and acetone, and insoluble in

5) M. Vrancken and G. Smets, ibid., **14**, 521 (1954); A. Conix, N. V. Mortsel and G. Smets, ibid., **15**, 221 (1955).

benzene, toluene and water. After hydrazinolysis of these copolymers, water soluble polyampholytes (X) were obtained. The pH-titration curves of these copolymers (Figs. 3 and 4) were of a typical polyampholyte-type, the structure of which was assumed to be as follows:

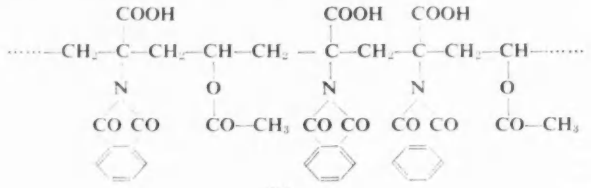

IX

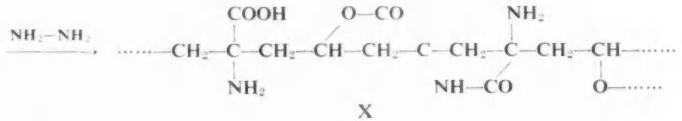

X

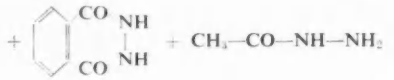

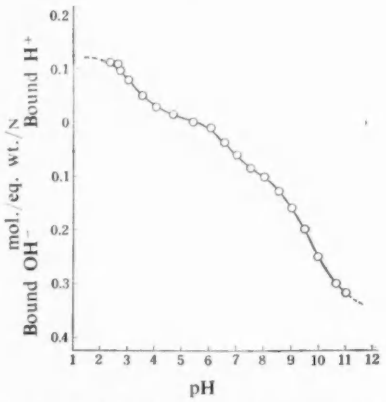

Fig. 3. pH-Titration curve of compound X-a.

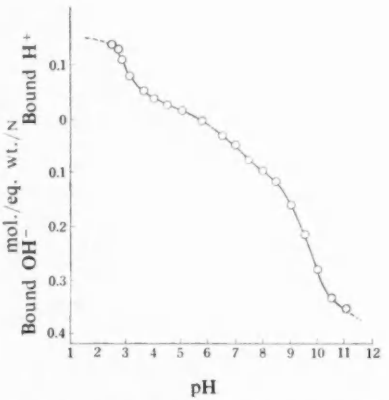

Fig. 4. pH-Titration curve of compound X-b.

If the sequence of co-monomer-segments was at random, five-membered lactam formation, as in poly-α-amino acrylic acid, should not occur. As shown in Figs. 3 and 4 however, the number of ionizable groups was about 30% of the theoretical value. The values increased inversely with the number of amino acid segments. In this cases, the number of amino groups was greater than that of carboxyl groups. Perhaps, amino acid segments may have been localized in the molecule. Moreover, partial intramolecular lactone formation may have occurred.

If copolymerization of small amounts of compounds I or II with vinyl monomers such as acrylonitrile were possible, these would improve the affinity for dyeing of the parent polymers. Moreover, these would be useful as key-substances for preparing graft-copolymer of vinyl- and amino acid-polymers.

Experimental*1

Polymerization of I to III.—A solution of I (2 g.) and azobisisobutylonitrile (0.1 g.) in purified ethyl acetate (20 ml.) was heated at 50°C in a sealed tube for about 4 hr. The opaque jelly formed, was crushed up finely and became powdery on addition of dry ether. The powder formed III was collected centrifugally, washed with ether and dried over phosphorus pentoxide in a desiccator; colored gradually above 180°C, sintered at about 250°C, yield 40% (0.8 g.).

Found*2: C, 44.5; H, 4.9; N, 15.8. Found*3:

*1 All melting points were determined by using capillary tubes in a Kanechlole-bath, maximum temperature of which was 300°C.

*2 Analyzed immediately after preparation.

*3 Analyzed after storing the same sample for 10 days in a desiccator over phosphorus pentoxide.

C, 46.9; H, 5.07; N, 16.9. Found*4 : C, 46.5; H, 4.1; N, 16.5. Calcd. for $C_4H_3O_2N$ (III): C, 42.5; H, 2.6; N, 12.4%. Calcd. for C_3H_3ON (IV): C, 52.2; H, 4.35; N, 20.3%.

Formation of VI from III.—The polymer obtained above (0.5 g.) was dissolved in aqueous N potassium hydroxide (20 ml.) and the solution was heated in a sealed tube at 105°C for about 20 hr. The hydrolyzate was dialyzed against distilled water for 2 days and then lyophilized. White spongy material (0.4 g.) was obtained, which was soluble in water at above pH 6. For analysis, this materials was dissolved in distilled water, and reprecipitated by adding hydrochloric acid. The precipitates formed were washed with water, ethanol and, ether and dried; colored gradually above 250°C without melting.

Found: C, 49.1; H, 5.1; N, 17.3. Calcd. for C_3H_3ON-0.1·CO_2-0.2·H_2O (VI): C, 48.5; H, 4.4; N, 18.2%; equiv. wt./N=77.0.

Polymerization of II to VII.—A solution of II (4 g.) and azobisisobutylonitrile (0.6 g.) in methanol (10 ml.) was heated in a sealed tube at 60°C for about 200 hr. The polymer formed (VII) precipitated on addition of ether and washed with methanol and ether, and dried; sintered at 250°C and melted at 270°C, yield 55% (2.2 g.).

Found: C, 60.3; H, 4.2; N, 6.8. Calcd. for $C_{11}H_7O_4N$ (VII): C, 60.8; H, 3.2; N, 6.4%.

Hydrazinolysis of VII.—The polymer VII (1.5 g.) was dissolved in hydrazine hydrate (15 ml.) and the solution was boiled for about 3 hr. The hydrazinolyzate was concentrated to drynes and the residue was redissolved in aqueous 0.1 N potassium hydroxide (5 ml.) and the phtaloyl hydrazide formed, precipitated on addition of enough acetic acid to reduce the pH to 5. The white precipitate formed was centrifuged off, and washed with water; 1.0 g. of phthaloyl hydrazide was recovered. The supernatant was concentrated to 5 ml. and poured into ethanol (about 100 ml.) to precipitate polymer VIII, which was centrifuged off, washed with ethanol, and dried in vacuo at room temperature; slightly brown powder (80 mg.) which colored gradually above 250°C.

Found: C, 43.9; H, 4.5; N, 17.5. Calcd. for C_3H_3ON-0.7·H_2O: C, 44.1; H, 5.4; N, 17.2%; equiv. wt./N=81.6.

Copolymerization of II with Vinyl Acetate.—A mixture of II (5 g.), vinyl acetate (20 g.) and azobisisobutylonitrile (0.5 g.) in methanol (20 ml.) was heated in a sealed tube at 60°C for about 100 hr. The gelatinous precipitates formed were centrifuged off, washed with methanol, and powdered from dimethyl formamide and ether (IX-a); m. p. 220~230°C, wt. 4.0 g.

Found: C, 56.9; H, 5.2; N, 5.0. Calcd. for $C_{11}H_7O_4N$-0.625·$C_4H_6O_2$-H_2O (IX-a): C, 56.1; H, 4.5; N, 4.9%; eq. wt./N=289.

From the methanolic mother liquor, polymer IX-b was precipitated by addition of ether. It was centrifuged off, washed with ether and dried; sintered at 160~170°C and melted at 200°C, wt. 4.6 g.

Found: C, 56.6; H, 6.3; N, 2.2. Calcd. for $C_{11}H_7O_4N$-4.8·$C_4H_6O_2$-0.67·H_2O (IX-b): C, 56.5; H, 5.8; N, 2.2%; equiv.wt./N=642.

Hydrazinolysis of IX-a and IX-b.—The polymer IX-a (3 g.) was dissolved in hydrazine hydrate (50 ml.) and the solution was boiled for about 3 hr. The hydrazinolyzate was concentrated to dryness, and the residue was redissolved in aqueous N potassium hydroxide (5 ml.) and the phthaloyl hydrazide formed precipitated on additon of acetic acid. The white precipitates were centrifuged off, and washed with water; about 1.6 g. of phthaloyl hydrazide was recovered. The supernatant and the washings were combined and after adding a few drops of N potassium hydroxide, the solution was dialyzed against distilled water for about 2 days. The dialyzed solution was lyophilized to yield a spongy material X-a; colored gradually above 250°C, wt. 0.5 g.

Found: C, 48.5; H, 7.6; N, 13.5. Calcd. for C_3H_3ON-0.625·C_2H_4O-0.5·H_2O: C, 48.5; H, 6.2; N, 13.3%; equiv.wt./N=105.5.

The polymer IX-b (4 g.) was similarly treated with hydrazine hydrate (50 ml.) as described above, and material X-b) (1.1 g.) was obtained as a white spongy material; m. p. 200~210°C.

Found: C, 51.2; H, 8.1; N, 6.0. Calcd. for C_3H_3ON-3.5·C_2H_4O-0.67·H_2O (X-b): C, 51.1; H, 7.8; N, 6.0%; equiv.wt./N=235.

pH-Titrations.—Each polyampholyte (VI, VIII, X-a or X-b) was weighed (50~150 mg.) and dissolved in 0.1 N potassium chloride (20.00 ml.) containing 0.30 ml. of 1.00 N potassium hydroxide. The solution was titrated with 1.00 N hydrochloric acid using an Agla micrometer-syringe under stirring in an atmosphere of nitrogen. Determination of pH-values was carried out by using a Beckman, GS pH-meter. The curves shown in Figs. 1, 2, 3 and 4 were obtained by Parke and Davis's method[6].

Summary

Homopolymers of *N*-carboxy-dehydroalanine anhydride (I) and of *N*-phthaloyl-dehydroalanine (II), and copolymers of II with vinyl acetate were synthesized. Hydrolysis or hydrazinolysis was carried out to obtain polymers containing α-amino acid structures. Actual structures of these polymers were discussed.

The author wishes to express his thanks to Professor Shiro Akabori and Professor Shunsuke Murahashi for their valuable advice and encouragement.

Institute for Protein Research
Osaka University
Kita-ku, Osaka

*4 Another example of analysis.

6) T. V. Parke and W. W. Davis, *Anal. Chem.*, **26**, 642 (1954).

The Acid Product Obtained in the Synthesis of 2-Phenyltropone Derivatives from 2-Phenylsuberone[1]

By Tadashi MUROI*

(Received February 20, 1960)

Previously Nozoe, Kitahara and others[2] reported that in the direct bromination-dehydrobromonation of suberone, a considerable amount of an acid product was sometimes obtained besides the 2, 4, 7-tribromotropone, and thereafter confirmed the structure of this acid product to be 2, 4, 7-tribromo-5-hydroxytropone[3].

The present author also reported[4] previously that by the application of 4~5 molar equivalents of bromine on 2-phenylsuberone (I), 4-bromo-and 4, 7-dibromo-2-phenyltropone (II and III) were obtained in a good yield and that these products were occasionally accompanied by a considerable amount of an acid substance (A), assumed to be a mixture of bromo-derivatives of 4-hydroxy-2-phenyltropone (IV). This paper describes the details of A and the four methyl ethers derived from A.

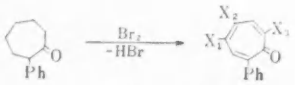

(I)

(II): X_1=Br, X_2=X_3=H
(III): X_1=X_3=Br, X_2=H
(IV): X_1=OH, X_2=X_3=H

Scheme I

The yield of A was found to increase remarkably, when somewhat impure I, or a solvent containing a trace of water was used, i. e. when fairly prolonged heating had to be applied in order to complete the reaction. Compound A separated as yellow needles or pale yellow scales of decomp. point ca. 200°C, and was sparingly soluble in chloroform, alcohol and acetic acid, and insoluble in benzene, ether and water. It gave no coloration with ferric chloride characteristic of tropolone or enol. It gave, however, a sparingly soluble yellow sodium salt when treated with sodium hydroxide or sodium carbonate solution. When treated with diazomethane, A afforded four kinds of methyl ethers; pale yellow needles (V), m. p. 173~174°C, yellow needles (VI), m. p. 131~132°C, yellow prisms (VII), m. p. 74~75°C, and pale yellow plates (VIII), m. p. 112~113°C. Their formation ratio was not constant but, in general, V and VI were always obtained in a better yield than VII or VIII and some times the yield of VII and VIII was so small that they can not be isolated.

Both V and VII had the molecular formula of $C_{14}H_{11}O_2Br$ and were obtained chiefly from the sparingly soluble portion of A in alcohol. On the other hand VI and VIII analyzed for $C_{14}H_{10}O_2Br_2$ and were obtained from the comparatively soluble portion of A.

Previously, Kitahara and others reported[5] that 2, 4, 7-tribromo-5-hydroxytropone (IXa) gave two kinds of methyl ethers and predicted from this fact that IXa existed as an equilibrium mixture of IXa and its tautomeric isomer, i. e. 2, 4, 6-tribromo-5-hydroxytropone (IXb).

(IXa) (IXb)

Scheme II

Acid hydrolysis of V gave yellow needles (X), $C_{13}H_9O_2Br$ m. p. ca. 210°C (decomp.), treatment of which with diazomethane afforded V and VII, with the former predominating. This fact indicates that X exists in a tautomeric mixture (Xa and Xb) and that V and VII are the respective methyl ethers of Xa and Xb.

When refluxed with sodium methoxide in absolute methanol, VII underwent aromatization, and the successive hydrolysis of its product yield pale yellow crystals (XI), m. p. 98~103°C. When treated with concentrated sulfuric acid, XI was converted to give yellow scales (XII), m. p. 93~94°C, which was proved to be 3-methoxyfluorenone[6] by mixed fusion with the authentic sample. It is, therefore, clear

* Present address, Hitachi Research Laboratory of Hitachi Ltd., Sukegawa-machi, Hitachi.

1) Presented at the 11th Annual Meeting of the Chemical Society of Japan, Tokyo, April, 3, 1958.

2) T. Nozoe, Y. Kitahara, T. Ando, S. Masamune and H. Abe, *Sci. Repts. Tohoku Univ., Ser.* I, **36**, 166 (1952).

3) T. Nozoe, Y. Kitahara and H. Abe, *Proc. Japan Acad.*, **29**, 347 (1953).

4) T. Muroi, This Bulletin, **33**, 1166 (1960).

5) Y. Kitahara, J. Shin and T. Toda, Presented at the Local Meeting of Tohoku District of the Chemical Society of Japan, Yamagata, Oct. 6, 1955.

6) F. Ullmann and H. Bleier, *Ber.*, **35**, 4272 (1902).

that XI is 4-methoxy-2-phenyl-benzoic acid and VII is 7-bromo-4-methoxy-2-phenyltropone, and X is a tautomeric mixture of 7-bromo-4-hydroxy-2-phenyltropone (Xa) and 5-bromo-4-hydroxy-3-phenyltropone (Xb).

Catalytic debromination of VII and V in the presence of palladium-carbon gave 4-methoxy-2-phenyltropone (XIII), m. p. 93～94°C, and 4-methoxy-3-phenyltropone (XIV), m. p. 75～76°C, respectively.

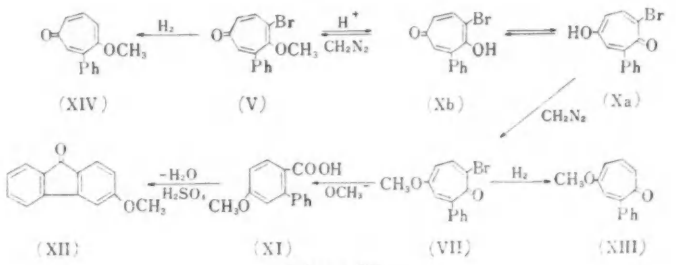

Scheme III

Acid hydrolysis of VI afforded pale yellow needles (XV), $C_{15}H_{10}O_2Br_2$ m. p. ca. 200°C (decomp.) which when treated with diazomethane, gave a mixture of VIII and VI. Catalytic debromination of VI gave XIII in a good yield. These facts indicate that XV also exists in a equilibrium mixture of two tautomeric forms (XVa and XVb) as in the case of IX and X, and moreover, that VI and VIII are respective methyl ethers of XVa and XVb.

When heated with alkali in alcohol, VI easily underwent aromatization to give colorless needles (XVI) m. p. 168～169°C, accompanied by a small amount of XV. When treated with concentrated sulfuric acid, XVI afforded yellow scales (XVII) m. p. 235～237°C, which was assumed to be monobromo-derivatives of XII. It follows therefore that one of the bromine atoms of VI occupies its C-7 position.

It was also found that VIII underwent aromatization very easily with alkali to give colorless needles (XVIII), m. p. 187～188°C, in a good yield. Catalytic debromination of XVIII gave colorless needles (XIX), m. p. 208～210°C. The structure of XIX is proved to be 4-methoxy-3-phenylbenzoic acid by the synthetic method shown in scheme IV.

These facts indicate, that VI and VIII are 5, 7-dibromo-4-methoxy-2-phenyltropone and 5, 7-dibromo-4-methoxy-3-phenyltropone, respectively, and XV is 5, 7-dibromo-4-hydroxy-2-phenyltropone as shown in the Scheme IV.

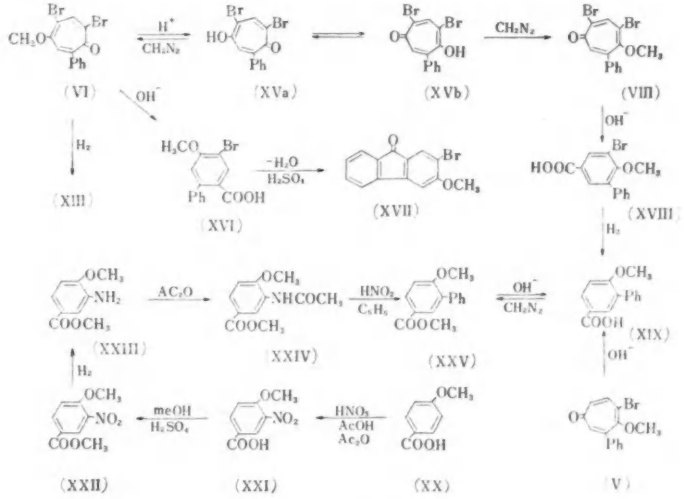

Scheme IV

From the fact mentioned above, the acid substance(A) is clarified to be a mixture of 7-bromo- and 5,7-dibromo-4-hydroxy-2-phenyltropone (Xa and XVa) and their respective tautomeric isomers. As the reaction of bromine on I is fairly complicated as reported previously[4], the mechanism of the formation of A can not be discussed at this stage. It is, however, assumed that A is derived through II or III by their hydroxylation or successive bromination during the reaction.

When treated with alkali, V was easily converted to give XIX in a good yield with the elimination of bromine at the C-5 position. Similar reaction was reported previously[7] by the present author, and this reaction is considered to be very interesting from the viewpoint that, in the rearrangement reaction of troponoid compound, the elimination of the substituents other than in C-2 (i.e. C-7) position has not been observed so far[8].

The synthesis and some reactions of IV and its bromoderivatives will be reported in the next paper.

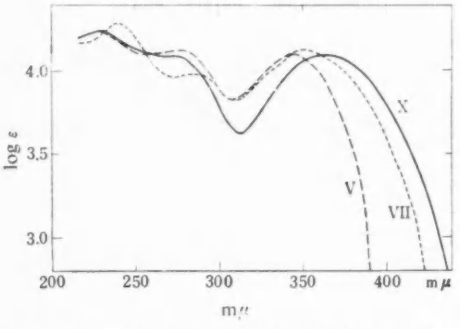

Fig. 1. Ultraviolet absorption spectra of V, VII and X in methanol.

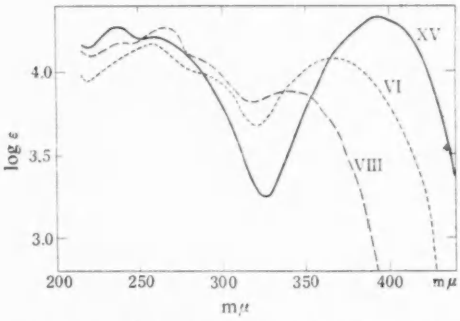

Fig. 2. Ultraviolet spectra of VI, VIII and XV in methanol.

7) T. Muroi, *J. Chem. Soc. Japan, Pure Chem. Sec.* (*Nippon Kagaku Zasshi*), **80**, 303 (1959).

Experimentals[9]

Formation of Acid Substance (A) from 2-Phenylsuberone(I).—i) To a mixture of 4.7 g. of I, (b. p. 110~111°C/0.3~0.4 mmHg, n_D^{20}: 1.5390) 7.5 cc. of acetic acid and 1 cc. of water, a solution of 20 g. of bromine dissolved in 3.5 cc. of acetic acid was added dropwise over a period of 2 hr. at 50~80°C. The whole was heated on a water bath for about 3 hr. until there were no liberations of hydrogen bromide, cooled, and diluted with about 200 cc. of methanol, and yellow crystals (a) thereby separated were collected by filtration. Yield, ca. 4.3 g., m. p. 110~130°C. Crystalline residue, obtained after the evaporation of the solvent under reduced pressure, was digested with water and chloroform to give 0.25 g. of yellow crystals (b), m. p. 200°C (decomp.). The chloroform solution was shaken with 10% sodium carbonate solution and the aqueous layer was acidified with hydrochloric acid to give pale yellow crystals (c), m. p. 195°C (decomp.). Yield, 0.25 g.

The crystals (a) were digested with benzene and the insoluble portion (d), m. p. 195°C (decomp.) was collected by filtration. Yield, 0.85 g. The crystals (b), (c), and (d) were combined and dissolved in sodium carbonate solution. After treated with active carbon, the solution was acidified again and an acid product (A) was obtained as pale yellow crystals, m. p. 195~200°C (decomp.). Yield, 1.3 g.

The benzene soluble parts of (a) gave 2.8 g. of III. Similarly, chromatographic separation of the chloroform solution (aforementioned)[4] through a silica-gel column gave small amounts of III, II and 7-bromo-2-phenyltropone.

ii) To a solution of 4.7 g. of impure I (b. p. 140~149°C/2~3 mmHg, n_D^{20}: 1.5339) dissolved in 7.5 cc. of acetic acid, a solution of 16 g. of bromine in 3 cc. of acetic acid was added dropwise at 50~80°C. The whole was heated on a water bath for about 20 hr. till the liberation of hydrogen bromide was ceased. The solvent was evaporated under reduced pressure and the residue was washed with chloroform and water by which 1.8 g. of yellow crystals (a), m. p. 150~180°C (decomp.) were obtained. After the treatment of the chloroform solution with 10% sodium carbonate solution as in the above case, 0.2 g. of pale yellow crystals (b), m. p. ca. 175°C (decomp.) were obtained. The combined crystals (a) and (b) were repeatedly recrystallized from ethanol. Yellow needles (A_1) m. p. 207~210°C (decomp.) and pale yellow scales (A_2) m. p. 195~198°C (decomp.) were obtained from the sparingly soluble portion and comparatively easily soluble portion in alcohol, respectively.

Further recrystallization did not give pure substances and the analytical values of A_1 and A_2 were as below:

8) a) S. Seto, *Sci. Repts. Tohoku Univ., Ser.* I., **37**, 377 (1953). b) Y. Kitahara, ibid., **38**, 280 (1954). b) T. Mukai, ibid., **39**, 250 (1956). d) P. L. Pauson, *Chem. Revs*, **55**, 9 (1955).

9) Melting points are uncorrected. The micro analyses and the measurement of U. V. spectra were carried out by Mrs. K. Kodaira of Tohoku University, to whom deep gratitude is hereby expressed.

A_1: Found: C, 51.08; H, 2.88. Calcd. for $C_{13}H_9O_2Br$: C, 56.35; H, 3.27%.

A_2: Found: C, 44.11; H, 2.33. Calcd. for $C_{13}H_8O_2Br_2$: C, 45.15; H, 2.33%.

The neutral portion, when treated as in i), gave a small amount of the bromo derivatives of 2-phenyltropone whose structures were confirmed by mixed fusion with their authentic samples, respectively.

Methylation of A.—i) To a suspension of 1.15 g. of A, m. p. 185~190°C (decomp.) in 10 cc. of ether, ethereal diazomethane was added and the whole was kept standing overnight in a refrigerator. The crystals, m. p. 110~115°C, thereby separated, were collected by filtration and recrystallized from benzene or methanol to give 0.5 g. of VI as yellow needles m. p. 131~132°C.

Found: C, 46.00; H, 2.84. Calcd. for $C_{14}H_{10}O_2Br_2$: C, 45.44; H, 2.74%.

The filtrate was evaporated and the residue, dissolved in a mixture of benzene and petroleum ether, was chromatographed through a silica-gel column. This was eluted successively with benzene-petroleum ether mixture, benzene, and chloroform to give 0.15 g. of VI and 0.05 g. of V.

ii) A mixture of 0.7 g. of A_1 and 5 cc. of ether was treated with diazomethane as in i). The raw crystals thereby obtained were recrystallized from benzene or methanol to give 0.2 g. of V, as pale yellow needles, m. p. 173~174°C.

Found: C, 58.53; H, 4.14. Calcd. for $C_{14}H_{11}O_2Br$: C, 58.09; H, 3.81%.

The mother liquor, chromatographed as above, gave 0.1 g. of VI, 0.05 g. of V and a trace of VII as in their respective raw crystals.

iii) A mixture of 0.7 g. of A_2 and 5 cc. of ether was treated with diazomethane as above, and 0.3 g. of VI was separated. The chromathographic separation of the mother liquor through a silica-gel column gave 0.03 g. of VII, 0.05. of VI and 0.03 g. of V.

Acid Hydrolysis of 5-Bromo-4-methoxy-3-phenyltropone (V).—To a solution of 0.2 g. of V dissolved in 0.6 cc. of concentrated sulfuric acid, 6 cc. of water was added and the mixture was refluxed for 2 hr. After cooling, additional 10 cc. of water was added and the yellow crystals that separated were collected by filtration and washed with hot benzene. Yield 0.23 g. Recrystallization from ethanol gave X as yellow needles, m. p. 210~212°C (decomp.).

Found: C, 56.30; H, 3.40. Calcd. for $C_{13}H_9O_2Br$: C, 56.35; H, 3.27%.

From benzene solution 0.05 g. of V was recovered.

Acid Hydrolysis of 5, 7-Dibromo-4-methoxy-2-phenyltropone (VI).—A mixture of 0.37 g. of VI, 2 cc. of concentrated sulfuric acid and 4 cc. of water was refluxed for 30 min. After cooling the whole, the separated crystals were collected by filtration and washed with benzene. Yield 0.32 g. Recrystallization from ethanol gave XV as yellow scales, m. p. 195~198°C. (decomp.).

Found: C, 45.63; H, 2.46. Calcd. for $C_{13}H_8O_2Br_2$: C, 45.15; H, 2.33%.

Methylation of 7-Bromo-4-hydroxy-2-phenyltropone (X). — Treatment of X (0.3 g.) with diazomethane in ether followed by the removal of the solvent gave crystalline residue. Recrystallization from benzene gave 0.16 g. of raw crystals of V, m. p. 160~165°C. The mother liquor, after the removal of the solvent, was dissolved in a mixture of benzene and petroleum ether and chromatographed through a silica-gel column. About 0.07 g. of yellow crystals of VII, m. p. 62~65°C and a small amount of V were obtained. Recrystallization of VII from cyclohexane or dilute methanol gave yellow needles, m. p. 73~74°C.

VII: Found: C, 58.09; H, 3.60. Calcd. for $C_{14}H_{11}O_2Br$: C, 58.09; H, 3.81%.

Methylation of 5,7-Dibromo-4-hydroxy-2-phenyltropone (XV).—In the usual manner, 0.3 g. of XV was treated with diazomethane in ether. The crystals that separated were recrystallized from benzene or methanol to give 0.18 g. of VI as yellow needles, m. p. 129~130°C and 0.02 g. of VIII as pale yellow plates, m. p. 112~113°C.

VIII: Found: C, 45.51; H, 2.68. Calcd. for $C_{14}H_{10}O_2Br_2$: C, 45.44; H, 2.72%.

Chromatographic separation of the mother liquor through a silica-gel column gave additional 0.03 g. of VIII and a trace of VI.

Reaction of 7-Bromo-4-methoxy-2-phenyltropone (VII) and Sodium Methoxide.—To a solution of 0.04 g. of metallic sodium in 4 cc. of absolute methanol, 0.2 g. of VII was added and the solution was refluxed over a period of 20 hr. on an oil bath. After removal of the solvent, 5 cc. of water was added, and the solution was refluxed for an additional period of 3 hr. The solution was shaken with chloroform to remove the neutral portions and the water layer was acidified with dilute sulfuric acid. The acidic product that separated was extracted with chloroform. After removal of the solvent, the crystalline residue was recrystallized from cyclohexane to give 0.03 g. of XI as yellow crystals, m. p. 95~100°C. This was dissolved in 0.5 cc. of concentrated sulfuric acid and heated on a water bath for several min. After cooling, the solution was diluted with water and extracted with benzene. The benzene extract, after being washed with dilute sodium hydroxide solution, was evaporated and the residue was recrystallized from cyclohexane to give yellow needles, m. p. 95~97°C. This was proved to be identical by mixed fusion with the authentic sample of 3-methoxyfluorenone (XI).

Reaction of 5, 7-Dibromo-4-methoxy-2-phenyltropone (VI) and Alkali.—A mixture of 0.12 g. of VI, 3 cc. of ethanol and 1 cc. of 2 N sodium hydroxide was refluxed for 30 min. After removal of ethanol, the residue was acidified and extracted with benzene. Benzene extract gave 0.06 g. of pale yellow crystals which were digested, with a small amount of yellowish brown crystals, m. p. 185~193°C (decomp.). This was proved to be XV from its analytical value.

Found: C, 43.88; H, 2.20. Calcd. for $C_{13}H_8O_2Br_2$; C, 45.15; H, 2.33%.

The benzene solution was passed through a short silica-gel column to give 0.03 g. of raw crystals of m. p. 140~155°C. Recrystallization from dilute methanol gave XVI as colorless needles, m. p. 168~169°C.

Found: C, 54.51; H, 3.46. Calcd. for $C_{14}H_{11}O_2Br$: C, 54.75; H, 3.61%.

When XVI was heated with concentrated sulfuric

acid on a water bath for several minutes and then diluted with water, there were obtained yellow crystals of m. p. 235~237°C.

Found: C, 57.52; H, 3.04. Calcd. for $C_{14}H_9O_2Br$; C, 58.16; H, 3.14%.

Reaction of 5, 7-Dibromo-4-methoxy-3-phenyltropone (VIII) and Alkali.—A mixture of 0.06 g. of VIII, 3 cc. of methanol and 10 cc. of 2 N sodium hydroxide was refluxed on a water bath for 30 min. After treated as in the case of VII, 0.05 g. of raw crystals of m. p. 175~180°C were obtained. Recrystallization from methanol gave XVIII as colorless needles of m. p. 187~188°C.

Found: C, 55.28; H, 3.60. Calcd. for $C_{14}H_{11}O_3Br$: C, 54.75; H, 3.61%.

Debromination of 0.03 g. of XVIII dissolved in 3 cc. of methanol, in the presence of palladium carbon catalyst and sodium acetate, gave 0.02 g. of colorless crystals m. p. 190~200°C. This was recrystallized from methanol to give colorless needles of m. p. 210~211°C, which was proved to be identical with the authentic sample of XIX obtained from V.

Reaction of 5-Bromo-4-methoxy-3-phenyltropone (V) and Alkali.—A mixture of 0.14 g. of V, 2.5 cc. of ethanol and 0.8 cc. of 2 N sodium hydroxide was refluxed for 30 min. After treated as in the above cases, 0.12 g. of pale yellow acidic crystals were obtained. This was digested with hot benzene to give a minute amount of yellow crystals of m. p. 205~208°C (decomp.). Which was proved to be identical with X from its analytical value and ultraviolet spectrum.

Found: C, 56.28; H, 3.34. Calcd. for $C_{13}H_9O_2Br$: C, 56.35; 3.27%.

From the benzene solution, colorless needles of m. p. 207~209°C were obtained. This was proved to be identical with the sample of XIX obtained from 4-methoxybenzoic acid (XX).

Found: C, 73.97; H, 5.04. Calcd. for $C_{14}H_{12}O_3$: C, 73.67; H, 5.30%.

Reduction of 7-Bromo-4-methoxy-2-phenyltropone (VII).—Catalytic reduction of 0.11 g. of VII dissolved in 3 cc. of ethanol, in the presence of 0.02 g. of sodium acetate and 0.02 g. of palladium carbon, resulted in absorption of hydrogen at room temperature. After removal of the catalyst by filtration, the filtrate was diluted with water and extracted with benzene. This extract, evaporated under reduced pressure, gave crystalline residue which was recrystallized from cyclohexane to give XIII as pale yellow needles m. p. 91~92°C.

Found: C, 79.63; H, 5.80. Calcd. for $C_{14}H_{12}O_2$: C, 79.22; H, 5.70%.

Reduction of 5, 7-Dibromo-4-methoxy-2-phenyltropone (VI).—Catalytic reduction of 0.1 g. of VI, as in the case of VII, gave 0.02 g. of XIII.

Reduction of 5-Bromo-4-methoxy-3-phenyltropone (V).—Catalytic reduction of 0.1 g. of V dissolved in 40 cc. of ethanol, in the presence of 0.1 g. of palladium carbon and 0.1 g. of sodium acetate, resulted in absorption of hydrogen at room temperature. After removal of the catalyst and the solvent, the residue was diluted with water and extracted with benzene. This solution, passed through a silica-gel column, gave raw crystals of m. p. 70~74°C. Recrystallization from cyclohexane gave XIV, as pale yellow prisms, m. p. 75~76°C.

Found: C, 78.31; H, 5.81. Calcd. for $C_{14}H_{12}O_2$: C, 79.22; H, 5.70%.

Synthesis of 4-Methoxy-3-phenylbenzoic Acid (XIX).—4-Methoxy-3-nitrobenzoic acid (XXI)[10], m. p. 191~192°C, was obtained by the nitration of 4-methoxybenzoic acid (XX) in a mixture of acetic acid and acetic anhydride with concentrated nitric acid.

The methylation of XXI with methanol and concentrated sulfuric acid gave methyl-4-methoxy-3-nitrobenzoate (XXII)[11] m. p. 110~111°C in a good yield. Catalytic reduction of XXII in ethyl acetate in the presence of Raney nickel catalyst (W-5), gave methyl-3-amino-4-methoxy benzoate (XXIII)[12], m. p. 83~85°C.

A solution of 0.7 g. of acetic anhydride and 3 cc. of acetic acid was heated for 30 min. To the cold reaction mixture, nitrous fume generated by the action of concentrated nitric acid to solid sodium nitrate, was passed in for a period of 1 hr. at about 5°C. When diluted with water, the reaction mixture separated a yellow oily product, which was extracted with benzene. After washed with water and dried over anhydrous sodium sulfate, the benzene solution was poured on a mixture of 0.7 g. of anhydrous sodium carbonate and 0.7 g. of anhydrous sodium sulfate. The whole was stirred for a period of 5 hr. and then kept to stand for 2 days. After removal of solid materials, the filtrate was evaporated to give 0.6 g. of an oily product. This was distilled under reduced pressure and about 0.2 g. of yellow crystalline oil was obtained. Recrystallization from ether and methanol gave methyl 4-methoxy-3-phenylbenzoate (XXV) as colorless prisms, m. p. 88~89°C. Hydrolysis of XXV gave XIX as colorless needles of m. p. 115~117°C which was proved to be identical by mixed fusion with the sample obtained from V or VII. Methylation of 0.04 g. of XIX with diazomethane gave about 0.03 g. of XXV.

The author takes this opportunity to express his sincere gratitude to Professor Tetsuo Nozoe of Tohoku University for his guidance and encouragement throughout the course of this work, to Professor Shuichi Seto, Professor Yoshio Kitahara of Tohoku University and to Assistant Professor Katsuo Kikuchi of Yamagata University for their very helpful and kind discussions.

Department of Chemistry
Faculty of Liberal Arts and Science
Yamagata University
Koshirakawa-machi, Yamagata

10) *Beilsteins Handbuch. Org. Chem.*, **10**, 181.
11) ibid., **10**, 182.
12) ibid., **14**, 594.

A Study on Anion Exchange aud Amine Extraction of Rare Earth Elements in Nitric Acid

By Fujio ICHIKAWA

(Received April 28, 1960)

The use of amine extraction for uranium, thorium and many other elements has recently been developed by a number of investigators[1-7]. It is reported that the mechanism of amine extraction is similar to that of anion exchange and the former is called commercially liquid anion exchanger. The author previously reported[8] the amine extraction and anion exchange of uranium, protactinium and thorium in nitric, hydrochloric and sulfuric acid. Peppard, Mckay and their coworkers[9-12] reported on the extraction of rare earth nitrates with tri-*n*-butyl phosphate.

In the present paper, the distribution coefficients of rare earth elements between anion exchange resin and nitric acid are compared with those between amine and nitric acid. Based on the resuls from these distribution studies, the mechanism of amine extraction is discussed.

Experimental

Materials.—Dowex 1, X8 (100~200 mesh), converted into nitrate form by nitric acid, is used as an anion exchange resin. Primene JM-T, Amberlite LA-2 and tri-*n*-octyl amine are respectively used as primary, secondary and tertiary amine. Amines are diluted with kerosene, and octyl alcohol is added to this solution to avoid the third phase formation, making phase separation clear. These amine solutions are converted into the nitrate form with 8 N nitric acid, as shown in the following equation.

$$RR'NH + HNO_3 \rightleftarrows RR'NH_2NO_3$$

Promethium-147 is used as a tracer of Pm. Other radioactive tracers of rare earth elements are prepared by neutron irradiation of rare earth oxides in J. R. R.-1 Reactor or by separation from isotopes of alkaline earth elements which are in a state of equilibrium with their daughter nuclides. The irradiated oxides are dissolved in 8 N nitric acid. The γ-ray spectrograms of these samples are obtained with a single channel pulse height analyzer and the radioactivities of these samples are measured by γ-ray or β-ray counting.

Table I shows the radioisotopes used in this experiment and the method for radioactivity measurement.

Table I. Radioisotopes of rare earth elements

Nuclide	Preparation	Counting method
^{140}La	Imported ^{140}Ba→^{140}La, coprecipitation with $Fe(OH)_3$, extraction of Fe by Amberlite LA-1 from 6 N HCl	γ
^{141}Ce	(n, γ)	γ
^{142}Pr	(n, γ)	β
^{147}Nd	(n, γ)	γ at 0.092 MeV. of ^{147}Nd
^{147}Pm	imported	β
^{152}Eu→^{154}Eu	(n, γ)	γ
^{159}Gd	(n, γ)	γ at 0.364 MeV. of ^{159}Gd
^{160}Tb	(n, γ)	γ
^{165}Dy	(n, γ)	γ
^{166}Ho	(n, γ)	γ
^{170}Tm	(n, γ)	γ
^{175}Yb	(n, γ)	γ at 0.396 MeV. of ^{175}Yb
^{176m}Lu→^{177}Lu	(n, γ)	γ

Sm and Er are omitted from this experiment because their γ-ray spectra resemble those of the daughters'.

Procedure.—The distribution coefficients in both anion exchange and amine extraction are measured by the batch method. Half a gram of dried resin is immersed in 5 ml. of nitric acid solution of rare earth elements and then shaken for 20 hr. at a constant temperature so that a state of equilibrium is attained. Then the sample is filtered and the activity of 1 ml. of the filtrate is compared with that of a reference solution.

In the case of the amine extraction, 2 ml. of 30% kerosene solution of amine is shaken for 1 min. with 2 ml. of nitric acid solution of rare earth element. Then resulting solution is then centrifuged and two phases are separated. The activity of both organic and aqueous solutions are measured. The distribution coefficient is calculated from the data which are obtained in these experiments.

1) D. J. Crouse et al., ORNL-2099 (1956).
2) J. C. Sheppard, HW-51958 (1957).
3) C. F. Coleman et al., A/Conf. 15/p/510 (1958).
4) K. B. Brown et al., ORNL-2269 (1957).
5) A. Preuss and J. Saunders, RMO-2533 (1955).
6) A. S. Wilson, A/Conf. 15/p/544 (1958).
7) D. J. Crouse and J. O. Denis, ORNL-1859 (1955).
8) F. Ichikawa and S. Uruno, This Bulletin, 33, 569 (1960).
9) D. P. Peppard et al., *J. Phys. Chem.*, 57, 294 (1953).
10) D. F. Peppard et al., *J. Am. Chem. Soc.*, 75, 6063 (1953).
11) H. A. C. Mckay et al., *J. Inorg. Nucl. Chem.*, 4, 304 (1957).
12) H. A. C. Mckay et al., idid., 9, 279 (1959).

Results

Distribution coefficients (K_d) of lanthanum, promethium and holmium are measured for the nitric acid solution of various concentrations.

Results are shown in Figs. 1—4. In the concentration range from 1 to 8 N nitric acid, the K_d value of anion exchange increases slowly and then decreases in acidities over 8 N. The distribution coefficients in primary amine extraction increases with the increase in the concentration of nitric acid. As is shown in Fig. 1, the maximum value of K_d decreases with increasing atomic number. In order to confirm this trend, values of K_d for rare earth elements in 8 N nitric acid is determined at 20°C. Fig. 5 shows the result of this experiment. For rare earth elements from lanthanum to gadolinium the K_d value decreases with increasing atomic number. The difference in the K_d value for rare earth elements of higher atomic number is very small and the relation between the K_d value and the atomic number is complicated.

In the case of amine extraction, the K_d values for rare earth elements are very small. Results are shown in Figs. 6—8. K_d decreases slowly from lanthanum to dysprosium in

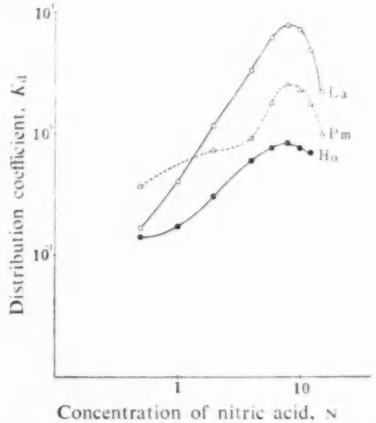

Fig. 1. Distribution coefficients of La, Pm and Ho between Dowex 1 and nitric acid.

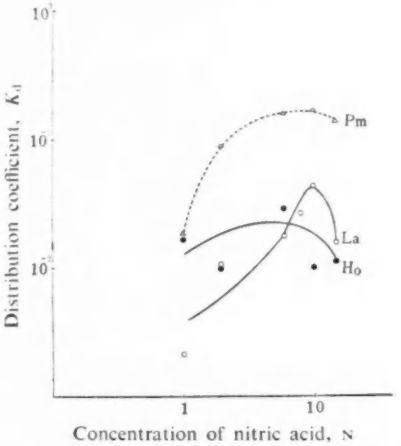

Fig. 3. Distribution coefficients of La, Pm and Ho between 30% Amberlite LA-2 and nitric acid.

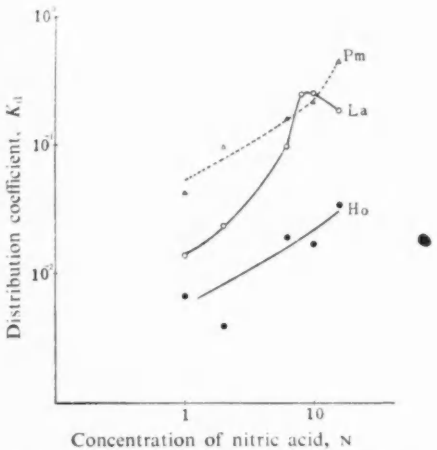

Fig. 2. Distribution coefficients of La, Pm and Ho between 30% Primene JM-T and nitric acid.

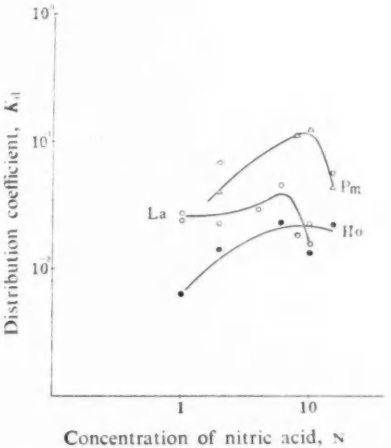

Fig. 4. Distribution coefficients of La, Pm and Ho between 30% tri-*n*-octyl amine and nitric acid.

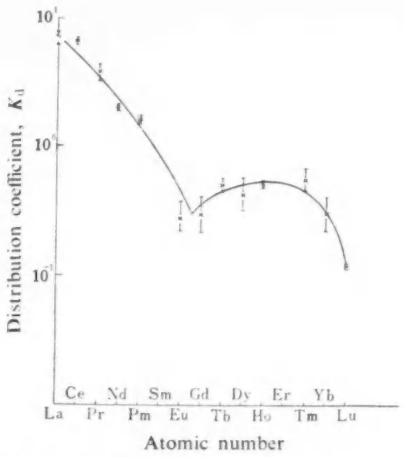

Fig. 5. Distribution coefficients of rare earth elements between Dowex 1 and 8 N nitric acid.

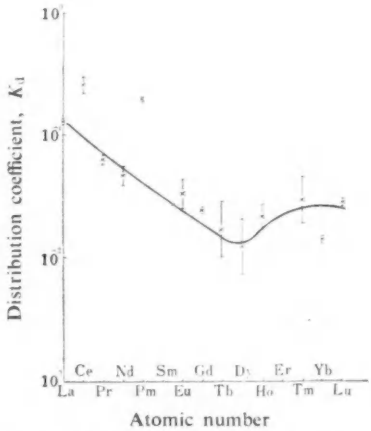

Fig. 6. Distribution coefficients of rare earth elements between 30% Primene JM-T and 8 N nitric acid.

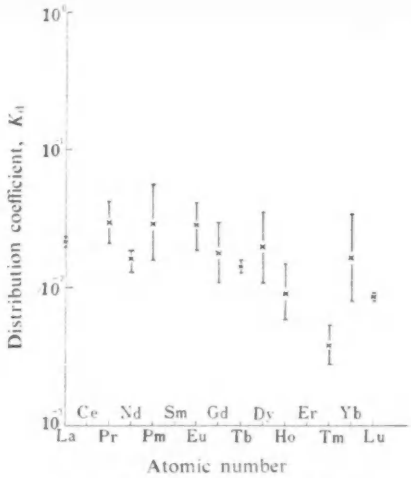

Fig. 7. Distribution coefficients of rare earth elements between 30% Amberlite LA-2 and 8 N nitric acid.

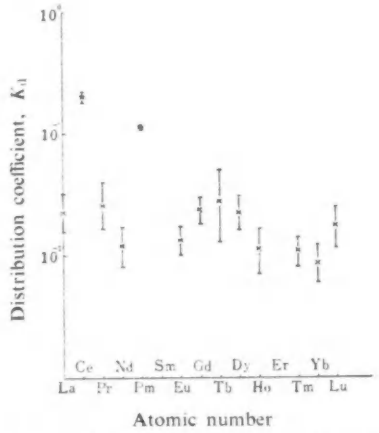

Fig. 8. Distribution coefficients of rare earth elements between 30% tri-*n*-octyl amine and 8 N nitric acid.

primary amine extraction. From holmium to lutetium, the difference in K_d value is very small. This is a tendency similar to that observed in anion exchange. As to the secondary amine extraction, a small decrease in K_d is found. But no significant variation in K_d is observed in tertiary amine extraction.

To compare these results, the extraction of rare earth elements by 100% TBP from 8 N nitric acid solution is studied. Fig. 9 shows the result. K_d value increases with increasing atomic number and this result is very different from those in anion exchange or amine extraction.

Discussion

Peppard and his coworkers[9,10] found the tendency of the increase in the extractability of rare earth nitrates by TBP with increasing atomic number. Mckay and his coworkers[11,12] reported that this trend is not always found in the subgroup from Gd to Lu. In the present experiment, the extractability of rare earth elements by 100% TBP from 8 N nitric acid solution also increased with increasing atomic number and some difference is found between lower and higher subgroups.

On the contrary, anion exchange study shows

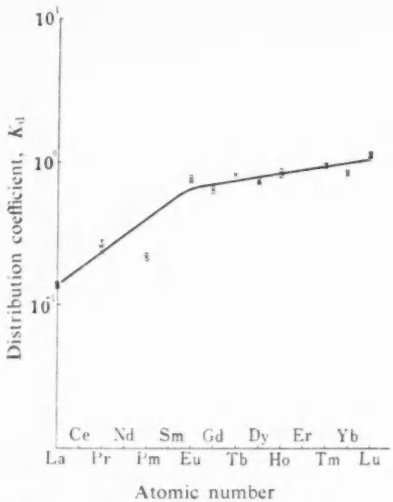

Fig. 9. Distribution coefficients of rare earth elements between 100% TBP and 8 N nitric acid.

decreasing of K_d value with increasing atomic number for rare earth elements of lower subgroup.

The different behavior of these two subgroups is probably due to the ionic radius, electronic structure and other characters. The reverse trend observed in TBP extraction and anion exchange might be due to the different probability of neutral complex formation and anionic complex formation in each circumstance.

From these points of view, the amine extraction behavior of these elements is very interesting. As is shown in Figs. 6—8, the difference in K_d value between rare earth elements of lower and higher atomic number is greater in the case of primary amine extraction than in secondary amine extraction. But, in both cases, decrease in K_d value with increasing atomic number is observed. It is suggested from these facts that the mechanism of amine extraction of rare earth elements resembles more the mechanism of anion exchange than TBP extraction does.

Summary

The amine extraction of rare earth elements in nitric acid is compared with anion exchange and TBP extraction with respect to the increase or decrease in K_d value with increasing atomic number of rare earth elements.

Concerning the relationship between distribution coefficient and atomic number of rare earth element, a similar trend is observed in anion exchange and amine extraction. The distribution coefficient decreases with increase in the atomic number. In TBP extraction, however, the corresponding value increases with increasing atomic number. It seems that the mechanism of amine extraction for rare earth element is similar to that of anion exchange.

The author expresses his gratitude to Dr. T. Nakai for his encouragement in this work. He also wishes to thank Miss. S. Uruno for assistance with experimental work.

Japan Atomic Energy Research Institute
Tokai, Ibaraki-ken

Vinyl Polymerization. XLVIII. Polymerization of Methylstyrenes and the Effect of Dimethylaniline on their Polymerization*

By Minoru IMOTO, Kiichi TAKEMOTO and Yuichi IIKUBO

(Received July 22, 1960)

Previously we have carried out polymerization of styrene and *p*-methylstyrene initiated by the azobisisobutyronitrile (ABIN)-dimethylaniline (DMA) system. Consequently a peculiar effect was observed in the polymerization of *p*-methylstyrene[1]. In this paper, the polymerization of *p*-methylstyrene with the ABIN-DMA system was studied repeatedly, and some different conclusions were obtained. The value of k_i in this system was also measured by the ferric chloride method of Bamford et al.[2]

* XLVII of this series: M. Imoto and I. Soematsu, in contribution.

1) M. Imoto and K. Takemoto, *J. Polymer Sci.*, **19**, 205 (1956).
2) J. C. Bamford, A. D. Jenkins and R. Johnston, *Proc. Roy. Soc.*, **A241**, 364 (1957).

As the polymerization of other monomethyl- and dimethylstyrenes has been little investigated, it was interesting to carry out the polymerization of these monomers. The polymerization with ABIN was studied in benzene, and rates of polymerization and intrinsic viscosities were determined.

Experimental

Syntheses of Monomers.—*Syntheses of p-Alkylstyrenes.*—*p*-Methyl-, *p*-ethyl- and *p-tert*-butylstyrene were synthesized from corresponding alkylbenzenes, according to the following sequence of reactions[3]:

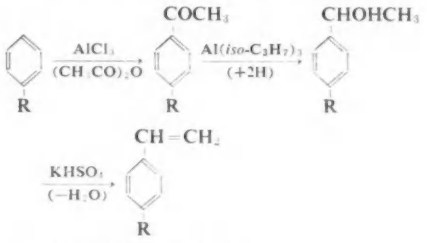

(R: CH_3, C_2H_5, *tert*-C_4H_9)

Synthesis of m-Methylstyrene.—*m*-Methylstyrene was synthesized from *p*-nitrotoluene as follows[4]:

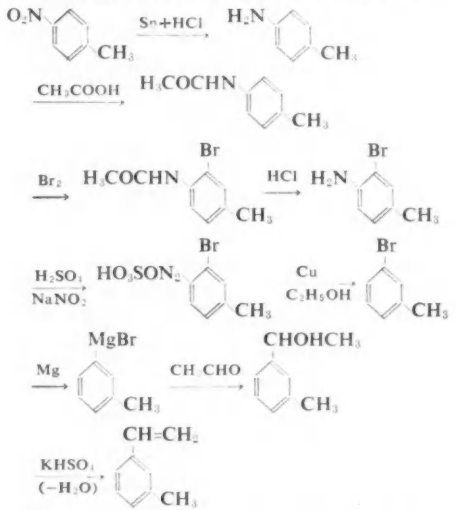

Syntheses of Dimethylstyrenes.—2,4-Dimethyl-, 2,5-dimethyl- and 3,4-dimethylstyrene were synthesized from corresponding xylenes in a manner similar to that used in the case of *p*-alkylstyrenes[5].

The Meerwein-Ponndorf reduction of the substituted acetophenones was found to be unsuccessful in the case of 3,4-dimethyl derivative. By the direct hydrogenation in autoclave, using copper-chromium oxide or Raney nickel as catalyst, 3,4-dimethylphenylcarbinol was obtained with yield of 90%.

Purification of Monomers.—All monomers were purified by distillation in vacuo under flushing of nitrogen after drying over calcium chloride. Before use, they were distilled again through a 40 cm. Stedman column. Reflux ratios were 10 : 1~6 : 1. Physical constants of the monomers were shown in Table I. Infrared spectroscopic analyses were also made for all the monomers to ascertain their structures.

Styrene was purified by distillation in the same manner as the substituted styrenes (b. p. 145 °C/760 mmHg).

Purification of Reagents.—2,2'-Azobisisobutyronitrile (ABIN) was purified by recrystallization from methanol and dried in vacuo (m. p. 103 °C). Dimethylaniline (DMA) was distilled in a nitrogen atmosphere and stored. Before use, it was again distilled under reduced pressure through a Vigreux column (b. p. 68 °C/10 mmHg). Benzene was distilled, after thiophene was removed, dried over calcium chloride and again distilled over metallic sodium (b. p. 80 °C). Ferric chloride ($FeCl_3 \cdot 6H_2O$), commercial pure grade, was used after crushing. Benzoquinone was synthesized from hydroquinone by oxidation with sodium dichromate and purified by sublimation under reduced pressure twice before use (m. p. 113~114 °C). Nitrogen was purified by washing through alkaline pyrogallol solution and concentrated sulfuric acid and by passing over reduced copper at 550 °C.

Procedures.—*Measurement of Rate of Polymerization.*—In order to determine the initial rate of polymerization, the dilatometric and usual sealed tube methods were adopted. In some experiments, the dilatometer reported earlier[6] was used. In another case, a dilatometer in a different form was used, the total capacity being about 4.5~5.5 ml. and the diameter of the capillary tube about 0.3~0.5 mm.

Polymerization was carried out as described in the previous paper. The polymerization temperature was regulated within ±0.02 °C in the case of dilatometry, and ±0.05 °C in the case of the sealed tube method.

Measurement of Intrinsic Viscosity.—Intrinsic viscosities $[\eta]$ of polymers were measured in benzene solution at 30±0.1 °C, using Ostwald's viscometer. Assuming that the following equation given by Tobolsky et al.[7] for polystyrene can also be available for substituted polystyrenes, the number-average polymerization degree $\bar{P}_n$ of all polymers was computed.

$$\bar{P}_n = 1770[\eta]^{1.40}$$

Measurement of Rate of Decomposition of ABIN.—The rate of decomposition of ABIN was measured, with the volume of nitrogen evolved[8].

3) C. G. Overberger, C. Frazier, J. Mandelman and H. G. Smith, *J. Am. Chem. Soc.*, **75**, 3326 (1951).
4) C. S. Marvel, C. G. Overberger, R. E. Allen and J. H. Saunders, ibid., **68**, 736 (1946).
5) C. S. Marvel, J. H. Saunders and C. G. Overberger, ibid., **68**, 1085 (1946).
6) M. Imoto and K. Takemoto, *J. Polymer Sci.*, **18**, 377 (1955).
7) D. H. Johnson and A. V. Tobolsky, *J. Am. Chem. Soc.*, **74**, 938 (1952).
8) M. Imoto, T. Otsu, T. Ota, H. Takatsugi and M. Matsuda, *J. Polymer Sci.*, **22**, 137 (1956).

TABLE I. PHYSICAL PROPERTIES OF SUBSTITUTED STYRENES

Styrene	B. p., °C (mmHg)	S. g.	Refractive index
p-Methylstyrene	58 (7)	$d_4^{25}=0.890$	$n^{25}=1.5393$
p-Ethylstyrene	68 (10)	$d_4^{20}=0.9070$	$n^{25}=1.5349$
p-tert-Butylstyrene	90~92 (10)	$d_4^{23}=0.8739$	$n^{20}=1.5212$
m-Methylstyrene	90~91 (30)	$d_{25}^{25}=0.9032$	$n^{24.5}=1.5392$
2,4-Dimethylstyrene	90 (25)	$d_{25}^{25}=0.9048$	$n^{20.5}=1.5425$
2,5-Dimethylstyrene	81~83 (23)	$d_{25}^{25}=0.9050$	$n^{20}=1.5389$
3,4-Dimethylstyrene	86~88 (20)	$d_{25}^{25}=0.9200$	$n^{20}=1.5420$

TABLE II. RATES OF POLYMERIZATION AND DEGREES OF POLYMERIZATION FOR SUBSTITUTED STYRENES

Monomer	Rate of polymerization: Sealed tube method, 50°C (mol./l. sec.)	Rate of polymerization: Dilatometry, 70°C (mol./l. sec.)	Degree of polymerization $\bar{P}_n$
Styrene	11.13×10^{-6}	5.10×10^{-6}	700
p-Methylstyrene	14.30	5.32	190
p-Ethylstyrene	—	2.13	—
p-tert-Butylstyrene	—	1.73	—
m-Methylstyrene	4.20	—	280
2,4-Dimethylstyrene	6.52	—	150
2,5-Dimethylstyrene	6.86	—	300
3,4-Dimethylstyrene	10.96	—	490

* Monomer concentration = 3.43 mol./l., ABIN concentration = 1.097×10^{-2} mol./l.
** Monomer concentration = 0.455 mol./l., ABIN concentration = 2.50×10^{-3} mol./l.

Results

Polymerization of Substituted Styrenes.—*Polymerization of p-Alkyl- and Dimethylstyrenes.*— Polymerizations of styrene, *p*-methyl-, *p*-ethyl- and *p-tert*-butylstyrene were carried out dilatometrically in benzene at 70°C. The linear time-conversion relationship was obtained for all runs. Polymerization of *m*-methyl-, 2,4-dimethyl-, 2,5-dimethyl and 3,4-dimethylstyrene were also carried out in benzene at 50°C by the sealed tube method. Time-conversion curves were shown in Fig. 1 (including the curves of styrene and *p*-methylstyrene), where the concentrations of monomer and initiator were kept constant at 3.43, and 1.097×10^{-2} mol./l., respectively. The linear time-conversion curves were also obtained. The rate for *p*-methylstyrene was greater than that for styrene. The rates for other monomers were smaller than that for styrene.

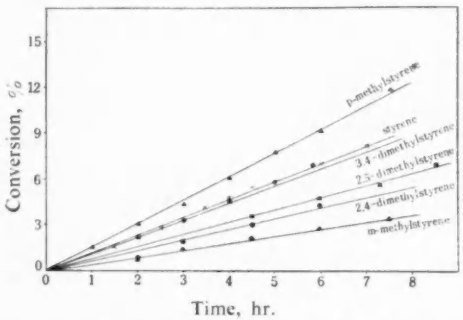

Fig. 1. Time-conversion curves for polymerization of substituted styrenes initiated by ABIN (sealed tube, in benzene, 50°C).
[M] = 3.43 mol./l.
[ABIN] = 1.097×10^{-2} mol./l.
50°C, in benzene

The values of the rate of polymerization obtained were tabulated in Table II. The table includes also the values of degree of polymerization. The polymers used for the determination of $[\eta]$ were obtained by 4.5 hr. polymerization.

Comparing the values of $\bar{P}_n$ and Rp of *p*-methylstyrene with these of styrene, it was assumed that *p*-methylstyrene easily underwent chain transfer reaction. This was because in spite of the larger value of Rp, the degree of polymerisation was smaller. In order to study the effect of solvents on reaction, polymerization of *p*-methylstyrene was carried out in acetone or dimethylformamide (DMF) in the same manner as in benzene. As shown in Table III, the rates of polymerization in acetone were nearly the same as that in benzene. But the value obtained in DMF was relatively low. Separation of the polymer from benzene or DMF solution was easy, because the polymer separated granulously when the reaction mixture was poured into an excess of methanol.

TABLE III. OVERALL RATES OF POLYMERIZATION OF *p*-METHYLSTYRENE IN SOME SOLVENTS (DILATOMETRY, 60°C)

Exp. run	Solvent	Rate of polymerization mol./l. sec.
1	Dimethylformamide	2.13×10^{-5}
2	〃	2.08
3	Benzene	2.47
4	〃	2.46
5	〃	2.56
6	Acetone	2.46
7	〃	2.47

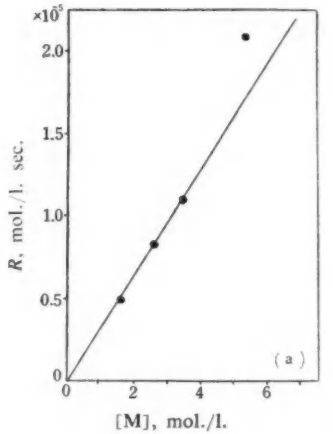

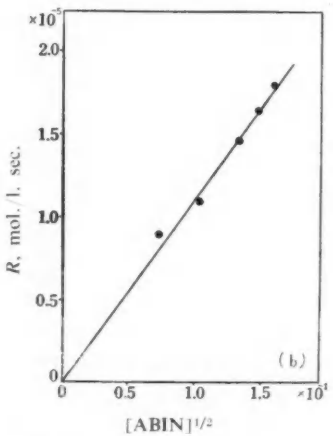

Fig. 2. Polymerization of 3,4-dimethylstyrene initiated by ABIN (sealed tube, in benzene, 50°C).
(a) Relationship of the initial rate of polymerization with the monomer concentration. ([ABIN] = 1.098×10^{-2} mol./l.)
(b) Relationship of the initial rate of polymerization with the initiator concentration. ([M] = 3.49 mol./l.)

However, when acetone was used, a turbid emulsion was obtained and the separation by filtration was much more difficult.

Rate Equation of Polymerization for Substituted Styrene.—From the results of 3,4-dimethylstyrene as shown in Fig. 2, the following equation was derived. This was identical with that for styrene.

$$R_p = k\,[\mathrm{M}]\,[\mathrm{ABIN}]^{1/2}$$

Determination of Rate Constants for Initiation.—The rate constants of initiation of the polymerization of styrene and *p*-methylstyrene were determined, according to the $FeCl_3$-method by Bamford et al.[2], using the following equation.

$$\tau = \frac{[FeCl_3\cdot6H_2O]}{2f\cdot k_d\,[ABIN]} = \frac{[FeCl_3\cdot6H_2O]}{2k_i\,[ABIN]}$$

where τ is the induction period (in minutes), f the initiator efficiency, and k_d and k_i the rate constants for decomposition of initiator and for initiation, respectively. The measurement of the value of τ for *p*-methylstyrene was carried out in DMF at 60°C.

In Fig. 3, examples of the time-conversion curve were illustrated. In Fig. 4, the relationship between the induction period and the amount of ferric chloride was shown. In Fig. 5, the relationship between the concentration of ABIN and the reciprocal of induction period was shown. The rate constants of initiation

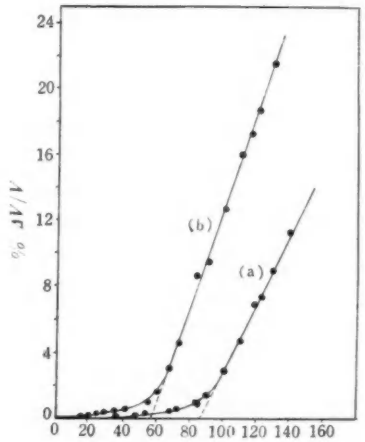

Fig. 3. Time-conversion curve for polymerization of *p*-methylstyrene initiated by ABIN in the presence of ferric chloride (in DMF, 60°C).
[M] = 2.17 mol./l.
[$FeCl_3\cdot6H_2O$] = 4.46×10^{-3} mol./l.
(a) [ABIN] = 6.12×10^{-2} mol./l.
(b) [ABIN] = 1.00×10^{-1} mol./l.

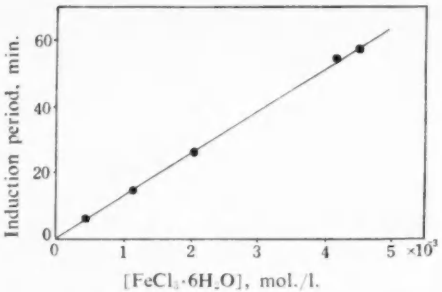

Fig. 4. Relationship between the induction period and the amount of ferric chloride in the polymerization of *p*-methylstyrene (in DMF, 60°C). [M]=2.17 mol./l., [ABIN]=1.00×10^{-1} mol./l.

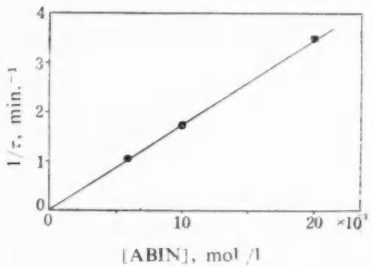

Fig. 5. Relationship between the induction period and the amount of ABIN in the polymerization of *p*-methylstyrene (in DMF, 60°C). [M]=2.17 mol./l., [$FeCl_3\cdot6H_2O$]=4.46×10^{-3} mol./l.

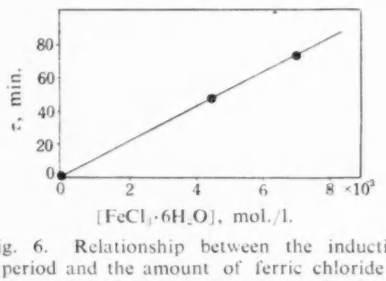

Fig. 6. Relationship between the induction period and the amount of ferric chloride in the polymerization of styrene (in DMF, 60°C). [M]=2.04 mol./l., [ABIN]=1.00×10^{-1} mol./l.

for the polymerization of *p*-methylstyrene were estimated as follows:

$$k_i=0.67\times10^{-5}\ (\mathrm{sec}^{-1})$$

Similar determination was also made for styrene in DMF at 60°C, and the result obtained was shown in Fig. 6. The value of k_i was as follows:

$$k_i=0.76\times10^{-5}\ (\mathrm{sec}^{-1})$$

This value was in good agreement with the value, $k_i=0.70\times10^{-5}$ (sec^{-1}), obtained by Bamford et al. From the agreement of our value with that by Bamford et al., the value of k_i for *p*-methylstyrene seemed to be reasonable.

As for k_t, the value for *p*-methylstyrene was found to be rather smaller than that for styrene. As shown in the former section of this paper, however, the overall rate of the polymerization of *p*-methylstyrene was greater than that of styrene. These results imply that in the sase of *p*-methylstyrene the rate constant for the propagation would be greater than that for styrene, or, that the rate constant of the termination k_t would be smaller. Further work will be done to clarify this point.

Polymerization of Substituted Styrene in the Presence of Dimethylaniline.—Polymerization of Styrene and *p*-Methylstyrene.—*a) Polymerization with Bz_2O_2-DMA.*—Polymerization of *p*-methylstyrene was carried out dilatometrically at 70°C, using a system of benzoyl peroxide (Bz_2O_2)-dimethylaniline (DMA) as initiator. Time-conversion curves were shown in Fig. 7, where the concentrations of monomer and Bz_2O_2 were kept constant at 0.455 and 2.50×10^{-3} mol./l., respectively, and the concentration of DMA was varied from 0 to 0.02 mol./l. Fig. 8 shows the results obtained, where the concentration of monomer and DMA were kept constant at 0.455 and 2.50×10^{-3} mol./l., respectively, and the concentration of Bz_2O_2 was varied from 0 to 0.085 mol./l. The initial rates of polymerization were determined by the extrapolation method previously reported[5].

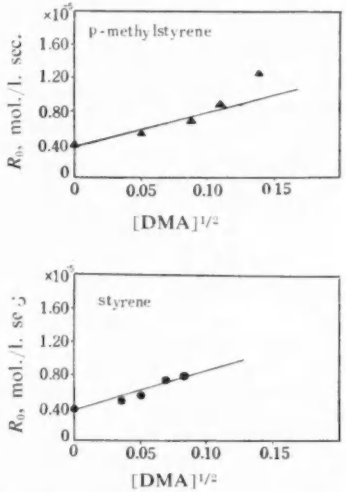

Fig. 7. Polymerization of styrene and *p*-methylstyrene initiated by Bz_2O_2 at 70°C (dilatometry).

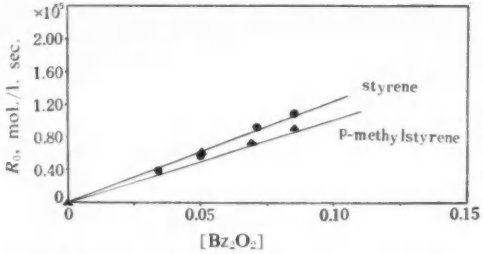

Fig. 8. Polymerization of styrene and *p*-methylstyrene initiated by Bz_2O_2 at 70°C (dilatometry).

The polymerization of styrene was carried out in parallel.

It was found that in the polymerization of *p*-methylstyrene, the initial rate of polymerization was also regarded as of 1/2-order with the concentrations of Bz_2O_2 and DMA, respectively.

$$R_i = k'[Bz_2O_2]^{1/2}[DMA]^{1/2}$$

This agrees well with the results reported for the polymerization of several vinyl monomers[9].

b) Polymerization with ABIN-DMA.—Polymerizations of styrene and *p*-methylstyrene were carried out dilatometrically at 70°C by the ABIN-DMA system. Keeping the concentrations of monomer and ABIN constant at 0.455 and 2.50×10^{-3} mol./l., respectively, and varying the concentration of DMA from 0 to 2.5×10^{-2} mol./l., the initial rates of polymerization were measured.

Previously, two of the present authors, M. Imoto and K. Takemoto, published a paper on the polymerization of *p*-methylstyrene by ABIN-DMA[1]. There an apparent conclusion was obtained that the initial rate of polymerization increased with the addition of a small

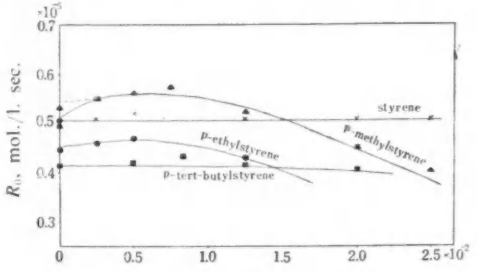

Fig. 9. Polymerization of styrene and *p*-alkylstyrenes initiated by ABIN in the presence of DMF at 70°C.
[M] = 0.455 mol./l.
[ABIN] = 2.50×10^{-3} mol./l.

9) M. Imoto, T. Otsu and T. Ota, *Makromol. Chem.*, **16**, 10 (1955).

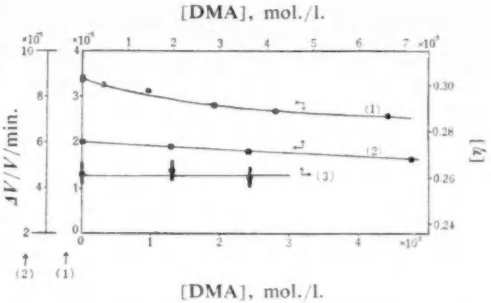

Fig. 10. Relationship of overall rate and intrinsic viscosity with the amount of DMA in the polymerization of *p*-methylstyrene initiated by ABIN at 60°C (in benzene).
[M] = 2.17 mol./l., [ABIN], (1) 1.00×10^{-1} mol./l., (2), (3) 2.68×10^{-3} mol./l.

quantity of DMA and then decreased with the increasing quantity of DMA, after passing a maximum value (Fig. 9). It had been assumed that this phenomenon was due to the acceleration of the hyperconjugation effect of the *p*-alkyl group by DMA. For four years the study to ascertain this phenomenon was carried out repeatedly. In many cases, it was observed that no such accelerating effect by DMA existed as shown in Fig. 10.

Granting the dotted line in Fig. 9 to be correct, the former observations coincided with the results obtained in this paper. (As stated above, the rate of polymerization of *p*-methylstyrene was surely greater than that of styrene.) It was now concluded that an accelerating effect by hyperconjugation might be denied, and that the initial rates of polymerization seemed to decrease with DMA as seen from Figs. 9 and 10.

Polymerization of Dimethylstyrenes and *m*-Methylstyrene.—We have carried out further

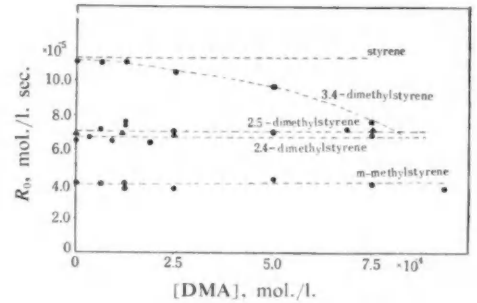

Fig. 11. Polymerization of *m*-methylstyrene and dimethylstyrenes initiated by ABIN in the presence of DMA at 50°C.
[M] = 3.43 mol./l.
[ABIN] = 1.097×10^{-2} mol./l.

experiments on the polymerization of dimethylstyrenes in order to examine the effect of DMA on the polymerization initiated by ABIN.

Polymerization was carried out by the sealed tube method at 50°C. The concentrations of the monomer and ABIN were kept constant at 3.43 and 1.097×10^{-2} mol./l. respectively, while the concentration of DMA was varied from 0 to 1.0×10^{-1} mol./l. As shown in Fig. 11, in the case of *m*-methylstyrene no effect of DMA on the initial rate was observed as in the case of styrene, while in the case of 2,4- and 3,4-dimethylstyrene a slight decrease with DMA was observed.

Measurement of Intrinsic Viscosity.—Intrinsic viscosities of the polymers obtained were measured in benzene at 30°C. Figs. 10 and 12 gave the plots of the intrinsic viscosities to the amounts of DMA added in the polymerization. From the results, it was concluded that no effect of DMA on the intrinsic viscosity was present.

Rate of Decomposition of ABIN in the Presence of DMA and Monomer.—The rate of decomposition of ABIN was measured at 50°C in benzene in the presence of monomer and DMA, using the apparatus described in the experimental part. The concentration of ABIN was kept constant at 9.84×10^{-2} mol./l.

It was established that the rate of decomposition of ABIN was independent of the concentrations of styrene and DMA as shown in Fig. 13.

Relationship between DMA and Induction Period.—(*a*) *In DMF, with Ferric Chloride.*—We have already shown that an induction period was observed in the polymerization of styrene or *p*-methylstyrene in the presence of ferric chloride. We have studied further the effect of DMA on the induction period for the polymerization of *p*-methylstyrene initiated by ABIN in DMF, where the concentrations of ABIN and ferric chloride were kept constant at 1.00×10^{-1} and 3.5×10^{-3} mol./l. respectively, and the concentration of DMA was varied from 0 to 2.4 mol./l. As can be seen from Fig. 14 and Table IV, it was found that no effect of DMA on the induction period was observed.

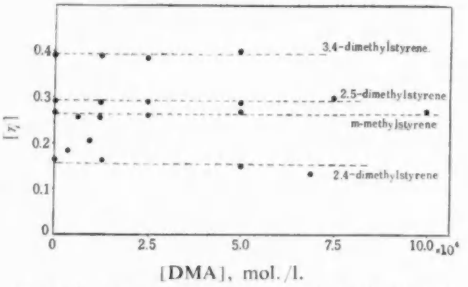

Fig. 12. Intrinsic viscosity for the substituted styrene polymers (30°C, in benzene).

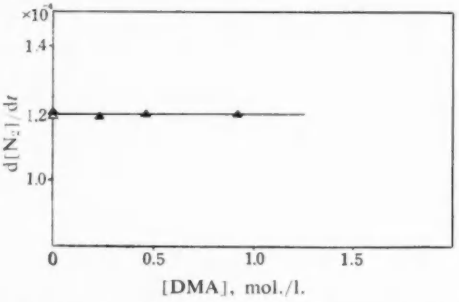

Fig. 13. Decomposition rate of ABIN in the presence of monomer and DMA at 50°C (in benzene).
[M] = 0.253 mol./l.
[ABIN] = 9.84×10^{-2} mol./l.
△ In the absence of monomer
▲ In the presence of monomer

TABLE IV. RELATIONSHIP BETWEEN INDUCTION PERIOD AND THE AMOUNT OF DMA AT 60°C (IN DMF)
[ABIN] = 1.00×10^{-1} mol./l., [M] = 2.17 mol./l.,
[$FeCl_3\cdot6H_2O$] = 3.5×10^{-3} mol./l.

Amount of DMA mol./l.	Induction period min.
5×10^{-3}	43.0
1×10^{-2}	43.0
3×10^{-1}	44.0
6×10^{-1}	44.5
1.2	43.5
2.4	39.0
0	43.0

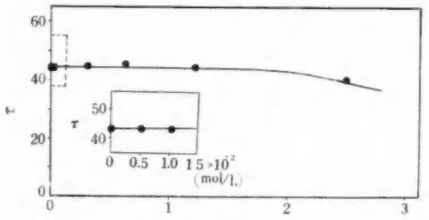

Fig. 14. Relationship between induction period and the amount of DMA in the polymerization of *p*-methylstyrene at 60°C (in DMF). [M] = 2.17 mol./l., [ABIN] = 1.00×10^{-1} mol./l., [$FeCl_3\cdot6H_2O$] = 3.5×10^{-3} mol./l.

(*b*) *In Benzene, with p-Benzoquinone.*—It could not be completely denied, that DMF reacted with a free radical. Therefore, it was

considered that DMF was not the most suitable solvent. Thus, in the following runs, benzene was chosen as solvent. However, ferric chloride did not dissolve in benzene. We have studied finally the polymerization of *p*-methylstyrene in the presence of *p*-benzoquinone and DMA in benzene and studied the effect of DMA on the induction period, on the rate of polymerization after induction period and on the intrinsic viscosity of polymers. As can be seen from Fig. 15 and Table V, the induction period was decreased with the amount of DMA, which was somewhat different from the result obtained when the ferric chloride-DMA system was used. The rate of polymerization after the induction period had a tendency to increase,

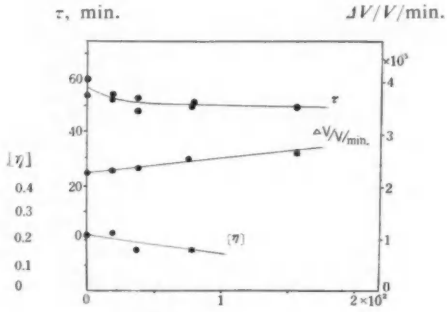

Fig. 15. Relationship of the amount of DMA with induction period, with over-all rate after induction period, and with intrinsic viscosity in the polymerization of *p*-methylstyrene at 60°C (in benzene). [M]=2.17 mol./l., [ABIN]=7.05×10^{-3}mol./l., [*p*-Benzoquinone] =1.06×10^{-3} mol./l.

Table V. Induction period, and over-all polymerization rate after induction period in the polymerization of *p*-methylstyrene in the presence of DMA at 60°C (in benzene)

DMA mol./l.	Induction period min.	Volume conversion $\Delta V/V$/min.	Rate$\times10^5$ mol./l./sec.
0	56.0	—	—
2×10^{-3}	54.0	—	—
4×10^{-3}	49.0	—	—
8×10^{-3}	52.0	—	—
0	60.5	2.24	1.69
1.8×10^{-3}	53.5	2.27	1.71
3.8×10^{-3}	54.0	2.27	1.71
7.8×10^{-3}	51.5	2.43	1.82
15.6×10^{-3}	49.5	2.60	1.95

while the intrinsic viscosities decreased with DMA.

Determination of the individual rate constants in the polymerization of *p*-methylstyrene is in progress using the sector method. The results will be reported in near future.

Summary

1. Solution polymerizations of styrene, *p*-methyl-, *p*-ethyl-, *p*-*tert*-butyl-, *m*-methyl-, 2,4-dimethyl-, 2,5-dimethyl- and 3,4-dimethylstyrene were carried out at 50 and 70°C by ABIN in benzene, and the rates of polymerization and $[\eta]$'s of the polymers were determined. For 3,4-dimethylstyrene, the same equation as for styrene was obtained:

$$R_0=k[\mathrm{M}][\mathrm{ABIN}]^{1/2}$$

2. Rate constants of initiation of the polymerizations of styrene and *p*-methylstyrene were determined, according to the $FeCl_3$-method as follows:

$$k_i=0.67\times10^{-5}\ (\mathrm{sec}^{-1})$$

(for *p*-methylstyrene)

$$k_i=0.76\times10^{-5}\ (\mathrm{sec}^{-1})\ \text{(for styrene)}$$

3. Polymerizations of styrene and *p*-methylstyrene were carried out at 70°C by the Bz_2O_2-DMA system, and the same equation as styrene was derived for *p*-methylstyrene as follows:

$$R_0=k'[\mathrm{Bz_2O_2}]^{1/2}[\mathrm{DMA}]^{1/2}$$

4. Polymerizations of styrene, *p*-methyl-, and dimethylstyrenes were carried out at 50 and 70°C by ABIN-DMA system, and the results for the rate of polymerization and the value of $[\eta]$ were discussed. A correction was made for the results previously obtained.

5. The effect of DMA on the induction period for the polymerization of *p*-methylstyrene was studied at 60°C. In the case of polymerization with $FeCl_3$ in DMF, no effect of DMA on the induction period was observed, while in the case of that with *p*-benzoquinone in benzene, the induction period was decreased with the amount of DMA.

Faculty of Engineering
Osaka City University
Kita-ku, Osaka
(*M. I. & K. T.*)

Onoda Cement Co. Ltd.
Onoda Factory
Onoda-shi, Yamaguchi-ken
(*Y. I.*)

Visco-elastic Behaviors of Aluminum Soap-Hydrocarbon Systems. I. Aluminum Stearate in Nujol

By Sukekuni SHIBA

(Received August 6, 1960)

Aluminum soaps dispersed in hydrocarbon oils exhibit many interesting flow properties. Gelling characteristics of aluminum soaps and flow properties of aluminum soap-hydrocarbon systems have been studied by many authors[1-3].

Flow properties have been studied usually for viscous or plastic properties under static conditions. The conception of "elastic fluid" for these systems was adopted first by Goldberg and Sandvik[4], who studied visco-elastic properties (dynamic viscosity and shear modulus) of aluminum soaps gelled in varsol, and found breakdown under steady shear at audio frequency. Garner, Nissan and Wood[5], studying elasto-viscous properties of aluminum stearate in petrol, found the correlation of free energy with the mechanical shearing of the system. Weber and Bauer[6], studying flow properties of aluminum dilaurate-toluene gels, found from the initial elastic axial extension in a capillary that pronounced elastic properties appear abruptly in the gels as the concentration of soap increases, and a concentration of 1% by weight of aluminum dilaurate in toluene is reached.

In the preceding paper[7], flow properties of aluminum soaps in nujol and time effects of flow under shear were studied in static conditions. In the present paper, dynamic visco-elastic behaviors of aluminum stearate dispersed in nujol were studied in a region of low frequency, rangining from 10^{0} to 10^{-3} cycles/sec. to examine the correlation of the rheological properties and dispersed states of the soaps.

Experimental

Materials.—Aluminum stearate was prepared from purified stearic acid by a metathetic process as described in the previous paper[7]. Stearic acid, found: m. p., 69.5°C; neutralization equivalent, 281.9. Analysis of the soap showed that the ratio of moles of acid per mole of aluminum was 1.72. Nujol, which was a paraffin-rich saturated hydrocarbon, was used as a vehicle. Physical constants were: $d_4^{25}=0.8429$; $\eta_{25}=0.217$ poise; $n_D^{20}=1.4672$. The purity of the materials was checked by infrared absorption measurements.

Apparatus.—A top-drive concentric cylinder rheometer, essentially the same as the apparatus designed by Nakagawa[8], was used. The outer cylinder was fixed in a thermostat; the inner cylinder was suspended coaxially on a torsion wire. The specimen was placed in the annular space between the two cylinders, and a sinusoidal torsional oscillation was applied at the top of the torsion wire. The oscillation of the inner cylinder was detected by a small mirror attached to the inner cylinder, and the oscillation was combined rectangularly with the driving oscillation optically. The resulting Lissajous' figure, which indicates the phase angle and amplitude ratio of the oscillations, was recorded on an oscillographic paper and analysed for visco-elasticity by an approximate method neglecting the inertia of the specimen. Details of the apparatus and analysis were reported elsewhere[9].

Procedure.—Aluminum stearate was added to the weighed portions of nujol and the mixture was heated at 110~120°C with stirring for 15 min. The resulting isotropic solution was cooled and kept in a desiccator over phosphorus pentoxide. The specimen thus prepared was aged more than 24 hr. at room temperature. Measurements were carried out under the following conditions:

Temperature; 15~100°C.
Period of oscillation; 2~1,000 sec.
Maximum shear strain; 0.01~0.3.
Soap concentration; up to 1 wt. %.

Experiments were performed avoiding effects of humidity as far as possible.

Results and Discussion

The systems both in gel and sol states behave always as visco-elastic bodies. A relatively dilute system (sol) shows linear visco-elastic behaviors, whereas a more concentrated system (gel) shows non-linear behaviors as seen in the case of static measurements[7]. In this experiment, the systems were treated as linear visco-elastic bodies, because the shear strain was

1) V. R. Gray and A. E. Alexander, *J. Phys. & Colloid Chem.*, **53**, 9 (1949).
2) H. Sheffer, *Can. J. Research*, **B-26**, 481 (1948).
3) E. K. Rideal et al., *Proc. Roy. Soc.*, **A200**, 135 (1950).
4) H. Goldberg and O. Sandvik, *Anal. Chem.*, **19**, 123 (1947).
5) F. H. Garner, A. H. Nissan and G. F. Wood, *Phil. Trans. Roy. Soc.*, **A243**, 37 (1950).
6) N. Weber and W. H. Bauer, *J. Phys. Chem.*, **60**, 270 (1956).
7) S. Shiba, This Bulletin, **33**, 1563 (1960).
8) T. Nakagawa and M. Senō, This Bulletin, **29**, 471 (1956).
9) S. Shiba, *Railway Technical Research Report*, **No. 112** (Feb. 1960).

small and approximation by linear behaviors was possible.

Aging.—It is necessary to examine the effect of aging in order to get reproducible results. Changes in dynamic viscosity η and shear modulus G with time are shown in Fig. 1.

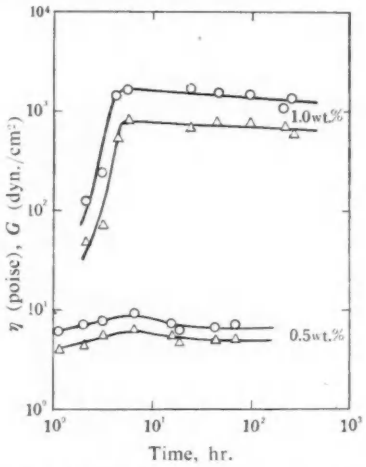

Fig. 1. Change in dynamic viscosity (○) and modulus (△) with time.
25°C, period $T=12$ sec.

Rapid increase in dynamic properties was found in the first stage of aging, then the properties approach constant values after they reach maximum values 4~6 hr. after preparation of the specimen. This result supports the results obtained by viscosity and flow birefringence measurements for benzene and nujol solutions of aluminum soaps[7-10]. However, the change in the properties of a gel was extraordinarily great compared with other cases. This fact indicates that the properties of the system which has not been disturbed by shear were measured in this experiment; whereas in the former reports, a state in which the weak structures formed by aging in the system had been broken, was measured.

Amplitude Dependence.—Effects of amplitude of oscillation which are a measure of non-linear behavior, were examined changing the amplitude of the oscillation given at the top of the torsion wire. Results are shown in Fig. 2, where γ_{max} is the maximum shear strain at the wall of the internal cylinder expressed as follows;

$$\gamma_{max}=\left[\frac{2Ar_e^2r_i^2}{(r_e^2-r_i^2)r^2}\right]_{r=r_i}=\frac{2Ar_e^2}{r_e^2-r_i^2} \qquad (1)$$

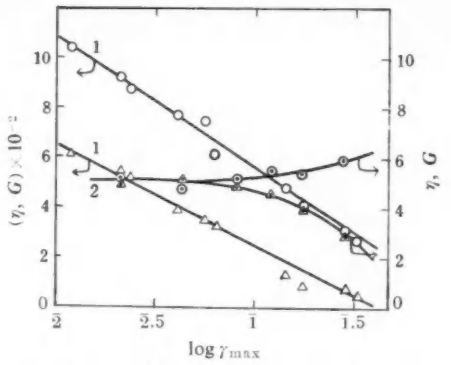

Fig. 2. Amplitude dependence of dynamic viscosity (○) and shear modulus (△), 25°C, period $T=12$ sec, 1. 1.0 wt. %, 2. 0.5 wt. %.

A is the amplitude of the oscillation of the internal cylinder; r_i and r_e are the radii of internal and external cylinders, respectively. The 1 wt. % gel shows marked amplitude dependence; for the 0.5 wt. % sol dependence is found for large values of γ, but is negligible for usual measurements carried out in the region of γ up to 0.1.

As was found from static measurements of viscosity[7], the aluminum soap-hydrocarbon gels undergo shear breakdown. Accordingly, amplitude dependence may be ascribed not only to the non-linearity but also to the shear breakdown of the rheological structures. In the first stage of flow, it requires a certain amount of work to begin deformation against the network structures in the gel, and this work results in the amplitude effect in this experiment. It is not clear, however, whether the effect is due completely to shear strain or to the rate of shear; because the maximum rate of shear changes proportionally to shear strain when other conditions are equal.

Because of this dependence, a series of experiments should be carried out under constant shear strain and shear rate, but the apparatus is not suitable for this purpose. The amplitude was kept as small and constant as possible to avoid these effects.

Frequency Dependence.—Frequency dependence of the dynamic rheological properties of the system was examined under various conditions. Fig. 3 shows the shear modulus, dynamic loss, and relaxation spectra of a gel containing 1 wt. % of soap in nujol. The spectra were obtained from shear modulus (E') and dynamic loss (E'') by the approximation method[11],

10) J. W. McBain and E. B. Working, *J. Phys. & Colloid Chem.*, **51**, 974 (1947).

11) F. Schwarzl, "Proceedings of the Second International Congress on Rheology" (Edited by V. G. W. Harrison), Butterworths Sci. Pub., London (1954), p. 197.

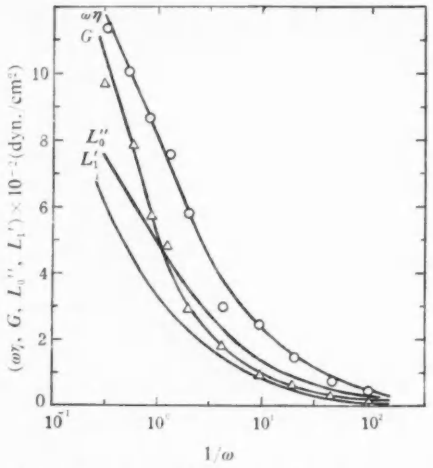

Fig. 3. Frequency dispersion of visco-elasticity and relaxation spectra, 25°C, 1.0 wt%.

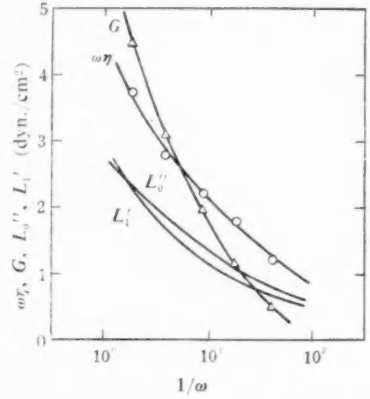

Fig. 4. Frequeny dispersion of visco-elasticity and relaxation spectra, 25°C, 0.5 wt. %.

$$L(t) \simeq L_1'(t) = [\mathrm{d}E'(\omega)/\mathrm{d}\log\omega]_{\omega=1/t} \qquad (2)$$

$$L(t) \simeq L_0''(t) = (2/\pi)\,[E''(\omega)]_{\omega=1/t} \qquad (3)$$

In these formulae L without index is the exact spectrum, whereas L with index indicates an approximation to the spectrum. The system shows typical visco-elastic properties. Curves of visco-elasticity show marked dispersion; the dynamic shear modulus and dynamic loss increase conspicuously with the increase of frequency. Relaxation spectra obtained from the two approximation methods show similar results. The spectra show a wedge type similar to the spectra found for polyisobutylene. This indicates that the gel resembles the polymer solution or gels in dynamic properties, accordingly the dispersed state of the soap crystallites as well. Fig. 4 shows the dispersion of a sol containing 0.5 wt. % of soap in nujol; similar results are observed in this case, although the visco-elasticity is far smaller than in the case of gel.

Frequency dependence at various temperatures is shown in Figs. 5 and 6. At each temperature, similar dispersion is found. It is possible to express these data by a single curve by the method of reduced variables[12]. The reduced curves for the dynamic shear modulus and dynamic loss are shown in Fig. 7. Good coincidence was found except for the data obtained at 80°C. The results suggest the

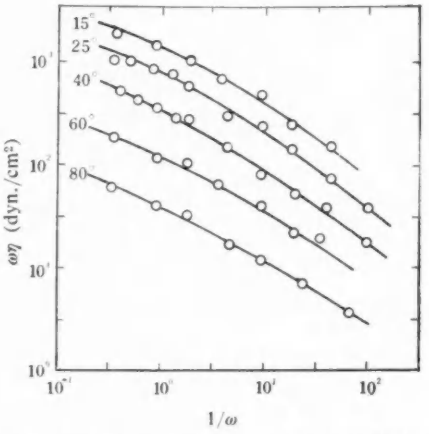

Fig. 5. Frequency dispersion of dynamic loss at various temperatures, aluminum stearate 1 wt. %.

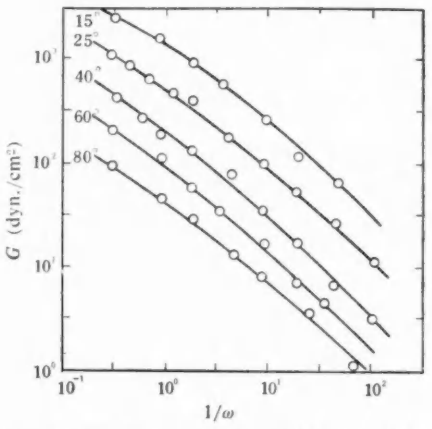

Fig. 6. Frequency dispersion of shear modulus at various temperatures, aluminum stearate 1 wt. %.

12) J. D. Ferry et al., *Ind. Eng. Chem.*, **44**, 703 (1952).

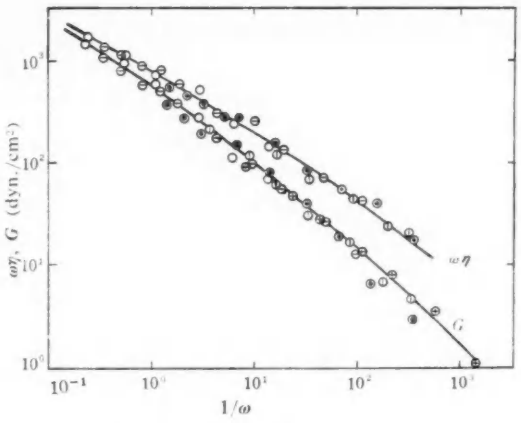

Fig. 7. Reduced curves.
○ 15°C ⊖ 25°C ⊙ 40°C ⊕ 60°C ⊜ 80°C

TABLE I. SHIFT FACTORS FOR ALUMINUM STEARATE-NUJOL GEL (1 wt. %)

Temperature (°C)	$\log a_T$
15	0.52
25	0
40	−0.53
60	−0.97
80	−1.38

absence of serious changes in rheological structures up to 60°C, that is, the system is thermo-rheologically simple in that temperature region. The shift factors for this transformation to 25°C are summarized in Table I. Change in the reducing factor with temperature is somewhat small compared with the data of usual polymers.

Concentration Dependence.—Change in shear modulus and dynamic viscosity with concentration at various temperatures is shown in Fig. 8. Modulus and viscosity show similar curves which are composed of two straight lines, and have a break point near concentration 1 wt. %. Above this point, modulus and viscosity increase abruptly. This point corresponds to the appearance of soft gel, therefore it is considered as the critical concentration for gel formation. Change in temperature has a minor effect both on the type of the curve and on the critical concentration. The critical concentrations of gel formation obtained from the curves at 15, 25 and 40°C are 0.86, 0.82, and 0.86 wt. % respectively. The curves were obtained from a single period of oscillation; however, these types of curves and critical concentrations are expected under various conditions, because the frequency dependence of the systems is similar,

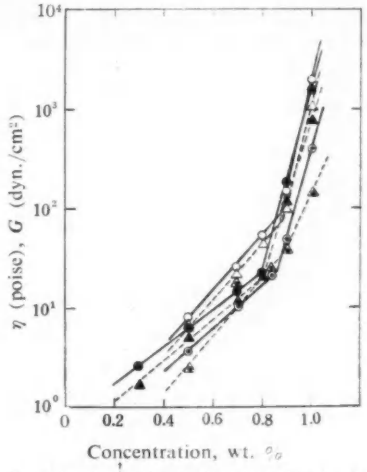

Fig. 8. Change in dynamic viscosity (—○—) and shear modulus (--△--) with concentration, period $T=12$ sec.
○ 15°C ● 25°C ⊙ 40°C

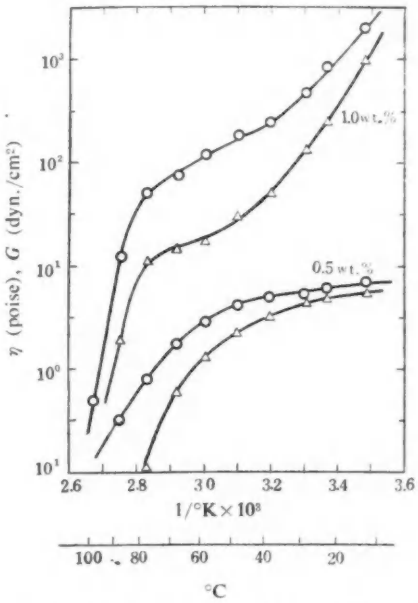

Fig. 9. Temperature dependence of dynamic viscosity (○) and shear modulus (△), period $T=12$ sec.

as shown in Figs. 5 and 6.

Below the critical concentration, the viscosity and elasticity change exponentially with concentration; this region corresponds to the sol in which the soap crystallites are dispersed with secondary interactions. Above the critical

concentration, an extraordinarily sudden increase in visco-elasticity occurs due to the strong network structures in the system, which is stable under a very low rate of shear. This was not observed in a static viscosity measurement carried out under a high rate of shear, owing to the degradation of the structure under shear.

Effect of Temperature. — Changes in visco-elasticity with temperature are shown in Fig. 9. Viscosity change of the vehicle is expressed approximately by the Andrade formula ; whereas the system shows complex thermal behaviors. The curves have deflection points near 80°C, which show some phase change in the structure of the systems, the transition from dispersion to isotropic solution. Below this transition temperature, the 1 wt. % gel shows greater temperature effect than the vehicle due to the effect of temperature on the strength of network structures ; that is, the gel structures change continuously with temperature. On the other hand, a 0.5 wt. % sol undergoes less temperature effect than the vehicle, which shows that the rheological structures remain unchanged by temperature.

Summary

Dynamic visco-elastic behaviors of the aluminum stearate nujol system were studied, using a concentric cylinder type forced oscillation rheometer. The system behaves always as a typical visco-elastic body in a wide range of concentrations and temperatures, and manifests conspicuous amplitude and frequency dependence, which indicates non-linear visco-elastic properties. Wedge type relaxation spectra of the system were obtained, and it was found that the system is thermo-rheologically simple in a confined region of temperatures. The time effect of the specimen and temperature dependence of dynamic properties were examined, and the rheological structures in the system under various conditions were discussed.

The author wishes to express his thanks to Professor H. Akamatu and Dr. T. Nakagawa, both of the University of Tokyo, for their kind advice and encouragement throughout this investigation.

Railway Technical Research Institute
Kunitachi, Tokyo

Visco-elastic Behaviors of Aluminum Soap-Hydrocarbon Systems. II. Aluminum Soaps in Nujol

By Sukekuni SHIBA

(Received August 6, 1960)

In the previous paper[1], dynamic behaviors of the aluminum stearate-nujol system were studied, and typical visco-elastic properties of the system were found. In this paper, visco-elastic behaviors of aluminum soaps from various fatty acids and aluminum stearates of different compositions dispersed in nujol were studied.

Experimental

Materials.—Aluminum soaps from various parent fatty acids were prepared from purified fatty acids. The purity of the fatty acids and method of preparation were described in the previous paper[2]. Results of aluminum analysis of the soaps are shown in Table I. Aluminum stearates of different compositions were prepared, varying the amount of excess of sodium hydroxide during the precipitation

TABLE I. COMPOSITIONS OF ALUMINUM SOAPS

Soap	No. of C atoms in acid	Al wt. % (analysed)	Mol. acid per mol. Al
Palmitate	16	5.80	1.62
Myristate	14	5.96	1.77
Laurate	12	6.38	1.87
Caprate	10	7.36	1.87
Caprylate	8	9.17	1.72

TABLE II. COMPOSITIONS OF ALUMINUM STEARATES

Excess NaOH %	Al wt. % (analysed)	Mol. acid per mol. Al
10	4.09	2.18
18	4.40	2.01
25	4.68	1.89
35	5.04	1.72
50	5.46	1.56
75	5.96	1.41

1) S. Shiba, This Bulletin, **34**, 194 (1961).
2) S. Shiba, ibid., **33**, 1563 (1960).

of the soaps. Compositions of the aluminum stearates are summarized in Table II.

The vehicle was the same nujol as in the previous work. Infrared absorption measurements showed no free fatty acid for the soaps from various fatty acids, whereas the spectra of aluminum stearates containing more than 2 acid molecules per aluminum showed the presence of free fatty acids.

Apparatus and Procedure. — Forced oscillation rheometer and the experimental procedure are the same as in the previous work[1].

Results and Discussion

Various aluminum soaps dispersed in nujol show thickening properties to some extent, and the system becomes an elastic gel at a high concentration or a viscous sol at lower concentrations. Gelling characteristics of the soaps were examined for varying fatty acids and soap compositions.

Frequency Dependence. — The frequency dependency of aluminum palmitate, caprate and caprylate in nujol is shown in Fig. 1. A gel

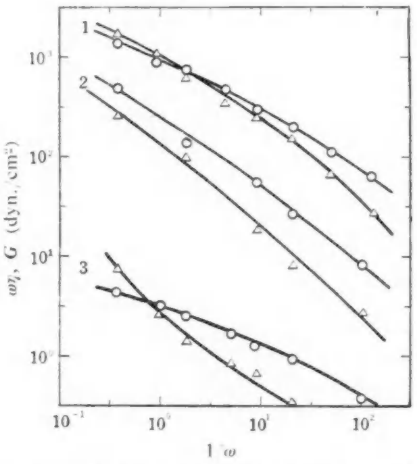

Fig. 1. Frequency dependence of dynamic loss (○) and shear modulus (△), aluminum soaps in nujol at 25°C.
1. Palmitate 1 wt. % 2. Caprate 2 wt. %
3. Caprylate 3 wt. %

containing 1 wt. % of palmitate shows frequency dispersion similar to stearate which indicates wedge type relaxation spectrum. A gel of aluminum caprate (2 wt. %) shows a dispersion which resembles that of palmitate as shown in Fig. 1, despite the higher concentration of the soap. Aluminum myristate and laurate show behaviors similar to palmitate; caprylate scarcely shows the elastic properties. That is to say, the visco-elastic properties of the systems decrease suddenly when the length of the fatty acid molecule decreases below ten carbon atoms.

Concentration Dependence. — The concentration dependences of visco-elastic properties for the systems are shown in Figs. 2 and 3.

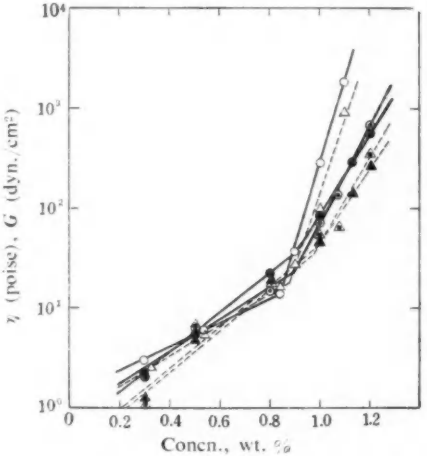

Fig. 2. Concentration dependence of dynamic viscosity (—○—) and shear modulus (--△--), 25°C period $T=12$ sec.
○ Palmitate ● Myristate ◦ Laurate

Palmitate, myristate and laurate show curves similar to stearate, and each curve consists of two straight lines in the concentration range above and below the break point. The break points correspond to the critical concentrations necessary to form gels, and the two straight lines represent the concentration dependence of visco-elasticity of gels and sols respectively. These curves are expressed by empirical formulae;

$$\log \eta_s = a_s + b_s c, \qquad \log \eta_g = a_g + b_g c \qquad (1)$$

$$\log G_s = a_s' + b_s' c, \qquad \log G_g = a_g' + b_g' c \qquad (2)$$

where η and G are dynamic viscosity (poise) and shear modulus (dyn./cm²), the subscripts s and g mean that the values are referred to the sol and gel states. Changes in critical concentration and constant b_g with soaps are summarized in Table III. The two values represent the gelling capacity of the soaps and the concentration dependence of the rheological properties of the resulting gel. The fatty acid of shorter hydrocarbon chain length gives an indistinct and higher critical concentration and a lower value of b_g. When the mole concentrations of the systems are considered, the difference will be larger. This tendency indicates the superiority of soaps from higher fatty acids as thickener. The results for laurate support those of Weber and Bauer[3], who found the appearance of pronounced elastic properties

TABLE III. CRITICAL CONCENTRATION AND CONSTANT b_g

Soap	Crit. conc. wt. %	b_g 1/wt. %
Stearate*	0.81	10.2
Palmitate	0.85	8.3
Myristate	0.92	4.1
Laurate	0.91	4.9
Caprate	2.0	1.4
Caprylate	—	—

* Obtained from Ref. 1.

in the gels as the concentration of soap increased over 1 wt. %.

Caprate and caprylate show a somewhat different type of concentration dependence, as shown in Fig. 3. Caprate has a critical concentration near 2 wt. % and visco-elasticity

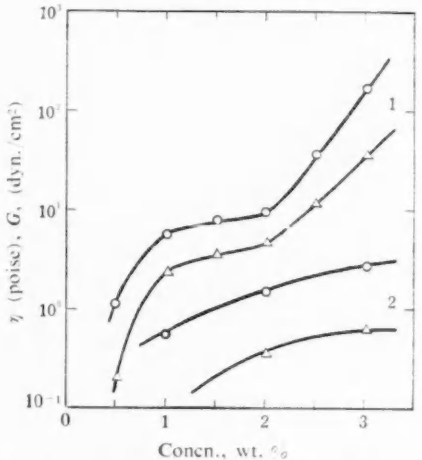

Fig. 3. Concentration dependence of dynamic viscosity (○) and shear modulus (△), 25 °C period T=12 sec.

1. Caprate 2. Caprylate

decreases rapidly at a concentration below 1 wt. %. Caprylate shows neither conspicuous thickening effect nor gelling property. Thus, the aluminum soaps from fatty acid lower than capric acid, show remarkably different rheological behaviors.

A mixture of the stearate and palmitate shows intermediate concentration dependence of both soaps.

The experiments were carried out under definite conditions, however results similar to the case of stearate[1] are expected under various conditions, due to their relatively similar dependence on frequency and temperature.

3) N. Weber and W. H. Bauer, *J. Phys. Chem.*, **60**, 270 (1956).

Temperature Dependence.—Changes in visco-elastic properties of aluminum soap-nujol systems with temperature are shown in Fig. 4. The soaps examined do not show linear relation as described by the Andrade formula. In this temperature region, distinct transition was not

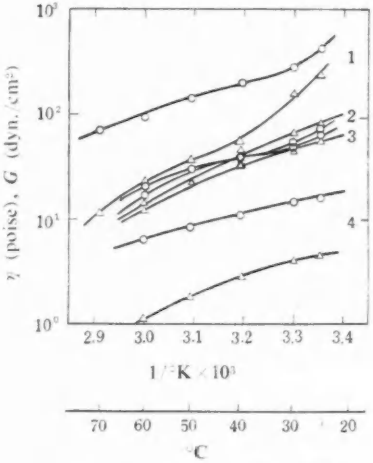

Fig. 4. Temperature dependence of dynamic viscosity (○) and shear modulus (△), aluminum soaps in nujol 1 wt. %, T=12 sec.

1. Palmitate 2. Myristate 3. Laurate 4. Caprate

observed; however, the transition from dispersion to solution found for stearate may exist in these cases. The curves show a convex type against temperature. This suggests that gradual transition or structural change occurs over a wide range of temperatures resulting in decrease in rheological properties. Therefore, the apparent activation energies of flow calculated from gradients of the curves are somewhat larger than that of the vehicle, nujol.

Effect of Soap Composition.—Aluminum stearate of different compositions that is, the soaps in which a different number of acids combined with the aluminum atom, in nujol were examined. Comparison of the results for 1 wt. % soaps in nujol is made in Fig. 5. An extraordinary difference was found; however, when the conspicuous concentration dependence of the systems as shown in Fig. 2 is considered, it is clear that the results expressed by single point observations on visco-elasticity do not reveal the full aspects of the properties of the soaps. The critical concentration was observed by a simple method: soap solutions of various concentrations were cooled in test tubes and kept still overnight; when the specimen did not flow in a minute after the

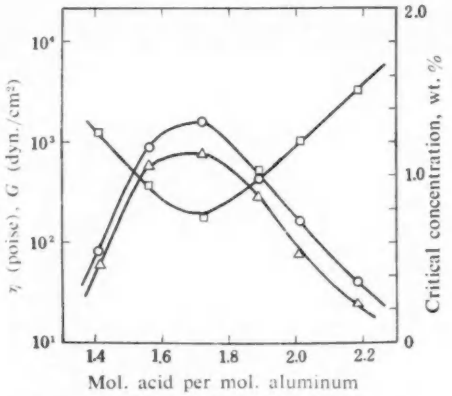

Fig. 5. Visco-elastic properties and critical concentrations of aluminum stearates in nujol at 25°C.
○ η, △ G for 1 wt. % soaps in nujol, T=12 sec., □ critical concentration.

tube was laid down, the specimen was judged to be a gel. The results are also shown in Fig. 5, which shows the maximum effects as thickener near 1.7 mol. acid per aluminum.

Rheological Structures in the Systems.—Visco-elastic behaviors of the systems show evidence of strong rheological structures in the systems. The system is essentially a colloidal dispersion of elongated aluminum soap crystallites in hydrocarbon media as ascertained by electron microscope observation[4]. The system containing soaps in more than the critical concentration exhibits typical visco-elastic properties of gels indicating the network structures of soap crystallites by secondary interactions. At lower concentrations the network is incomplete, resulting in a sol with fluidity. At elevated temperatures, e. g. above 80°C, the soaps disperse homogeneously to a transparent solution. Transition from dispersion to solution is expected from conspicuous change in rheological properties.

Static flow properties of the system under constant shear were discussed elsewhere[2]. Network structures suffer a breakdown by shear and result in relatively high fluidity in that case. In this experiment, extraordinarily high values of visco-elasticity were obtained, since the specimen was treated so as not to be affected by shear. The effects of weak secondary interactions which undergo breakdown are recognized as the difference between the two results.

4) D. Evans and J. B. Matthews, *J. Colloid Sci.*, **9**, 60 (1954).

Summary

Dynamic visco-elastic behaviors of aluminum soaps from various fatty acids and aluminum stearates of different compositions in nujol were studied, using a forced oscillation rheometer. The systems behave always as typical visco-elastic bodies in a wide range of concentrations and temperatures. Aluminum palmitate, myristate, and laurate show properties similar to stearate, whereas caprate and caprylate show less effects on rheological properties. Optimum composition of aluminum stearate as thickener was obtained. Rheological structures in the systems were discussed and comparison of the results by static and dynamic measurements was made.

The author wishes to express his thanks to Professor H. Akamatu and Dr. T. Nakagawa, both of the University of Tokyo, for their kind advice and encouragement throughout this investigation.

Railway Technical Research Institute
Kunitachi, Tokyo

Infrared Studies of the Librations of Water Molecules in the Solid Matrices at 20°K

By Tatsuo MIYAZAWA

(Received July 28, 1960)

The matrix isolation technique has been applied for the infrared absorption studies in the rocksalt or potassium bromide regions[1-4], however, not in the cesium iodide region so far. In the cesium iodide region (400~190 cm^{-1}) librational frequencies of small molecules in the crystalline state as well as internal rotation frequencies and bending frequencies are observed. These intramolecular vibrations are coupled with rotational motions in the vapor phase and quite complicated vibration-rotation bands are observed. In the solid matrices at sufficiently low temperatures, however, translational diffusion as well as rotational diffusion of trapped molecules are generally hindered, and the overall rotational motions are reduced to librational motions. No rotation envelope is apparent, and complicating effects frequently arising from rotational motions in the vapor phase are absent.

In carrying out matrix isolation experiments it is necessary to purify the matrix material carefully since the molar ratio (M/R) of the matrix (M) and the reactive species (R) may be as high as 1000 or more. It is not possible to remove the trace of water in nitrogen gas by simply passing the gas through a liquid nitrogen bath. It was necessary first to measure the spectra of water in the nitrogen matrix at various M/R ratios. Spectroscopic studies of water itself are also interesting in relation with hydrogen bonds and with the effects of matrix solids on the low frequency vibrations.

Experimental Results

For spectroscopic measurements in the region 400~190 cm^{-1} a Perkin Elmer Model 12C spectrometer was used with the cesium iodide optics[5]. The experimental technique of the matrix isolation method has been described[1]. The infrared spectra of water in the solid nitrogen matrix at 20°K were measured for the molar ratios (N_2/H_2O) of 1000, 200, 80 and 40. In each case 55 micromoles of water was dispersed in the matrix over an area of about 2 cm^2. The nitrogen gas used in the measurement was purified by being passed over copper at 600°C and then through a liquid nitrogen bath. The observed spectra are shown in Fig. 1. It may be seen that the intensity of the

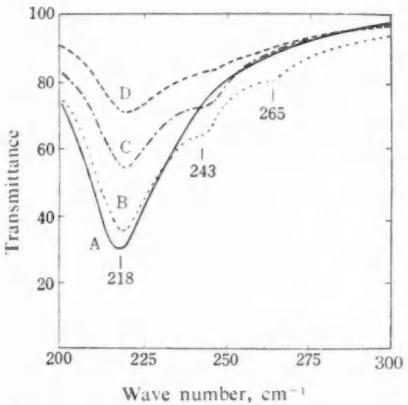

Fig. 1. Infrared spectra of water in the solid nitrogen matrix at 20°K. A: M/R =1000, B: M/R=200, C: M/R=80, D: M/R=40.

band at 218 cm^{-1} increases as M/R is increased from 40 to 1000. The intensity of the band at 243 cm^{-1} increases as M/R is increased from 40 to 80, reaches its maximum for M/R of 80~200 and then decreases as M/R is increased to 1000. The band at 265 cm^{-1} appears to exhibit its intensity maximum for M/R of 200.

In order to measure the effect of isotopic substitution on the water bands, 55 micromoles of heavy water was also suspended in the solid nitrogen matrix for M/R of 200; however, in this case no bands were observed in the region above 190 cm^{-1}.

The infrared spectrum of water (55 micromoles, M/R of 200) was also measured in the solid argon matrix at 20°K. Argon gas was

1) E. Whittle, D. A. Dows and G. C. Pimentel, *J. Chem. Phys.*, **22**, 1943 (1954); E. D. Becker and G. C. Pimentel, ibid., **25**, 224 (1956).
2) M. Van Thiel, E. D. Becker and G. C. Pimentel, ibid., **27**, 486 (1957).
3) E. Catalano and D. E. Miligan, ibid., **30**, 45 (1959).
4) M. Van Thiel, E. D. Becker and G. C. Pimentel, ibid., **27**, 95 (1957); G. C. Prinental, *Spectrochim. Acta*, **12**, 94 (1958); T. Miyazawa and K. S. Pitzer, *J. Chem. Phys.*, **30**, 1076 (1959).
5) T. Miyazawa, ibid., **29**, 421 (1958). The measurements were made at the University of California.

purified by being passed over copper heated to 600°C and then through a dry ice-acetone bath. In this case no bands were observed in the region 400~190 cm^{-1}, in contrast with the case of the nitrogen matrix.

Discussion

Infrared spectra of water in the solid nitrogen matrix have been measured in the region 3500~3000 cm^{-1} by Van Thiel, Becker and Pimentel[2]. Eleven peaks have been observed at various M/R ratios, and the bands at 3725 cm^{-1} and 3627 cm^{-1} have been assigned to the monomeric species, and the other bands have been assigned to the dimeric, trimeric, and polymeric species.

Assignment of Low Frequencies. — In the present study in the cesium iodide region three bands were observed at 218, 243 and 265 cm^{-1}. The intensity of the band at 218 cm^{-1} is plotted against M/R in Fig. 2, along with the corresponding curve for the 3725 cm^{-1} band. It

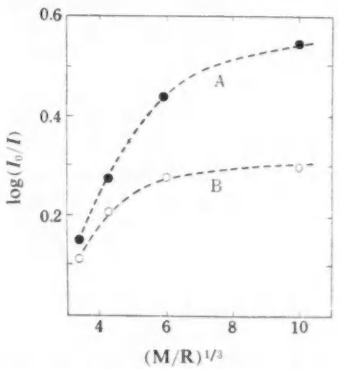

Fig. 2. Peak intensities vs. $(M/R)^{1/3}$.
A: 218 cm^{-1}, B: 3725 cm^{-1}.

may be seen that the intensity of the 218 cm^{-1} band changes in iust the same manner as the intensity of the 3725 cm^{-1} band of the monomeric species. The 218 cm^{-1} band is therefore assigned to the monomeric species. The 243 cm^{-1} band is observed as a shoulder of the 218 cm^{-1} band and its intensity change with M/R appears to correspond most closely with the 3691 cm^{-1} band of the dimeric species[2].

218 cm^{-1} Band of Monomer.—All the intramolecular vibrations of the monomeric species have already been observed[2] at 3725, 3627 and 1600 cm^{-1}. The 218 cm^{-1} band is, therefore, undoubtedly due to translational or rotational modes in the solid matrix. The translational and rotational motions are restricted in the matrix and become vibrational motions giving rise to vibrational infrared bands.

Lattice Vibrations of Ice. — Prior to more detailed discussions of the matrix spectra the infrared bands of crystalline ice due to these translational or rotational vibrations will be briefly reviewed. The infrared bands due to the translational lattice vibrations of water and heavy water (at −190°C) have been observed at 229 and 222 cm^{-1} respectively[6]. The observed frequency ratio (ν_{H_2O}/ν_{D_2O}) of 1.03 agrees with the theoretical ratio of $1.05=(M_{D_2O}/M_{H_2O})^{1/2}$ for the translational mode. On the other hand the rotational lattice vibrations (librations) of water and heavy water (at −170°C) have been observed at 850 and 630 cm^{-1} respectively[7] and in this case the frequency ratio of 1.35 is much greater than the ratio of 1.03 for the translational mode.

Three Librations in the Nitrogen Matrix.—The 218 cm^{-1} band in question disappears on deuteration and the corresponding band of heavy water has not been observed in the region above 190 cm^{-1}. The isotopic frequency ratio for this mode is definitely greater than the ratio of 1.05 expected for the translational mode. The 218 cm^{-1} band may thus be assigned to a librational mode of the monomeric species in the nitrogen matrix.

So far we have not specified the types of librations in the matrix. For the monomeric species of water there are three types as shown in Fig. 3; one around the twofold axis (the B axis), one around the axis perpendicular to

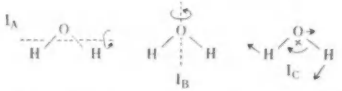

Fig. 3. Librational modes of monomer.

the molecular plane (the C axis), and the last one around the axis of the least moment of inertia (the A axis). The first one will not be infrared active since the B axis is parallel to the dipole moment of the molecule. The other two involve rotations of the molecular dipole moment and will give rise to strong infrared bands.

Intensity of Libration Bands.—The infrared intensities of these libration bands may be estimated assuming that the molecules carry out librations about the axes passing through the center of the mass. The moments of inertia about the three axes are

$$I_A = 2m_H r^2 (m_O/M_{H_2O}) \cos^2 \alpha$$

$$I_B = 2m_H r^2 \sin^2 \alpha$$

6) R. Zimmermann and G. C. Pimentel, unpublished.
7) K. B. Harvey and P. A. Giguère, *Can. J. Chem.*, **34**, 798 (1956); N. Ockman, *Advances in Physics*, **7**, 199 (1958); D. F. Hornig, H. F. White and F. P. Reding, *Spectrochim. Acta*, **12**, 338 (1958).

and $I_C = I_A + I_B$

where m_H and m_O are the masses of the hydrogen and oxygen atoms, respectively, r the bond length and 2α the interbond angle. Now if the monomeric species is randomly oriented in the matrix the infrared intensities, D_A and D_C, of the A and C librations are expressed analogous to the vapor intensities, and

$$D_i \propto |\partial\mu/\partial Q_i|^2 = |\partial\mu/\partial\theta_i|^2 \cdot |\partial\theta_i/\partial Q_i|^2 = \mu^2 \cdot I_i$$

where μ is the dipole moment, Q_i the ith normal coordinate, θ_i the angle of rotation around the ith axis, and I_i the corresponding moment of inertia. The intensity ratio of the A and C bands is calculated to be $D_A/D_C = 2.7$ for the H_2O molecule with the bond angle of 105°. The 218 cm^{-1} band of the monomeric species is considered to be primarily due to the A librational mode.

Librational Frequencies. — The three librational frequencies may be estimated assuming that the potential energy arises from Cartesian displacements of the hydrogen atoms in the matrix. The potential energy possibly arising from Cartesian displacements of the oxygen atom was not considered in the present treatment. The Cartesian displacements of the hydrogen atoms, ξ_A, ξ_B and ξ_C, due to the rotations around the three axes are

$$\xi_A = \theta_A (m_O/M_{H_2O}) r \cos\alpha$$

$$\xi_B = \theta_B r \sin\alpha$$

and

$$\xi_C = \theta_C r [\sin^2\alpha + (m_O/M_{H_2O})^2 \cos^2\alpha]^{1/2}$$

Taking into account the potential energies for the two hydrogen atoms, the librational frequencies, ν_A, ν_B and ν_C, are found to be

$$(2\pi\nu_A)^2 = (K/m_H)(m_O/M_{H_2O})$$

$$(2\pi\nu_B)^2 = (K/m_H)$$

and

$$(2\pi\nu_C)^2 = (K/m_H)\{\tan^2\alpha + (m_O/M_{H_2O})^2\}/\{\tan^2\alpha + (m_O/M_{H_2O})\}$$

whre K is the potential constant. The value of K is calculated to be 0.032 millidyne/A from the ν_A frequency (218 cm^{-1}) of water, and other librational frequencies were calculated to be $\nu_B = 231$ and $\nu_C = 226$ cm^{-1} for H_2O and $\nu_A' = 146$, $\nu_B' = 164$ and $\nu_C' = 157$ cm^{-1} for D_2O.

The ν_C frequency of 226 cm^{-1} is slightly higher than the observed ν_A frequency of 218 cm^{-1} and the intensity of the ν_C band is considered to be weaker than the intensity of the ν_A band as mentioned before. In fact the 218 cm^{-1} band has an ill-defined shoulder on the high frequency side around 230 cm^{-1}, in agreement with the result of the present treatment*. The librational frequencies calculated for D_2O are much lower than 190 cm^{-1}, again in agreement with the result of the present measurement on D_2O.

243 cm^{-1} Band of the Ring Dimer. — The structure of the dimeric species of water in the solid nitrogen matrix has been found to be a ring dimer by Van Thiel et al.[2]. The ring dimer has a center of symmetry and there will be three infrared active low frequency vibrations as shown in Fig. 4. The b_u vibration

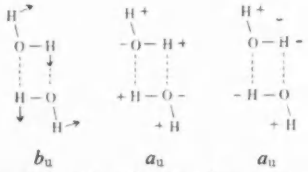

Fig. 4. Infrared active low frequency modes.

involves the stretching of the O···H hydrogen bonds and its frequency will be appreciably higher than the two a_u frequencies involving only the bending of the hydrogen bonds. The observed frequency of 243 cm^{-1} is slightly higher than the monomeric frequency and this is most probably due to either one of the two a_u modes of the ring dimer.

Libration in the Argon Matrix. — The librational frequencies of water in the argon matrix have not been observed in the region above 190 cm^{-1}. It has been found that the nitrogen and argon matrices have different effects on the monomeric bands of water. Catalano and Milligan have observed seven sharp peaks (1654~1554 cm^{-1}) due to the bending vibration in the argon matrix but only one peak at 1600 cm^{-1} in the nitrogen matrix[3]. The observed fine structure in the argon matrix has been ascribed to overall rotations of the monomeric species in the argon matrix**. The rotations may not be unrestricted of course; however, they should be much less restricted in the argon matrix than in the nitrogen matrix. The present observation in the cesium iodide region is in accord with the conclusion drawn by Catalano and Milligan[2].

The author wishes to thank Professor K. S. Pitzer and Professor G. C. Pimentel of the University of California for their interest and

* In crystalline ice the ν_A and ν_C librations give rise to a band at 850 cm^{-1} (at −170°C). The two librations, however, have not been resolved from each other[7].

** It is interesting to note that NH_2 radical has been found to carry out almost free rotation in the argon matrix[8].

8) G. W. Robinson and M. McCarty, Jr., *J. Chem. Phys.* **30**, 999 (1959).

encouragement. The present work was partly supported by the American Petroleum Institute Research Project 50.

Institute for Protein Research
Osaka University
Kita-ku, Osaka

Studies on Dehydroalanine Derivatives. III. Formation of Amino Acids from Poly-dehydroalanine

By Shumpei SAKAKIBARA

(Received July 13, 1960)

In the previous papers of this series[1,2], the synthesis of *N*-carboxy-dehydroalanine anhydride and of poly-dehydroalanine was described. However, the synthesis of analytically pure poly-dehydroalanine was unsuccessful, and it was found that the polymer contained only about 10% dehydroalanyl residues in the molecule[2]. This suggested that the dehydroalanyl groups in the polypeptide chain are very reactive. The present investigation is on the reactivity of dehydroalanyl residues in polypeptide chains. Poly-dehydroalanine was used as test material, and the reagents used for the reaction were potassium carbonate, potassium cyanide, benzyl mercaptane and acetonitrile. The amino acids derived from the poly-dehydroalanine were examined after hydrolysis of the reaction products.

Experimental

Meterial.—Poly-dehydroalanine was prepared from *N*-carboxy-dehydroalanine anhydride[1]. It was polymerized in pyridine as described in the previous paper[2]. The freshly prepared polymer was used in these experiments.

Reaction Conditions and Detection of Amino Acids Formed.—The reaction mixtures shown in Table I were hydrolyzed for about 15 hr. at 105°C after addition of concentrated hydrochloric acid (an equal volume to that of the reaction mixture), and then concentrated to dryness. These concentrates were analyzed by Dowex 50 column chromatography using the conditions of Moore and Stein[3] (Fig. 1) and/or by two dimensional paper chromatrgraphy after dinitrophenylation under the improved conditions of Levy[4] (Fig. 2). Amino acids formed were analyzed quantitatively by Levy's method (Table II). The spot corresponding to DNP-aspartic or glutamic acid in Fig. 2 was rechromatographed on paper by descending method using 2.5 M phosphate buffer as solvent, as shown Fig. 4. Since the spot corresponding to DNP-aspartic acid from reaction mixture 3 contained a little DNP-glutamic acid, these two compounds were separated on a buffered celite column using 0.2 M phosphate-citric acid as buffer and chloroform-ether (90 : 10) as developer[5] (Fig. 3). Then, the bands corresponding to DNP-aspartic acid (A) and DNP-glutamic acid (B) were reconfirmed and repurified by paper

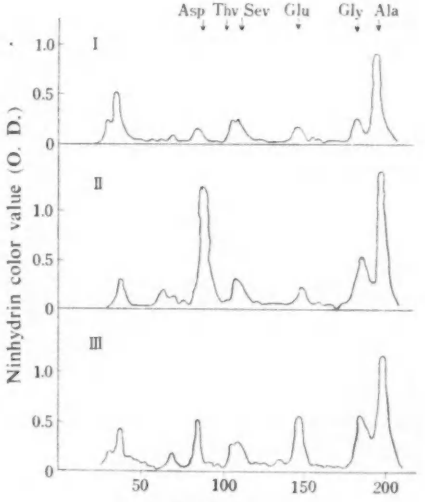

Fig. 1. Chromatographic analysis of ninhydrin-positive materials in the HCl-hydrolyzates (per 10 mg. of poly-dehydroalanine): I. Reaction mixture 1; II. Reaction mixture 3; III. Reaction mixture 5 (cf. Table I). Column: Dowex 50-X8, 100×0.9 cm.
Arrows indicate the position of the peaks of standard amino acids.

1) S. Sakakibara, This Bulletin, **32**, 13 (1959).
2) S. Sakakibara, ibid., **33**, 814 (1960).
3) S. Moore and W. H. Stein, *J. Biol. Chem.*, **192**, 663 (1951).
4) A. L. Levy, *Nature*, **174**, 126 (1954); G. Koch and W. Weidel, *Z. physiol. Chem.*, **303**, 213 (1956).
5) A. Courts, *Biochem. J.*, **58**, 70 (1954).

TABLE I. REACTIONS OF POLY-DEHYDROALANINE WITH VARIOUS REAGENTS

Reaction No.	Poly-dehydroalanine* apparent wt. (calcd. wt.) mg.	Reagent g.	Water ml.	Reaction conditions
1	5 (4.10)	K_2CO_3 0.04	2	A**
2	10 (8.20)	K_2CO_3 0.08	4	B†
3	65 (53.4)	KCN 0.4	20	A**
4	15 (12.3)	K_2CO_3 0.12 Benzyl mercaptane 0.1	6	C††
5	10 (8.20)	K_2CO_3 0.08 CH_3CN 1	4	B†

* Soluble poly-dehydroalanine contained 17.9% of volatile components. Since completely dry polymer was partially insoluble[2], the actual weight was calculated from the apparent weight.
** Kept at room temp. for about 15 hr. and then heated at 80°C for 1 hr. in a sealed tube.
† Irradiated with an UV-lamp (Mazda 15 W sterilizing lamp at the irradiation distance of 10 cm.) for 24 hr. at room temp. in a petridish (dia. 5 cm.) covered with cellophane (0.05 mm. thick).
†† Shaken at room temp. for about 15 hr. in a sealed tube.

TABLE II. QUANTITATIVE ESTIMATION OF DNP-AMINO ACIDS ANALYZED BY LEVY'S CHROMATOGRAPHICAL METHOD (FIG. 2) : μM/10 mg. OF DRIED POLY-DEHYDROALANINE

Spot No. in Fig. 2		1	2	3	4	5	6	7	8	9	10	11		12	13
Corresponding amino acid			Ala	Gly	Thr	Ser						Asp	Glu		*S*-Bz-CyS*
No. of reaction mixt.**	1	2.24	1.81	0.18	0.05	0.13	0.05	0.07	0.10	0.07	0.14	0.29	0.42	0.25	—
	2	2.78	1.74	0.18	0.18	0.20	0.06	0.06	0.23	0.09	0.17	0.50	0.90	0.19	—
	3	0.88	2.15	0.24	0.03	0.11	—	0.03	0.17	0.07	0.16	2.11	0.44	0.27	—
	4	1.01	1.27	0.19	0.05	0.25	—	0.12	0.16	0.12	0.13	0.14	0.19	0.09	0.96
	5	2.47	1.89	1.93	0.15	0.29	0.06	0.04	0.23	0.16	0.13	0.74	1.09	0.27	—

* Bz=Benzyl
** Confer Table I

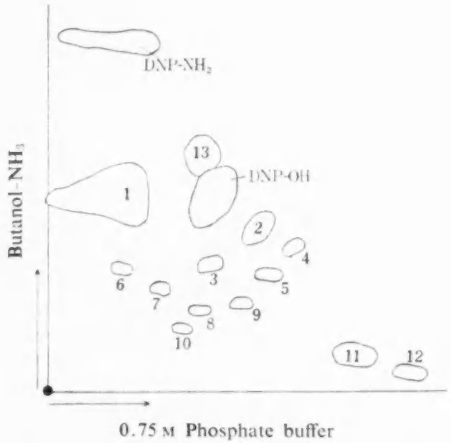

Fig. 2. Standard map of two-dimensional paper chromatogram of DNP-amino acids derived from every reaction mixture.
Details are listed on Table II.

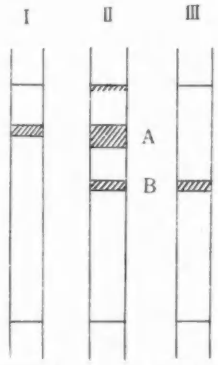

Fig. 3. Chromatographic separation of spot 11 in Fig. 2, reaction mixture 3; I. Standard DNP-aspartic acid: II. Spot 11 in Fig. 2, reaction mixture 3; III. Standard DNP-glutamic acid.
Column: Buffered celite; pH 4.2, 0.2 M phosphate-citric acid buffer.
Solvent: Chloroform-ether (90 : 10).

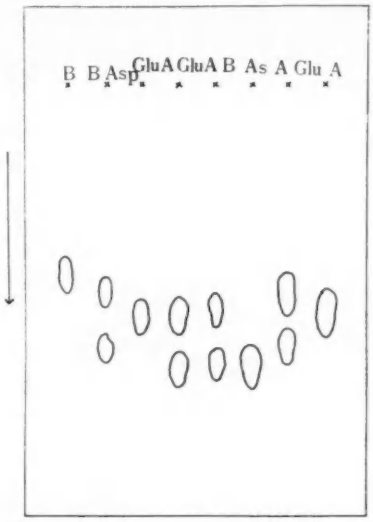

Fig. 4. Paper chromatogram for identification of bands A and B in Fig. 3 with authentic samples.
Solvent: 2.5 M phosphate buffer.
Descending method.

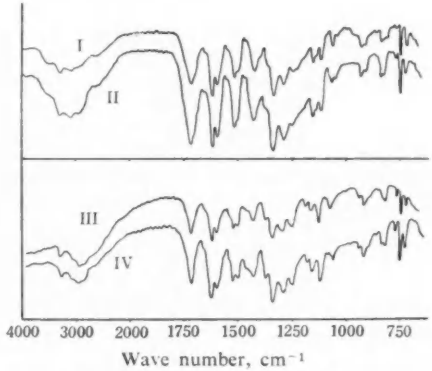

Fig. 5. Infrared absorption spectra of DNP-aspartic acid and DNP-alanine; I. Standard DNP-DL-aspartic acid; II. DNP-aspartic acid derived from the reaction mixture 3; III. Standard DNP-DL-alanine; IV. DNP-alanine derived from the reaction mixture 3.
Recorded on a Shimadzu IR spectrophotometer.
Liquid layer on KRS-5 plate.

chromatography (Fig. 4). The resulting DNP-aspartic acid was reconfirmed by comparison of its infrared absorption spectrum with that of an authentic sample (Fig. 5, I and II). The DNP-alanine formed in reaction mixture 3 was, like DNP-aspartic acid, identified by its infrared absorption spectrum (Fig. 5, III and IV).

In reaction mixture 4, *S*-benzyl cysteine was qualitatively detected by one-dimensional paper

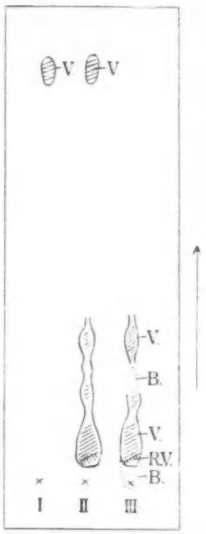

Fig. 6. One dimensional paper chromatogram of reaction mixtures 1 and 4. Identification of *S*-benzyl-cysteine formed in reaction mixture 4. I. Standard *S*-benzyl-cysteine; II. Reaction mixture 4; III. Reaction mixture 1.
V.···violet B.···brown R. V.···reddish violet

chromatography (butanol : acetic acid : water, 4:1:1) (Fig. 6).

Results and Discussion

Before hydrolysis, reaction mixtures 1 and 3 were clear light-brown solutions, 2 and 5 were clear light-yellow solutions, and 4 was a stable white emulsion. The hydrochloric acid hydrolyzates of these reaction mixtures contained small amounts of huminic material as mentioned in the previous paper[2]. As can be seen in the chromatograms of each reaction mixture (Figs. 1 and 2), several unknown bands and spots were observed besides bands and spots corresponding to natural-type amino acids such as alanine, glycine, serine, threonine, glutamic acid and aspartic acid. Formation of glycine and serine in each case could be explained by the following scheme.

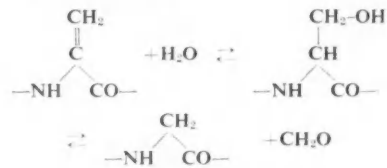

However, formation of amino acids such as alanine, glutamic acid, aspartic acid and threonine could not be explained. Perhaps, compounds such as carbon dioxide, formaldehyde,

ammonia and hydrochloric acid may react in various complex ways with the dehydroalanyl groups. It was very interesting to find spot 1 in the chromatogram shown in Fig. 2. This might correspond to di- or poly-DNP-derivative of some amino acid. Since the structure has not yet been confirmed, some kinds of basic amino acids or polyamino polycarboxylic acids may be derived from dehydroalanine.

Ultraviolet-radiation of dehydroalanyl groups resulted in the liberation of greater amounts of glycine.

As shown in Figs. 1, 2, 3, 4 and 5, and in Table II, formation of considerable amounts of aspartic acid in reaction mixture 3 was definitely confirmed, and this was explained by the following reactions:

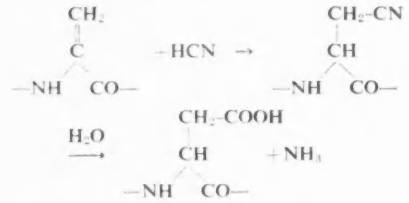

In reaction mixture 5, the liberation of greater amounts of glycine, aspartic acid and glutamic acid was observed. However, the reason of their formation is as yet unknown.

S-Benzyl cysteine was clearly detected in reaction mixture 4 (Figs. 2 and 6). It was expected that cystine would have been found in some reaction mixtures containing sodium sulfide and thiosulfate, but this could not be confirmed. Similary, attempts to detect formation of tryptophane and tyrosine residues in the polymer using indol and phenol reagents, were unsuccessful because of the difficulty of detecting small amounts of these amino acids. Nevertheless, it was interesting that many kinds of amino acids were liberated from polydehydroalanine.

A few years ago, Akabori[6,7] proposed a hypothesis on the mechanism of formation of primordial protein. He suggested that initially polyglycine was formed by the polymerization of amino-acetonitrile[8] on the surface of clay. Then, many kinds of side chains were introduced into polyglycine through the reactions of this material with simple substances such as aldehydes or olefines. Subsequently, he confirmed experimentally the formation of serine, threonine[9] and leucine[7] from polyglycine, dispersed on kaolinite, on treatment with formaldehyde, acetoaldehyde and butene-2, respectively. If it is assumed that dehydroalanyl residues are formed from polyglycine during the dehydration reaction with formaldehyde, the formation of residues such as aspartic acid, glutamic acid, alanine and threonine, from polyglycine would be rationally explained. This suggestion is supported by the fact, as shown in the following communication, that *N*-phthaloyl-dehydroalanine can be derived from serine and phthalic anhydride. Furthermore, if experimental confirmation is possible, the formation of amino acids such as cystine, tryptophane and tyrosine could also be explained in a similar way.

Summary

Reaction of poly-dehydroalanine with various reagents such as potassium carbonate, potassium cyanide, benzyl mercaptane and acetonitrile were studied. In every reaction mixture, alanine, glycine, serine, threonine, glutamic acid, aspartic acid and several unknown amino acids were detected. Ultraviolet-radiation resulted in the liberation of greater amounts of glycine. It was observed that considerable amounts of aspartic acid, *S*-benzyl-cysteine and glutamic acid were formed in reaction mixtures of potassium cyanide, benzyl mercaptane and acetonitrile, respectively.

The author wishes to express his thanks to Professor Shiro Akabori and Professor Shunsuke Murahashi for their valuable advice and encouragement.

Institute for Protein Research
Osaka University
Kita-ku, Osaka

6) S. Akabori, *Science* (*Kagaku*), **25**, 54 (1955).
7) S. Akabori, Proc. International Symposium on "The Origin of Life on the Earth", Pergamon Press, London (1959), p. 189.
8) H. Hanafusa and S. Akabori, This Bulletin, **32**, 626 (1959).
9) S. Akabori, K. Okawa and M. Sato, ibid., **29**, 608 (1956).

The Beckmann Rearrangement of the Geometrical Isomers of Cyclohexyl Phenyl Ketoxime in Liquid Sulfur Dioxide[1]

Ritsuro TADA, Yoichi MASUBUCHI and Niichiro TOKURA

(Received May 21, 1960)

In the previous report[1] of this series some effects of reagents on the products of the Beckmann rearrangement have been reported. It is currently accepted[2] that the Beckmann rearrangement is accompanied by exclusive trans migration. However, Some anomalies on the migratory aptitude in this rearrangement have been observed. Recently, Brown, van Gulic and Schmid[3] have reported that when pivalophenoxime was subjected to the Beckmann rearrangement with hydrochloric acid in acetic acid, similar products were obtained either from the *syn*-oxime or from the *anti*-isomer. This phenomena could be accounted for by a preliminary isomerization of the oximes before the rearrangement. On the other hand, Yukawa, Hanabusa and Kin[4] have examined the Beckmann rearrangement of cyclohexyl phenyl ketoximes and found that the migratory aptitude varied according to the reagents applied.

In addition, in the light of the publications hitherto reported[5~7], the geometrical structures of the cyclohexyl phenyl ketoximes are still ambiguous. Contradictory geometrical structures have been assigned to the oximes by Meyer and Scharvin[5,6] and also by Meisenheimer and Theilacher[7]. Moreover, since its first synthesis in 1897 by Meyer and Scharvin[5], the establishment of the geometrical structures mainly depended upon the analysis of the migrated products of the Beckmann rearrangement and the above-mentioned random migratory aptitude was ignored.

It is the purpose of the present writers to carry out the rearrangement in liquid sulfur dioxide of this compound to obtain further information on the geometrical structures of this ketoxime and the migration tendency in the Beckmann rearrangement by subjecting it to a more moderate condition. The isomeric cyclohexyl phenyl ketoximes were prepared and separated by the well-known precedure[5], to give the α-oxime, m. p. 156~157°C., and β-oxime, m. p. 113~114°C, respectively after repeated fractional precipitations from acetic acid solution by the addition of water.

The authentic specimens of the acid amides,

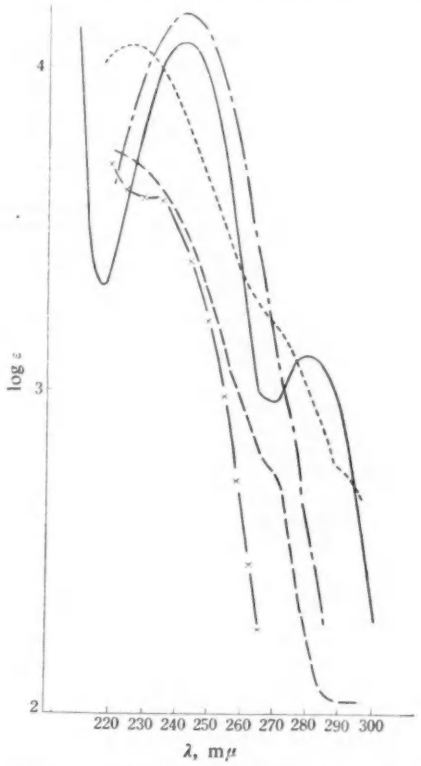

Fig. 1. Ultraviolet absorption spectra of cyclohexyl phenyl ketoximes and the derived acid amides.

---- α-Cyclohexyl phenyl ketoxime (I)
-×- β-Cyclohexyl phenyl ketoxime (II)
------ *N*-Cyclohexyl benzamide (III)
—·— Cyclohexanecarboxyanilide (IV)
—— Cyclohexyl phenyl ketone (V)

1) Part VI; On the Beckmann rearrangement in liquid sulfur dioxide. Previous papers on this series: IV. R. Tada, H. Sakuraba and N. Tokura, This Bulletin, **31**, 1003 (1958). V. N. Tokura, R. Tada and H. Suzuki, ibid., **32**, 654 (1959).
2) B. Jones, *Chem. Revs.*, **23**, 335 (1944).
3) R. F. Brown, M. M. van Gulic and G. H. Schmid, *J. Am. Chem. Soc.*, **77**, 1094 (1955).
4) Y. Yukawa, "Jikken Kagaku Koza", Vol. 18, Maruzen Co. Ltd., Tokyo, (1957), p. 426.
5) V. Meyer and W. Scharvin, *Ber.*, **30**, 1942 (1897).
6) W. Scharvin, ibid., **30**, 2862 (1897).
7) J. Meisenheimer and W. Theilacher, "Stereochemie", edited by Freudenberg Leibzig (1933), p. 2103.

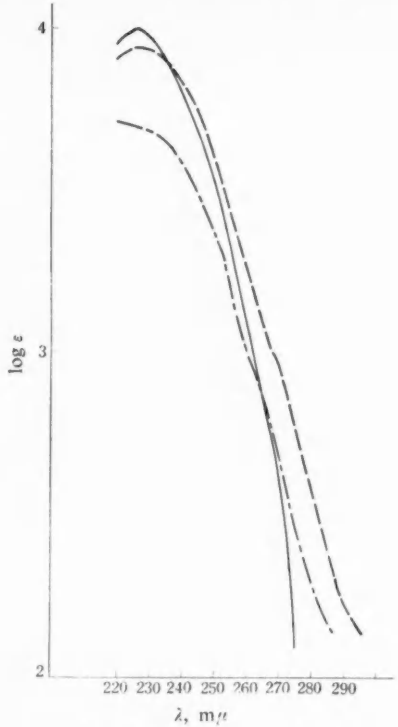

Fig. 2. Ultraviolet spectra of the reaction products from α-oxime I in liquid SO_2 at −70°C.
—— $SOCl_2$
----- $SOCl_2$ in ether
– – – Bromine

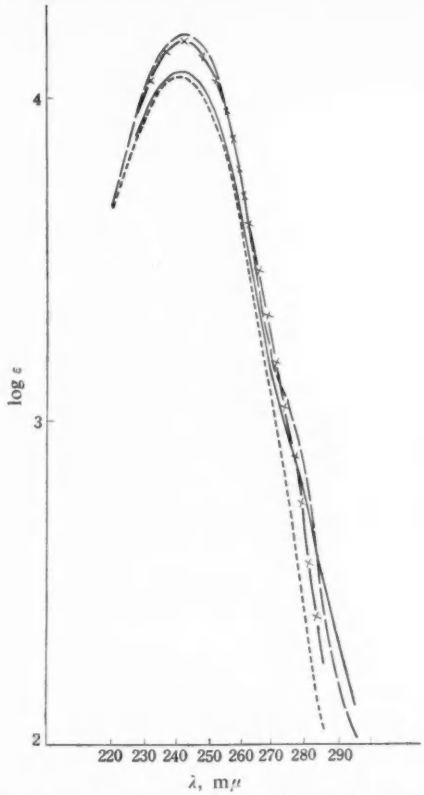

Fig. 3. Ultraviolet spectra of the reaction products from β-oxime II in liquid SO_2 at −70°C.
—— $SOCl_2$ in ether
—— Bromine
-×- $SOCl_2$
------ $C_6H_5SO_2Cl$

which should be expected to produce by the Beckmann rearrangement from the ketoximes, *N*-cyclohexyl benzamide (III), m. p. 148~149°C (reportedly[8] 146°C) and cyclohexanecarboxyanilide (IV), m. p. 146.5~147°C (reportedly 139°C)[9] respectively, were also prepared for identification of the reaction product and the ultraviolet spectra of the respective amides were compared. Although the melting point of the two compounds were close to each other, the mixed melting point of the two authentic acid amides, III and IV, was depressed to 112~116°C.

A preliminary test was performed to confirm the stability of the oximes in liquid sulfur dioxide. In the range of this experimental condition the α-oxime was sufficiently stable whereas the β-oxime isomerized to the α-oxime gradually in liquid sulfur dioxide. Accordingly, special attention was paid to carry out the Beckmann rearrangement of the β-oxime.

8) W. Markownikoff, *J. Chem. Soc.*, **87**, 92 (1892).
9) J. S. Lumsden, *Ann.*, **302**, 27 (1905).

TABLE I. REARRANGEMENT OF CYCLOHEXYL PHENYL KETOXIMES IN LIQUID SULFUR DIOXIDE

Reagent	−70±0.2°C, 1 hr.	
	Product	Rearrangement
α-Oxime I		
$SOCl_2$	III	trans
$C_6H_5SO_2Cl$	I	No
Bromine	III	trans
HCl	I	No
HBr	I	No
$SOCl_2$ in ether	I	No
β-Oxime II		
$SOCl_2$	IV	trans
$C_6H_5SO_2Cl$	IV	trans
Bromine	IV	trans
HCl	I+V	No, deoximation
HBr	I+V	No, deoximation
$SOCl_2$ in ether	IV	trans

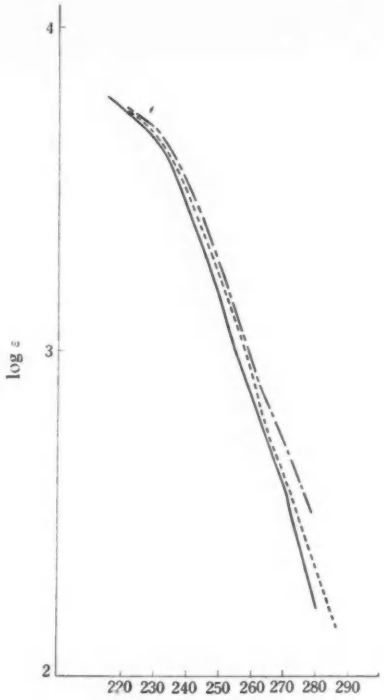

Fig. 4. Ultraviolet spectra of the reaction products from α-oxime I by hydrogen halides in liquid SO_2 at −70°C.
---- HCl —— HBr
—·— α-Oxime (I)

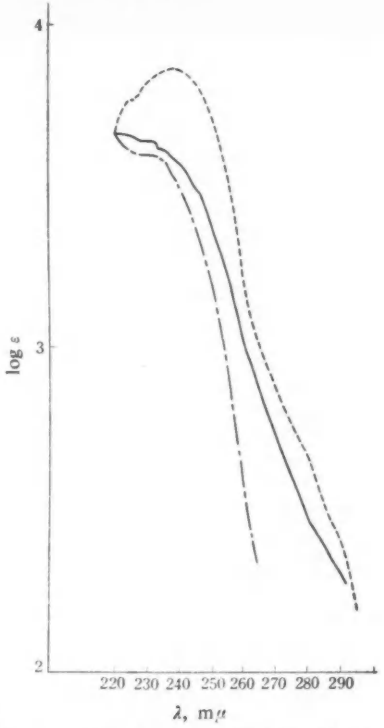

Fig. 5. Ultraviolet spectra of the reaction products from β-oxime II in liquid SO_2 at −70°C.
---- HCl —— HBr
—— β-oxime (II)

The Beckmann rearrangement were carried out in liquid sulfur dioxide at −70°C to avoid any undesirable side reaction. The reagents adopted for the rearrangement were thionyl chloride, benzenesulfonyl chloride, bromine and hydrogen halides. The result of the rearrangement is listed in Table I.

When the Beckmann rearrangement was carried out with thionyl chloride at −70°C in liquid sulfur dioxide, neither the α-oxime nor the β-oxime showed the random migratory aptitude, affording only *N*-cyclohexyl benzamide(III) from α-oxime I, and cyclohexanecarboxyanilide (IV) from β-oxime II, respectively. The mixed melting point and the superimposability of the ultraviolet spectra with those of the authentic specimen have proved that the rearrangement was progressing only in one direction, producing a single acid amide of the two.

The similar results were also obtained by other reagents, by which the different migratory aptitudes were not displayed in the rearrangements.

Chart 1.

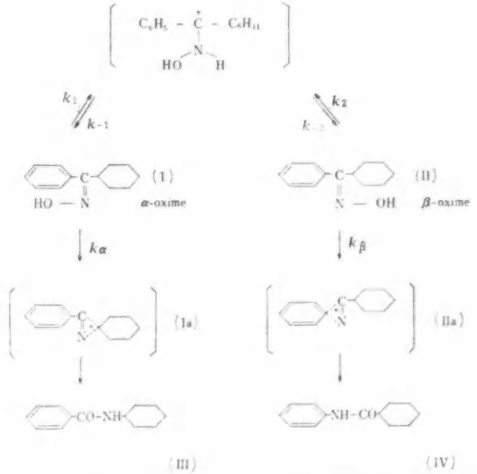

Thus, among a variety of reagents examined, within the range of these experimental conditions, thionyl chloride and bromine were only effective for the rearrangement of the α-oxime,

from which both reagents yielded the compound III exclusively as the result of trans migration.

As for the less stable β-oxime, the rearrangements were effected by thionyl chloride, benzenesulfonyl chloride and bromine to yield the amide IV exclusively, again the trans migration being predominant.

Hydrogen chloride and hydrogen bromide were both ineffective for the rearrangement, recovering the original α-oxime when it was started from the α-oxime or yielding a mixture of cyclohexyl phenyl ketoxime (V) and the α-oxime isomerized when the β-oxime was reacted. It is not surprising that the β-oxime unreacted was transformed to the more stable α-oxime (Chart 1, $k_2 > k_{-2}$ and $k_{-1} > k_1$) and the ketone V was recovered as the result of deoximation in liquid sulfur dioxide (Chart 2).

Chart 2.

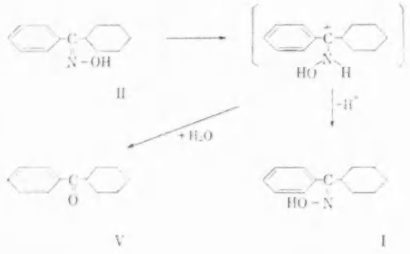

The ultraviolet spectra of the respective specimens and the crude products were recorded in methanol solutions and are seen in Fig. 1—5.

The products were obtained in the pure state or in a comparatively pure state. Sometimes the melting points of the crude products (after being washed with water and dried in vacuo) were in a range such as 135~142°C, but the ultraviolet spectra showed no contamination of another amide and were almost superimposable to the authentic acid amide. It is worthy to note that the formation of the ketone V and the possible contamination of the ketone in small quantity would make the quantitative analysis of the β-oxime impossible by ultraviolet spectrometry, because the ultraviolet spectrum of the ketone V was closely resembling that of the β-oxime. (Fig. 1)

It is a plausible conclusion that the more stable α-oxime I is in the *syn*-phenyl structure VII and the less stable β-oxime II is in the *anti*-phenyl structure VI.

When R (alkyl) is methyl[10], the structure of the oxime is principally of the *anti*-phenyl oxime VI,

because the Beckmann rearrangement affords mainly acetanilide, the phenyl groups migrating. Thus the *anti*-phenyl structure VI of the oxime is favored. As the bulkiness of the alkyl group increases, the presence of the *syn*-phenyl structure becomes more favorable[11].

When R is cyclohexyl, the *anti*-structure VII will be predominant because the steric interference between the hydroxyl group and the puckered cyclohexane ring will be more serious than that between the hydroxyl group and the planer phenyl group. Thus, the α-oxime, structure I, viz. *syn*-phenyl VII, is the more stable form, from which the Beckmann rearrangement should give III by the trans migration.

The rearrangement reaction in liquid sulfur dioxide was so rapid that the isomerization of one isomer to the other or the equilibration between the two oximes could not be competitive against the Beckmann rearrangement reaction, ($k_\alpha \gg k_1$, $k_\beta \gg k_2$, Chart 1). Even the labile β-oxime afforded only the trans migrated product IV on the Beckmann rearrangement. On this occasion the elucidation of Brown et al.[3] may again be recalled to account for the discrepancy of our result.

The complication of the result may be increased if the isomerization and the deoximation of the oxime were accompanied competitively with the rearrangement.

Another point of interest is that when the Beckmann rearrangement was carried out at −70°C in ether as the solvent in place of sulfur dioxide with thionyl chloride as the reagent, α-oxime could not be rearranged, whereas β-oxime rearranged to the acid amide IV smoothly with trans migration. The difference of the reactivity in these solvents and oximes may perhaps depend on the different solvations of the two solvents on oximes and the difference of the reactivity of the two oximes.

That the β-oxime II is more reactive than the α-oxime I is satisfactorily explicable by the facility of producing the intermediate azirinum cation[12] (IIa) by phenyl group participation, and the release of the steric hindrance by rearranging.

In conclusion, the assignment of Meisenheimer and Theilacher[7] has been verified for

10) D. E. Pearson and F. Ball, *J. Org. Chem.*, **14**, 118 (1949).

11) Y. Yukawa, Y. Tsuno and A. Tsukamoto, Abstracts of the 7th Annual Meeting of Chem. Soc. of Japan., April, 1954.

12) R. Huisgen, J. Witte and I. Ugi, *Chem. Ber.*, **90**, 1844, 1850 (1957).

the geometrical structure of cyclohexyl phenyl ketoximes, the α-oxime being of the *syn*-phenyl and the β being of the *anti*-structure.

Experimental

Material.—The purification and the manipulation of the liquid sulfur dioxide has already been published elsewhere. Thionyl chloride and benzenesulfonyl chloride were used after one distillation respectively[1]. Bromine was washed with concentrated sulfuric acid and distilled.

Preparation and Separation of Cyclohexyl Phenyl Ketoxime (I) and (II).—Essentially the method of Meyerand Scharvin[2] was used and modified slightly. A Grignard reagent from cyclohexyl bromide was reacted with benzaldehyde to obtain the corresponding carbinol, b. p. 130~135°C (5 mmHg), 26%, which was spontaneously oxidized in the air to cyclohexyl phenyl ketone (V), fine crystals, m. p. 57~58°C. The oxidation of the ketone resulted in a mixture of the geometrical isomers in good yield. The oximes were dissolved in acetic acid and fractionally precipitated by adding water gradually to obtain first the β-oxime, fine crystals, m. p. 113~114°C (II), then the α-isomer, fine needles, m. p. 156~157°C (I), respectively. For compound I. Found: N, 6.64. Calcd. for $C_{13}H_{17}ON$: N, 6.89%. For compound II. Found: N, 6.80. Calcd. for $C_{13}H_{17}ON$: N, 6.89%.

***N*-Cyclohexyl Benzamide(III).**—This material was prepared by the known method[3], from cyclohexyl amine and benzoyl chloride in a yield of 82.3%, fine needles, m. p. 148~149°C (methanol). Found: N, 6.51. Calcd. for $C_{13}H_{17}ON$: N, 6.89%.

Cyclohexanecarboxyanilide (IV).—Aniline and cyclohexanecarboxylic acid was refluxed for several hours and the resulting mass was twice recrystallized from ethanol[3], long pillars, m. p. 146.5~147°C. Found: N, 6.60. Calcd. for $C_{13}H_{17}ON$: N, 6.89%.

Mixed Melting Point of III and IV.—Though the melting points of the two acid amides III and IV, were very close to each other, the mixed melting point of the two materials, III and IV, was depressed to 112~126°C.

Isomerization of α- or β-Oxime, I or II in Liquid Sulfur Dioxide.—α-Oxime I, (1.0 g.) was dissolved in 300 ml. of liquid sulfur dioxide at -70 ± 0.2°C and allowed to stand for 24 hr. No change of melting point of I, 156~157°C, was seen after the recovery of the material (0.89 g.), which showed no depression of mixed melting point with an authentic specimen. On the contrary, the same treatment on the β-oxime II was carried out at -70°C for 24 hr. and α-oxime was obtained as the result of isomerization which was identified by the mixed melting point measurement with the authentic α-oxime.

The Beckmann Rearrangement.—To a solution of 0.5g. (0.0025 mol.) of the α-oxime in 100 ml. of liquid sulfur dioxide, a reagent (0.0025 mol.), e. g. 0.3 g. of thionyl chloride in a small ampoule was added and the vessel was cooled to a definite temperature in a constant temperature bath. After the mixture reacted to the temperature (-70 ± 0.2°C) the vessel was vigorously shaken in order to break the ampoule in the mixture. The mixture was allowed to stand at this temperature for one hour. Then the mixture was filtered and the filtrate was poured into ice-water. The precipitate afforded was collected, washed with water and dried in vacuo. The product was examined as to its melting point and the mixed melting point with the authentic acid amide, and ultraviolet spectrum of the product was compared in methanolic solution.

As the β-oxime was so unstable in liquid sulfur dioxide that the oxime in a glass ampoule was placed in a mixture of a reagent and sulfur dioxide. The rearrangement by hydrogen chloride or hydrogen bromide was carried out by passing the dry hydrogen halide gas into the reaction mixture at -70°C, followed by the crushing of the ampoule of the oxime.

Ultraviolet Spectra Measurement.—A Hitachi EPU-2A type spectrophotometer was used. All the measurements were carried out in methanolic solution.

Results of the Rearrangements.—*α-Oxime by Thionyl Chloride.*—The melting point of the product (0.42 g.) was 142~145°C, the mixed melting point with III being 144~147°C, whereas with IV, the melting point depressed to 112~116°C. The ultraviolet spectrum was superimposable with that of III. (Fig. 2)

β-Oxime by Thionyl Chloride.—The melting point of the product (0.43 g) was 145~146°C. No melting point depression with IV, whereas with III it was depressed. The ultraviolet spectrum was superimposable on that of IV. (Fig. 3)

α-Oxime by Benzenesulfonyl Chloride.—The product was recovered α-oxime (0.46 g), melting point and mixed melting point being 155~157°C.

β-Oxime by Benzenesulfonyl Chloride.—The reaction gave a product (0.44 g.) of meltng point 135~142°C. The mixed melting point with IV was 136~145°C. The ultraviolet spectrum was superimposable on that of IV. (Fig. 3) The wide range of the melting point will mean that the reaction was not complete in one hour.

α-Oxime by Bromine.—The result in this case was somewhat complicated, as the Beckmann rearrangement of a phenyl ketoxime by bromine was often accompanied by a bromination of the benzene nucleus[13]. The ultraviolet spectrum of the crude product was close to that of III. (Fig. 2), however, the melting point of the product (0.43 g.) was 112~120°C. A fractional crystallization from alcohol yielded two crystals, one melting at 116~120°C and containing bromine (by the Beilstein test), but was a very small quantity for its further identification. The other was the acid amide III, m. p. 145~146°C (0.30 g.) and mixed melting point with III was 146~147°C.

β-Oxime by Bromine.—From the crude product (0.46 g.), the fractional precipitation (from acetic acid solution by adding water), yielded crystals of m. p. 131~139°C, which was negative for the Beilstein test but was not pure enough. However, the ultraviolet spectrum of this material was resembling well that of IV, (Fig. 3).

α-Oxime by Hydrogen Chloride.—α-Oxime (0.47

13) N. Tokura, R. Asami and R. Tada, *J. Am. Chem. Soc.*, **79**, 3135 (1957).

g.), melting point and mixed m. p. 154~157°C was recovered. (Fig. 4)

β-Oxime by Hydrogen Chloride.—The ultraviolet spectrum of the product was reproduced in Fig. 5. Two kinds of crystals were separated by fractional precipitation as above mentioned. One, melting point and mixed m. p. 55.56°C (0.40 g.) was the ketone V, 2,4-dinitrophenyl hyrazone, m. p. 198~199.5°C, Found: N, 15.68. Calcd. for $C_{19}H_{20}O_4N_4$: N, 15.21%. The other, (0.12 g.), melting point and mixed m. p. 156~158°C was the α-oxime[1] isomerized from the β-oxime II.

α-Oxime by Hydrogen Bromide.—α-Oxime (0.48 g.), melting point and mixed m. p., 155~157°C was recovered.

β-Oxime by Hydrogen Bromide.—The ketone V, (0.15 g.), meltng point and mixed m. p. 53~55°C, and the α-oxime (0.23 g.), melting point and mixed m. p. 156~158°C, were separated and identified respectively, as above.

α-Oxime by Thionyl Chloride in Ether at −70°C.—The α-oxime (0.33g.) was recovered, melting point and mixed m. p. 155~157°C, (ultraviolet spectrum, Fig. 2).

β-Oxime by Thionyl Chloride in Ether at −70°C.—The product (0.43 g.), melting point and mixed m. p. 142~143.5°C was proved to be the IV. The ultraviolet spectrum was superimposable. (Fig. 3)

Summary

The Beckmann rearrangement of the isomeric cylcohexyl phenyl ketoximes was carried out in liquid sulfur dioxide at low temperature (−70°C) with thionyl chloride, benzenesulfonyl chloride, bromine and hydrogen halides. In liquid sulfur dioxide, the β-oxime was unstable and isomerized slowly to the α-oxime with no reagent. The α-oxime yielded *N*-cyclohexyl benzamide and the β-oxime yielded cyclohexanecarboxyanilide, respectively, by the Beckmann rearrangement in liquid sulfur dioxide. The geometrical structure of the isomers and isomerization between them were discussed. As for the β-oxime, the rate of the rearrangement by far surpassed the rate of the isomerization. The principle of the trans migration in the Beckmann rearrangement has been confirmed within the range of this experiment. The deoximation of the oxime to the parent ketone, cyclohexyl phenyl ketone was observed in the reaction of β-oxime with hydrogen chloride and bromide.

We are indebted to the Befu Chemical Industries Ltd., for the donation of liquid sulfur dioxide. The present authors are also grateful to Professor Y. Yukawa of Osaka University for his courtesy in carrying out this project.

Chemical Research Institute of Non-Aqueous Solutions Tohoku University, Sendai

---

On the Reactivity of Various Silicate Minerals toward Acids

By Hanzo MASE

(Received May 31, 1960)

As for the relative difficulty of dissolution of oxyacids and their salts toward water, a few qualitative rules have been proposed on the standpoint of ionic potential[1]. However, it is not too much to say that no comprehensive treatises on the reactivity of various silicate minerals toward ordinary acids (except hydrofluoric acid) have been reported, although the studies on the individual one have been undertaken by many investigators[2].

Previously, the author pointed out the requirements for the frothing reaction of silicate minerals toward water and concentrated sulfuric acid. Those requirements were summarized as follows: 1) the silicates belonging to either the neso- or the phyllo-silicates are generally reactive; 2) in the phyllosilicates, most of those of the 1:1 type (e. g., serpentine) are as a rule reactive, but those of the 2:1 type are not at all or only slightly reactive; and 3) the more electropositive the metallic components are, the more reactive the silicates become. But the electropositivity of metals was not discussed in detail.

1) G. H. Cartledge, *J. Am. Chem. Soc.*, **50**, 2855 (1928); V. M. Goldschmidt, *J. Chem. Soc.*, **1937**, 655; F. E. Wickman, *Arkiv. Kemi, Min. Geol.*, **19B**, No. 2 (1944); R. Tsuchida, *Chemistry (Kagaku)*, **6**, 6 (1951); **7**, 88 (1952).

2) W. Eitel, "The Physical Chemistry of the Silicates", The University of Chicago Press, Chicago, Illinois (1954), p. 965; S. Nagai and Y. Arai, *Gypsum and Lime (Sekko to Sekai)*, **34**, 7 (1958); J. Ando, *J. Chem. Soc. Japan, Ind. Chem. Sec. (Kogyo Kagaku Zasshi)*, **63**, 83 (1960).

In this paper, the author attempted to make this problem clear by using various terms concerning the combining forces between the cations and the silicate ions, and also to explain it energetically from the bonding energies of silicate minerals.

Results from the Electropositivity of the Constituent Metals

It is well known in the field of crystal chemistry that the bonding force between various cations and silicate ions is related to the polarizing power of the cations or their tendencies to form covalent bonds with oxygen atoms. One may say that a cation with strong polarizing power or a pronounced tendency to make covalent bonds loosens bonds within a silicate ion, thus causing a splitting up of it into free acids. On the contrary, cations with small polarizing power allow strong bonds to form within the silicate ion and do therefore make stable silicate.

This polarizing power of cations is qualitatively or approximately measured with their ionic potentials (e. g., cation charge/cation radius), the ratio of cation charge to the square of cation radius (Goldschmidt's polarizing power), or the field strength around the cations[3], etc. (hereafter referred to as ϕ, ϕ' or F. S., respectively.)

Therefore, the author tried to calculate and to view the above mentioned values of various cations contained in silicate minerals. The results were listed in the following table[4].

ϕ; more than 4	Ti, Be, Al, Cr, V(III), Zr, Fe(III), Mn(III).
3~4	Th, Sc.
2~3	Y, Mg, Ni, Ce, La, Fe(II), Zn, Mn(II).
less than 2	Cu, Ca, Sr, Pb, Ba, Li, Na, K.
ϕ'; more than 6	Be, Ti, Al, Cr, V(III), Fe(III), Mn(III).
4~6	Zr, Sc.
2~4	Th, Mg, Ni, Y, Fe(II), Zn, Mn(II), Ce, La.
less than 2	Cu, Ca, Li, Sr, Pb, Na, Ba, K.
F. S.; more than 0.7	Ti, Th, Al, Cr, Zr, V(III), Fe(III), Be, Mn(III).
0.5~0.7	Sc, Y.
0.4~0.5	Ce, La, Mg, Ni, Fe(II), Zn, Mn(II).
less than 0.4	Cu, Ca, Sr, Pb, Ba, Li, Na, K.

As shown in this table, the polarizing power of the following cations seems to be extremely great, and further the electropositivity of them to be small: e. g., Ti, Be, Al, Cr, V(III), Fe(III), Mn(III), Zr, etc. Thus the existence of these metals may contribute to the decrease of reactivity of silicate minerals. This conclusion is in agreement with the experimental results that kaolinite is not completely decomposed, although serpentine is easily attacked by acids.

As is generally known, all the silicate minerals were now divided into five classes structurally; namely, neso-, soro-, ino-, phyllo-, and tecto-silicate. According to this classification, it was at first in Tables I—V[5] examined whether or not the singularity of the above eight metal ions is applicable to those silicates. In Tables I—V the results of reactions toward acids are made an entry. Most of them are cited from the data of Lange's Handbook[6], Dana's Textbook of Mineralogy[7], and Mellor's Treatise[8]. The parenthesized passage is refered to the author's prediction.

Nesosilicate Minerals.—The nesosilicates are termed the silicates having the structures with separated tetrahedra $(SiO_4)^{4-}$ groups, and involve the following minerals listed in Table I.

Generally speaking, the results in Table I seem to indicate that the majority of nesosilicate minerals are able to react with acids, and to be decomposed with the formation of gelatinous silica, except the garnet group and a few particular complex silicate minerals. Also it is confirmed that one of the above eight metallic elements is inevitably contained in these insoluble nesosilicate minerals.

For example, phenacite (Be_2SiO_4) is not attacked by acids. This fact is probably due to the existence of Be atoms, which have very large ϕ, ϕ' and F. S. For the same reason, the garnet group minerals, euclase, topaz, zunyite, andalusite, sillimanite, mullite, kyanite, sapphirine, etc. may be not decomposed by acids. Moreover titanosilicate minerals containing Ti atoms are inactive toward acids. Although

3) A. Dietzel, *Naturwiss.*, **29**, 537 (1941); *Electrochem.*, **48**, 9 (1942).

4) The values of the ionic radii of various cations were quoted from C. W. Stillwell's "Crystal Chemistry", McGraw-Hill Book Co., Inc., New York (1938).

5) The classification, species and structural formula of silicate minerals are based upon Sudo's system (which is primarily cited from Berman's and Swartz's systems and is revised and enlarged with the latest data.) and Strunz's Tables (H. Strunz, "Mineralogische Tabellen" (1958)).

H. Berman, *Am. Mineralogist*, **22**, 342 (1937); O. K. Swartz, ibid., **22**, 1073, 1161 (1937); T. Sudo, "Mineral Chemistry (Kobutsu Kagaku) (II)", Kyoritsu Shuppan Co., Ltd. (1959), p. 259.

6) Lange's Handbook of Chemistry (1949).

7) Dana's Textbook of Mineralogy (1959).

8) W. Mellor, "A Comprehensive Treatise on Inorganic and Theoretical Chemistry", Vol. VI (1925).

Table I. Reactivity of nesosilicate minerals toward acids

Minerals	Chemical formula	Reactivity toward acids	Bonding energy (kcal.)
Olivine series (Ca, Mn, Mg, Fe, Pb) (Mg, Fe, Mn, Zn) SiO_4			
Forsterite	Mg_2SiO_4	Gel. a.	29796
Olivine	$(Mg, Fe)_2SiO_4$	Gel. a.	(29904)*1)
Hortonolite	$(Mg, Fe, Mn)_2SiO_4$	Gel. a.	
Fayalite	Fe_2SiO_4	Gel. a.	(29880)
Knebelite	$(Fe, Mn)_2SiO_4$	Gel. a.	
Tephroite	$(Mn, Zn, Mg)_2SiO_4$	Gel. a.	
Roepperite	$(Fe, Mn, Zn)_2SiO_4$	Gel. HCl	
Glaucochroite	$CaMnSiO_4$	Gel. HCl	
Monticellite	$CaMgSiO_4$	Gel. HCl	(29358)
Larsenite	$PbZnSiO_4$	Sol. HNO_3	
Calcium Larsenite	$(Pb, Ca)ZnSiO_4$	Sol. HNO_3	
Larnite	Ca_2SiO_4	Sol. HCl	(28920)
Merwinite	$Ca_3Mg(SiO_4)_2$	Sol. HCl	(29139)
Phenacite group X_2SiO_4			
Phenacite	Be_2SiO_4	Insol.	
Willemite	Zn_2SiO_4	Gel. a.	
Troostite	$(Zn, Mn)_2SiO_4$	Gel. a.	
Trimerite	$CaMn_2(BeSiO_4)_3$	Sol. HCl	
Humite group $nMg_2SiO_4 \cdot Mg(OH, F)_2$			
Norbergite	$Mg_2SiO_4 \cdot Mg(OH, F)_2$	Gel. a.	(27632)*2)
Chondrodite	2 〃 . 〃	Gel. a.	(28498)*2)
Humite	3 〃 . 〃	Gel. a.	(28869)*2)
Clinohumite	4 〃 . 〃	Gel. a.	(29075)*2)
Hodgkinsonite group $X_{2+x}(SiO_4)_2(OH, F)_2$			
Hodgkinsonite	$(Zn, Mn)(SiO_4)(OH)_2$	Sol. a.	
Alleghanyite	$Mn_5(SiO_4)_2(OH, F)_2$	Sol. a.	
Leucophoenicite	$Mn_7(SiO_4)_4(OH)_2$	Sol. a.	
Garnet group $X_3Y_2(ZO_4)_3$	X=Mg, Fe, Mn, Ca Y=Al, Fe(III), Cr, Ti, Mn Z=Si, Ti		
(1) Almandite series $(Mg, Fe, Mn)_3Al_2(SiO_4)_3$			
Pyrope	$Mg_3Al_2(SiO_4)_3$	Insol.	(31836)
Almandite	$Fe_3Al_2(SiO_4)_3$	Insol.	31878
Spessartite	$Mn_3Al_2(SiO_4)_3$	Insol.	
(2) Andradite series			
Grossularite	$Ca_3Al_2(SiO_4)_3$	Insol.	(31398)
Andradite	$Ca_3Fe_2(SiO_4)_3$	Insol.	
Uvarovite	$Ca_3Cr_2(SiO_4)_3$	Insol.	
Titanium Garnet	$Ca_3(Al, Fe(III), Fe(II), Ti)_2[(Si, Ti)O_4]_3$	Insol.	
Zircon group $XSiO_4$			
Zircon	$ZrSiO_4$	Mostly insol.	
Thorite	$ThSiO_4$	Gel. a.	
Wöhlerite group $W_2X(ZO_4)_2(F, OH)$			
Rosenbuschite	$(Na, Ca)_3(Fe, Ti, Zr)(SiO_4)_2F$	Sol. HCl	
Wöhlerite	$(Ca, Na)_3(Zr, Ta)(SiO_4)_2F$	Sol. HCl	
Hiortdahlite	$(Ca, Na)_{13}(Fe, Mn, Zr, Ti)(SiO_4)_5(F, OH)$	(Sol. HCl)	
Guarinite	$(Ca, Na)_5(Fe, Mn, Zr, Ta)(SiO_4)_2(O, F, OH)$	Gel. HCl	
Johnstrupite	$(Ca, Na, Ce)_3(Al, Mg, Ti, Ce)(SiO_4)_2(F, OH)$	Sol. HCl	(29850)*3)
Rinkite	$(Ca, Na)_6(Ce, Zr, Ti)_2(SiO_4)_{10}F_2$	Decomp. H_2SO_4	
Rinkolite	$(Ca, Na)_6(Ce, Ti)_3(SiO_4)_4(F, OH)_4$	(Decomp. a.)	
Mosandrite	$(Ca, Na)_{12}Ce_3(Zr, Ti, Mg)_4(SiO_4)_{10}F_5$	Sol. HCl	
Lavenite	$(Ca, Na)(Zr, Ta, Fe, Ti, Mn)(SiO_4)F$	Sl. sol. HCl	
Britholite	$Ca_3Ce_4[(Si, P)O_4]_4(OH, F)_3$	(Decomp. a.)	
Hellandite	$Ca_3(Y, Er)_4(Al, Fe(III), Mn(III))_5(SiO_4)_6(OH)_3$	Sol. HCl	

TABLE I. (Continued)

Minerals	Chemical formula	Reactivity toward acids	Bonding energy (kcal.)
Lessingite	$Ca_2(Ce, La, Na)_2(SiO_4)_3(OH, F)$	(Decomp. a.)	
Beckelite		Sol. a.	
Datolite group			
Datolite	$Ca_2B_2(SiO_4)_2(OH)_2$	Gel. HCl	
Euclase	$Al(BeOH)SiO_4$	Insol.	
Homilite	$Ca_2Fe(II)Be_2(SiO_4)_2O$	Gel. HCl	
Gadolinite	$Y_2Fe(II)Be_2(SiO_4)_2O_2$	Gel. a.	
Misc.			
Topaz	$Al_2SiO_4(F, OH)_2$	Sl. decomp. H_2SO_4	31712
Ilvaite	$Ca(Fe, Mn)_2Fe(III)(SiO_4)_2(OH)$	Gel. a.	
Afwillite	$Ca_3(SiO_3OH)_2 \cdot 2H_2O$	(Decomp. a.)	
α-Eucryptite	α-$LiAl(SiO_4)$	Gel. HCl	
Eulytite	$Bi_4(SiO_4)_3$	Gel. HCl	
Zunyite	$Al_{12}(Si_2O_7)_2(SiO_4)(AlO_4)(OH, F)_{15}Cl$	Insol.	
Quasi-silicates			
Aluminum silicates			
Andalusite	Al_2SiO_5	Insol.	
Sillimanite	Al_2SiO_5	Insol.	31957
Mullite	$(Al_2O)_6(SiO_4)_6(Al_2O_7)$	Insol.	
Kyanite	Al_2SiO_5	Insol.	
Staurolite	$Fe(II)Al_4Si_2O_{10}(OH)_2$	Sl. decomp. H_2SO_4	31828
Kentrolite group			
Kentrolite	$Pb_2Mn(III)_4Si_2O_{15}$	Sol. a.	
Melanotekite	$Pb_2Fe(III)_4Si_2O_{15}$	Decomp. HNO_3	
Titanosilicates			
Titanite	$CaTiSiO_5$	Sol. H_2SO_4	(32942)
Lorenzenite	$Na_2(Zr, Ti)_2Si_2O_9$	Insol. HCl	
Ramsayite	$Na_2Ti_2Si_2O_9$	(Insol.)	(33845)
Lamprophyllite	$Na_3Sr_2Ti_3(SiO_4)_4(O, OH, F)_2$	(Insol.)	
Fersmanite	$Ca_4Na_4Ti_4Si_2O_{18}F_2$ (?)	(Insol.)	
(App.)			
Dumortierite	$(Al, Fe)_7BSi_3O_{18}$	Insol. HF	
Serendibite	$(Ca, Mg)_5Al_5BSi_4O_{20}$	(Insol.)	
Sapphirine	$Mg_2Al_4SiO_{10}$	Insol.	(31283)
Ardennite	$Mn_5Al_5(V, As)O_4Si_5O_{20}(OH)_2 \cdot 2H_2O$	(Insol.)	
Kornerupine	$(Mg, Fe, Al)_4(Al, B)_6Si_4O_{16}(O, OH)_{5\sim6}$	(Insol.)	
Cappelenite	$(Ba, Ca, Ce, Na)_3(Y, Ce, La)_6B_6Si_6O_{27}$	Sol. HCl	
Melancocerite	$Ca_{16}Na_4(Y, La)_2(Zr, Ce)_6B_2Si_{12}O_{57}F_{12}$	Decomp. HCl	
Uranosilicates			
Uranophane	$Ca(H_3O)_2(UO_2)(SiO_4)_2 \cdot 3H_2O$	Gel. HCl	
Sklodowskite	$MgU_2O_2(OH)_2(SiO_4)_2 \cdot 4H_2O$	Gel. HCl	
Kasolite	$PbUO_2SiO_4 \cdot H_2O$	Gel. a.	
Soddyite	$(UO_2)_2SiO_4 \cdot 2H_2O$ (?)	Gel. HCl	

(Abbreviations used in Tables I—V.)
a.: acids; abbr.: abbreviation; app.: appendix; conc.: concentrated; decomp.: decomposed (by); gel.: gelatinize; insol.: insoluble (in, or, in acids); misc.: miscellanea; sl.: slightly; sol: soluble (in); undecomp.: undecomposed (by).
(The minerals cited in the appendixes in these tables are unassigned up to the present.)
*1) This value was calculated regarding the compositional formula of olivine as $9Mg_2SiO_4 \cdot Fe_2SiO_4$.
*2) These values were calculated regarding $nMg_2SiO_4 \cdot Mg(OH, F)_2$ as $nMg_2SiO_4 \cdot Mg(OH)_2$.
*3) This value was calculated regarding the chemical formula of johnstrupite as ideally $Ca_3Al(SiO_4)_2(OH)$.

TABLE II. REACTIVITY OF SOROSILICATE MINERALS TOWARD ACIDS

Minerals	Chemical formula	Reactivity toward acids	Bonding energy (kcal.)
Benitoite	$BaTi(Si_3O_9)$	Sol. HF	
Rhodonite series			
Rhodonite	$(Mn, Ca)_5Si_5O_{15}$	Sl. sol. HCl	
Pyroxmangite	$(Mn, Ca)_7Si_7O_{21}$	Insol. a.	
Wollastonite group			
Wollastonite	$Ca_3Si_3O_9$	Decomp. HCl	
Bustamite	$(Ca, Mn)_3Si_3O_9$	(Decomp. HCl)	
Pectolite	$Ca_2NaH(SiO_3)_3$	Gel. HCl	
Alamosite	$PbSiO_3$	(Gel. HNO_3)	
Catapleiite series			
Catapleiite	$Na_2Zr(Si_3O_9)\cdot H_2O$	Sol. HCl	
Eudialyte	$(Na, Ca, Fe)_6ZrSi_6O_{15}(OH, Cl)$	Gel. HCl	
Steenstrupine	$(Ca, Na)_4Mn(Ce, La, Al, Fe(III))_6(Si, Ti)_9O_{27}(OH)_7\cdot 3H_2O$ (?)	Decomp. a.	
Tourmaline series	$WX_3Y_6(Z_3O_9)_3(O, OH, F)_4$		
Dravite	$NaMg_3B_3Al_3(Al_3Si_6O_{27})(OH)_4$	Undecomp. a.	
Uvite	$CaMg_3B_3Al_3(Al_3Si_6O_{27})(O, OH)_4$	Undecomp. a.	
Indigolite	$Na(Al, Fe(II), Li, Mg)_3B_3Al_3(Al_3Si_6O_{27})(O, OH, F)_4$	Undecomp. a.	
Tourmaline	$(Na, Ca)(Mg, Fe(II), Fe(III))_3B_3Al_3(Al_3Si_6O_{27})(O, OH)_4$	Undecomp. a.	
Schorl	$NaFe_3B_3Al_3(Al_3Si_6O_{27})(OH)_4$	Undecomp. a.	
Misc.			
Dioptase	$Cu_6(Si_6O_{18})\cdot 6H_2O$	Gel. HCl	
Axinite	$(Fe, Mn)Ca_2Al_2(BO_3)(Si_4O_{12})(OH)$	Undecomp. a.	
Beryl	$Al_2Be_3Si_6O_{18}$	Insol.	
Osumilite	$(K, Na, Ca)(Mg, Fe(II))_2(Al, Fe(III), Fe(II))_3(Si, Al)_{12}O_{30}\cdot H_2O$	(Sl. decomp. a.)	
Indialite	$(Mg, Fe)_2Al_3(Si_5, Al)O_{18}$	(Sl. decomp.)	(31920)*1)
Cordierlite	$(Mg, Fe)_2Al_3(Si_5, Al)O_{18}$	Sl. decomp. a.	(31920)*1)
Thalenite group			
Thalenite	$Y_2Si_2O_7$	(Insol. a.)	
Thortveiteit	$(Sc, Y)_2Si_2O_7$	Insol. HCl	
Cerite	$(Ce, Y, Pr, Nd)_2Si_2O_7\cdot H_2O$	Gel. HCl	
Rowlandite	$(Y, Ce, La)_4Fe(II)(Si_2O_7)_2F_2$	Gel. HCl	
Melilite series			
Åkermanite	$Ca_2MgSi_2O_7$	Gel. HCl	30391
Gehlenite	$Ca_2Al(AlSiO_7)$	Gel. HCl	26890
Melilite	$(Ca, Na)_2(Al, Mg)(Si, Al)_2O_7$	Gel. HCl	
Hardystonite	$Ca_2ZnSi_2O_7$	Gel. HCl	
Leucophanite	$(Ca, Na, H)_2BeSi_2O_6(OH, F)$ (?)	Sol. HF	
Meliphanite	$(Ca, Na)_2(Be, Al)Si_2O_6F$	(Insol.)	
Barysilite group			
Barysilite	$Pb_3Si_2O_7$	Gel. HNO_3	
Ganomalite	$Pb_9Ca_4(Si_2O_7)_3(OH)_2$	Gel. HNO_3	(27383)*2)
Nasonite	$Pb_6Ca_4(Si_2O_7)_3Cl_2$	Gel. HNO_3	
Hemimorphite group			
Hemimorphite	$Zn_4(OH)_2Si_2O_7\cdot H_2O$	Gel. a.	
Clinohedrite	$Ca_2Zn_2Si_2O_7(OH)_2\cdot H_2O$	Gel. HCl	
Bertrandite	$Be_4Si_2O_7(OH)_2$	Insol. a.	
Cuspidine	$Ca_4Si_2O_7(F, OH)_2$	(Gel. HCl, HNO_3)	(28427)*3)
Molybdophyllite	$Pb_2Mg_2Si_2O_7(OH)_2$	(Gel. HNO_3)	
Murmanite	$NaTiSiO_4(OH)$ (?)	(Insol. a.)	(32, 164) (?)
(App.)			
Barylite	$BaBe_2Si_2O_7$	Insol.	
Lawsonite	$CaAl_2Si_2O_7(OH)_2\cdot H_2O$	Insol.	(31,030)
Danburite	$CaB_2Si_2O_8$	Sl. decomp. HCl	

TABLE II. (Continued)

Minerals	Chemical formula	Reactivity toward acids	Bonding energy (kcal.)
Astrophyllite	$(K_2, Na_2, Ca)(Fe, Mn)_4(Ti, Zr)Si_4O_{14}(OH)_2$	Decomp. HCl	
Aenigmanite	$(Na, Ca, K)_4(Fe(II), Mn, Fe(III), Ti, Al)_{13}(Si_2O_7)_6$ (?)	Sl. sol. a.	
Vesuvianite	$Ca_{10}Al_4(SiO_4)_5(Si_2O_7)_2 \cdot 2(Mg, Fe)(OH)_2$	Sl. decomp. HCl	
Epidote group	$W_2Y_3(ZO_4)(OH)(Z_2O_7)O$		
Zoisite	$Ca_2Al_3(SiO_4)(Si_2O_7)O(OH)$	Insol.*4)	
Epidote series			
Clinozoisite	$Ca_2Al_3(SiO_4)(Si_2O_7)O(OH)$	Insol.	
Epidote	$Ca_2(Al, Fe)_3(SiO_4)(Si_2O_7)O(OH)$	Sl. decomp. HCl	
Piedmontite	$Ca_2(Al, Fe, Mn)_3(SiO_4)(Si_2O_7)O(OH)$	(Sl. decomp. a.)	
Allanite series			
Allanite	$(Ca, Ce, La, Na)_2(Al, Fe, Mn, Be, Mg)_3(SiO_4)(Si_2O_7)O(OH)$	Gel. HCl	
Nagatelite	$(Ca, Ce)_2(Al, Fe(III), Fe(II))_3[(P, Si)O_4][(P, Si)_2O_7]O(OH)$	Sol. HCl, HNO_3	
Pumpellyite	$Ca_4(Mg, Fe, Mn)(Al, Fe, Ti)_5Si_6O_{23}(OH)_3 \cdot 2H_2O$	(Sol. HCl)	

*1) These values were calculated regarding $(Mg, Fe)_2Al_3(Si_5, Al)O_{15}$ as $Mg_2Al_3(Si_5, Al)O_{15}$.
*2) This value was calculated regarding the chemical formula of ganomalite as $Ca_{10}(Si_2O_7)_3(OH)_2$.
*3) This value was calculated regarding $\cdots\cdots(F, OH)_2$ as $\cdots\cdots(OH)_2$.
*4) The fine powder of zoisite is completely decomposed by boiling hydrochloric acid.

TABLE III. REACTIVITY OF INOSILICATE MINERALS TOWARD ACIDS

Minerals	Chemical formula	Reactivity toward acids	Bonding energy (kcal.)
Pyroxene group $W(X, Y)(Z_2O_6)$	W=Ca, Na, K, Mg, Mn. X, Y=Mg, Fe(II), Al, Ti, Li, Mn, Fe(III), Cr, Ni. Z=Si, Al.		
(1) Enstatite series WXZ_2O_6			
Enstatite	$MgSi_2O_6$	Insol. HCl	32344
Hyperthene	$(Mg, Fe)_2Si_2O_6$	Insol. a.	
(2) Pigeonite series			
Clinoenstatite	$Mg_2Si_2O_6$	Insol. a.	
Pigeonite	$(Ca, Mg)(Mg, Fe)Si_2O_6$	(Insol. a.)	
(3) Diopside series $W(X, Y)Z_2O_6$			
Diopside	$CaMgSi_2O_6$	Insol. a.	32052
Hedenbergite	$CaFeSi_2O_6$	Insol. HCl	(32080)
Augite	$(Ca, Mg)(Mg, Fe, Al)(Al, Si)_2O_6$	Insol. a.	30728
Schefferite	$Ca(Mg, Fe, Mn)Si_2O_6$	(Insol. a.)	
Jeffersonite	$Ca(Mg, Mn, Zn)Si_2O_6$	(Insol. a.)	
(4) Acmite-Jadeite series WYZ_2O_6			
Acmite	$NaFe(III)Si_2O_6$	Very sl. sol. a.	
Jadeite	$NaAlSi_2O_6$	Insol. a.	(33848)
Aegirite	$(Ca, Na)(Mg, Fe(III), Al)Si_2O_6$	Insol. a.	
Spodumene	$LiAlSi_2O_6$	Insol. a.	
(App.)			
Margarosanite	$(Pb, Ca, Mn)SiO_3$	Gel. HNO_3	
Babingtonite	$Ca_2Fe(II)Fe(III)Si_5O_{14}(OH)$	Gel. HCl	
Taramellite	$BaFeSi_2O_6(OH)$	Insol. a.	
Hyalotekite	$(Pb, Ca, Ba)_4BSi_6O_{17}(F, OH)$	Insol. a.	
Neptunite	$Na_2FeTiSi_4O_{12}$	Insol. HF	(33938)

Table III. (Continued)

Minerals	Chemical formula	Reactivity toward acids	Bonding energy (kcal.)
Calcium metasilicates			
Inesite	$Ca_2Mn_7H_2Si_{10}O_{30}\cdot 5H_2O$	(Sol. HCl)	
Hillebrandite	$Ca_2SiO_4\cdot H_2O$	Sol. HCl	(28027)*1)
Riversideite	$Ca_5H_2Si_6O_{18}\cdot 2H_2O$	Sol. HCl	(31285)
Copper metasilicates			
Chrysocolla	$CuSiO_3\cdot nH_2O$	Decomp. a.	
Shattuckite	$8CuSiO_3\cdot 4H_2O$	(Decomp. a.)	
Plancheite	$14CuSiO_3\cdot 4H_2O$	(Decomp. a.)	
The others			
Carpholite	$MnAl_2Si_2O_6(OH)_4$	Insol. HCl	
Stokesite	$CaSnSi_3O_9\cdot 2H_2O$	Insol. a.	
Searlesite	$NaBSi_2O_6\cdot H_2O$	Decomp. HCl	
Bavenite	$Ca_4AlBe_2HSi_9O_{27}\cdot H_2O$	(Sl. sol. a.)	
Cainosite	$Ca_2(Ce, Y)_2Si_4O_{12}CO_3\cdot 1\sim 2H_2O$	Sol. HCl	
Epididymite	$NaBeSi_3O_7(OH)$	Very sl. sol. a.	
Elpidite	$Na_2(Zr, Ti)Si_6O_{15}\cdot 3H_2O$	(Sl. sol. a.)	
Leucosphenite	$Ba(Na, Ca)_4Ti_2BSi_5O_{17}$	Decomp. HF	
Ussingite	$Na_2Al(Si_3O_8)(OH)$	Gel. HCl	
Amphybole group $(W, X, Y)_{7\sim 8}(Z_4O_{11})_2(O, OH, F)_2$			
(1) Anthophyllite series			
Anthophyllite	$(Mg, Fe)_7Si_8O_{22}(OH)_2$	Insol.	
Gedrite	$(Mg, Fe, Al)_7(Al, Si)_8O_{22}(OH)_2$	(Insol.)	
(2) Cummingtonite series $X_7(Z_4O_{11})_2(OH)_2$			
Cummingtonite	$(Mg, Fe)_7Si_8O_{22}(OH)_2$	(Insol.)	
Grunerite	$(Mg, Fe, Mn)_7Si_8O_{22}(OH)_2$	Insol. a.	
Kupfferite	$Mg_7Si_8O_{22}(OH)_2$	(Insol.)	(32430)
(3) Tremolite series			
Tremolite	$Ca_2Mg_5Si_8O_{22}(OH)_2$	Insol.	32284
Actinolite	$Ca_2(Mg, Fe)_5Si_8O_{22}(OH)_2$	Insol.	
(4) Hornblende series $W_0(X, Y)_{10}(Z_4O_{11})_4(O, OH, F)_4$			
Edenite	$Ca_4Na_2Mg_{10}Al_2Si_{14}O_{44}(OH, F)_4$	(Insol.)	(31272)*2)
Pargasite	$Ca_4Na_2Mg_9Al_4Si_{13}O_{44}(OH, F)_4$	(Insol.)	(31088)*3)
Hastingsite	$Ca_4Na_2Mg_5Al_6Si_{12}O_{44}(OH, F)_4$	(Insol.)	(30904)*3)
Hornblende	$Ca_4Na_2(Mg, Fe(II))_5(Al, Fe(III), Ti)_6Si_{12}O_{44}(OH, O)_4$	Insol. a.	
Kaersutite	$Ca_4Na(Mg, Fe(II))_7(Al, Fe(III))_6Ti_2Si_{12}O_{46}(OH)_2$	(Insol.)	
Arfvedosonite	$Na_6Mg_5Al_2Si_{16}O_{44}(OH, F)_4$	Insol. a.	(32538)*2)
〃	$Ca_2Na_4Fe(II)_7(Al, Fe(III))_6Si_{13}O_{44}(OH)_4$	Insol. a.	
Holmquistite	$CaNaLi_2Mg_6Al_2Si_{15}O_{44}(OH)_2$	(Insol. a.)	
Glaucophane	$Na_4Mg_6Al_4Si_{16}O_{44}(OH, F)_4$	Insol. a.	(33182)*2)
Riebeckite	$Na_6Fe(II)_6Fe(III)_4Si_{16}O_{46}(OH)_2$	Insol. a.	
Narsarsukite	$Na_2(Ti, Fe(III))Si_4(O, OH, F)_{11}$	Insol. a.	
Chrysotile	$(Mg, Fe)_6Si_4O_{11}(OH)_6\cdot H_2O$	Decomp. H_2SO_4	(29468)*3)
(App.)			
Sepiolite	$Mg_5H_2(Si_4O_{11})_3\cdot 3H_2O$	Decomp. HCl	(32627)
Attapulgite	$Mg_5Si_8O_{20}(OH)_2\cdot 8H_2O$	(Decomp. a.)	(31076)

*1) This value was calculated regarding the chemical formula of hillebrandite as $Ca_2SiO_3(OH)_2$.
*2) These values were calculated regarding ……$(OH, F, or, OH, O)_4$ as …… $(OH)_4$.
*3) This value was calculated regarding $(Mg, Fe)_6$…… as Mg_6…….

TABLE IV. REACTIVITY OF PHYLLOSILICATE MINERALS TOWARD ACIDS

Minerals	Chemical formula	Reactivity toward acids	Bonding energy (kcal.)
	Phyllosilicates of aluminum. $Y_pSi_4O_{10}(OH)_{2p-4}\cdot sH_2O$ Y=Al, Fe(III), rarely Cr; $p=2\sim3$; $s=0\sim4$.		
2 : 1 Type			
Pyrophyllite	$Al_2Si_4O_{10}(OH)_2$	Sl. decomp. HCl	32558
1 : 1 Type kaolin minerals	$Al_4Si_4O_{10}(OH)_8$		
Kaolinite	$Al_4Si_4O_{10}(OH)_8$	Sl. decomp. HCl	
Dickite	〃	(Sl. decomp. HCl)	32165
Nacrite	〃	(Sl. decomp. HCl)	
	Phyllosilicates of iron, magnesium, calcium and manganese.		
2 : 1 Type			
Talc	$Mg_3Si_4O_{10}(OH)_2$	Undecomp. a.	(32516)
Minnesotaite	$(Fe(II), Mg)_{5.5}(Si, Al, Fe(III))_8O_{18.5}(OH)_{5.5}$	(Undecomp. a.)	
Chlorite graup (abbr.)			
Clinochlore	(abbr.)	Decomp. H_2SO_4	
Penninite	(abbr.)	Decomp. H_2SO_4	
Prochlorite	(abbr.)	Decomp. hot H_2SO_4	
Montmorillonite group			
Montmorillonite	$(E.C.)^{*1}_{0.67}(Al_{3.33}Mg_{0.67})Si_8O_{20}(OH)_4$	Decomp. boiling a.	
Beidellite	$(E.C.)^{*1}_{0.67}Al_4(Si_{7.33}Al_{0.67})O_{20}(OH)_4$	(Decomp. boiling a.)	
Nontronite	$(E.C.)^{*1}_{0.67}Fe_4(Si_{7.33}Al_{0.67})O_{20}(OH)_4$	Gel. HCl	
Saponite	$(E.C.)^{*1}_{0.67}Mg_6(Si_{7.33}Al_{0.67})O_{20}(OH)_4$	Decomp. H_2SO_4	
Iron-saponite	$(E.C.)^{*1}_{0.67}(Mg, Fe)_6(Si_{7.33}Al_{0.67})O_{20}(OH)_4$	(Decomp. a.)	
Sauconite	$(E.C.)^{*1}_{0.67}(Mg, Fe, Zn)_6(Si_{7.33}Al_{0.67})O_{20}(OH)_4$	(Decomp. a.)	
Vermiculite group			
Vermiculite	$(Mg, Fe)_{2\sim3}(Si, Al, Fe(II))_4O_{10}(OH)_2\cdot4H_2O$	(Decomp. a.)	
Brittle mica group			
Chalcodite	$(Mg, Fe)_{13}Al_4Si_{15}O_{50}(OH)_{10}\cdot10H_2O$	(Decomp. a.)	
Epichlorite	$(Mg, Fe)_{10}Al_6Si_{15}O_{49}(OH)_{10}\cdot8H_2O$	(Decomp. a.)	
Stilpnomelane	$(K, Na, Ca)_{0\sim1}(Fe(II), Mg, Al, Fe(III))_{7\sim8}Si_8O_{22\sim24}(OH)_{2\sim4}\cdot H_2O$	(Decomp. a.)	
Margarite	$CaAl_2(Al_2Si_2)O_{10}(OH)_2$	Sl. decomp. HCl	(30914)
Prehnite	$Ca_2Al_2Si_3O_{10}(OH)_2$	Sl. decomp. HCl	(31496)
Chloritoid	$(Fe, Mg)_2Al_4Si_2O_{10}(OH)_4$	Decomp. H_2SO_4	(29976)*2)
Clintonite	$X_4Z_4O_{10}(OH)_2$ X=Mg : Ca : Al=3 : 2 : 1, Al : Si=2 : 1.	Decomp. hot & conc. a.	
Xanthophyllite	$(Mg, Ca, Al)_4(Si, Al)_4O_{10}(OH)_2$	(Decomp. a.)	
Mica group			
(1) Muscovite series			
Muscovite	$KAl_2(AlSi_3)O_{10}(OH, F)_2$	Insol.	32494
Phengite	$K_4Mg_2Al_8Si_{14}O_{40}(OH)_8$	Insol.	(32858)
Alurgite	$K_4Mg_4Al_7Si_{14}O_{39}(OH)_9$	(Insol.)	
Paragonite	$Na_4Al_{12}Si_{12}O_{40}(OH)_8$	Insol. HCl	(32540)
Roscoelite	$K_4V_8Al_4Si_{12}O_{40}(OH)_8$	Sl. decomp. H_2SO_4	
(2) Biotite series			
Biotite	$K_4(Mg, Fe)_{12}Al_4Si_{12}O_{40}(OH)_8$	Decomp. H_2SO_4	30475
Phlogopite	$K_4Mg_{12}Al_4Si_{12}O_{40}(OH)_8$	Decomp. H_2SO_4	(30454)
Cryophyllite	$K_4Mg_{10}Al_8Si_{10}O_{40}(OH)_8$	(Decomp. H_2SO_4)	(30090)
(3) Lepidolite series			
Lepidolite	$K_4Mg_4Li_4Al_8Si_{12}O_{40}(OH)_4F_4$	Very sl. sol. HCl	
〃	$K_4Li_6Al_8Si_{14}O_{42}(OH)_4F_2$	(〃)	
〃	$K_4Li_6Al_7Si_{14}O_{39}(OH)_2F_7$	(〃)	
Zinnwaldite	$K_4Fe(II)_4Li_4Al_8Si_{12}O_{40}(OH)_4F_4$	Sl. sol. HCl	
Polylithionite	$K_4Li_8Al_4Si_{16}O_{40}F_8$	(Sl. sol. HCl)	

Table IV. (Continued)

Minerals	Chemical formula	Reactivity toward acids	Bonding energy (kcal.)
(Misc.)			
Glauconite	$K_{2\sim3}(Mg, Fe, Ca)_{1\sim3}(Fe(III), Al)_{3\sim6}(Si_{13\sim14}Al_{2\sim3})O_{35\sim40}(OH)_{6\sim10}$	Decomp. HCl	
(App.)			
Pholiodolite	$KMg_6AlSi_7O_{20}(OH)_4\cdot3H_2O$	(Decomp. HCl)	(30733)
Cookeite	$(Li, Al)_4(Si, Al)_4O_{10}(OH)_4\cdot2H_2O$	Decomp. H_2SO_4	
Bityite	$CaLiAl_3BeSi_2O_{10}(OH)_2$	(Insol.)	
Ganophyllite	$NaMn_6Al_2(Si_4O_{10})_2(OH)_{11}$ (?)	(Decomp. a.)	
1 : 1 Type			
Antigorite	$Mg_6Si_4O_{10}(OH)_8$	Decomp. H_2SO_4	(29445)
Greenalite	$(Fe(II), Mg)_9Fe(III)_2Si_2O_{22}(OH)_{12}\cdot2H_2O$	(Decomp. H_2SO_4)	
Neponite	$(Mg, Ni)_6Si_4O_{10}(OH)_8$	(Decomp. H_2SO_4)	
Connarite	$(Ni, Mg)_5(Si_4O_{10})_3(OH)_4\cdot6H_2O$	(Decomp. H_2SO_4)	
Amesite	$(Mg, Al, Fe(II))_3(Si, Al)_2O_5(OH)_4$	(Decomp. H_2SO_4)	
Cronstedite	$(Mg, Ca, Fe(II), Fe(III), Al)_{3\sim4}(Si, Al)_2O_5(OH)_4$	(Decomp. H_2SO_4)	
Chamosite	$(Al, Fe(II), Fe(III), Mg, Ti)_3(Si, Al)_2O_5(OH)_4$	(Decomp. H_2SO_4)	
(App.)			
Zeophyllite	$Ca_5Si_6O_{15}(OH, F)_{10}$	(Decomp. HCl, HNO_3)	(29376)*3)
Friedelite	$Mn_5Si_6O_{15}(OH, Cl)_{10}$	Gel. HCl	
Pyrosmalite	$(Mn, Fe)_5Si_6O_{15}(OH, Cl)_{10}$	Gel. HCl	
Schallerite	$Mn_5(Si, Al)_6O_{15}(OH, Cl)_{10}$	(Gel. HCl)	
Ferroschallerite	$(Fe, Mn)_5(Si, Al)_6O_{15}(OH, Cl)_{10}$	(Gel. HCl)	
Centrallasite	$Ca_4Si_6O_{15}(OH)_2\cdot5H_2O$	Decomp. HCl	(30844)
Truscottite	$(Ca, Mg)_4Si_6O_{15}(OH)_2\cdot5H_2O$	(Decomp. HCl)	
Gyrolite	$Ca_4Si_6O_{15}(OH)_2\cdot3H_2O$ (?)	(Decomp. HCl, HNO_3)	(31457) (?)
Bementite	$Mn_7Si_4O_{10}(OH)_6$	Gel. hot HCl	
Errite	$Mn_4Si_4O_{10}(OH)_4\cdot3H_2O$	(Gel. a.)	
Apophyllite	$KCa_4(Si_4O_{10})_2F\cdot8H_2O$	Decomp. a.	
Okenite	$Ca_2(Si_4O_{10})\cdot4H_2O$	Gel. HCl	(31354)
	Anhydrous phyllosilicates containing no aluminum.		
Gillespite	$BaFeSi_4O_{10}$	(Decomp. HCl, HNO_3)	
Sanbornite	$Ba_2Si_4O_{10}$	(Decomp. HCl, HNO_3)	

*1) E. C.=Exchangeable cations (Na, K, Ca, etc.)

*2) This value was calculated regarding the chemical formula of chloritoid as $Fe_2Al_4Si_2O_{10}(OH)_4$.

*3) This value was calculated regarding $\cdots\cdots(OH, F)_{10}$ as $\cdots\cdots(OH)_{10}$.

Table V. Reactivity of tectosilicate minerals toward acids

Minerals	Chemical formula	Reactivity toward acids	Bonding energy (kcal.)
	W=Ca, Na, K; Li, Cs(rare); Mn, Fe, Zn(very rare) Z=Si, Al; Be(rare); N=S, Cl, CO_3, SO_4, H_2O		
Silica group			
Quartz	SiO_2	Insol.	37320
Petalite group			
Petalite	$(Li, Na)AlSi_4O_{10}$	Insol.	
Milarite	$KCa_2AlBe_2Si_{12}O_{30}\cdot\frac{1}{2}H_2O$	Insol.	
Leifite	$Na_4Al_2Si_9O_{22}F_2$	(Insol.)	
Feldspar group WZ_4O_8, W=Na, Ca, K, Ba; Z=Si, Al; Si : Al=3 : 1~1			
(1) Monoclinic system			
Orthoclase	$KAlSi_3O_8$	Insol.	34266
Soda orthoclase	$(K, Na)AlSi_3O_8$	Insol.	
Hyalophane	$(K, Na, Ba)Al(Al, Si)Si_2O_8$	Insol.	
Celsian	$BaAl_2Si_2O_8$	Sol. HCl	

TABLE V. (Continued)

Minerals	Chemical formula	Reactivity toward acids	Bonding energy (kcal.)
(2) Triclinic system			
(a) Microcline series :—			
Microcline	$KAlSi_3O_8$	Insol.	(34521)
Soda microcline	$(K, Na)AlSi_3O_8$	(Insol.)	
Anorthoclase	$(Na, K)AlSi_3O_8$	Insol.	
(b) Plagioclase series :—			
Albite	$NaAlSi_3O_8$	Insol.	34335
Anorthite	$CaAl_2Si_2O_8$	Decomp. HCl	31935
Leucite	$KAlSi_2O_6$	Decomp. HCl	(33248)
Nepheline group WZ_2O_4			
Nepheline	$KNa_3(AlSiO_4)_4$	Gel. a.	(31465)
Kaliophyllite	$KAlSiO_4$	Gel. a.	(31212)
β-Eucryptite	β-$LiAlSiO_4$	Gel. HCl	
Cancrinite group			
Cancrinite	$(Na, K)_6Ca_2(SO_4)_2(AlSiO_4)_6$	Sol. HCl	
Davyne	$(Na_2, Ca)_4(CO_3)(H_2O)_{0\sim3}(AlSiO_4)_6$	Gel. HCl	
Sodalite group			
Sodalite	$Na_8Al_6Si_6O_{24}Cl_2$	Sol. HCl	
Noselite	$Na_8(AlSiO_4)_6\cdot Na_2SO_4$	Gel. HCl	
Hauyne	$(Na, Ca)_{8\sim4}(SO_4)_{2\sim1}(AlSiO_4)_6$	Sol. HCl	
Helvite	$Mn_8S_2(BeSiO_4)_6$	Sol. HCl	
Danalite	$Fe_8S_2(BeSiO_4)_6$	Gel. HCl	
Scapolite series $W_4Z_{12}O_{24}N$			
Marialite	$(Na, Ca)_4Al_3(Al, Si)_3Si_6O_{24}(Cl, CO_3, SO_4)$	Sl. decomp. HCl	
Meionite	$(Ca, Na)_4Al_3(Al, Si)_3Si_6O_{24}(Cl, CO_3, SO_4)$	Decomp. HCl	
Zeolite group			
Mordenite	$(Ca, K_2, Na_2)Al_2Si_{10}O_{24}\cdot 7H_2O$	Decomp. a.	(32590)
Heulandite group			
Clinoptilolite	$Ca_2Na_3Al_7Si_{33}O_{80}\cdot 23H_2O$ (?)	Decomp. a.	(32974) (?)
Heulandite	$CaAl_2Si_7O_{18}\cdot 6H_2O$	Decomp. a.	(32375)
Epistilbite	$CaAl_2Si_6O_{16}\cdot 5H_2O$	Decomp. HCl	(32268)
Brewsterite	$(Sr, Ba, Ca)Al_2Si_6O_{16}\cdot 5H_2O$	Decomp. HCl	
Desmine group			
Desmine	$CaAl_2Si_7O_{18}\cdot 7H_2O$	Decomp. HCl	(32069)
Harmotome	$BaAl_2Si_6O_{16}\cdot 6H_2O$	Decomp. HCl	
Phillipsite	$KCaAl_3Si_5O_{16}\cdot 6H_2O$	Gel. HCl	(30815)
Gismondite	$CaAl_2Si_2O_8\cdot 4H_2O$	Gel. HCl	(29530)
Erionite	$(K_2, Na_2, Ca)Al_2Si_6O_{16}\cdot 6H_2O$ (?)	Sol. HCl	
Chabazite group			
Chabazite	$(Ca, Na_2)Al_2Si_4O_{12}\cdot 6H_2O$	Decomp. HCl	
Gmelinite	$(Na_2, Ca)Al_2Si_4O_{12}\cdot 6H_2O$	Decomp. HCl	
Levynite	$CaAl_2Si_4O_{12}\cdot 6H_2O$	Gel. a.	(30727)
Thomsonite group			
Thomsonite	$NaCa_2[Al_4(Al, Si)_2Si_4]O_{20}\cdot 5H_2O$	Gel. HCl	
Gonnardite	$(Ca, Na)_3(Al, Si)_{10}O_{20}\cdot 6H_2O$	(Gel. HCl)	
Ashcroffine	$KNa(Ca, Mg, Mn)Al_4Si_2O_{15}\cdot 8H_2O$	(Gel. HCl)	
Natrolite group			
Natrolite	$Na_2Al_2Si_3O_{10}\cdot 2H_2O$	Gel. a.	(31240)
Mesolite	$Na_2Ca_2Al_6Si_9O_{30}\cdot 8H_2O$	Gel. a.	(31143)
Scolesite	$CaAl_2Si_3O_{10}\cdot 3H_2O$	Gel. a.	(31098)
Edingtonite	$BaAl_2Si_3O_{10}\cdot 3H_2O$	Gel. a.	
Unassigned			
Yugawaralite	$Ca_4Al_7Si_{20}O_{54}\cdot 14H_2O$	(Gel. a.)	(32657)
Analcite	$NaAlSi_2O_6\cdot H_2O$	Gel. HCl	(32109)
Faujasite	$CaNa_2Al_4Si_8O_{24}\cdot 16H_2O$	Decomp. HCl	(30009)
Laumonite	$CaAl_2Si_4O_{12}\cdot 4H_2O$	Gel. HCl	(31478)
Ferrierite	$(Na, K)_2MgAl_3Si_{15}O_{36}(OH)\cdot 9H_2O$	(Gel. HCl)	
Questionable			
Didymolite	$(Ca, Mg, Fe)Al_2Si_3O_{10}$	Insol. a.	
D'Achiardite	$(K, Na)CaH_3Al_2Si_9O_{24}\cdot 6H_2O$	Decomp. HCl	

trimerite contains Be, it is dissolved by hydrochloric acid. This fact may be due to the presence of a considerable amount of electropositive Mn(II) and Ca.

Generally, it may safely be assumed that 1) of the above-mentioned requirements and the singularity of the above eight metallic elements hold in the case of nesosilicates.

Furthermore, it is noteworthy that the nesosilicate minerals containing Ca, Sr, Ba and Pb react with difficulty with sulfuric acid, because sulfates of these metals are hardly soluble. Of these metals, lead chloride is soluble with difficulty in water, and so the silicate minerals containing Pb do not react easily with hydrochloric acid at ordinary temperatures.

Sorosilicate Minerals.—The results for the solosilicate minerals are listed in Table II. The above inductive rules appear also to be applicable in this case as well as in the case of the nesosilicate minerals. For example, osumilite, indialite, cordierite, the tourmaline and the epidote series minerals may be scarcely attacked by acids, because of the presence of great amounts of Al, and Fe(III); and then for the same reason, schorl probably appears to be undecomposed by acids. In the thalenite group minerals, the fact that thortveiteit is insoluble in acids, in spite of the reactivity of cerite toward acids, is presumably due to the existence of scandium atoms having comparatively large values of ϕ, ϕ' or F. S. Similarly, the fact that bertrandite only in the hemimorphite group is undecomposed by acids appears to be due to the presence of Be. Beryl containing Al and Be is insoluble as shown from the above results. In addition, in the melilite series, leucophanite and meliphanite are slightly decomposed by hydrochloric acid (and perhaps nitric acid) owing to the existence of Be.

From this standpoint, it appears to be deducted that thalenite and rowlandite are probably attacked by acids. Moreover, it is noteworthy that dioptase ($Cu_6Si_6O_{18}\cdot 6H_2O$) having the structure identical with that of beryl[9] is easily decomposed by acids, because Cu^{2+} has remarkably smaller ϕ, ϕ' or F. S. than those of Be^{2+}. But the unreactivity of the rhodonite series[10] seems to be impossible to explain from this viewpoint, and appears to indicate the necessity of consideration for their structures, but now no satisfactory explanation has been offered as to this fact.

Inosilicate Minerals.—As is generally known, the inosilicate minerals are structurally classified in the pyroxene and the amphybole group. The former consists in structure with infinite single chain $(SiO_3)^{2-}_{\infty}$ of $(SiO_4)^{4-}$ tetrahedra with common corners, and the latter is characterized by the double chains of the type $(Si_4O_{11})^{6-}_{\infty}$.

The results are listed in Table III.

From Table III, it would be presumably derived that these inosilicate minerals could not for the most part be decomposed by acids. Taken in connection with their structures, this fact would seem to prove that these silicates are probably constructed by the compact arrangements of metallic ions and $(SiO_3)^{2-}_{\infty}$ or $(Si_4O_{11})^{6-}_{\infty}$ ions; in other words, their metal ions are compactly surrounded with the above-cited giant ions. Relating to this structure, it is noteworthy that the inosilicates containing alkali metals, e. g., the acmite-jadeite series and hornblende series, are not decomposed by acids. Therefore, it seems that the structural factor adds a striking effect to the reactivity toward acids in these cases. But the chemical composition of these silicates also has a comparative effect on their reactivity. For example, the inertness of the above-mentioned acmite-jadeite series and epididymite are probably in part due to the existence of Be and Al; and from the same viewpoint, it is presumably best to deduct the inertness of carpholite and bavenite. Furthermore, the fact that sepiolite and attapulgite are easily decomposed by acids would probably be due to the existence of large voids such as caves passing through between chains of $(Si_4O_{11})^{6-}_{\infty}$ ions[11].

Phyllosilicate Minerals.—As stated above, it is confirmed from the Table IV that all the 1 : 1 type phyllosilicate minerals are easily decomposed by acids, except the aluminum ones (e. g., the kaolin minerals) as was expected. On the contrary, in the 2 : 1 type phyllosilicate minerals, the magnesium type (talc) also is unattacked by acids, as well as the aluminum type (pyrophyllite). This seems to be mainly due to its 2 : 1 type structure; namely, all the magnesium ions in talc are compactly sandwiched with the two infinite layerous ions $(Si_2O_5)^{2-}_{\infty}$. Furthermore, the inertness of the muscovite and lepidolite series appears to be in part due to the above-cited structure and in part to the existence of aluminum. The biotite series contain no aluminum for positive ions, and then these would perhaps be attacked by acids.

Tectosilicate Minerals.—Table V seems to indicate that the reactivity of tectosilicate minerals toward acids are scarcely connected

9) N. V. Belov, *Compt. Rend. Acad. Sci. Russ.* **37**, 139 (1942).

10) E. H. Kraus, W. F. Hunt and L. S. Ramsdell, "Mineralogy, An Introduction to the Study of Minerals and Crystals", 3rd. Ed., McGraw-Hill Book Co., Inc., New York and London (1936), p. 368.

11) W. T. Grandquist and R. C. Amero, *J. Am. Chem. Soc.*, **70**, 3265 (1948).

with their chemical compositions. For example, the fact that orthoclase, microcline, and albite are insoluble to acids, and leucite and nepheline are decomposed by acids, cannot be explained from their chemical compositions. Therefore, in this case, it is suggested that their structures have an important effect on their reactivity.

As for their structures, the position and state of metallic ions in their crystal lattices would seem to carry on connection with their reactivity.

Results from the Bonding Energies

It appears that the bonding energies of the silicate minerals are closely related to their reactivity. Especially the bonding energies of the tectosilicate minerals would seem to be important. As for this problem, Keller[12] made a computation by adding the energies of the bonds between their constituent cations and oxygen, starting with the elements in the gaseous state, on the basis of the data from Huggins and Sun[13].

The author computed the bonding energies of the various silicate minerals by adding the bonding energies of their constituent elements, utilizing data compiled by Huggins and Sun[13], and Keller[12]. Of the valuse in Tables I—V, those in parentheses are computed by the author, and the rest are reprinted from Keller's paper.

It is reasonable to assume that there are some deep relationships between the reactivity and the bonding energies of silicate minerals. Judging from the comparison of these two properties in Tables I—V, the following results were obtained. Generally speaking, the neso-, soro-, ino-, and phyllo-silicate minerals of which bonding energies are less than about 30500 kcal. and the tectosilicate minerals of which these energies are less than about 33500 kcal. seem to be decomposed by acids. The fact that the tectosilicate minerals alone are in particular different from others appears presumably to be relative to the singularity of themselves; namely, this seems to depend primarily upon their ultimately polymerized structures—the three-dimentional frameworks—constructed by complete sharing of all oxygens in all the tetrahedra contained in their structures.

12) W. D. Keller, *Am. Mineralogist*, **39**, 783 (1954).
13) M. L. Huggins and K-H. Sun, *J. Phys. Chem.*, **50**, 319 (1946).

Summary

In this paper, the author proposed a classified table of metals contained in silicate minerals, and the qualitative and conventional rules in which it appeared possible to predict the reactivity of all the known silicate minerals toward ordinary mineral acids. In the classification and rules, ionic potential, Goldschmidt's polarizing power, and field strength of the metals in the silicate minerals play important roles.

The rules are summarized as follows: 1) the silicate minerals—especially, the neso- and soro-silicate ones composed of the comparative simple ionic crystal lattices—containing the less electropositive metals (e. g., Ti, Be, Al, Cr, V(III), Fe(III), Mn(III), Zr, etc.) are generally unattacked by acids; 2) in the ino-, phyllo-, and tecto-silicate minerals, which contain various polymerized and giant silicate ions, their structures exert a favorable influence upon their reactivity toward acids. Thus, in these minerals, it is necessary for us to take their structural effects into consideration, besides the above rule 1); and 3) the bonding energies of silicate minerals are closely related to their reactivity. In general, the neso-, soro-, ino-, and phyllo-silicate minerals of which bonding energies are less than about 30500 kcal. and the tectosilicate ones of which the energies are less than about 33500 kcal. seem to be decomposed by acids.

Department of Applied Chemistry
Faculty of Industry
Iwate University
Ueda, Morioka

Studies on Mass Spectra and Appearance Potentials of Acetic Acid and Deuteroacetic Acid CD_3COOH

By KOZO HIROTA, KAZUO NAGOSHI* and MOTOYOSHI HATADA

(Received June 8, 1960)

Recently the data of mass spectra have often been utilized in the discussion of radiation-induced reactions of organic compounds[1]. On such an occasion it is indispensable to determine the chemical species corresponding to each peak in the spectra by some methods, e. g. by comparing the spectra of the compounds marked by isotopes. For the same purpose, ionization potentials of these compounds are required, if possible. Although the data of this kind have been accumulated to some extent, those of the appearance potentials which are necessary to produce fragment ions do not exist so much yet in spite of their increasing importance. Such being the situation, as a part of our research on radiation chemistry of oxygen-containing compounds, mass spectra of acetic acid and deuteroacetic acid CD_3COOH were measured at several accelerating voltages and temperatures of the ion source on one hand, and also the appearance potentials of parent ions and main fragment ions of these acids on the other hand.

Experimental

Materials.—The purest commercial acetic acid was used without any treatment. Deuteroacetic-d_3 acid was synthetized as follows; carbon suboxide C_3O_2 obtained by dehydrating commercial malonic acid with phosphorus pentoxide was reacted with deuterium oxide. The deuteromalonic acid thus produced was decomposed thermally into deutero-acetic-d_3 acid-d CD_3COOD. The deuterium atom of the carboxylic group of this acid was replaced by protium atom, bubbling gaseous hydrogen chloride through the acid. The result of mass spectrometric analysis of the acid thus obtained showed that the amount of CD_3COOH in the deuterated acid was 95.6 atomic per cent, while CD_2HCOOH was the major parts of the impurities, CH_3COOH being negligibly small.

Apparatus.—The specifications of the mass spectrometer (Hitachi type RMU-5) are as follows: 90° focusing type, the temperature of the ion source is variable from 120 to 240°C, and electron accelerating voltage is also variable between 0 and 200 V. The standard conditions for gas analysis were as follows: electron accelerating voltage, 82 eV.: ion accelerating voltage, 1500 V., total emission current, 130 μA; target current, 35 μA; standard temperature of the ion source, 130°C.

Results

Mass Spectra.—Mass spectra of both acids are shown in Table I, where each peak height is per cent of total ion yield. From the table, the peak heights of the ions produced from CH_3COOH are in the order: $m/e=43>45>15>60>29$. The result is concordant with that of some other research[2], but not with that of Kambara[3] who found the ion of $m/e=28$ to be the most abundant followed by the ions of $m/e=43>45>15>14>12$ (cf. Table II). The discrepancy between the two data is too great to be explained by the discrimination peculiar to the respective apparatus. However, larger values of the peaks of $m/e=28$, 14 and 12 of Kambara may be explained by the contamination of carbon monoxide and nitrogen, and this explanation is supported by the fact that the peak at $m/e=28$ in the mass spectrum of

TABLE I. MASS SPECTRA OF CH_3COOH AND CD_3COOH

m/e	CH_3COOH %	CD_3COOH %	m/e	CH_3COOH %	CD_3COOH %
1	0.9	0.6	30	0.3	1.9
2	0.03	0.6	31	2.0	0.1
3	—	0.03	32	0	0.1
4	—	0.03	33	0	0.6
12	0.7	0.5	40	0.4	0.2
13	1.8	0.1	41	1.3	0.1
14	4.0	1.5	42	4.5	0.8
15	11.0	0.6	43	26.5	0.7
16	1.7	3.6	44	1.0	3.3
17	1.4	2.7	45	21.2	19.9
18	2.6	13.8	46	0.9	28.4
19	—	1.4	47	0	0.3
24	0.2	0.1	60	9.4	0.3
25	0.4	0	61	—	0
26	0.4	0.4	62	—	0.7
27	0.1	0.1	63	—	13.0
28	1.6	1.9	64	—	0.3
29	4.7	1.0			

* Research fellow dispatched from Kurashiki Rayon Co. (1958~1959).

1) For instance, see, J. G. Burr, *J. Phys. Chem.*, **61**, 1483 (1957).

2) Catalog of Mass Spectral Data of the American Petroleum Institute, Project. 44, Spectrum Serial No. 640.

3) T. Kambara, *J. Phys. Soc., Japan*, **5**, 84 (1950).

TABLE II. MASS SPECTRA OF CH_3COOH IN THE LITERATURE

m/e	Ions	Relative peak height* Kambara[3]	API Table No. 640	The present research
12	C^+	34		4
13	CH^+	16		7
14	CH_2^+	43		15
15	CH_3^+	64		42
25	C_2H^+	4		2
26	$C_2H_2^+$	5	1.3	2
27	$C_2H_3^+$	5	0.40	0
28	$C_2H_4^+$, CO^+	130	5.6	6
29	CHO^+	33	15.6	18
30	CH_2O^+	1	0.7	1
31	CH_3O^+	8.5	4.5	8
32	—	—	0.1	0
41	C_2HO^+	19	4.5	5
42	$C_2H_2O^+$	28	14.5	17
43	$C_2H_3O^+$	100	100	100
44	$C_2H_4O^+$, CO_2^+	12	4.9	4
45	CHO_2^+	81	93.6	80
46	$CH_2O_2^+$	—	1.2	3
55		—	0.08	—
56		—	0.13	—
57		—	0.06	—
60	$C_2H_4O_2^+$	29	57.7	36

* The peak height of $m/e=43$ is normalized to 100.

CD_3COOH obtained under the same experimental condition is also small. Moreover, the heights of the main peaks of both spectra of CH_3COOH and CD_3COOH can be explained without contradiction, i. e., the peaks at $m/e=$ 43, 15 and 60 in CH_3COOH, corresponding to CH_3CO^+, CH_3^+ and CH_3COOH^+, shift to those at $m/e=46$, 18 and 63 in CD_3COOH, corresponding to CD_3CO^+, CD^+ and CD_3COOH^+, while the peak of $COOH^+$ ($m/e=45$) occupies the second height in both spectra. Therefore it may be concluded that our spectra are free from the peaks due to some impurities or thermally decomposed products.

In Fig. 1, the effect of temperature on the mass spectrum of acetic acid is shown over a temperature range 130~230°C, taking the temperature of the ion source as abscissa and the percentage of the peak height as ordinate. It is found that the observed effect is not so large, as to be explained by such a mechanism as that the fragment ions are produced monomolecularly from the parent ions with some activation energies for bond breaking processes. However, considering that the gaseous acetic acid molecules may not be in thermal equilibrium completely with the wall of the ion source this result may not be curious. But from this figure, it might be said that the temperature effect has the following tendencies: ions $m/e=15$, 43 and 45 are practically independent on temperature, while others

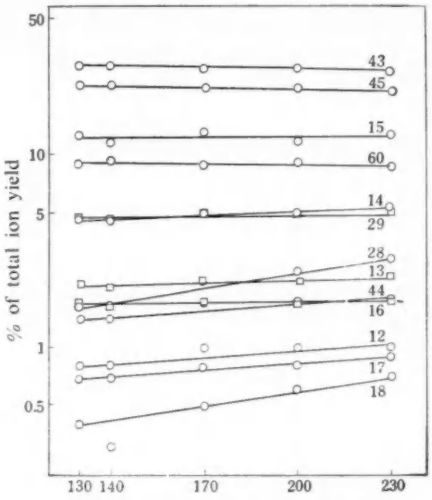

Fig. 1. The effect of ion source temperature on the mass spectrum of acetic acid.

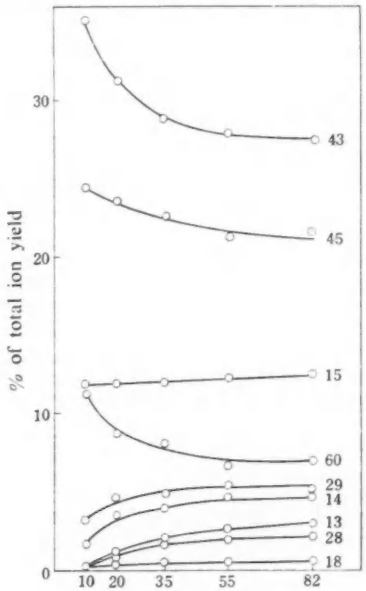

Fig. 2. The effect of electron accelerating voltage on the mass spectrum of acetic acid.

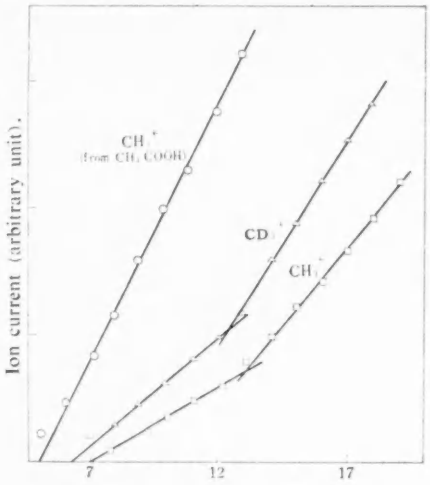

Fig. 3. Ionization efficiency curves of CH_3^+, CD_3^+ and $COOH^+$ ions.

increase, especially those of CO_2^+ ($m/e=44$), CO^+ ($m/e=28$) and H_2O^+ ($m/e=18$), HO^+ ($m/e=17$) and C^+ ($m/e=12$), which are the parent and fragment ions from molecules probably produced by the thermal decomposition of acetic acid.

The effect of electron accelerating voltage on the spectrum of acetic acid is shown in Fig. 2, where the voltage is varied from 9 to 82 V., and the sum of each peak height is normalized to 100 at each voltage. It is evident that the main peaks can be classified into three groups, i. e., the first group, CH_3^+ ion is practically constant, the second group, CH_3COOH^+ ($m/e=60$), CH_3CO^+ ($m/e=43$) and $COOH^+$ ($m/e=45$) ions, decreases and the residual third group, COH^+ ($m/e=29$) and CH_2^+ ($m/e=14$) increases with the increasing electron accelerating voltage. These tendencies may be reasonable if it is assumed, as is done by King and Long[4] on the mass-spectra of formic esters, that most of the ions which belong to the first and the third groups are produced from the ions of the second group. Detailed mechanism of production of CH_3^+ will be discussed again.

Appearance Potential.—As described above, the ions, CH_3^+, CH_3CO^+, $COOH^+$ and CH_3COOH^+ can be regarded as the main peaks in the spectrum of CH_3COOH, because the total contribution of the other ions to the spectrum is below 30%. The appearance potential of the above four ions were measured by the following procedure. The ionization efficiency curve for the ion under investigation was determined up to about 10 V. above the expected value of appearance potential and then the accurate one was determined by extrapolating the linear portion of the curve to the voltage axis. Thus, the obtained value of the ionization potential was calibrated by use of Moore's photo-ionization datum of argon ion, i. e., 15.76 V.[5]

In Fig. 3, the measurements on CH_3^+, CD_3^+ and $COOH^+$ are plotted against apparent voltage of electron acceleration. The results of these and other ions are summarized in Table III.

TABLE III. APPEARANCE POTENTIALS IN VOLT

Ions	CH_3COOH	CD_3COOH
CH_3COOH^+ or CD_3COOH^+	10.7_2	10.7_1
CH_3CO^+ or CD_3CO^+	12.6_9	12.9_7
$COOH^+$	14.1_5	14.0_8
CH_3^+ or CD_3^+	16.0_8	15.5_6
Break point of CH_3^+ or CD_3^+ curve	22.3	21.5

General discussion.—In order to confirm the reliability of our data, the appearance potential of the parent ion CH_3COOH^+ (10.7_2 V.) was compared with those in the literatures. Among the latter values, our appearance potential coincides fairly well with those obtained by the critical slope method of Honig (10.70[6] and 10.6_5[7] V.), but is higher than the value $10.3_3\pm$ 0.03 V. obtained by the method of photo-ionization[8]. Such a situation may be plausible considering the generally accepted fact that the former method as well as our linear extrapolation method gave higher values than the latter.

Thus it has been found that the degree of accuracy of our measurement is sufficient for discussing the appearance potentials of other fragment ions and of other ions produced from CD_3COOH. The first point to be discussed will be the fact that the appearance potentials of the parent ions of both acids are 10.7_2 and 10.7_1 V.; i. e., they coincide with each other within the experimental errors, while those of the corresponding fragment ions differ definitely from each other.

Secondly, it may be noteworthy that the appearance potential of CD_3CO^+ ion is higher by 0.3 V. than that of CH_3CO^+ ion. On the other hand, the appearance potentials of $COOH^+$ (from deuterated acid) and CD_3^+ ions are lower than those of $COOH^+$ and CH_3^+ ions by 0.1 and 0.5 V., respectively. According

4) A. King and F. Long, *J. Chem. Phys.*, **29**, 374 (1958).

5) D. P. Stevenson, *Trans. Faraday Soc.*, **49**, 867 (1953).

6) J. D. Morrison and A. J. C. Nicholson, *J. Chem. Phys.*, **20**, 1021 (1952).

7) I. Omura, K. Higasi and H. Baba, This Bulletin, **29**, 504 (1956).

8) K. Watanabe, *J. Chem. Phys.*, **26**, 542 (1957).

to the results hitherto published, it seems to be a rule that the ionization potential of a molecule increases by deuteration; e. g. 13.04 V. for CH_3^+ against 13.21 V. for CD_3^+ [9]. Our data, therefore, seem to be an exceptional case. At present, such an anomaly can not be explained easily. The next point to be mentioned may be the breaks of the curves observed in cases of CH_3^+ and CD_3^+ ions. The breaks occur at about 6 V. higher than the corresponding appearance potentials in both cases.

The occurrence of these breaks might be explained by assuming that above this break point the simultaneous fragmentation process (1b) of the parent ion at two bonds occurs in addition to the single fragmentation process (1a) to form CH_3^+ ion:

$$CH_3COOH \rightarrow CH_3^+ + COOH \qquad (1a)$$

$$\searrow CH_3^+ + CO_2 + H \qquad (1b)$$

However, according to the theoretical result[10] which has been derived by the quasi-equilibrium theory, most of the CH_3^+ ions must be produced secondarily, i. e., by the decomposition of highly excited CH_3CO^+ ion. This explanation may not be extraordinary, because a similar shape of ionization efficiency curve of CH_3NO_2, in which a sharp break point occured about 4.3 V. above the first appearance potential of NO_2^+, was explained reasonably by the existence of a bent excited state of NO_2^+ [11]. Therefore, the mechanism of producing the CH_3^+ ions whose appearance potentials are different is not such as that described by Scheme 1, but both ions are produced by Scheme 2,

$$CH_3COOH \rightarrow CH_3CO^+ + OH$$

$$\rightarrow CH_3^+ + CO + OH \qquad (2)$$

The states of the CH_3^+ produced below and above the break point in the curve are therefore different.

9) R. E. Honig, ibid., **16**, 105 (1948).
10) Cf. K. Fueki and K. Hirota, *J. Chem. Soc. Japan, Pure Chem. Sec.* (*Nippon Kagaku Zasshi*), **81**, 356 (1960).
11) J. Collin, *J. Chem. Phys.*, **30**, 1621 (1959).

Summary

In order to obtain information on the decomposition process of acetic acid in radiation chemistry, not only mass spectra of both acetic acid and deuteroacetic acid but also appearance potentials of parent and main fragment ions of both acids have been measured.

By studying the effects of ion source temperature and of electron accelerating voltage on the spectra, and by comparing the mass spectra of both acids, it has been possible to identify the chemical species produced by electron impact without ambiguity and also to estimate the process of their production to some extent.

It has been found that, although the appearance potentials of the parent ion of both acids coincide fairly well, those of CH_3^+ and $COOH^+$ from CH_3COOH are higher than those of corresponding ions from deuterated acid. The breaks of ionization-efficiency curves have been observed in CH_3^+ and CD_3^+ ions at about 6 volts higher than the appearance potentials suggesting a possibility of the presence of an excited state of the product ions.

The authors express their sincere thanks to Dr. I. Kanomata of Tokyo Metropolitan University and also to Dr. K. Fueki of Osaka University for their discussions.

Osaka Laboratory
Japanese Association for Radiation Research on Polymers
508, Mii, Neyagawa, Osaka
(K. H., K. N. & M. H.)

Faculty of Science
Osaka University
Nakanoshima, Osaka
(K. H.)

Theoretical Reactivity Index of Addition in the "Frontier Electron Theory"

By Kenichi FUKUI, Chikayoshi NAGATA, Teijiro YONEZAWA and Keiji MOROKUMA

(Received August 8, 1960)

It is well known that many polycondensed aromatic hydrocarbons undergo addition such as that of the Diels-Alder type and oxidation with osmium tetroxide: the former is the addition of e. g. quinone or maleic anhydride to the reactive para position and the latter is the addition to the reactive ortho bond.

It is suggested that the frontier electron density and superdelocalizability which have been proved to be good indexes of substitution reaction in conjugated compounds[1-3] will also be applicable to interpreting the reactivity in simultaneous addition reactions stated above, because the substitution and addition seem to be not so greatly different in nature from each other, at least until the activated complex is formed. In substitution reaction, the hydrogen atom of the attacking position and the reagent was considered to form a pseudoatom and the hyperconjugation energy due to the charge transfer between the pseudoatom and the orbital at the attacking position was assumed to make the reaction easy[4]. The situation in the addition reaction can be considered to resemble the substitution reaction in the sense that the delocalization energy due to the charge transfer in the transition state play a dominant role in decreasing the activation energy of the reaction. The circumstances will be clearly seen in the following example: the addition of maleic anhydride to the para position of polycondensed aromatic hydrocarbon, e. g. anthracene is deemed to proceed by a one-step process as follows:

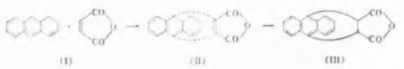

(I) (II) (III)

The charge transfer between the maleic anhydride and the substrate molecule through the orbitals at the ethylenic bond of the former and the para position of the latter will occur in the transition state (II), and the delocalization energy due to the charge transfer is naturally considered a measure of easiness of addition reaction because the activation energy is decreased according as the increase of delocalization energy. In this connection, the frontier electron density and the superdelocalizability which could be derived from the delocalization energy are expected to be a good measure of the addition reaction.

In the present paper, the theoretical index for addition reaction in the frontier electron theory is derived and the index is compared with the rate of reactions hitherto carried out.

Theoretical Treatment

The secular equation of the π part of the transition complex which includes the orbitals of reagent and substrate π electron system is written as

$$D(\varepsilon) = \begin{vmatrix} \alpha_h-\varepsilon & 0 & 0 & \gamma & 0 & 0 & \cdots & 0 \\ 0 & \alpha_h-\varepsilon & \gamma & 0 & 0 & 0 & \cdots & 0 \\ 0 & \gamma & a_{11}-\varepsilon & a_{12} & a_{13} & a_{14} & \cdots & a_{1n} \\ \gamma & 0 & a_{21} & a_{22}-\varepsilon & a_{23} & a_{24} & \cdots & a_{2n} \\ 0 & 0 & a_{31} & a_{32} & a_{33}-\varepsilon & a_{34} & \cdots & a_{3n} \\ \cdots & \cdots & \cdots & \cdots & \cdots & \cdots & \cdots & \cdots \\ \cdots & \cdots & \cdots & \cdots & \cdots & \cdots & \cdots & \cdots \\ 0 & 0 & a_{n1} & a_{n2} & \cdots & \cdots & \cdots & a_{nn}-\varepsilon \end{vmatrix}$$

$$= (\alpha_h-\varepsilon)^2\Delta(\varepsilon) - \gamma^2[(\alpha_h-\varepsilon)\{\Delta_{rr}(\varepsilon) + \Delta_{ss}(\varepsilon)\}] + \gamma^4\Delta_{rrss}(\varepsilon) = 0 \qquad (1)$$

where

$$\Delta(\varepsilon) = \begin{vmatrix} a_{11}-\varepsilon & a_{12} & a_{13} & \cdots & a_{1n} \\ a_{21} & a_{22}-\varepsilon & a_{23} & \cdots & a_{2n} \\ a_{31} & a_{32} & a_{33}-\varepsilon & \cdots & a_{3n} \\ \cdots & \cdots & \cdots & \cdots & \cdots \\ \cdots & \cdots & \cdots & \cdots & \cdots \\ a_{n1} & a_{n2} & \cdots & \cdots & a_{nn}-\varepsilon \end{vmatrix}$$

is the secular determinant for the substrate π-electron system and $\Delta_{rr}(\varepsilon)$ and $\Delta_{ss}(\varepsilon)$ are the minors of $\Delta(\varepsilon)$ corresponding to the *rr*- and *ss*-elements, and a_{ii} and $a_{ij}(i \neq j)$ are the

1) K. Fukui, T. Yonezawa and H. Shingu, *J. Chem. Phys.*, **20**, 722 (1952).
2) K. Fukui, T. Yonezawa, C. Nagata and H. Shingu, ibid., **22**, 1433 (1954).
3) K. Fukui, T. Yonezawa and C. Nagata, ibid., **27**, 1247 (1957).
4) K. Fukui, T. Yonezawa and C. Nagata, This Bulletin, **27**, 423 (1954).

Coulomb and the resonance integrals, respectively. For simplicity, the values of these integrals are assumed to be the same as those in an isolated molecule. α_h and γ are the Coulomb integral of the reagent*, and the resonance integral between the reagent and the rth and the sth atom of the substrate molecule at which the reaction takes place, respectively.

When the conjugation between the substrate molecule and reagent is small, i.e., in the case of $0<\gamma\leqq 1$, the perturbed orbital energy of the complex are given by the following formula

$$\varepsilon_j' = \varepsilon_j + \delta\varepsilon_j\gamma^2 + 0(\gamma^4) + \cdots\cdots \quad (2a)$$

$$\alpha_h' = \alpha_h + \delta_h\gamma^2 + 0(\gamma^4) + \cdots\cdots \quad (2b)$$

The values of $\delta\varepsilon_j$ and $\delta\alpha_h$ are easily obtained by the perturbation treatment as

$$\delta\varepsilon_j = \frac{\Delta_{rr}(\varepsilon_j) + \Delta_{ss}(\varepsilon_j)}{(\alpha_h - \varepsilon_j)\Delta'(\varepsilon_j)}\gamma^2 + \cdots\cdots \quad (3)$$

$$\delta\alpha_h = -\frac{\{\Delta_{rr}(\alpha_h) + \Delta_{ss}(\alpha_h)\}}{2\Delta(\alpha_h)} \pm \frac{\sqrt{\{\Delta_{rr}(\alpha_h) - \Delta_{ss}(\alpha_h)\}^2 + 4\{\Delta_{rs}(\alpha_h)\}^2}}{2\Delta(\alpha_h)} \quad (4)$$

ε_j' and α_h' are the roots of $D(\varepsilon)=0$ and they correspond to the energy of the molecular orbital of the unperturbed system $\Delta(\varepsilon)$ and the orbitals of the reagent, respectively. We assumed that $\Delta(\varepsilon)=0$ has no multiple roots here, but in the case in which $\Delta(\varepsilon)=0$ has double roots, the final result is not altered.

The delocalization energy $\mathcal{H}_{r+s}$ is derived by treatment analogous to the case of substitution reaction[3]. It is given according as the type of reaction as follows:
for electrophilic reaction,

$$\mathcal{H}_{r+s} \cong 2\sum_{j=1}^{m}\frac{\Delta_{rr}(\varepsilon_j) + \Delta_{ss}(\varepsilon_j)}{(\alpha_h - \varepsilon_j)\Delta'(\varepsilon_j)}\gamma^2 = 2\sum_{j=1}^{m}\frac{(C_r^j)^2 + (C_s^j)^2}{\varepsilon_j - \alpha_h}\gamma^2 \quad (5)$$

for radical reaction**,

$$\mathcal{H}_{r+s} \cong \left[-\sum_{j=1}^{m}\frac{\Delta_{rr}(\varepsilon_j) + \Delta_{ss}(\varepsilon_j)}{(\varepsilon_j - \alpha_h)\Delta'(\varepsilon_j)} - \sum_{j=m+1}^{n}\frac{\Delta_{rr}(\varepsilon_j) + \Delta_{ss}(\varepsilon_j)}{(\alpha_h - \varepsilon_j)\Delta'(\varepsilon_j)}\right]\gamma^2 = \left[\sum_{j=1}^{m}\frac{(C_r^j)^2 + (C_s^j)^2}{\varepsilon_j - \alpha_h} + \sum_{j=m+1}^{n}\frac{(C_r^j)^2 + (C_s^j)^2}{-(\varepsilon_j - \alpha_h)}\right]\gamma^2 \quad (6)$$

for nucleophilic reaction,

$$\mathcal{H}_{r+s} \cong -2\sum_{j=m+1}^{n}\frac{\Delta_{rr}(\varepsilon_j) + \Delta_{ss}(\varepsilon_j)}{(\alpha_h - \varepsilon_j)\Delta'(\varepsilon_j)}\gamma^2 = 2\sum_{j=m+1}^{n}\frac{(C_r^j)^2 + (C_s^j)^2}{-(\varepsilon_j - \alpha_h)}\gamma^2 \quad (7)$$

where C_r^j is the coefficient of the rth atomic orbital of jth molecular orbital of non-perturbed substrate molecule and the relation $-\Delta_{rr}(\varepsilon_j)/\Delta'(\varepsilon_j) = (C_r^j)^2$ was used in deriving the last terms of the right hand side of the above equations.

When the value of α_h is equal to α, the Coulomb integral of carbon atom in benzene, the coefficients of γ^2 in Eqs. 5, 6 and 7 are nothing but $(S_r + S_s)$ for electrophilic, radical and nucleophilic reactions, respectively. Therefore, the theoretical index for addition reaction at two positions r and s is the sum of the superdelocalizability at r and s positions. It is clearly seen in the expression in Eqs. 5, 6 and 7 that the contribution of the frontier orbital is the greatest, hence as in the case of the treatment of substitution reaction[3], the one term approximation taking into consideration the frontier orbital alone, will be allowed.

It is noted that the present treatment gives the same result regardless whether one considers the reaction as a simultaneous or two-step one. This indescernability is also seen in other treatments such as static and localization methods. Therefore, it is impossible to decide whether the reaction is one-step or not by comparing the theories and experimental results.

The theoretical index derived above is qualified as a good index for predicting the reactivity in simultaneous addition reaction as a result of comparison with the experiment. For instance, the data of the attacking positions in the Diels-Alder reaction are in agreement without an exception with the predicted most reactive position in a molecule (Table I). The relative rate of these compounds in the Diels-Alder reaction has not been measured in one

* In this treatment, the attacking reagent was assumed to be composed of two non-conjugating components. In other words, the reaction was considered to occur with two reagents. The one reagent attacks the r position and the other the s position simultaneously or stepwise. In the case of the addition of maleic anhydride to polycondensed aromatic hydrocarbons, the reagent as well as the substrate is a conjugated system, and the whole π electron system of maleic anhydride should be taken into consideration. In this case, however, the reaction was considered as an addition of two reagents to the substrate separately.

** For a radical reaction twice the second term (the energetically lower term) of Eq. 4 are omitted in deriving Eq. 6. It is because one may conclude that the term has no connection with the simultaneous addition reaction. That is to say, from the configuration interaction's point of view, it originates in the interaction between the initial configuration (initial state of reaction) and the configuration corresponding to one-electron transfer from a component of the reagent to another component. Not involving the charge transfer between the reagent and the substrate molecule but between the two components of reagents, this interaction seems to have no connection with the reaction.

TABLE I. SUM OF THE SUPERDELOCALIZABILITY AT PARA CARBON ATOMS IN SOME AROMATIC HYDROCARBONS (S_r+S_s) IN COMPARISON WITH EXPERIMENTS

Compound	Para position	S_r+S_s	Experiment; position of attack
Hexacene	6, 15	4.011	6, 15[b]
	5, 16	3.459	
	1, 4	2.355	
Pentacene	6, 13	3.589	6, 13[b]
	5, 14	3.269	
	1, 4	2.308	
Naphthacene	5, 12	3.010	5, 12[b]
	1, 4	2.243	
Anthracene	9, 10	2.627	9, 10[b]
	1, 4	2.147	
1, 2-Benzanthracene	9, 10	2.437	9, 10[a,c]
	5, 8	2.098	
	1', 4'	1.915	
1, 2, 3, 4-Dibenz-anthracene	9, 10	2.303	9, 10[a,d,b]
	5, 8	2.056	
	1', 4'	1.853	
1, 2, 5, 6-Dibenz-anthracene	9, 10	2.292	9, 10[e]
	1', 4'	1.919	
Naphthalene	1, 4	1.989	No addition[f]
Phenanthrene	1, 4	1.918	No addition[g]
Chrysene	1, 12	1.907	No addition[g]
Benzene		1.667	No addition[f]

a) E. Clar, *Ber.*, **64**, 2194 (1931); **65**, 503 (1932); **72**, 1817 (1939).
b) O. Diels, K. Alder and S. Beckmann, *Ann.*, **486**, 1191 (1931).
c) E. Clar, *Ber.*, **65**, 519 (1932).
d) E. Clar and L. Lombardi, *Ber.*, **65**, 1411 (1932).
e) J. W. Cook, *J. Chem. Soc.*, **1931**, 3273.
f) E. Clar, "Aromatische Kohlenwasserstoffe" p. 12 (1941).
g) R. N. Jones, C. J. Gogek and R. W. Sharpe, *Can. J. Res.*, **B26**, 719 (1948).
h) E. J. Moriconi, W. F. O'Conner and F. T. Wallenberger, *J. Am. Chem. Soc.*, **81**, 646 (1959).

TABLE II. SUM OF THE SUPERDELOCALIZABILITY AT TWO ADJACENT CARBON ATOMS IN SOME AROMATIC HYDROCARBONS (S_r+S_s) IN COMPARISON WITH EXPERIMENTS

Compound	Bond ($r-s$)	S_r+S_s	Experiment; position of attack
1, 2-Benzanthracene	3, 4	2.079	3, 4[a]
	5, 6	1.963	
	7, 8	1.953	
	3', 4'	1.849	
	1', 2'	1.832	
	6, 7	1.818	
	2', 3'	1.766	
1, 2, 5, 6-Dibenz-anthracene	3, 4	2.062	3, 4[a,e]
	3', 4'	1.848	
	1', 2'	1.842	
	2', 3'	1.771	
Pyrene	1, 2	2.052	1, 2[b]
	3, 4	1.944	
Chrysene	1, 2	1.997	1, 2[b]
	3, 4	1.857	
	5, 6	1.852	
	4, 5	1.762	
Phenanthrene	9, 10	1.995	9, 10[a,b,d]
	1, 2	1.837	
	3, 4	1.832	
Anthracene	1, 2	1.995	1, 2, 3, 4[a,c]
	2, 3	1.843	
Naphthalene	1, 2	1.867	1, 2[c]
	2, 3	1.746	
Benzene		1.667	No addition[c]

a) G. M. Badger, *J. Chem. Soc.*, **1949**, 456; Ref. 5.
b) J. W. Cook and R. Schoental, ibid., **1948**, 170.
c) J. W. Cook and R. Schoental, *Nature*, **161**, 237 (1948).
d) N. L. Drake and T. R. Sweeney, *J. Org. Chem.*, **11**, 67 (1946).
e) E. J. Moriconi, W. F. O'Conner, W. J. Schmitt, G. W. Cogswell and B. P. Fürer, *J. Am. Chem. Soc.*, **82**, 3441 (1960).

and the same condition. However, considering the experimental data which have been so far reported (cf. references in Table I), one can conclude that the following order of reactivity might exist: hexacene > pentacene > naphthacene > anthracene > 1, 2-benzanthracene > 1, 2, 5, 6-dibenzanthracene > naphthalene, phenanthrene, benzene. This is in excellent accord with the order of magnitude of S_r+S_s of these compounds.

As is seen in Table II, the experimental position of attack of osmium tetroxide to the double bond of some polycondensed aromatic hydrocarbons agree very well with the prediction by the theory. The reactive rate of reaction of these compounds is not determined completely; however, the experiment by Badger and Reed showed that 1, 2-benzanthracene reacts with osmium tetroxide faster than phenanthrene does[5]. This fact is explained well by our calculated result.

Faculty of Engineering
Kyoto University
Sakyoku, Kyoto

5) G. M. Badger and R. I. Reed, *Nature*, **161**, 238 (1948).

Diamagnetic Behavior of Some Aliphatic Molecules in Crystals

By A. Mookherji, S. N. Mookherji and D. Neogy

(Received May 18, 1960)

According to Pauling[1] the normal susceptibility in the plane of the aromatic molecules is due to the bound electrons, contributing to the susceptibility equally in all directions, and the electrons which are free to precess only in the plane of the molecule in orbits, provided by the entire molecular ring system, contribute only to the susceptibility along the normal to the molecular plane. When such anisotropic molecules are regularly arranged in crystals, the crystal as a whole will exhibit magnetic anisotropy. Hence anisotropy of the diamagnetic crystals is obviously due to the anisotropy of its constituent molecules.

Krishnan and Banerji[2] and Banerji[3] showed that, if the molecular anisotropy is known, it is possible to obtain much useful information regarding the orientation of the molecules in crystals relative to one another.

In a recent paper (Mookherji et al.)[4] studying the susceptibilities of a few dibasic aliphatic acids and their salts observed that,

a) Unlike the normal aliphatics the maximum diamagnetic susceptibility for the these salts lies normal to the plane of the carboxylic groups.

b) This extra diamagnetism could be attributed to resonance which exists in these molecules.

From X-ray studies and chemical considerations one may be led to think that the carboxylic groups in mono- and dibasic aliphatic acids and their salts can be represented by two or more structures and hence in these molecules resonance will exist. It would be therefore interesting to study the diamagnetic anisotropy of the crystals of the above mentioned acids and their salts and to find whether a similar diamagnetic behaviour like succinic and tartaric acids and their salts could be observed.

Experimental

Crystals were grown out of aqueous solution at room temperature by slow evaporation. The chemicals used were Merk's extra pure reagent quality prewar variety.

The magnetic anisotropy and the orientation of the crystals in magnetic field were carried out by the well known method of Krishnan and Banerji[2]. The absolute susceptibility in any convenient direction was measured by a modified quartz balance (Bose)[5]. The magnetic field used for the purpose had a constant gradient over a considerable volume by using pole pieces as devised by Dutta Roy[6]. The standard crystal for calibration of this balance was a well developed crystal of naphthalene for which mass susceptibility is accurately known (Banerji)[7].

Results

The results of measurements are collected in Tables I and II, and are expressed in the usual units i.e. c.g.s. E.M. units. χ_3 is the gram molecular susceptibility along b-crystallographic axis of a monoclinic crystal; the algebraically greater of the two values in the symmetry plane (010) is denoted by χ_1 and the smaller by χ_2; ϕ is the angle that χ_1-direction makes with c-crystallographic axis taken positive from c-axis towards a-axis through obtuse β.

In orthorhombic crystals, the gram molecular susceptibilities along the crystallographic axes a, b and c are represented by χ_a, χ_b and χ_c, respectively.

Discussion

Magnetic Analysis of Molecular Orientation in Crystals.—We proceed now to discuss the magnetic anisotropy in the light of the orientation of the molecules in the unit cell of the crystal. The crystals are discussed individually.

Oxalic Acid Dihydrate.—Complete X-ray studies by Robertson and Woodword[8] revealed that the crystal is monoclinic in the space group C_{2h}^5 with two molecules in the unit cell. The molecules are centro symmetric, approximately plane, and are magnetically nearly uniaxial.

Let us represent the axes of symmetry of the two molecules by Z_1 and Z_2 and the principal susceptibilities of the molecule by $K_\perp$ and $K_\parallel$ in the plane of the molecule and normal to it respectively.

1) L. Pauling, *J. Chem. Phys.*, **4**, 673 (1936).
2) K. Krishnan and S. Banerji, *Philos. Trans.*, **A 234**, 265 (1935); *Z. Kristallogr*, **A 99**, 499 (1938).
3) S. Banerji, *Z. Kristallogr.*, **A 100**, 316 (1938).
4) A. Mookherji, R. Mittal and D. Neogy, *Bull. Nat. Inst. Sci. India*, No. 14 (1959).
5) A. Bose, *Ind. Jour. Phys.*, **21**, 275 (1947).
6) S. Datta Roy, idid., **29**, 429 (1955).
7) S. Banerji, *Report Symposium. Ind. Association for the cultivation of Science*, 19 (1957).
8) J. M. Robertson and J. Woodward, *J. Chem. Soc.*, **1936**, 1817.

TABLE I. MAGNETIC ANISOTROPY AT 30°C

Sl. No.	Name and structural formula of the crystal	Crystallographic data	Mode of suspension	Orientation in the field	$\Delta\chi \times 10^6$	Magnetic anisotropy
1	2	3	4	5	6	7
1.	Oxalic acid dihydrate	Monoclinic	"b" axis vertical	$\theta = 15.2°$	2.1	$\chi_1 - \chi_2 = 2.10$
		C_{2h}^5	"a" axis vertical	"b" axis normal to the field	8.39	$\chi_1 - \chi_3 = 8.53$
	COOH | COOH $+2H_2O$	$a = 6.12$ $b = 3.6$ $c = 12.0$ $\beta = 106° 12'$ $z = 2$	001 Plane horizontal	"b" axis normal to the field	6.56	$\theta_{cal} = 14.7°$ $\theta_{obs} = 15.2°$
2.	Ammonium oxalate monohydrate	Orthorhombic	"c" axis vertical	"a" axis along the field	1.108	$\chi_a - \chi_b = 1.108$
		$P_{2_12_12}$	"a" axis vertical	"c" axis normal to the field	13.17	$\chi_b - \chi_c = 13.17$
	$COONH_4$ | $COONH_4$ $+H_2O$	$a = 8.04$ $b = 10.27$ $c = 3.82$ $z = 2$	"b" axis vertical	"a" axis along the field	14.16	Cal. $\Delta\chi = 0.99$
3.	Potassium oxalate monohydrate	Monoclinic	"b" axis vertical	$\theta = 61.0°$	1.6	$\chi_1 - \chi_2 = 1.6$
		$C_{2/c}$	"b" & "c" axes horizontal	"b" axis normal to the field	8.8	$\chi_1 - \chi_3 = 10.0$
	COOK | COOK $+H_2O$	$a = 9.32$ $b = 6.17$ $c = 10.65$ $\beta = 110° 58'$ $z = 4$	"a" axis vertical	"b" axis normal to the field	9.5	$\theta_{cal} = 59.5°$ $\theta_{obs} = 61.0°$
4.	Ammonium bi-oxalate monohydrate	Orthorhombic	"b" axis vertical	"b" axis along the field	9.09	$\chi_c - \chi_a = 9.09$
		$a : b : c =$ $0.4524 : 1 : 0.5593$	"c" axis vertical	"b" axis along the field	10.78	$\chi_b - \chi_a = 10.78$
	$COONH_4$ | COOH $+H_2O$		"a" axis vertical	"b" axis along the field	2.06	Cal. $\Delta\chi = 1.70$
5.	Potassium bi-oxalate monohydrate	Monoclinic	"b" axis vertical	$\Psi = 4.0$	9.00	$\chi_1 - \chi_2 = 9.00$
		$P_{2_1/c}$	"c" axis vertical	"b" axis along the field	10.2	$\chi_3 - \chi_2 = 10.3$
	COOK | COOH $+H_2O$	$a = 4.32$ $b = 12.88$ $c = 10.32$ $\beta = 133° 29'$ $z = 4$	"b" & "c" axes horizontal	"b" axis along the field	1.4	$\phi_{cal} = 3.9$ $\phi_{obs} = 4.0$
6.	Calcium formate	Orthorhombic P_{Cab}	"b" axis vertical	"c" axis along the field	1.722	$\chi_c - \chi_a = 1.722$
	H—COO H—COO Ca	$Z = 8$ $a = 10.16$ $b = 13.38$ $c = 6.27$	"c" axis vertical	"a" axis normal to the field	1.287	$\chi_b - \chi_a = 1.287$
			"a" axis vertical	"b" axis normal to the field	0.3118	Cal. $\Delta\chi = 0.435$
7.	Barium formate	Orthorhombic	"c" axis vertical	"a" axis along the field	0.621	$\chi_a - \chi_b = 0.621$
		$a : b : c =$ $0.765 : 1 : 0.8638$	"b" axis vertical	"b" axis normal to the field	1.729	$\chi_c - \chi_b = 1.729$
	H—COO H—COO Ba		"b" axis vertical	"c" axis along the field	0.9279	Cal. $\Delta\chi = 1.108$
8.	Barium acetate trihydrate	Monoclinic	"b" axis vertical	$\theta = 33.5°$	1.18	$\chi_1 = \chi_2 = 1.18$
		$a : b : c =$ $2.1362 : 1 : 1.222$	"a" axis vertical	"b" axis along the field	0.776	$\chi_1 - \chi_3 = 0.458$
	$CH_3—COO$ $CH_3—COO$ Ba $+3H_2O$	$\beta = 113° 27'$	001 Plane horizontal	"b" axis along the field	1.27	$\phi_{cal} = 33.5°$

TABLE II. ABSOLUTE SUSCEPTIBILITIES

Sl. No.	Name of the crystal	Temp. °C	Direction along which suscept. was measured	Volume suscept.	Corresponding χ_M	Principal gram molecular suscept.	Mean suscept. $\bar{\chi}_m$	Pascal's value $\bar{\chi}_m$
1	2	3	4	5	6	7	8	9
1.	Oxalic acid dihydrate, Monoclinic	33.00	Along "b" axis	−0.4214	−53.1	$\chi_1=-53.1$ $\chi_2=-55.2$ $\chi_3=-61.63$	−56.64	−60.42
2.	Ammonium oxalate monohydrate, orthorhombic	33.00	Along "b" axis	−0.4257	−60.4	$\chi_a=-60.4$ $\chi_b=-61.51$ $\chi_c=-74.68$	−65.33	−68.20
3.	Potassium oxalate monohydrate, monoclinic	33.00	Along "b" axis	−0.3740	−68.82	$\chi_1=-68.82$ $\chi_2=-70.42$ $\chi_3=-78.82$	−72.68	−67.20
4.	Ammonium bi-oxalate monohydrate, orthorhombic	33.00	Along "b" axis	−0.3417	−42.72	$\chi_a=-42.72$ $\chi_b=-31.94$ $\chi_c=-33.63$	−36.09	−56.83
5.	Potassium bi-oxalate monohydrate, monoclinic	33.00	Along "b" axis	−0.2954	−43.13	$\chi_1=-43.13$ $\chi_2=-52.13$ $\chi_3=-41.93$	−45.73	−57.33
6.	Calcium formate orthorhombic	33.00	Along "b" axis	−0.2650	−34.46	$\chi_c=-34.46$ $\chi_a=-36.182$ $\chi_b=-34.895$	−35.179	−44.70
7.	Barium formate orthorhombic	33.00	Along "b" axis	−0.2892	−65.77	$\chi_c=-65.77$ $\chi_b=-67.50$ $\chi_a=-66.88$	−66.71	−65.40
8.	Barium acetate trihydrate, monoclinic	33.00	Along "b" axis	−0.3772	−116.7	$\chi_1=-116.7$ $\chi_2=-117.88$ $\chi_3=-116.242$	−116.94	−128.00

Then χ_1 will lie in the direction, normal to the plane containing Z_1 and Z_2 axes and χ_2 will be the internal bisector of the angle 2Ψ between Z_1 and Z_2 and hence,

$$\left.\begin{aligned}\chi_1&=K_\perp\\ \chi_2&=K_{\parallel}\cos^2\Psi+K_\perp\sin^2\Psi\\ \chi_3&=K_{\parallel}\sin^2\Psi+K_\perp\cos^2\Psi\end{aligned}\right\} \quad (1)$$

and $$\bar{\chi}=(\chi_1+\chi_2+\chi_3)/3=\frac{K_{\parallel}+2K_\perp}{3}$$

substituting the values of $(\chi_1-\chi_2)$ and $(\chi_1-\chi_3)$ in Eq. 1 we have $(K_\perp-K_{\parallel})=10.7\times10^{-6}$ and $\Psi=63.5°$, which agrees well with X-ray findings, i.e. 61.9°.

Ammonium Oxalate Monohydrate.—Fine structure studies by X-ray methods (Hendricks, and Hendricks and Jefferson[9,10]) reveal that there are two molecules in the unit cell in space group $P_{2_12_12}$ and that the two parts of the COOH group are in planes making an angle COOH of 20° whereas in oxalic acid both parts are in the same plane. The planes containing the oxygens of the oxalate groups are almost parallel to (001) plane. Following Mookherji[11] we can attribute the abnormal diamagnetism to oxygen atoms of the oxalate groups. Hence according to X-ray findings (001) plane should approximately be a plane of magnetic symmetry, whereas normal to this plane we should expect algebraically maximum susceptibility. From Table I we find that in the (001) plane $\Delta\chi=\chi_a-\chi_b=1.1\times10^{-6}$, whereas it is 14.2×10^{-6} in the plane normal to it.

We may therefore conclude that for oxalate molecules, which are in strained condition because of its two parts being in two different planes $\Delta K=K_\perp-K_{\parallel}=14.0\times10^{-6}$, more by 4 units for the oxalate groups, where both the parts are in the same plane.

Ammonium Bi-oxalate.—From Table I it is seen that the two susceptibilities in the (001) plane are nearly equal and numerically less than the third susceptibility by about 10 units, which is almost equal to the value of the oxalate group in oxalic acid dihydrate. Thus we conclude that in this crystal all the oxalate groups are oriented parallel with (001) plane. At present no X-ray data are available to verify the above conclusions.

Potassium Oxalate Monohydrate.—Hendricks[9] by X-ray methods found that the crystal is

9) S. B. Hendricks, *Z. Kristallogr.*, **91**, 48 (1935).
10) S. B. Hendricks and M. E. Jefferson, *J. Chem. Phys.*, **4**, 102 (1936).
11) A. Mookherji, *Acta Cryst.*, **10**, 25 (1957).

monoclinic in the space group of $C_{2/c}$ with four molecules in the unit cell; they form a set of two pairs with the two molecular planes in each pair being parallel. If the slight tilt between the two pairs is neglected then the molecules may be taken oriented parallel to the plane (010).

Evidently, $K = \chi_1$, $K_\perp \approx \chi_2 \approx \chi_3$

Hence, $\frac{1}{2}[(\chi_1-\chi_2)+(\chi_2-\chi_3)] = K_\perp - K$

Thus it is observed that $(K_\perp - K)$ for oxalate group in the crystal is 9.2 as against 10.7 for that in the oxalic acid. This is evidently due to the neglect of the tilt. On calculating the tilt comes out as 15.0° with the (010) plane.

Potassium Bi-oxalate.—According to Hendricks[5], the crystal has four molecules in the unit cell and the molecular planes are oriented parallel to (100) plane. Hence $K_\perp - K = 10.0 \times 10^{-6}$, which is almost the same as found with other oxalate groups.

Calcium Formate.—It crystallises in the orthorhombic system in the space group P_{cab} with eight molecules in the unit cell (Nitta and Osaki[12]). If n, m and l are the direction cosines of the normal to the formate group, following Banerji[3] we have,

$$l^2-m^2=\frac{\chi_b-\chi_a}{K_\perp-K}, \qquad l^2-n^2=\frac{\chi_c-\chi_a}{K_\perp-K}$$

and $l^2+m^2+n^2=1$

In order to calculate m, l and n one must know $(K_\perp - K) = \Delta K$ for COOH group. This may be estimated as follows:

According to Pauling and Sherman[13] resonance energy in monobasic acids is 1.20 electron volts. Now according to Pauling[14], if one attributes to ΔK this resonance energy then,

$$\Delta K = \frac{E \times M}{3.22 \times \rho} = 8.36 \times 10^{-6}$$

where E is kinetic energy, M the molecular weight and ρ the density. On substituting this value and $(\chi_b - \chi_a)$ and $(\chi_c - \chi_a)$ from Table I we find that the formate groups are inclined at 48.1, 56.0 and 59.8° to a, b and c crystallographic axes respectively.

Barium Formate.—The crystal is orthorhombic. The orientation of the formate group is calculated following the same method as in the case of calcium formate, which show that the normal to the formate group is inclined at 54.0° to a-axis 35.8° to b-axis and 38.8° to c-axis.

12) I. Nitta and K. Osaki, *X-Rays*, **5**, 37 (1948).
13) L. Pauling and J. Sherman, *J. Chem. Phys.*, **1**, 679 (1933).
14) L. Pauling, *Phys. Rev.*, **34**, 954 (1929).

Diamagnetic Anisotropy and Resonance Energy.—According to Pauling, mono- and dicarboxylic acids and their salts exhibit resonance with two contributing forms and the actual resonance structure is a resonance hybrid intermediate between the contributing forms. Taking into account the empirical values of the polar effect and the dissociation constants of fatty acids Pauling calculated the resonance energy in carboxylic groups. One direct consequence of such resonance is the abnormal diamagnetism normal to the plane of the groups. Therefore it would be very interesting to correlate the measured abnormal diamagnetism with the resonance energy as obtained empirically. As already stated the kinetic energy E of the resonating electron is related to ΔK by expression

$$E = 3.22 \times \frac{\Delta K \times \rho}{M}$$

Using the above relation we have calculated the resonance energy for formates, oxalates, succinates and tartrates using ΔK-values which are given in Table III. We have also taken

TABLE III

Substances	$\Delta K \times 10^6$	Extra resonance energy calculated By Pauling	Extra resonance energy calculated From magnetic values
	Aromatics		
Diphenyl	118.6	86.88	84.65
Naphthalene	114.0	74.66	82.62
Anthracene	182.6	104.70	100.30
Stilbene	141.6	94.26	101.00
	Aliphatics		
Succinic acid	10.7	54.86	52.00
Tartaric acid	9.6	54.86	52.00
Oxalic acid	10.7	54.86	53.31

some of the ΔK-values for some typical aromatics as determined by Krishnan and Banerji[2] and calculated resonance energy. The agreement between the observed and calculated values is very encouraging.

Influence of Resonance Energy on Diamagnetism.—Adopting the conventional structural formulae for oxalates, formates and acetates, we have calculated mean gram molecular susceptibilities $\bar{\chi}_m$ for them on the basis of Pascal's additive law which are given in Table II. On comparing with our measured values of $\bar{\chi}_m$ a lowering is observed. This lowering is well understood if we recall that the resonance occuring in these groups impart on them some amount of double bond character (unsaturated) which lowers $\bar{\chi}_m$. A similar comparison of $\bar{\chi}_m$ deduced on the basis of Pascal's law and those measured by Krishnan and Banerji[2] for a number of aromatic substances

points to the same findings. Matsunaga[15] found with azobenzene the same value as Banerji[3] which is lower than Pascal's value Thus one can safely conclude that resonance lowers diamagnetic values.

The above point of view is further strengthened by our findings that for molten oxalic acid dihydrate $\bar{\chi}_m$ is -60.89×10^{-6} (100°C) while that for the powder state is -56.4×10^{-6} (30°C). In molten state the crystal lattice completely breaks down so that the double bond character almost vanishes and hence there is an increment of $\bar{\chi}_m$ approaching Pascal's value.

Summary

The principal magnetic susceptibilities of single crystals of some aliphatic mono- and di-basic acids and their salts have been measured and the results have been correlated with the fine structure studies of the crystals by X-ray methods. It is observed that the anisotropy per -COOH group is 5 units, which increases by nearly 2 units if two parts of COOH groups are not in the same plane.

The observed extra diamagnetism normal to the plane of the carboxylic groups, if attributed to resonance, the calculated energy compares very favourably with that deduced by Pauling from a consideration of the heat of formation of molecules and the lowering of the susceptibility from Pascal's value is then well understood.

We take this opportunity to thank the Ministry of Education, Govt. of India for the individual (A. M.) research grants and to U. P. S. R. G. C. for the award of scholarship to one of us (D. N.).

Physics Labratries
Agra College
Agra, India

15) Y. Matsunaga, This Bulletin, **29**, 308 (1956).

The Surface Tension and the Critical Micelle Concentration in Aqueous Solution of β-D-Alkyl Glucosides and their Mixtures

By Kozo Shinoda, Tokio Yamaguchi and Ryohei Hori

(Received August 11, 1960)

There have not been many research works on the pure non-ionic agents[1-3]. Future progress in this field should be assured by the study of pure non-ionic agents. Some colloid chemical properties of a series of pure octyl polyol ethers in aqueous solution have been studied to determine the effect of differences in the hydrophilic group[3]. In the present paper, we have measured the surface tension vs. concentration of octyl, decyl and dodecyl glucosides in order to know the effect of paraffin chain length on the physico-chemical properties of alkyl glucosides. The CMC was determined from the inflexion of the surface tension vs. concentration curve. The surface tension of mixtures of alkyl glucosides solutions and the effect of added salts on the surface tension of octyl glucoside were also measured.

Experimental

The procedures and purifications of alkyl glucosides were similar[4] as in the case of octyl glucoside[5]. The melting points and specific rotations of β-D-octyl, decyl and dodecyl glucosides were m. p. 63.8~65°C, $[\alpha]_D^{20}=-33.8°$ (H_2O); m. p. 135°C, $[\alpha]_D^{25}=-27.8°$ (H_2O); m. p. 143.5°C, $[\alpha]_D^{25}=-24.7°$ (H_2O), respectively.

The materials were further purified by foam fractionation. The concentration of the solution foam fractionated was chosen slightly below the CMC, because the foam stability and the efficiency of the elimination of highly surface active impurities were optimum in this concentration[5]. Surface

1) C. R. Bury and J. Browning, *Trans. Faraday Soc.*, **49**, 209 (1953).
2) T. Nakagawa et al., *J. Chem. Soc. Japan, Pure Chem. Soc.* (*Nippon Kagaku Zasshi*), **77**, 1563 (1956); **79**, 345, 348 (1958).
3) K. Shinoda, T. Yamanaka and K. Kinoshita, *J. Phys. Chem.*, **63**, 648 (1959).
4) R. Hori, Ph. D. Dissertation, Kyoto University (1959) (in Japanese).
5) K. Shinoda and K. Mashio, *J. Phys. Chem.*, **64**, 54 (1960).

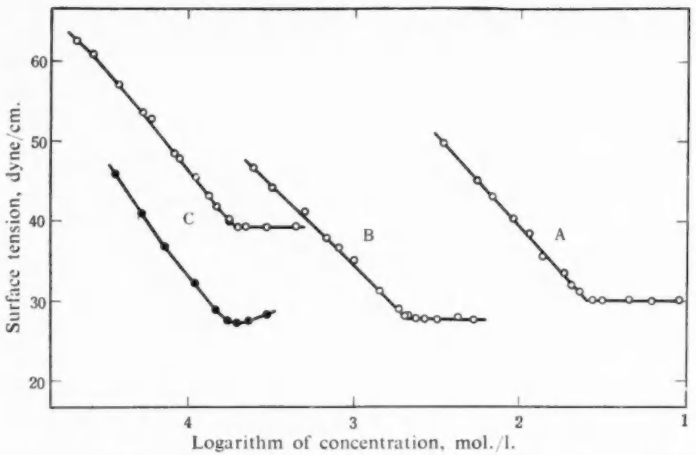

Fig. 1. The surface tension vs. log. concentration curves of β-D-alkyl glucosides at 25°C: A, octyl glucoside; B, decyl glucoside; C, dodecyl glucoside; ●, before foam fractionation.

tension was measured by the drop weight method, with a tip 0.576 cm. in diameter in an air thermostat at 25±0.2°C. The correction of Harkins et al.[6] was applied. There was appreciable change, 2~4 dyne/cm. of surface tension, with time durations of 4~20 min. and 10~60 min. for decyl and dodecyl glucosides, respectively.

Results

The surface tension vs. concentration relations are shown in Fig. 1 and summarized in Tables I, II and III. There was great change in surface tension between foam fractionated unfractionated solution of dodecyl glucoside. However, there was no appreciable change in solutions of octyl and decyl glucosides.

TABLE I. THE SURFACE TENSION IN AQUEOUS SOLUTION OF β-D-OCTYL GLUCOSIDE AT 25°C

Concentration, mol./l. ×10²	Time per drop in min.	Number of measurements	Surface tension dyne/cm.	Mean variation dyne/cm.
0.343	20	4	49.8	0.2
0.549	15	4	45.0	0.6
0.686	10	4	43.1	0.35
0.915	10	4	40.3	0.4
1.14	10	4	38.4	0.2
1.37	10	4	35.6	0.3
1.83	5	8	33.6	0.9
2.05	5	4	32.1	0.05
2.29	5	2	31.2	0.05
2.75	5	4	30.2	0.3
3.07	5	3	30.3	0.2
4.61	5	4	30.4	0.1
6.15	5	3	29.9	0.6
9.23	5	2	30.1	0.0

TABLE II. THE SURFACE TENSION IN AQUEOUS SOLUTION OF β-D-DECYL GLUCOSIDE AT 25°C

Concentration, mol./l. ×10²	Time per drop in min.	Number of measurements	Surface tension dyne/cm.	Mean variation dyne/cm.
0.255	20	2	46.7	0.1
0.325	15	3	44.2	0.1
0.513	15	4	41.2	0.3
0.683	10	4	37.8	0.1
0.816	10	2	36.7	0.0
1.025	10	4	35.0	0.3
1.46	10	2	31.2	0.2
1.91	5	3	29.0	0.0
2.06	5	3	28.1	0.1
2.14	5	2	28.3	0.0
2.41	5	4	27.8	0.1
2.67	5	2	27.7	0.1
3.22	5	3	27.7	0.1
4.28	5	3	28.0	0.3
5.35	5	4	27.7	0.5

The inflexion in the surface tension vs. logarithm of concentration curve was distinct and there was no minimum in foam fractionated solution. The surface tension of mixtures of alkyl glucosides has been measured. The results are summarized in Fig. 2. The surface tension vs. concentration curve showed the minimum in the mixture of octyl-decyl glucosides. The effect of added sodium chloride, calcium chloride and sodium sulfate on the surface tensions of aqueous solution of octyl glucoside has also been measured. The results are shown in Fig. 3.

6) W. D. Harkins and F. E. Brown, *J. Am. Chem. Soc.*, **41**, 519 (1919).

TABLE III. THE SURFACE TENSION IN AQUEOUS SOLUTION OF β-D-DODECYL GLUCOSIDE AT 25°C

Concentration, mol./l. $\times 10^4$	Time per drop in min.	Number of measurements	Surface tension dyne/cm.	Mean variation dyne/cm.
0.213	60	3	62.5	0.1
0.270	60	3	60.8	0.3
0.385	60	3	57.0	1.0
0.540	50	3	53.6	1.1
0.609	40	3	52.8	0.1
0.835	30	3	48.5	0.1
0.900	20	3	47.9	0.2
1.13	20	4	45.4	0.4
1.35	15	4	43.1	0.3
1.51	15	4	41.8	0.4
1.81	10	4	40.2	0.2
1.82	10	4	39.8	0.9
2.00	10	4	39.3	0.25
2.26	10	4	39.3	0.1
3.01	10	4	39.4	0.15
3.77	10	4	39.4	0.4

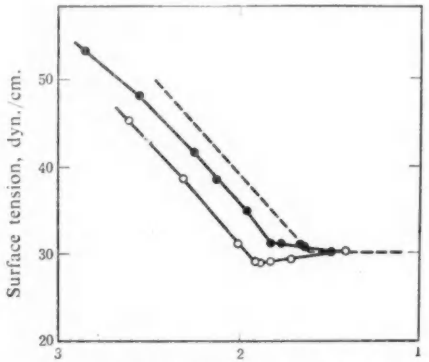

Fig. 2. The surface tension vs. log. concentration of mixtures of alkyl glucosides at 25°C: ○, decyl and octyl glucosides in mole ratio of 0.089 to 0.911; ●, dodecyl and octyl glucosides in mole ratio of 0.0084 to 0.9916; dotted curve shows pure octyl glucoside.

Discussion

The CMC was obtained from the inflexions in the curves. As the surface tension remains constant, the activity of solute is constant over the flat portion of the surface tension vs. concentration curve. Because, in Gibbs adsorption isotherm,

$$\left(\frac{\partial\gamma}{\partial \ln c_2}\right)_T\left(\frac{\partial \ln c_2}{\partial \ln a_2}\right)_T = -RT\Gamma_2 \qquad (1)$$

if $(\partial\gamma/\partial \ln c_2)_T=0$ and $\Gamma_2>0$, then $(\partial \ln a_2/\partial \ln c_2)_T=0$ and therefore $a_2=$const. with concentration.

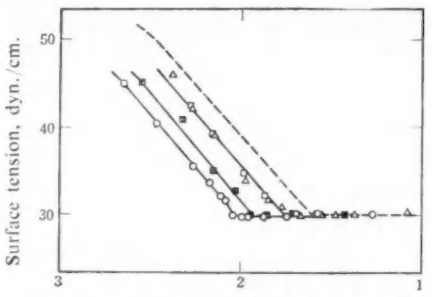

Fig. 3. The effect of added salts on the surface tension of β-D-octyl glucoside at 25°C: △, 0.93 N $CaCl_2$; □, 0.47 N NaCl; ■, 0.93 N NaCl; ○, 0.93 N Na_2SO_4.

The fact that the activity vs. concentration remains constant suggests that something similar to a phase separation is occurring in the solution. Namely, the micelle formation begins above the concentration of inflexion and the concentration of single species stays constant.

Table IV gives the CMC, surface excess and residual area per molecule calculated from the data in Tables I, II and III under the assumption that $(\partial \ln a_2/\partial \ln c_2)_T=1$ below the concentration of inflexion point.

TABLE IV. THE CMC, SURFACE EXCESS AND RESIDUAL AREA OF β-D-ALKYL GLUCOSIDES AT 25°C

Substance	CMC mol./l.	Surface excess 10^{-10} mol./cm²	Residual area Å²
Octyl glucoside	0.025	3.9	42
Decyl glucoside	0.0022	3.5	47
Dodecyl glucoside	0.00019	4.6	36

The CMC of ionic agents was given as a function of hydrocarbon chain length and the concentration of gegenions[7-10],

$$\log \mathrm{CMC} = -\frac{m\omega}{kT} + K_6 \ln C_i + \text{const.} \qquad (2)$$

where ω is the cohesive energy change per methylene group passing from the bulk of the solution to the micelle, m the number of carbon atoms in hydrocarbon chain, K_6 the experimental constant, C_i the concentration of uni-valent gegenions.

As there is no electrical work accompanying

7) A. B. D. Cassie and R. C. Palmer, *Trans. Faraday Soc.*, **37**, 156 (1941).
8) H. Lange, *Kolloid-Z.*, **117**, 48 (1950).
9) M. E. Hobbs, *J. Phys. & Colloid Chem.*, **55**, 675 (1951).
10) K. Shinoda, This Bulletin, **26**, 101 (1953).

the formation of micelles of non-ionic agents, the electrical term in Eq. 2 disappears. The change in CMC as a function of the paraffin chain length may be expressed as,

$$\log \mathrm{CMC} = -\frac{m\omega}{kT} + \text{const.} \quad (3)$$

Actually the CMC of octyl, decyl and dodecyl glucosides decreased to 1/3.4 per one additional methylene group. This relation is similar to that of ionic agents under the condition of a definite concentration of gegenions[11] as will be expected from Eq. 2. In a case where no salt is added, the decrease in CMC of ionic agent is much smaller. Lange has found similar results for octyl, decyl and dodecyl polyoxyethylene ether[12].

The CMC's of mixtures of ionic agents have been studied and interpreted rather well[13,14]. As there is no electrical energy involved in micellization of non-ionic agent, the theoretical treatment is far simpler and the CMC is given as a function of the mole composition of the mixture.

$$\sum \mathrm{CMC}_{mi} \cdot x_i = \mathrm{CMC}_{\mathrm{mix}} \quad (4)$$

$$\sum \mathrm{CMC}_{mi} \frac{x_i' \exp(m_i\omega/kT)}{\sum x_i' \exp(m_i\omega/kT)} = \mathrm{CMC}_{\mathrm{mix}} \quad (5)$$

Where x_i is the mole fraction of the ith component in the micelle and x_i' the mole fraction of the ith component in the bulk of the solution. The comparison between the calculated and observed CMC values is shown in Table V.

Table V

Substance	Mole fraction of the latter compound	CMC mol./l.	Calcd. CMC mol./l.
Octyl/Decyl glucoside	0.089	0.0125	0.013
Octyl/Dodecyl glucoside	0.0084	0.015	0.012

It seems very interesting to us that the surface tension vs. concentration curve showed the minimum in the mixture of decyl and octyl glucoside, but the mixture of dodecyl octyl glucoside did not show the recognizable minimum as shown in Fig. 2. The existence of the minimum in the former and non-existence in the latter can be explained as being based on the change in composition at the surface. In the mixture of decyl and octyl glucosides, the more surface-active molecule, decyl glucoside, has lower suface tension over the flat portion, as shown in Fig. 1. The mole fraction of decyl glucoside is relatively large at the surface at the minimum, i.e., at the beginning of micelle formation, whereas the fraction of decyl glucoside decreases above the CMC, due to the increase of the micellar species, and the surface tension approaches that of pure octyl glucoside solution. This discussion may hold for the mixture of homologous compounds of non-ionic agents.

The addition of salts to solutions of non-ionic agents has a relatively small effect compared with ionic agents. Moreover, the slope of surface tension vs. logarithm of concentration curve does not change appreciably in contrast with ionic agents[15]. The effect is not electrical and probably rather indirect. Sodium chloride showed a greater effect than calcium chloride depressing the cloud point[16] and increasing relative viscosity and turbidity[17] of non-ionic agents. The same trend was observed in depressing the CMC. Sodium sulfate of the same concentration shows an even greater effect than sodium chloride. The CMC obtained from the inflexions of surface tension vs. concentration curves are summarized in Table VI.

Table VI. The effect of added salts on the CMC determined by surface tension measurements at 25°C

Substance	Medium	CMC mol./l.
Octyl glucoside	H_2O	0.025
〃	0.93 N $CaCl_2$	0.017
〃	0.47 N NaCl	0.017
〃	0.93 N NaCl	0.012
〃	0.93 N Na_2SO_4	0.009

The salts of the same ionic strengths do not exhibit the same effect. The volume of salts added, including hydration water, may change the effective concentration of agents and the change in solvent property may decrease the hydration and the CMC decreases.

Summary

The surface tension in aqueous solutions of β-D-alkyl glucoside and their mixtures at 25°C has been measured. The CMC was determined from the inflexions of the curves; octyl glucoside, 0.025 mol./l., decyl glucoside 0.0022 mol./l., dodecyl glucoside, 0.00019 mol./l. The effect of hydrocarbon chain length was explained theoretically. The CMC of mixtures has been also explained by the extension of the theory of ionic agents. The effect of added sodium chloride, calcium chloride and sodium sulfate

11) K. Shinoda, *J. Phys. Chem.*, **59**, 432 (1955).
12) H. Lange, *Kolloid-Z.*, **163**, 9 (1959).
13) H. Lange, ibid., **131**, 96 (1953).
14) K. Shinoda, *J. Phys. Chem.*, **58**, 1136 (1954).
15) H. Lange, *Kolloid-Z.*, **153**, 155 (1957).
16) W. N. Macley, *J. Colloid Sci.*, **11**, 272 (1956).
17) T. M. Doscher, G. E. Myers and D. C. Atkins, Jr., ibid., **6**, 223 (1951).

on the surface tension in aqueous solution of octyl glucoside has been measured. The effect of added salts on the CMC was determined from the inflexions of the surface tension vs. logarithm of concentration curves.

We wish to thank Mr. K. Ito for some of the measurements and the Ministry of Education for their support.

Department of Chemistry
Faculty of Engineering
Yokohama National University
Minami-ku Yokohama
(K. S. & Y. T.)

Department of Pharmacy
Kyoto University
Sakyo-ku, Kyoto
(H. R.)

*Some Copper Complexes of Diazoaminobenzene Derivatives and their Properties**

By Hiraku YAMADA, Hiroshi OHTA, Masaru YAMAGUCHI and Tokuichi TSUMAKI

(Received August 13, 1960)

It is well known that the copper(I) complexes of diazoaminobenzene and its derivatives are, in some organic solvents, more stable than the copper(II) complexes. Dwyer et al.[1-6] found that in solution the copper(II) complex of diazoaminobenzene decomposed rapidly into the copper(I) complex by auto-reduction, splitting off the organic fragments. But they did not investigate these fragment. In the present paper are described the synthesis of the copper(II) complexes of diazoaminobenzene derivatives and the isolation and identification of their thermal decomposition products.

As the starting materials for the synthesis of the copper(II) complexes, we chose 4,4'-dichloro-, 4,4'-dimethoxy-, 4-chloro-, 4-methoxy- and 4-ethoxydiazoaminobenzenes. The synthesis of their copper(II) complexes was fairly difficult owing to their extreme instability in solution. The synthesis was, therefore, carried out successfully at low temperature, and, in some cases, at temperature as low as possible by cooling with an ethanol-dry ice bath. The complexes were obtained as dark green crystals or powder. In the dry state they are stable, but in solution they become much less stable; and, when heated, they decompose very rapidly into black brown solutions containing tarry substances.

From the tarry substances we could obtain by chromatography on alumina, the copper(I) complexes as yellow to orange-red crystals. From the solution after the separation of the copper(I) complexes a considerable amount of azobenzene derivatives was obtained.

In order to obtain some knowledge concerning the decompositon mechanism, we furthermore investigated the thermal decomposition products of bis(diazoaminobenzene)copper(II) [or bis(1,3-diphenyltriazenato)copper(II)] and estimated quantitatively nitrogen gas evolved by the thermal decomposition of the copper(II) complexes of diazoaminobenzene derivatives. From bis(diazoaminobenzene)copper(II), only biphenyl, not azobenzene, was obtained. Further it was ascertained that one molecule of nitrogen was evolved per molecule of each of the complexes during the decomposition. It is, therefore, considered most probable that the decomposition of the copper(II) complexes proceeds in the manner shown below.

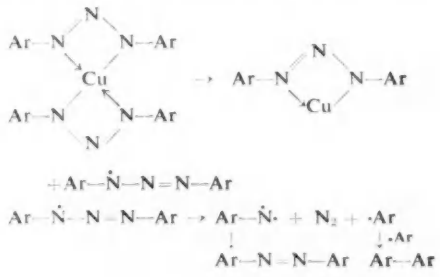

* "Co-ordinate Valency Rings" XXIX. XXVIII of this series: Y. Kihara, H. Ohta and T. Tsumaki, *Mem. Faculty Sci., Kyushu Univ., Ser. C, Chem.*, **3**, 137 (1960).

1) F. P. Dwyer, *J. Soc. Chem. Ind.*, **58**, 110 (1939); *Chem. Abstr.*, **33**, 5818 (1939).
2) F. P. Dwyer, *Australian Chem. Inst. J. and Proc.*, **6**, 348 (1939); *Chem. Abstr.*, **34**, 733 (1940).
3) F. P. Dwyer, ibid., **6**, 362 (1939); *Chem. Abstr.*, **34**, 734 (1940).
4) F. P. Dwyer, *J. Am. Chem. Soc.*, **63**, 79 (1941).
5) F. P. Dwyer et al., ibid., **63**, 81 (1941).
6) F. P. Dwyer et al., *Chemistry and Industry*, **1940**, 136; *Chem. Abstr.*, **34**, 3245 (1940).

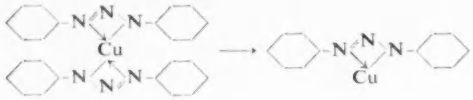

Experimental

The following diazoaminobenzene derivatives were synthesized:

4,4'-dichlorodiazoaminobenzene[7],
4,4'-dimethoxydiazoaminobenzene[8],
4,4'-diethoxydiazoaminobenzene[9],
4-chlorodiazoaminobenzene[10],
4-methoxydiazoaminobenzene[11],
and 4-ethoxydiazoaminobenzene[12]

The Synthesis of the Copper(II) Complexes of Diazoaminobenzene Derivatives.—*General Remarks*: Since the copper(II) complexes of diazoaminobenzene and its derivatives are very unstable in solution, the synthesis must always be carried out below 0 °C.

Bis(4, 4'-dichlorodiazoaminobenzene)copper(II).—To a solution of 5 g. of 4,4'-dichlorodiazoaminobenzene in 50 cc. of ethanol is added a solution of 1.8 g. of copper acetate in 100 cc. of the same solvent. The solvent is removed in vacuo, till the precipitate deposits. The precipitate is filtered off and washed with water and then with ethanol. The precipitate is then dissolved in cold acetone and concentrated under reduced pressure at room temperature, when dark green crystals separate out. Dark green plates, which decompose violently at 114 °C. Soluble in acetone, ethanol, benzene and chloroform.

Found: C, 48.02; H, 3.02; N, 18.18; Cu, 11.43. Calcd. for $C_{24}H_{16}N_6Cl_4Cu$: C, 48.54; H, 2.72; N, 14.15; Cu, 10.70%.

Bis(4, 4' - dimethoxydiazoaminobenzene)copper(II).—To a solution of 5.2 g. of 4,4'-dimethoxydiazoaminobenzene in 100 cc. of ether is added a solution of 1.8 g. of copper acetate in 200 cc. of ethanol, and the mixture is cooled in an ethanol-dry ice bath and stirred well. The color of the solution becomes green. After standing for an hour, the solvent is removed under reduced pressure at room temperature. The precipitate produced is filtered and washed successively with water, ethanol, acetone and ether, and dried. Dark green micro-crystals, which decompose at 200~204 °C. Soluble in acetone, ethanol, benzene and chloroform. In solution it is extremely unstable.

Found: C, 58.45; H, 5.08; N, 14.47; Cu, 11.08. Calcd. for $C_{28}H_{28}N_6O_4Cu$: C, 58.37; H, 4.90; N, 14.59; Cu, 11.03%.

Bis(4, 4'-diethoxydiazoaminobenzene)copper(II).—To a solution of 5.7 g. of 4,4'-diethoxydiazoaminobenzene in 200 cc. of acetone is added a solution of 1.8 g. of copper acetate in 100 cc. of ethanol, and the mixture is maintained between −10~−20 °C for an hour, and after that concentrated under reduced pressure. The precipitate is filtered and washed successively with water, acetone and ether, and dried. Dark green plates, which decompose at 150 °C. Soluble in ether, acetone and ethanol.

Found: C, 60.28; H, 6.05; N, 13.20; Cu, 9.92. Calcd. for $C_{32}H_{36}N_6O_4Cu$: C, 60.79; H, 5.74; N, 13.29; Cu, 10.05%.

Bis(4-chlorodiazoaminobenzene)copper(II).—To a solution of 4.5 g. of 4-chlorodiazoaminobenzene in 100 cc. of ethanol is added a solution of 1.8 g. of copper acetate in 100 cc. of ethanol, and the mixture is maintained between −10~−20 °C for an hour, and then concentrated under reduced pressure at room temperature. The precipitate is filtered, washed successively with water, ethanol, and ether, and dried. Dark green powder, which decomposes at 85~87 °C. Soluble in acetone, ethanol and benzene.

Found: C, 57.07; H, 3.84; N, 15.97; Cu, 12.05. Calcd. for $C_{24}H_{18}N_6Cl_2Cu$: C, 54.92; H, 3.46; N, 16.01; Cu, 12.10%.

Thermal Decomposition of the Copper(II) Complexes of Diazoaminobenzene Derivatives in Solution.—One per cent solution of each of the copper(II) complexes in acetone, benzene or ether is refluxed on a water-bath. In 15~30 min. the color of the solution changes from green to black-brown, and a tarry precipitate is produced. After 1~3 hr. the decomposition is complete. The tarry precipitate is filtered off from the solution, dissolved in benzene-chloroform-petroleum ether mixture and chromatographed on alumina, when the copper(I) complexes were obtained. The effluent was combined with the filtrate from the tarry precipitate and the combined solution was used for the later operations.

The following copper(I) complexes were obtained.

4, 4' - Dichlorodiazoaminobenzenecopper(I).—Yellow needles, which decompose at 242 °C explosively. Readily soluble in benzene and chloroform, soluble with difficulty in ether and acetone.

Found: C, 43.47; H, 2.46; N, 12.20; Cu, 19.34. Calcd. for $C_{12}H_8N_3Cl_2Cu$: C, 43.85; H, 2.45; N, 12.78; Cu, 19.33%.

4, 4' - Dimethoxydiazoaminobenzenecopper(I).—Orange-red needles, which decompose at 228 °C, giving tarry substance. Readily soluble in benzene and chloroform, soluble with difficulty in ether and acetone.

Found: C, 52.95; H, 4.56; N, 13.88; Cu, 19.78. Calcd. for $C_{14}H_{14}N_3O_2Cu$: C, 52.58; H, 4.41; N, 13.14; Cu, 19.87%.

4, 4'-Diethoxydiazoaminobenzenecopper(I).—Orange-colored needles, which decompose at 240 °C, giving tar. Readily soluble in benzene and ethanol, soluble with difficulty in ether and acetone.

Found: C, 55.59; H, 5.55; N, 12.01; Cu, 18.12. Calcd. for $C_{16}H_{18}N_3O_2Cu$: C, 55.24; H, 5.22; N, 12.08; Cu, 18.26%.

The above-mentioned combined solution was extracted with 1 N hydrochloric acid after the addition of 3~4 times its volume of ether. From this acid extract no identifiable substance was obtained. The remaining ether solution was chromatographed on alumina, using petroleum ether, petroleum benzine and acetone as eluents, when

7) R. Meldola et al., *J. Chem. Soc.*, **53**, 670 (1888).
8) M. Busch and E. Bergmann, *Chem. Zentr.*, **1905 I**, 1102.
9) R. Henriques, *Ber.*, **25**, 3064 (1892).
10) A. Hantzsch et al., ibid., **30**, 1413 (1897).
11) D. Vorländer, ibid., **62**, 2830 (1929).
12) D. Vorländer, ibid., **62**, 2825 (1929).

five fractions were obtained. From the first fraction the following azobenzene derivatives were obtained, and identified by the measurement of the mixed melting point with the authentic samples: 4,4'-dichloroazobenzene, 4,4'-dimethoxyazobenzene, and 4,4'-diethoxyazobenzene. From the fractions following we could not obtain any identifiable substances. We could, further, obtain biphenyl from the decomposition products of bis(diazoaminobenzene)copper(II) in benzene, but in this case we could not notice azobenzene.

Determination of Nitrogen Gas Evolved during the Decomposition of the Copper(II) Complexes in Solution.—The solution of 20~25 mg. of the complex in 10 cc. of benzene was heated in an airtight vessel in a stream of carbon dioxide. After removal of benzene vapour through the efficient trap cooled by dry ice, the nitrogen gas evolved was collected on an azotometer. The results are shown below:

Copper(II) complexes (one mole)	Nitrogen gas evolved (mole)
Bis(4, 4'-dichlorodiazoaminobenzene)copper(II)	0.754
Bis(4, 4'-dimethoxydiazoaminobenzene)copper(II)	0.952
Bis(4, 4'-diethoxydiazoaminobenzene)copper(II)	0.836
Bis(4-chlorodiazoaminobenzene)-copper(II)	0.748

The authors wish to express their gratitude to Mr. Michio Shido, Miss Sachiko Indo and Miss Takeko Tahara for the microanalyses.

Department of Chemistry
Faculty of Science
Kyushu University
Hakozaki, Fukuoka

Studies on Heavy-Nitrogen Labeled Compounds. III.[1] *Preparation of ^{15}N-Labeled α-Hydroximinopropionic Acid*

By Yoshishige SATO, Teruhiko MESHI and Norio SUGIMOTO

(Received July 16, 1960)

There are a number of methods of preparing ^{15}N-labeled compounds by using $(^{15}NH_4)_2SO_4$ as a starting substance but there are not many methods which resort to $K^{15}NO_3$. However, the use of $K^{15}NO_3$ as a starting substance will be required, when reactions including diazotization are performed. In 1950, Clusius et al.[2] succeeded in preparing $Na^{15}NO_2$ by the reaction of aqueous solution of sodium hydroxide with a mixture of oxygen and nitric oxide obtained by decomposition of $K^{15}NO_3$. Using $Na^{15}NO_2$ obtained, they prepared potassium azide-^{15}N[3], phenyl hydrazine ^{15}N[2] and diphenyl hydrazine-^{15}N[4]. Bothner-By and Friedman[5], in 1951, synthesized 3,5-dinitrobenzoylazide-3-^{15}N according to the same method as described above.

In this paper synthesis of α-hydroximinopropionic acid-^{15}N was performed by using $K^{15}NO_3$ as a starting substance. For preliminary experiment, $K^{14}NO_3$, $K^{14}NO_2$ and $^{14}NH_2OH\cdot HCl$ were employed for preparing $K^{14}NO_2$, $^{14}NH_2OH\cdot(1/2)H_2SO_4$ and $CH_3C(^{14}NOH)COOH$, respectively. Then, using $K^{15}NO_3$, $CH_3C(^{15}NOH)\cdot COOH$ was prepared without separating the intermediate products: $K^{15}NO_2$ and $^{15}NH_2OH\cdot(1/2)H_2SO_4$.

Experimental and Results

Preliminary Experimental by Use of ^{14}N-Compound. — *Preparation of $K^{14}NO_2$ from $K^{14}NO_3$.* — In order to reduce KNO_3 to KNO_2, lead, copper, sodium bisulfite, sodium formate and zinc were used and potassium hydroxide was sometimes employed as an accelerating agent for the reduction in a fused state. The amount of potassium nitrite was measured by the titration with N/10-$KMnO_4$ solution. The data are shown in Table I.

When a mixture of potassium hydroxide with copper, sodium formate or zinc is employed as a reducing agent, a high yield can be obtained as seen from this table.

On the other hand, in the case of the reduction of the aqueous solution, it was found that potassium nitrite was obtained with a greater yield than in the case of the fusion method. The procedure is as follows. Ten milliliter of aqueous solution containing 4 g. of potassium nitrate was

1) Part II: Y. Sato, T. Meshi, T. Takahashi, I. Chibata, M. Kisumi and Y. Ashikaga, *Radiation and Isotops*, **3**, 31 (1960).
2) K. Clusius and M. Hoch, *Helv. Chim. Acta.*, **33**, 2122 (1950).
3) K. Clusius and H. Hurzeler, ibid., **36**, 1326 (1953).
4) K. Clusius and M. Vecchi, ibid., **36**, 933 (1953).
5) A. A. Bothner-By and L. Friedman, *J. Am. Chem. Soc.*, **73**, 5391 (1951).

TABLE I. YIELD OF KNO_2, THE REDUCING AGENTS AND THE REDUCTION TIME

Reducing agents	Yield of KNO_2 %	Amounts of reduction agents for 2 g. of KNO_3 g.	Fusion time, hr.	
Pb	64*	2.4	2	6)
Pb	80.2*	2		5)
Pb	65~70*	4		7)
Pb	91~93*	2.4		8)
Pb	62	6	0.5	
Pb+KOH	50	Pb 4, KOH 1.2	2	
$NaHSO_3$	59	2		
HCOONa +KOH	80	HCOONa 1.4, KOH 1	0.5	
Cu	82	1.37	1	
Cu+KOH	83	Cu 1.37, KOH 1.2	1	
Zn+KOH	79	Zn 1.3, KOH 1.2	1	

* From literature.

mixed with 30 ml. of 30% aqueous ammonia solution and the mixture was kept below 10°C. Then, 2.6 g. of zinc dust was added in small portions to the mixture. The zinc-oxide was filtered off and the filtrate was concentrated to 3 ml. under vacuo. The yield of potassium nitrite was found to be 85%, when measured by titration with potassium permanganate solution.

Synthesis of Hydroxylamine Hydrochloride. —Using potassium nitrite as a starting substance, hydroxylamine hydrochloride was synthesized according to the method of organic syntheses[9]. The aqueous solution of potassium carbonate saturated with sulfur dioxide gas was added to the aqueous solution containing 1.7 g. of potassium nitrite in a vessel, the temperature of which was kept at 0°C. The mixed solution was kept at pH 3 with 7% aqueous solution of sulfurous acid. Two milliliter of acetone was added to it. The acetoxime was hydrolized with concentrated hydrochloride. The yield of hydroxylamine hydrochloride was about 70%.

Synthesis of α-Hydroximinopropionic Acid.—In 4 ml. of aqueous solution containing 0.9 g. of pyruvic acid, 0.732 g. of hydroxylamine hydrochloride was added and allowed to stand for one hour. Hydrochloric acid was neutralized by addition of 0.7 g. potassium carbonate powder. After the aqueous solution was neutralized, the solution was concentrated to dryness in vacuo. The solid residue was extracted with 100 ml. of ether, and α-hydroximinopropionic acid was obtained by removing ether. The yield is 85% on the basis of hydroxylamine hydrochloride and about 50% on the basis of potassium nitrate.

Synthesis of α-Hydroximinopropionic Acid-^{15}N. —α-Hydroximinopropionic acid-^{15}N was synthesized by the method described above. The procedure is as follows. Two and a half grams of $K^{15}NO_3$ (^{15}N atom % : 88%) was dissolved in an aqueous ammonia solution and kept below 10°C. Zinc powder (1.6 g.) was added for the reduction of $K^{15}NO_3$ to $K^{15}NO_2$. After the deposited zinc oxide was removed by filtration, the solution was concentrated to 10 ml., kept at 0°C and made pH 3 with 7% sulfurous acid. Further 0.4 ml. of concentrated sulfuric acid was added to the solution in order to hydrolize the reaction product and refluxed for five hours. Into the hydrolized solution, 50% aqueous solution containing 1.5 g. pyruvic acid was added and allowed to stand for one hour. Using the powder of potassium carbonate, the liberated sulfuric acid was neutralized and its solution was concentrated to dryness in vacuo. The residue was extracted with 100 ml. of ether. Water in the extracted ether solution was removed by anhydrous sodium sulfate and ether was removed in vacuo to give α-hydroximinopropionic acid-^{15}N. The yield is 1.55 g. and 61.5% on the basis of $K^{15}NO_3$.

Summary

By use of $K^{15}NO_3$ as a starting material, α-hydroximinopropionic acid-^{15}N was synthesized in accordance with the following reactions:

$$K^{15}NO_3 \rightarrow K^{15}NO_2 \rightarrow {}^{15}NH_2OH$$
$$\rightarrow CH_3C(={}^{15}NOH)COOH$$

The above reactions were carried out without separating any intermediate products. The yield of α-hydroximinopropionic acid-^{15}N was about 61% on the basis of $K^{15}NO_3$.

Osaka Research Laboratory
Tanabe Seiyaku Co., Ltd.
Kashimacho, Higashiyodogawa-ku
Osaka

6) W. R. Vaughan, D. I. McCane and G. B. Sloan, ibid., 73, 2298 (1951).
7) S. Feldhaus, *Ann.*, 126, 71 (1863).
8) V. I. Maimind, B. V. Tokarev, E. Gomes, R. G. Vdovina, K. M. Ermolaev and M. M. Shemyakin, *J. Gen. Chem. (U. S. S. R.)*, 26, 2187 (1956).
9) Organic Syntheses, 3, 61 (1923); W. L. Semon, *J. Am. Chem. Soc.*, 45, 188 (1923).

*The Resonance Effect of Amide Group on the Polymerizability of Lactam Derivatives. I. The Infrared Spectrum of N-Methyl Lactams**

By Naoya OGATA

(Received July 7, 1960)

The amide linkage of chain amide molecule tends to take a planar structure owing to the resonance in the molecule[1]. The two configurations of cis and trans forms shown below are possible:

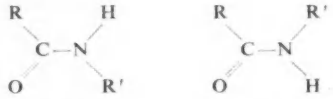

trans form cis form

It it known that the trans form of an amide group is more stable than the cis form and monosubstituted acid amide RCONHR′ takes the trans[1,2] form, while lactams of less than 9 membered rings take the cis form owing to the steric hindrance[3].

It has been reported on the polymerizability of ε-caprolactam that the configuration of the amide group relates to its reactivity[4] and *N*-alkyl-substituted derivatives of the cis amide such as *N*-methyl-ε-caprolactam are too stable to polymerize[5].

The great stability of *N*-alkyl-substituted lactams can not be explained from the difference in the ring strain or in the thermodynamical character[6] caused by the intramolecular rotational isomerism, but it is supposed to be due to the increase of resonance in the amide group[7]. Therefore, the infrared spectra of several chain and cyclic amide compounds have been measured with special interest in the range of 1600~1800 cm^{-1}, and the effect of the resonance on the characteristic band of the amide group has been investigated.

Experimental

The infrared spectra of several amide compounds were measured with a Hitachi model EPI-2 spectrophotometer in the range of 2~15 μ, with a rock salt prism. The cell thickness was 0.01 mm.

The infrared spectra of chloroform solution of *N*-alkyl-substituted chain or cyclic amides were measured in the range of 5.5~6.5 μ at various concentrations and temperatures. The cell thickness was selected suitably so that the transmittance at the absorption maximum is within the range of 20~80%. Although it is desirable to use a nonpolar solvent such as carbon tetrachloride, *N*-methyl lactams do not dissolve in carbon tetrachloride.

Results

The infrared spectra of several amide compounds are shown in Figs. 1—5. The frequencies of the carbonyl absorption (amide I band) of these compounds are shown in Table I, in which values in parentheses mean the frequencies of shoulders in the amide I band. The absorptions of the chloroform solution of *N*-methyl lactams are shown in Fig. 6. *N*, *N*-Disubstituted chain amide shows a sharp absorption at 1626 cm^{-1} (Fig. 7), while the amide I band of *N*-methyl lactams splits into

Table I. The frequencies of the carbonyl absorption

Kind of amide	Frequency, cm^{-1}	State
N-Hexylacetamide	1653	Liquid
N, *N*-Dibutylacetamide	1650	〃
ε-Caprolactam	1645	KBr disk
N-Methyl-ε-caprolactam	(1739), 1634	Liquid
α-Piperidone	1664	〃
N-Methyl-α-piperidone	(1739), 1672, 1631	〃
α-Pyrrolidone	1680	〃
N-Methyl-α-pyrrolidone	1681, (1629)	〃

Table II. The molar extinction coefficient of *N*-methyl-ε-caprolactam in chloroform solution

Concn. mol./l.	1733 cm^{-1}			1634 cm^{-1}		
	20°C	40°C	60°C	20°C	40°C	60°C
0.02	26.8	26.8	28.8	554	506	483
0.05	24.4	25.9	27.4	484	406	379
0.1	—	29.7	—	545	552	484
0.2	—	31.2	29.2	467	520	456
0.3	—	21.6	27.5	—	—	—
0.5	—	21.0	26.3	—	—	—
1.0	—	26.0	24.4	—	—	—
Mean	25.6	26.0	27.3	512	496	451

* Presented at the 13th Annual Meeting of the Chemical Society of Japan, Tokyo, April, 1960.

1) M. Tsuboi, This Bulletin, **22**, 215 (1949).
2) S. Mizushima et al., *J. Am. Chem. Soc.*, **72**, 3490 (1950).
3) R. Huisgen and H. Walz, *Chem. Ber.*, **89**, 2616 (1956).
4) N. Ogata, *Makromol. Chem.*, **30**, 212 (1959).
5) J. Procházka, *Chem. Listy*, **37**, 158 (1943).
6) H. Yumoto, *J. Chem. Phys.*, **29**, 1234 (1958).
7) N. Ogata, This Bulletin, **32**, 813 (1959).

TABLE III. THE MOLAR EXTINCTION COEFFICIENT OF *N*-METHYL-α-PIPERIDONE IN CHLOROFORM SOLUTION

Concn. mol./l.	1736 cm^{-1}			1669 cm^{-1}			1631 cm^{-1}		
	20°C	40°C	60°C	20°C	40°C	60°C	20°C	40°C	60°C
0.02	22.8	—	—	167	—	150	83	87	118
0.05	25.5	30.2	—	182	145	150	93	100	142
0.1	23.3	27.9	18.5	182	139	113	88	130	163
0.2	24.9	28.6	19.5	176	186	—	103	119	—
0.3	—	—	19.2	166	174	112	99	114	150
0.5	—	—	18.7	167	164	—	99	101	—
1.0	—	—	18.0	168	149	—	109	88	—
Mean	24.1	28.9	18.8	173	159	131	96	106	143

TABLE IV. THE MOLAR EXTINCTION COEFFICIENT OF *N*-METHYL-α-PYRROLIDONE IN CHLOROFORM SOLUTION

Concn. mol./l.	1675 cm^{-1}			1630 cm^{-1}		
	20°C	40°C	60°C	20°C	40°C	60°C
0.01	—	—	538	—	—	—
0.02	583	562	538	—	—	—
0.05	464	438	—	42.1	37.0	35.8
0.1	634	636	473	45.5	41.3	36.4
0.2	512	644	425	46.2	40.6	36.0
0.3	—	582	441	—	—	—
0.5	—	497	426	—	—	—
1.0	—	—	—	—	—	—
Mean	548	560	474	44.6	39.6	36.1

TABLE V. THE MOLAR EXTINCTION COEFFICIENT OF CHAIN AMIDE IN CHLOROFORM SOLUTION

Concn. mol./l.	*N*-Hexylacetamide 1653 cm^{-1}		*N*,*N*-Dibutylacetamide 1626 cm^{-1}		
	20°C	40°C	20°C	40°C	60°C
0.1	478	462	568	642	557
0.2	442	433	528	582	—
0.3	443	397	512	563	—
0.5	350	—	453	—	—
1.0	—	—	413	—	—
Mean	428	431	515	596	557

TABLE VI. THE FREQUENCIES OF THE AMIDE I BAND OF *N*-METHYL LACTAM

Lactam	Ring member	I-a	I-b	I-c
N-Methyl-α-pyrrolidone	5	—	1675*	1630
N-Methyl-α-piperidone	6	1736	1669*	1631
N-Methyl-ε-caprolactam	7	1733	—	1634*

* Maximum absorption

two or three absorptions. The molar extinction coefficients at the absorption maximum of the amide I band for these *N*-methyl lactams are almost constant regardless of concentrations, but change with temperature, as shown in Tables II—V.

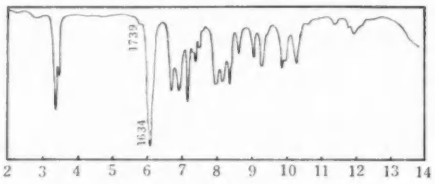

Fig. 1. The infrared spectrum of *N*-methyl-ε-caprolactam (Liquid).

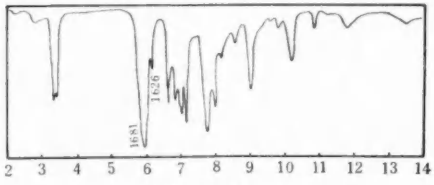

Fig. 2. The infrared spectrum of *N*-methyl-α-pyrrolidone (Liquid).

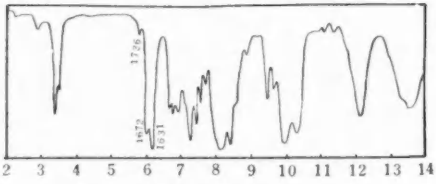

Fig. 3. The Infrared spectrum of *N*-methyl-α-piperidone (Liquid).

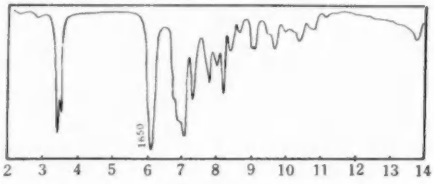

Fig. 4. The infrared spectrum of *N*, *N*-dibutyl-acetamide (Liquid).

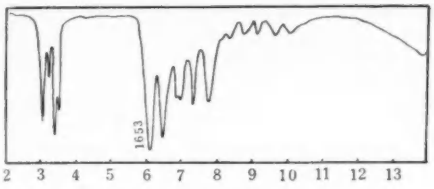

Fig. 5. The infrared spectrum of *N*-hexylacetamide[8](Liquid).

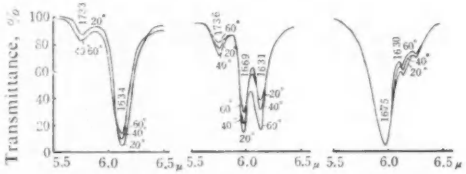

Fig. 6. The carbonyl absorption of *N*-methyl lactams in chloroform solution at the concentration of 0.1 mol./l.

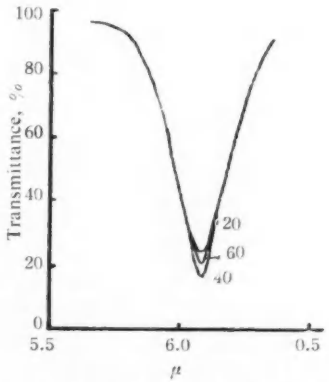

Fig. 7. The carbonyl absorption of *N*, *N*-dibutylacetamide in chloroform solution at the concentration of 0.1 mol./l.

TABLE VII. THE INTEGRATED ABSORPTION INTENSITY OF THE AMIDE I BAND (5.5~6.5 μ) OF *N*-METHYL LACTAM

Lactam	Temp. °C	Intensity, $mol^{-1}l.\,cm^{-2}$
N-Methyl-α-pyrrolidone	20	2.5×10^4
	40	2.5 〃
	60	2.0 〃
N-Methyl-α-piperidone	20	1.8×10^4
	40	1.7 〃
	60	1.8 〃
ε-Caprolactam	20	2.5×10^4
	40	2.5 〃
	60	2.4 〃

Discussion

N-Methyl-ε-caprolactam is too stable to polymerize at a temperature over 200°C and *N*-methyl-ε-aminocaproic acid transforms easily into *N*-methyl-ε-caprolactam by heating[8].

The rate of hydrolysis[7] of *N*-methyl-ε-caprolactam into *N*-methyl-ε-aminocaproic acid is much slower than that of ε-caprolactam. Since the cyclic structure of *N*-methyl-ε-caprolactam is the same as that of ε-caprolactam, it is supposed that this stability of *N*-methyl-ε-caprolactam is not due to the change in the ring strain, but to the increase of the resonance in the amide group as shown below by the −I effect of the methyl group:

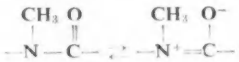

All *N*-monosubstituted acid amides show a strong absorption band usually near 1640 cm^{-1} in the solid state[8,9]. The lower frequencies of the carbonyl absorption of these amides are considered to be due to the resonance with the ionic form. The shifts of the carbonyl absorption towards lower frequencies by the *N*-alkyl substitution, therefore, seem to suggest the increase of the resonance in the amide group.

As stated before, the infrared spectra of *N*-methyl lactams with less than 7 membered rings exhibit a doublet or triplet in the region of the amide I band, and this is not caused by the interaction among molecules or by the solvent effect, since the molar extinction coefficients of these amide I bands in the chloroform solution are hardly influenced by the change of the amide compounds. The changes with temperature of the molar extinction coefficients of these absorption peaks are different from each other, as can be seen from Fig. 6. The elucidation of the cause of this interesting fact requires further investigation. The frequency of the maximum intensity among these doublets or triplets shifts towards lower frequencies with the enlargement of the ring. These bands are now named amide I-a, I-b and I-c in the order of the increasing frequency, respectively. These are shown in Table VI.

The integrated intensity of these split amide I bands was measured as follows: a point by point measurement of $\log(I_0/I)$ was made at intervals of 0.02 μ in the range of 5.5~6.5 μ and these data were plotted against the wavelength and the area under the curve was

8) H. Yumoto, K. Ida and N. Ogata, ibid., **31**, 249 (1958).
9) H. K. Hall, Jr. and R. Zbinden, *J. Am. Chem. Soc.*, **80**, 6428 (1958).

graphically determined. The true integrated absorption intensities were obtained by the method proposed by Ramsey[10]. The integrated absorption of the amide I band is almost unaltered with the ring size, as shown in Table VII. Therefore, these split absorptions are estimated to be due to the amide group.

Summary

The infrared spectra of several *N*-methyl lactams and acid amides have been measured in chloroform solution in order to investigate the correlation between the polymerizability of lactams and the frequencies of the carbonyl absorption of the amide group. The observed frequency lowering of the amide I band by *N*-methyl substitution can be related to the increasing contribution of the ionic structure to the resonance in the amide group, and to the low polymerizability. The infrared spectra of *N*-methyl lactams exhibit doublets or triplets in the carbonyl stretching region.

The author wishes to express his sincere gratitude to Dr. H. Kobayashi and Dr. H. Yumoto for their instruction in these studies and for their permission to publish the results. Thanks are also due to Mr. M. Nakata who collaborated with him in experiments.

Research Department
Toyo Rayon Co., Ltd.
Minato-ku, Nagoya

10) D. A. Ramsey, ibid., **74**, 72 (1952).

The Resonance Effect of Amide Group on the Polymerizability of Lactam Derivatives. II. The Basicity of Amide Group of Lactams***

By Naoya OGATA

(Received July 23, 1960)

Th polymerizability of lactams becomes very small by *N*-alkyl substitution[1,2]. *N*-Methyl-ε-caprolactam, for instance, is too stable to polymerize at a temperature above 200°C and *N*-methyl-ε-aminocaproic acid converts easily into *N*-methyl-ε-caprolactam by heating. The increase in the stability of the ring structure by the *N*-alkyl substitution of lactams is explained[3] from the increase of resonance in the amide group as shown below:

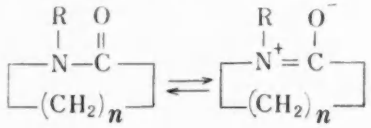

If the resonance effect of the amide group increases by *N*-alkyl substitution, it is expected that the basicity of the amide group will decrease. In this connection, an addition reaction of hydrogen chloride with several cyclic or chain amides has been investigated by the measurement of the infrared spectrum.

Experimental

Measurement ot the Infrared Spectrum of Addition Products of Hydrogen Chloride and Amide Compounds.—A chloroform solution of hydrogen chloride of 0.15 mol./l. was prepared by introducing dry hydrogen chloride gas into chloroform. This hydrogen chloride solution was diluted with chloroform to the concentrations of 0.08, 0.04, 0.02 and 0.01 mol./l. and 3.5 cc. of each of the solutions was mixed with 3.5 cc of a chloroform solution of several amide compounds of 0.04 mol./l.

The infrared spectra of the mixtures and the amide solutions were measured by a Hitachi model EPI-2 spectrophotometer with a rock salts prism, using hydrogen chloride-chloroform solution or pure chloroform as reference, respectively.

Determination of Equilibrium Constant of the Addition Reaction between the Amide Group and Hydrogen Chloride.—The equilibrium constants of the addition reaction between the amide group and hydrogen chloride were determined for several cyclic or chain amides by the intensity measurement of the carbonyl absorption in the infrared spectra.

The calibration curves for several amide compounds in chloroform were determined by measuring absorbances of the amide I band at 20°C which are shown in Figs. 1 and 2. The calibration curves at

* I, This Bulletin, **34**, 245 (1961).
** Presented at the 13th Annual Meeting of the Chemical Society of Japan, Tokyo, April, 1960.
1) J. Procházka, *Chem. Listy*, **37**, 202 (1943), *Chem. Abstr.*, **40**, 2113 (1946).
2) H. Yumoto, K. Ida and N. Ogata, This Bulletin, **31**, 249 (1948).
3) N. Ogata, ibid., **32**, 813 (1959).

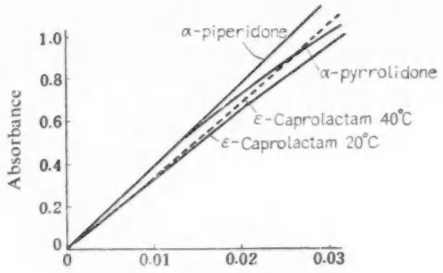

Fig. 1. The calibration curves for several lactams in chloroform solutions.

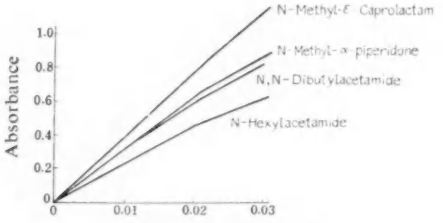

Fig. 2. The calibration curves for several amides in chloroform solutions.

40 and 55°C were almost the same as those at 20°C.

The concentrations of amide [-NHCO-] in chloroform solutions in the presence of hydrogen chloride were determined by these calibration curves. As hydrogen chloride has a tendency to be volatilized with rise of temperature, infrared spectra were measured for the narrow range of 1400～1800 cm^{-1} to avoid the change of concentration. The concentration of hydrogen chloride in chloroform was determined by titrating with N/100 sodium hydroxide.

The equilibrium constant K of the addition reaction between the amide group and hydrogen chloride can be calculated as follows:

$$[-NH_2{}^+CO-] = [-NHCO-]_0 - [-NHCO-]_{HCl}$$

$$[H^+] = [HCl] - [-N^+H_2CO-]$$

$[-NHCO-]_0$: Initial concentration of amide

$[-NHCO-]_{HCl}$: Concentration of amide in the presence of HCl

$$K = \frac{[-N^+H_2CO-]}{[-NHCO-][H^+]}$$

Results

Figs. 3—9 show the spectra, where a solid line represents the spectrum of the chloroform solution of the amide compound in the presence of hydrogen chloride and a dotted line the spectrum of the amide compound only.

In the presence of equal moles of hydrogen chloride and amide, the N—H absorption of cyclic or chain amides in the 3400～3500 cm^{-1} region is replaced by a broad absorption in the 2000～2400 cm^{-1} region and the intensity of the C=O absorption near 1650 cm^{-1} becomes weaker, accompanied by the appearance of a weak absorption in the 1750～1800 cm^{-1} region as shown in Table I.

The whole infrared spectrum of secondary or tertiary chain amide is not much altered in the presence of hydrogen chloride, while that of cyclic amide is altered considerably, accompanying a new absorption in the 1560～1640 cm^{-1} region.

The broad absorption in the 2000～2400 cm^{-1} region which appears in the chloroform solution of the amides in the presence of hydrogen chloride is supposed to be due to the $\rangle N^+H_2$ stretching motion.

The values of K at various concentrations of hydrogen chloride at 20, 40 and 55°C are shown in Table II. Table III shows the mean values of K for several amide compounds. The value of K decreases with the rise of temperature. K for chain amides is considerably smaller than that for cyclic amides. The values of K for cyclic amides increase with the enlargement of the lactam ring and those for tertiary amides are smaller than those for the corresponding secondary amides, especially for lactams.

From the slope of the linear relationship between the logarithm of K and reciprocals of absolute temperatures as shown in Fig. 10, heats of the addition reaction of the amide with hydrogen chloride are obtained. These are shown in Table IV. The heats of the addition reaction for cyclic amides become lower

Table I. The carbonyl absorption of several amides in the presence of HCl

Kind of lactam	Ring member	The C=O absorption band, cm^{-1}				
		Lactam alone	In the presence of HCl			
α-Pyrrolidone	5	1689	1800	1689*	1639	
α-Piperidone	6	1658	1800	1658*	1577	1565
ε-Caprolactam	7	1658	1800	1659*	1575	

* Maximum absorption

TABLE II. THE VALUES OF K

Sample	Temp. °C	Concn. of HCl mol./l.	Absorbance of C=O	Concn. of [-NHCO-] mol./l.	Concn. of [H^+] mol./l.	Concn. of [$-N^+H_2CO-$] mol./l.	K
α-Pyrrolidone	20	0.0030	0.654	0.0174	0.0009	0.0021	134
		0.0058	0.586	0.0157	0.0020	0.0038	121
		0.0112	0.456	0.0117	0.0034	0.0078	196
		0.0224	0.275	0.0069	0.0098	0.0126	186
	40	0.0030	0.552	0.0148	0.0018	0.0012	45
		0.0058	0.514	0.0135	0.0033	0.0025	56
		0.0114	0.421	0.0108	0.0062	0.0052	78
		0.0220	0.283	0.0072	0.0132	0.0088	93
α-Piperidone	20	0.0048	0.686	0.0175	0.0013	0.0035	154
		0.0094	0.564	0.0143	0.0027	0.0067	174
	40	0.0054	0.632	0.0161	0.0025	0.0029	72
		0.0084	0.548	0.0140	0.0041	0.0043	75
		0.0106	0.495	0.0125	0.0041	0.0065	51
		0.0168	0.376	0.0095	0.0080	0.0088	116
		0.0330	0.266	0.0068	0.0215	0.0115	79
ε-Caprolactam	20	0.0098	0.721	0.0218	0.0016	0.0082	235
		0.0132	0.697	0.0212	0.0035	0.0097	131
		0.0264	0.419	0.0118	0.0073	0.0191	222
		0.0375	0.353	0.0098	0.0173	0.0202	119
	40	0.0054	0.580	0.0173	0.0024	0.0030	72
		0.0104	0.485	0.0140	0.0041	0.0063	110
		0.0204	0.291	0.0080	0.0081	0.0123	190
	55	0.0040	0.586	0.0175	0.0017	0.0023	77
		0.0076	0.529	0.0155	0.0033	0.0043	84
		0.0280	0.269	0.0073	0.0155	0.0125	111
N-Methyl-α-piperidone	20	0.0022	0.737	0.0192	0.0014	0.0008	30
		0.0046	0.695	0.0182	0.0028	0.0018	35
		0.0092	0.604	0.0158	0.0050	0.0042	53
		0.0190	0.433	0.0112	0.0102	0.0088	77
	40	0.0036	0.609	0.0160	0.0023	0.0013	35
		0.0071	0.577	0.0150	0.0048	0.0023	32
		0.0144	0.479	0.0125	0.0096	0.0048	40
		0.0286	0.355	0.0092	0.0205	0.0081	43
N-Methyl-ε-caprolactam	20	0.0060	0.616	0.0195	0.0043	0.0017	20
		0.0124	0.530	0.0165	0.0077	0.0047	37
		0.0246	0.395	0.0122	0.0156	0.0090	47
	40	0.0037	0.593	0.0188	0.0030	0.0007	12
		0.0074	0.559	0.0175	0.0054	0.0020	21
		0.0146	0.486	0.0151	0.0102	0.0044	29
		0.0288	0.393	0.0141	0.0234	0.0054	16
	55	0.0060	0.569	0.0178	0.0050	0.0010	11
		0.0114	0.548	0.0172	0.0098	0.0016	10
		0.0200	0.492	0.0153	0.0165	0.0035	14
		0.0374	0.423	0.0131	0.0317	0.0057	14
N,*N*-Dibutyl-acetamide	20	0.0028	0.627	0.0213	0.0016	0.0012	35
		0.0054	0.602	0.0203	0.0032	0.0022	34
		0.0106	0.548	0.0182	0.0063	0.0043	38
		0.0222	0.467	0.0150	0.0147	0.0075	34
	40	0.0042	0.570	0.0190	0.0032	0.0010	17
		0.0076	0.539	0.0178	0.0054	0.0022	23
		0.0148	0.482	0.0155	0.0103	0.0045	28
		0.0288	0.420	0.0135	0.0223	0.0065	22
N-Hexyl-acetamide	20	0.0034	0.422	0.0183	0.0017	0.0017	55
		0.0067	0.382	0.0166	0.0033	0.0034	62
		0.0130	0.329	0.0142	0.0072	0.0058	57
	40	0.0044	0.413	0.0180	0.0024	0.0020	46
		0.0078	0.381	0.0165	0.0043	0.0035	49
		0.0154	0.329	0.0143	0.0097	0.0057	41

TABLE III. THE EQUILIBRIUM CONSTANT OF THE ADDITION REACTION OF SEVERAL AMIDES AND HCl

Sample	Configuration of amide	K		
		20°C	40°C	60°C
α-Pyrrolidone	5 membered cyclic cis amide	159	68	—
α-Piperidone	6 membered cyclic cis amide	164	79	—
ε-Caprolactam	7 membered cyclic cis amide	177	124	91
N-Methyl-α-piperidone	6 membered cyclic tertiary amide	49	38	—
N-Methyl-ε-caprolactam	7 membered cyclic tertiary amide	35	20	12
N,*N*-Dibutylacetamide	tertiary chain amide	35	22	—
N-Hexylacetamide	secondary trans amide	58	48	—

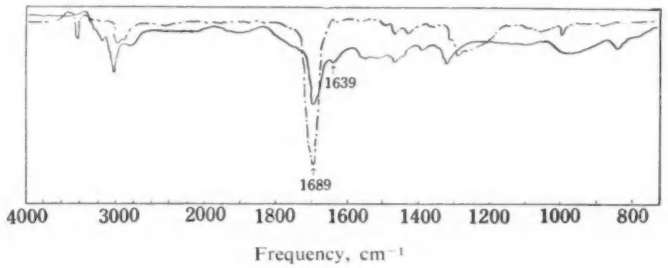

Fig. 3. The infrared spectrum of α-pyrrolidone in the presence of HCl (Chloroform solution).

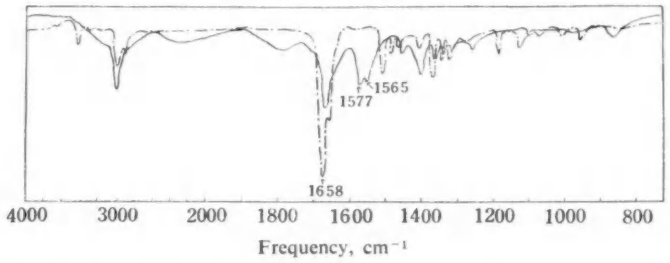

Fig. 4. The infrared spectrum of α-piperidone in the presence of HCl (Chloroform solution).

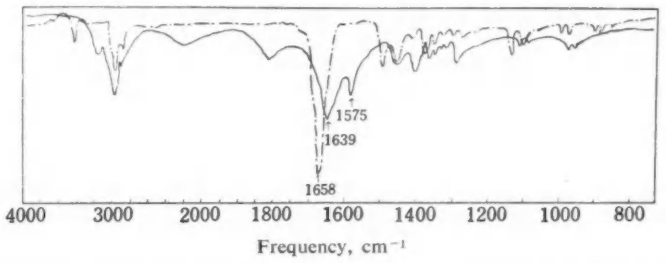

Fig. 5. The infrared spectrum of ε-caprolactam in the presence of HCl (Chloroform solution).

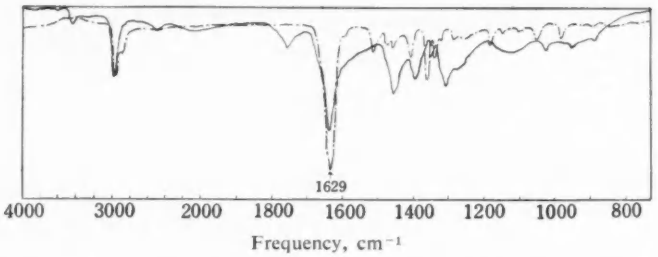

Fig. 6. The infrared spectrum of *N*-methyl-α-piperidone in the presence of HCl (Chloroform solution).

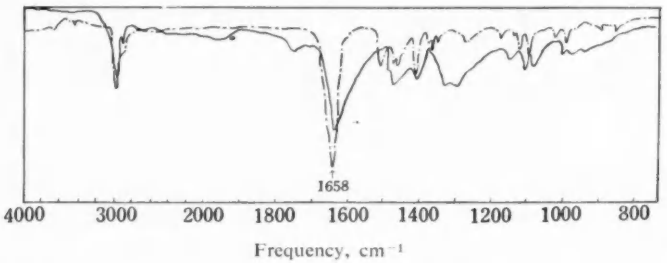

Fig. 7. The infrared spectrum of *N*-methyl-ε-caprolactam in the presence of HCl (Chloroform solution).

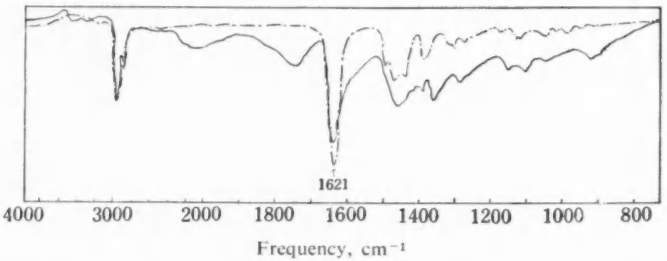

Fig. 8. The infrared spectrum of *N*, *N*-dibutylacetamide (Chloroform solution).

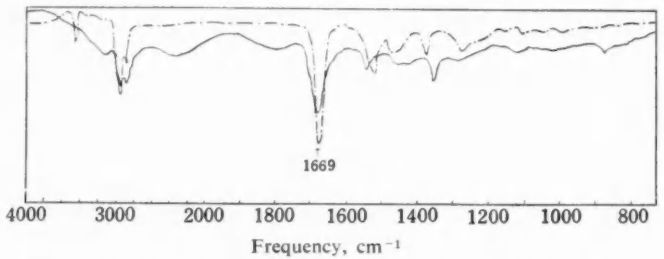

Fig. 9. The infrared spectrum of *N*-hexylacetamide in the presence of HCl (Chloroform solution).

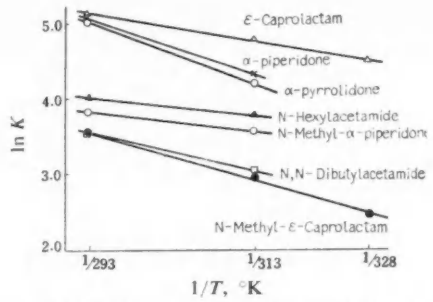

Fig. 10. The relationship between ln K and $1/T$.

TABLE IV. THE HEAT OF ADDITION REACTION OF SEVERAL AMIDES AND HCl

Sample	$-\Delta H$, kcal./mol.
α-Pyrrolidone	7.6
α-Piperidone	6.6
ε-Caprolactam	3.2
N-Methyl-α-piperidone	2.3
N-Methyl-ε-caprolactam	5.1
N,*N*-Dibutylacetamide	4.1
N-Hexylacetamide	2.2

with the enlargement of the ring and those for chain amides are generally lower than those for cyclic amides.

Discussion

The configuration of the amide group takes a planar structure owing to the resonance and two configurations of trans and cis forms are possible. It is known[4-7] that chain amides take the trans form, while cyclic amides of less than 9 membered rings take the cis form.

Although the basicity of the nitrogen atom of the amide becomes very weak by the +E effect of the carbonyl group, the amide group acts as a base, adding a proton[8]. It has been reported[9] that chain amide reacts with hydrogen chloride forming an addition product with 1/2 or 1 mol. of hydrogen chloride to 1 mol. of amide. The structure of the 1/2 mol. salt is proposed[9] as follows:

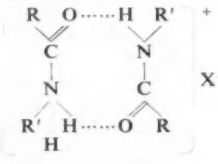

The intensity of the absorption which appears in lactams near 1800 cm^{-1} in the presence of hydrogen chloride becomes stronger with the enlargement of the lactam ring. This absorption shifts towards 1759 cm^{-1} in the case of *N*-methyl lactams or tertiary amide.

It has been presumed[10] that the higher frequencies of the carbonyl absorption of acid halide, which appears near 1800 cm^{-1}, is due to the strong +I effect of the halogen atom. Therefore, it is expected that the absorption near 1800 cm^{-1} in the amide-hydrogen chloride addition product may be the free carbonyl absorption which shifts towards higher frequencies by the increase in the electron affinity of the nitrogen atom of the amide.

It is supposed that a proton adds to the nitrogen atom of the amide group as shown in the following equation, since the N—H absorption disappears and new absorption due to the $>N^+H_2$ and the free C=O stretching motion (near 1800 cm^{-1}) appear in the infrared spectrum of the amide hydrogen chloride addition product.

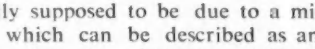

Primary and secondary amides show a strong absorption in the 1600~1500 cm^{-1} region, which is absent from those of cyclic lactams, and this band is refered to generally as the amide II band. The origin of the amid II band is generally supposed to be due to a mixed vibration which can be described as an out-of-phase combination of OCN and NH vibrations. The frequency of the amide II band of secondary amide shifts from 1530 cm^{-1} to 1550 cm^{-1} in the presence of hydrogen chloride, as shown in Fig. 9. This is explained from the increase in the ionic character of the N—H linkage by the addition of a proton.

The addition products of lactams and hydrogen chloride show a sharp absorption in the region of 1570~1640 cm^{-1}. This absorption does not appear in *N*-methyl lactams or tertiary chain amides in the presence of hydrogen chloride. It is supposed that this band may be assigned to the N—H deformation vibration. The assignment of this band to the C—N stretching motion is not accepted, since no absorption in the 1570~1640 cm^{-1} region appears in tertiary cyclic or chain amides in the presence of hydrogen chloride.

4) M. Tsuboi, ibid., **22**, 215 (1949).
5) R. Huisgen and H. Walz, *Chem. Ber.*, **89**, 2616 (1956).
6) H. K. Hall, Jr., *J. Am. Chem. Soc.*, **80**, 6404 (1958).
7) N. Ogata, *Makromol. Chem.*, **30**, 212 (1959).
8) M. J. S. Dewar, "The Electronic Theory of Organic Chemistry", Oxford University Press, London (1949), p. 96.
9) E. H. White, *J. Am. Chem. Soc.*, **77**, 6215 (1955).
10) L. J. Bellamy, "The Infrared Spectra of Complex Molecules", John Wiley & Sons, Inc., New York (1958), p. 125.

The equilibrium constants K of the addition reaction of hydrogen chloride and cyclic amide (cis form) are considerably greater than those of chain amide (trans amide). It is supposed that the basicity of the nitrogen atom of the cis amide may increase owing to the decrease of resonance in the amide group. The addition of hydrogen chloride to cyclic amide becomes easier with the enlargement of the ring, as shown by the greater value of K and the lower heat of addition reaction.

The values of K for N-methyl lactams are considerably smaller than those for the corresponding lactams and they are almost the same as those for tertiary chain amide. The heat of the addition reaction of hydrogen chloride with amide becomes higher with the N-methyl substitution of an amide hydrogen in lactams. This is expected to be due to the fact that the amide group is stabilized by hyperconjugation of methyl group as well as the increase in resonance by the $-I$ effect of methyl group. It is presumed that the small polymerizability of N-methyl-substituted lactams is due to the increase of resonance in the amide group.

Summary

The addition reaction of hydrogen chloride with several cyclic or chain amides has been investigated by the infrared absorption measurement in order to study the correlation between the polymerizability of lactams and the resonance in the amide group. The equilibrium constant K for the addition reaction with cyclic amide (cis form) is 150~180 and it becomes greater with enlargement of the ring size, while K for N-methyl lactams is about 30~40. The K value for secondary chain amide (trans form) is 60. The heat of the addition reaction of hydrogen chloride with lactams becomes lower with the enlargement of the lactam ring and also with the N-methyl substitution of the amide hydrogen.

The stronger basicity of the cis amide compared with the trans amide may be due to the decrease of resonance in the amide group, and the stabilization of the lactam ring by the N-methyl substituion may be ascribed to the increase in resonance by hyperconjugation of the methyl group.

The author wishes to express his sincere gratitude to Dr. H. Kobayashi and Dr. H. Yumoto who instructed him through these studies and permitted him to publish the results. Thanks are also due to Mr. M. Nakata for his collaboration in experiments.

Research Department
Toyo Rayon Co. Ltd.
Minato-ku, Nagoya

Studies on the Thiocarbamoylthiocarbonates. I. Synthesis of Aryl Thiocarbamoyldithiocarbonates

By Aritsune KAJI

(Received July 26, 1960)

O-Alkyl S-(N, N-disubstituted-thiocarbamoyl)-thiocarbonates were studied by Cambron[1] and Lo[2]. Lo reported that these alkyl esters, except isopropyl ester, were unstable and decomposed even at room temperature. No report on the aryl esters of this thiocarbonic acid has been given. The present author succeeded in the synthesis of these aryl esters.

Results and Discussion

Aryl chloroformates reacted with sodium dimethyldithiocarbamate in acetone, giving O-aryl S-(N, N-dimethylthiocarbamoyl)thiocarbonates as shown in Table I.

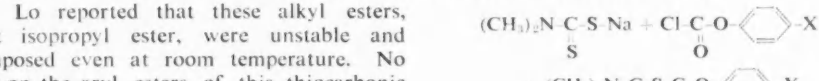

(X: -H, $-CH_3$, -Cl) (1)

But these esters were unstable and decomposed even at room temperature within a few weeks.

Aryl chlorothionoformates reacted with sodium or ammonium dialkyldithiocarbamates, giving various O-aryl S-(N, N-dialkylthiocarbamoyl)dithiocarbonates in good yields as

1) A. Cambron, *Can. J. Res.*, **2**, 341 (1930).
2) C. Lo and W. E. Craig, Japanese Pat. 253207 (1958).

TABLE I. *O*-ARYL *S*-(*N*,*N*-DIMETHYLTHIOCARBAMOYL) THIOCARBONATES

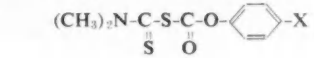

X	M. p., °C	Yield, %	Formula	Anal. C% Found (Calcd.)	Anal. H% Found (Calcd.)
-H	97.5~ 98.5	51.5	$C_{10}H_{11}NO_2S_2$	49.79 (50.43)	4.56 (4.32)
4-CH_3	105.5~106.5	50.5	$C_{11}H_{13}NO_2S_2$	51.76 (51.65)	5.10 (4.99)
3-Cl	122 ~123	24	$C_{10}H_{10}ClNO_2S_2$	43.56 (44.09)	3.29 (3.80)

TABLE II. *O*-ARYL *S*-(*N*,*N*-DIMETHYLTHIOCARBAMOYL) DITHIOCARBONATES

R	Appearance	M. p., °C	Yield, %	Formula	Anal. C % Found (Calcd.)	Anal. H % Found (Calcd.)
Phenyl	Yellow pillars	68 ~ 69	86	$C_{10}H_{11}NOS_3$	46.30 (46.69)	3.95 (4.28)
2-Tolyl	Yellow prisms	74 ~ 75	90	$C_{11}H_{13}NOS_3$	48.20 (48.70)	5.13 (4.80)
4-Tolyl	Yellow needles	88 ~ 89	78	$C_{11}H_{13}NOS_3$	48.97 (48.70)	4.71 (4.80)
4-Methoxyphenyl	Yellow needles	87.5~ 88.5	80	$C_{11}H_{13}NO_2S_3$	46.03 (45.99)	4.42 (4.53)
4-Chlorophenyl	Yellow prisms	104 ~105	80	$C_{10}H_{10}ClNOS_3$	41.40 (41.17)	3.56 (3.43)
2,4-Dichlorophenyl	Yellow needles	138 ~139	78	$C_{10}H_9Cl_2NOS_3$	36.95 (36.80)	2.54 (2.76)
2,4,5-Trichlorophenyl	Yellow prisms	113.5~114.5	75	$C_{10}H_8Cl_3NOS_3$	33.34 (33.29)	1.84 (2.22)
4-Bromophenyl	Yellow needles	110 ~111	74	$C_{10}H_{10}BrNOS_3$	35.95 (35.71)	2.60 (2.98)
2,4,6-Tribromophenyl	Yellow needles	118 (decomp.)	69	$C_{10}H_8Br_3NOS_3$	24.50 (24.30)	1.49 (1.69)
4-Chloro-2-tolyl	Yellow prisms	113 ~113.5	56	$C_{11}H_{12}ClNOS_3$	43.22 (43.20)	3.73 (3.93)
2-Chloro-4-tolyl	Yellow prisms	131.5~132.5	52	$C_{11}H_{12}ClNOS_3$	43.50 (43.20)	3.63 (3.93)
2,6-Dichloro-4-tolyl	Yellow prisms	133 ~134	60	$C_{11}H_{11}Cl_2NOS_3$	39.05 (38.82)	3.47 (3.24)
4,6-Dichloro-2-tolyl	Yellow needles	115 ~116.5	56	$C_{11}H_{11}Cl_2NOS_3$	39.30 (38.82)	3.41 (3.24)
3,5-Dimethyl-4-chlorophenyl	Yellow prisms	113 ~114.5	85	$C_{12}H_{14}ClNOS_3$	44.74 (45.07)	4.25 (4.38)
2-Phenyl-4-chlorophenyl	Yellow prisms	107 ~108	61	$C_{16}H_{14}ClNOS_3$	52.55 (52.24)	3.68 (3.81)
2-Biphenylyl	Yellow needles	135 ~136	84	$C_{16}H_{15}NOS_3$	57.83 (57.66)	4.62 (4.50)
4-Acetylphenyl	Yellow needles	117.5~118	78	$C_{12}H_{13}NO_2S_3$	48.50 (48.16)	4.10 (4.35)
2-Methoxycarbonyl-phenyl	Yellow prisms	102.5~103.5	60	$C_{12}H_{13}NO_3S_3$	45.80 (45.71)	4.10 (4.13)
4-Nitrophenyl	Yellow prisms	114 ~115	90	$C_{10}H_{10}N_2O_3S_3$	40.05 (39.75)	3.52 (3.31)
1-Chloro-2-naphthyl	Yellow prisms	126.5~127	91	$C_{14}H_{12}ClNOS_3$	49.20 (49.20)	3.60 (3.51)
1-Bromo-2-naphthyl	Yellow prisms	141 ~142	76	$C_{14}H_{12}BrNOS_3$	43.55 (43.52)	2.92 (3.11)

TABLE III. *O*-ARYL *S*-(*N*,*N*-DIETHYLTHIOCARBAMOYL)DITHIOCARBONATES

$(C_2H_5)_2N\text{-}\overset{\overset{S}{\|}}{C}\text{-}S\text{-}\overset{\overset{S}{\|}}{C}\text{-}O\text{-}R$

R	Appearance	M. p., °C	Yield, %	Formula	Anal. C % Found (Calcd.)	Anal. H % Found (Calcd.)
2-Biphenylyl	Yellow plates	76 ~ 77	72	$C_{18}H_{19}NOS_3$	60.30 (59.83)	5.34 (5.26)
2-Chloro-4-tolyl	Yellow needles	93 ~ 94	81	$C_{13}H_{16}ClNOS_3$	47.15 (46.78)	5.15 (4.80)
2,6-Dichloro-4-tolyl	Yellow needles	91.5~ 93	70	$C_{13}H_{15}Cl_2NOS_3$	42.85 (42.39)	3.92 (4.08)
3,5-Dimethyl-4-chlorophenyl	Yellow needles	92 ~ 93	69	$C_{14}H_{18}ClNOS_3$	48.45 (48.35)	4.57 (5.18)
2,4,6-Tribromophenyl	Yellow needles	114 (decomp.)	69	$C_{12}H_{12}Br_3NOS_3$	27.40 (27.59)	2.82 (2.30)
2-Nitro-4-tolyl	Yellow scales	104.5~105.5	84	$C_{13}H_{16}N_2O_3S_3$	46.17 (45.35)	4.75 (4.65)
2-Naphthyl	Yellow prisms	62 ~ 63	64.5	$C_{16}H_{17}NOS_3$	57.08 (57.31)	5.25 (5.07)
1-Chloro-2-naphthyl	Yellow prisms	143 ~144	60	$C_{16}H_{16}ClNOS_3$	52.50 (51.96)	4.40 (4.33)
3-Chloro-2-naphthyl	Yellow needles	107.5~108.5	72	$C_{16}H_{16}ClNOS_3$	51.80 (51.96)	4.57 (4.33)
1-Bromo-2-naphthyl	Yellow prisms	142 ~144	73	$C_{16}H_{16}BrNOS_3$	46.10 (46.38)	3.67 (3.86)

TABLE IV. *O*-ARYL *S*-(PIPERIDINOTHIOCARBONYL)DITHIOCARBONATES

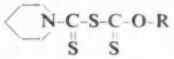

R	Appearance	M. p., °C	Yield, %	Formula	Anal. C % Fonnd (Calcd.)	Anal. H % Found (Calcd.)
Phenyl	Yellow needles	95~ 96	61	$C_{13}H_{15}NOS_3$	52.70 (52.53)	4.84 (5.05)
4-Tolyl	Yellow needles	102~103	74	$C_{14}H_{17}NOS_3$	53.90 (54.02)	5.15 (5.47)
2-Naphthyl	Yellow needles	127~128	71	$C_{17}H_{17}NOS_3$	59.10 (58.79)	4.85 (4.90)
1-Chloro-2-naphthyl	Yellow needles	131~132	76	$C_{17}H_{16}ClNOS_3$	53.42 (53.47)	4.25 (4.19)

TABLE V. *O*-ARYL *S*-(MORPHOLINOTHIOCARBONYL)DITHIOCARBONATES

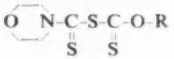

R	Appearance	M. p., °C	Yield, %	Formula	Anal. C % Found (Calcd.)	Anal. H % Found (Calcd.)
4-Tolyl	Yellow needles	136 ~137	51.5	$C_{13}H_{15}NO_2S_3$	50.20 (49.84)	4.75 (4.79)
4-Chlorophenyl	Yellow needles	134 ~135	53.5	$C_{12}H_{12}ClNO_2S_3$	43.55 (43.18)	3.69 (3.60)
2-Biphenylyl	Yellow needles	130.5~131	53	$C_{18}H_{17}NO_2S_3$	57.35 (57.60)	4.15 (4.53)
2-Methoxycarbonyl-phenyl	Yellow prisms	115 ~116	72	$C_{14}H_{15}NO_4S_3$	47.73 (47.06)	3.75 (4.20)
1-Chloro-2-naphthyl	Yellow needles	149 ~150	73	$C_{16}H_{14}ClNO_2S_3$	50.31 (50.07)	3.78 (3.65)

TABLE VI. *O*-ARYL *S*-(ARYLTHIOCARBAMOYL)DITHIOCARBONATES

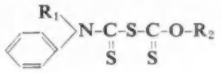

R_1	R_2	Appearance	M. p., °C	Yield, %	Formula	Anal. C % Found (Calcd.)	Anal. H % Found (Calcd.)
Methyl	4-Toyl	Yellow prisms	98～99	72	$C_{16}H_{15}NOS_3$	57.95 (57.66)	4.11 (4.50)
Methyl	4-Chloro-phenyl	Yellow prisms	133～134	85	$C_{15}H_{12}ClNOS_3$	51.20 (50.92)	3.72 (3.39)
Phenyl	4-Tolyl	Orange needles	110～111	73	$C_{21}H_{17}NOS_3$	63.90 (63.80)	4.51 (4.30)
Phenyl	4-Chloro-phenyl	Orange prisms	118～119	60	$C_{20}H_{14}NOS_3$	58.00 (57.76)	3.36 (3.37)

TABLE VII. *O*-ARYL *N*,*N*-DISUBSTITUTED-THIONOCARBAMATES

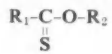

R_1	R_2	Appearance	M. p., °C	Yield, %	Formula	Anal. C, % Found (Calcd.)	Anal. H, % Found (Calcd.)
Dimethyl-amino	4-Tolyl	Colorless pillar	95 ～ 96	62	$C_{10}H_{13}NOS$	61.80 (61.53)	6.59 (6.67)
Dimethyl-amino	4-Chlorophenyl	Colorless needles	58 ～ 59	64	$C_9H_{10}ClNOS$	50.45 (50.12)	4.31 (4.64)
Dimethyl-amino	2,4,5-Trichloro-phenyl	Colorless prisms	136 ～137	72.5	$C_9H_5Cl_3NOS$	38.38 (37.96)	2.37 (2.81)
Dimethyl-amino	4-Acetylphenyl	Slight amber needles	102.5～103.5	61.5	$C_{11}H_{13}NO_2S$	59.26 (59.19)	5.83 (5.83)
Morpholino	1-Chloro-2-naphthyl	Colorless plates	138 ～139	81	$C_{15}H_{14}ClNO_2S$	58.80 (58.54)	4.23 (4.55)
N-Methyl-anilino	4-Chloro-phenyl	Colorless needles	104 ～105.5	78	$C_{14}H_{12}ClNOS$	60.05 (60.54)	4.19 (4.32)

shown in Tables II—V. *O*-Aryl *S*-(*N*-alkyl-*N*-arylthiocarbamoyl)dithiocarbonates and *O*-aryl *S*-(*N*,*N*-diarylthiocarbamoyl)dithiocarbonates were also given by the similar reaction and listed in Table VI. In these reactions, water, methanol, ethanol, acetone and benzene can be used as the reaction medium. These aryl esters of *S*-(*N*,*N*-disubstituted-thiocarbamoyl)-dithiocarbonic acid, isolated as yellow or orange crystals when recrystallized from acetone-ethanol, were stable at room temperature.

O-Aryl *S*-(*N*-monosubstituted-thiocarbamoyl)-dithiocarbonates could not be isolated by the reaction between aryl chlorothionoformates and sodium *N*-monoalkyl- or *N*-monoaryl-dithiocarbamates, because of their decomposition during the reaction period.

It was concluded that both of the two hydrogen atoms connected with the nitrogen atom of the thiocarbamoyl group must be substituted to stabilize these dithiocarbonates.

The substituents of the aryl group, as shown in Tables II—VI, did not have such strong effects on the stability of the esters which were kept at a lower temperature than their respective melting points.

Aryl esters of *S*-(*N*,*N*-disubstituted-thiocarbamoyl)dithiocarbonic acid decomposed when heated at the melting points for a long period, giving carbon disulfide and *O*-aryl *N*,*N*-disubstituted thionocarbamate as shown in Table VII.

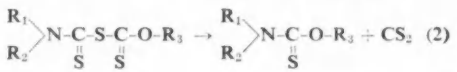

(2)

These thionocarbamates showed no depression of the melting point on the admixture with *O*-aryl *N*,*N*-disubstituted-thionocarbamates prepared from *N*,*N*-disubstituted-amines and aryl chlorothionoformates.

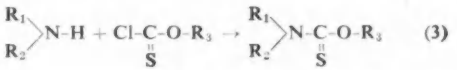

(3)

Experimental

Starting Materials.—Sodium or ammonium salts of *N*,*N*-disubstituted-dithiocarbamic acid were synthesized by the known methods[3]. Aryl esters of chlorothionoformic acid were prepared as follows: To a solution of 1 mol. of thiophosgen and 1 mol. of phenol in chloroform was added gradually 1 mol. of sodium hydroxide (5% aqueous solution) under vigorous agitation. The temperature was kept at 5~10°C during the reaction period of 30 min. The chloroform layer was washed with water and dried over calcium chloride. The removal of chloroform gave esters which could be used in the following reaction without further purification.

***O*-(3,5-Dimethyl-4-chlorophenyl) *S*-(*N*,*N*-dimethylthiocarbamoyl)dithiocarbonate.**—To a solution of 14.3 g. (0.1 mol.) of sodium dimethyldithiocarbamate in 100 cc. of water was added gradually 23.5 g. (0.1 mol.) of 3,5-dimethyl-4-chlorophenyl chlorothionoformate keeping the temperature at 10~15°C during the reaction period of 2 hr. By the filtration of the reaction mixture, 27.2 g. (yield, 85%) of yellow crystals with m. p. 112~114°C were obtained. Recrystallization from acetone-ethanol gave yellow prisms with m. p. 113~114.5°C.

***O*-(4-Chlorophenyl) *S*-(*N*-methyl-*N*-phenylthiocarbamoyl)dithiocarbonate.**—To a solution of 20 g. (0.1 mol.) of ammonium *N*-methyl-*N*-phenyldithiocarbamate in 200 cc. of acetone was added gradually 21 g. (0.1 mol.) of 4-chlorophenyl chlorothionoformate keeping the temperature at 5~10°C during the reaction period of 1 hr. The reaction mixture, poured into 500 cc. of cold water, gave 31 g. (yield, 85%) of yellow precipitates with m. p. 132~134°C. Recrystallization of the preceipitates from acetone-ethanol gave yellow prisms with m. p. 133~134°C.

The other esters shown in Tables II—VI were synthesized in the similar way.

4-Tolyl *N*,*N*-dimethylthionocarbamate.—In an oil bath, 0.45 g. of *O*-(4-tolyl) *S*-(*N*,*N*-dimethylthiocarbamoyl)dithiocarbonate was kept at 160°C for 1 hr. After the subsidence of evolution of carbon disulfide, the reaction mixture was cooled to room temperature. Twice repeated recrystallization of the reaction mixture from 0.5 cc. of ethanol, gave 0.2 g. (yield, 62%) of 4-tolyl *N*,*N*-dimethylthionocarbamate with m. p. 95~96°C.

The author wishes to express his sincere thanks to Professor Dr. Ryozo Goto, Kyoto University, for his guidance and encouragement throughout this work.

Takaoka Factory, Nippon Soda Co., Ltd.
Mukaino-honmachi, Takaoka, Toyama-ken

3) Houben-Weyl, "Methoden der organischen Chemie", 9, Georg Thieme Verlag, Stuttgart (1955), p. 826.

Spectrophotometric Determination of Submicrogram Quantities of Orthophosphate in Natural Waters

By Ken SUGAWARA and Satoru KANAMORI

(Received August 13, 1960)

In advanced researches of natural waters, need is felt for a method of determining phosphate more sensitive than the current Dénigè's colorimetric method[1] especially when the quantity of the sample is limited. Such a need is partly filled with the radioactivation method[2,3]. However, a nuclear reactor is not easily accessible. Furthermore, irradiation and cooling are time-consuming. This situation initiated the present work.

It is true that there have been made various trials to increase the sensitivity of the determination of phosphate by the use of solvent extraction of phosphomolybdate[4-7] where the yellow complex is extracted with an organic solvent to be directly or after reduction to molybdenum blue subjected to spectrophotometry. These methods, however, are not sufficiently sensitive to determine submicrogram quantities of the compound. The authors' idea was to step up this increased sensitivity. Thus the phosphomolybdate which was once extracted in an *n*-butanol-chloroform mixture is decomposed into the components. Then, the

1) G. Dénigè, *Compt. rend.*, **171**, 802 (1920).
2) L. M. Foster and D. C. Gaitanis, *Anal. Chem.*, **27**, 1342 (1955).
3) J. A. James and D. H. Richards, *Nature*, **176**, 1062 (1955); **177**, 1230 (1956).
4) T. Kiba and M. Ura, *J. Chem. Soc. Japan, Pure Chem. Sec.* (*Nippon Kagaku Zasshi*), **76**, 520 (1955).
5) Coe Wadeline with M. G. Mellon, *Anal. Chem.*, **25**, 1668 (1953).
6) C. M. Proctor and D. W. Hood, *J. Marine Res.*, **13**, 122 (1954).
7) C. H. Lueck and D. F. Boltz, *Anal. Chem.*, **28**, 1168 (1956).

liberated molybdenum is separated to be spectrophotometrically determined as thiocyanate complex whereby 0.02～1.00 μg. of phosphorus as phosphate in a water sample less than 250 ml. can be determined with an accuracy of an error less than 5%.

Experimental

Apparatus.—Absorbance was measured with a Beckman spectrophotometer model DU by using 10 mm. cells of Pyrex glass.

Reagents.—Hydrochloric acid, concentrated.

n-Butanol and chloroform, distilled.

n-Butanol-chloroform mixture: *n*-Butanol and chloroform are mixed in the proportion of 3 : 7 by volume.

Ammonium molybdate solution, 10%.

Washing solution. Thirty mlliliter of *n*-butanol is dissolved in 500 ml. of 0.5 N nitric acid.

Sodium hydroxide solution, 1N.

Ferrous ammonium sulfate solution: In 100 ml. of 0.2 N sulfuric acid 1 g. of the hexahydrate is dissolved.

Potassium thiocyanate solution, 10%.

Stannous chloride solution: In 100 ml. of 1 N hydrochloric acid 10 g. of the dihydrate is dissolved.

Phosphate standard solution: The stock solution which contains 1 mg. of phosphorus as phosphate per ml. is prepared by dissolving 0.439 g. of dihydrogen potassium phosphate in distilled water and making it up to 100 ml. The addition of a few drops of chloroform keeps the solution from mold growth. The working standard solutions are prepared by properly diluting the stock solution.

Procedure.—A sample is properly diluted or evaporated so that 250 ml. contains 0.02～1.0 μg. of phosphorus. After having been filtered, if necessary, this 250 ml. is placed in a 500 ml. separatory funnel. Then, 10 ml. of hydrochloric acid, 15 ml. of *n*-butanol and 10 ml. of the *n*-butanol-chloroform mixture are added. The funnel is shaken for 1 min. to saturate the aqueous phase with the mixed solvent. When two layers clearly separate, the organic layer is drawn out to be replaced by a new addition of 5 ml. of the ammonium molybdate solution and 5 ml. of the mixed solvent. Two minutes shaking follows whereby the phosphomolybdate is formed and extracted into the solvent. The extract is transferred into a 100 ml. funnel. The extraction is repeated by using another 5 ml. of the mixed solvent. The two extracts are combined and shaken for 1 min. with 50 ml. of the washing solution, whereby the uncombined molybdate is completely washed out. The remaining organic layer which contains exclusively phosphomolybdate is transferred into a 50 ml. separatory funnel. After the addition of 10 ml. of 1 N sodium hydroxide solution and 5 ml. of distilled water, the funnel is shaken for 1 min. to strip the phosphomolybdate completely from the oily phase by the aqueous alkali solution. After 15 min. standstill during which the decomposition of the phosphomolybdate into molybdate and phosphate is complete, the organic layer is drawn off. With swirling, 3 ml. of concentrated hydrochloric acid, 1 ml. of ferrous ammonium sulfate solution, 3 ml. of thiocyanate solution and 3 ml. of stannous chloride solution are added successively. An amber color develops immediately. This is extracted with two small portions of the mixed solvent and made up to 5 ml. To the joint extract a few small crystals of stannous chloride are recommended to be added to protect the ferrous iron from oxidation. Otherwise ferric thiocyanate is formed to cause a high blank value because of its red coloration. The quantity of phosphate is determined from the absorbance reading at 475 mμ in reference to the standard curve. The curve has previously been constructed by following the same procedure with the standard solutions at different dilutions.

Discussion

Extraction of Phosphomolybdate.—The extraction must proceed on a condition where following two requirements are satisfied: 1) The extraction must be complete. 2) The possible contaminations of arseno-, germano- and silicomolybdate must be avoided. To this

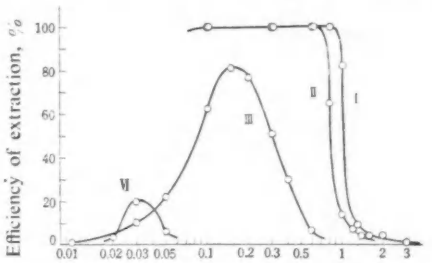

Fig. 1. Effect of the acidity on the extraction of heteromolybdates with *n*-butanol.
I Phosphomolybdate
II Arsenomolybdate
III Germanomolybdate
IV Silicomolybdate

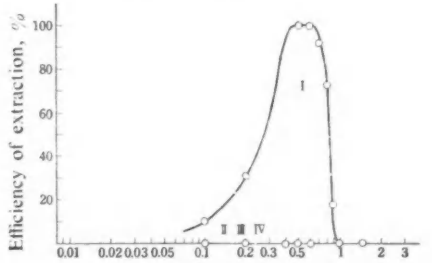

Fig. 2. Effect of the acidity on the extraction of heteromolybdates with the *n*-butanol-chloroform mixture.
I Phosphomolybdate
II Arsenomolybdate
III Germanomolybdate
IV Silicomolybdate

aim an appropriate solvent and the range of acidity where the solvent is most efficiently active were sought. Two sets of 50 ml. of arsenate, germanate and silicate solutions, each containing 10 μg. of one of the three elements, As, Ge and Si, were prepared and adjusted to various acidities with hydrochloric acid. Then, after the addition of 1 ml. of 10% ammonium molybdate solution, one of the sets was extracted with *n*-butanol, while another set with the *n*-butanol-chloroform mixture. The extracts were processed with 1.0% stannous chloride solution (1 N in hydrochloric acid) to reduce and strip the extracted heteropolyacids which were subjected to spectrophotometry to determine the efficiency of these extractions. As is seen from Figs. 1 and 2, the results point to the fact that the extraction is practically complete in a wider range of acidity from 0.1 to 0.8 N with *n*-butanol as compared with the range from 0.5 to 0.6 N with the mixed solvent. However, in these ranges, separation of phosphate from arsenate, germanate and silicate is not complete with *n*-butanol, while it is nearly complete with the mixed solvent. Thus the *n*-butanol-chloroform mixture is only acceptable as a solvent.

Standard Curve*.—Standard curves for three different methods are compared in Fig. 3, where the high sensitivity of the authors' method is quite evident.

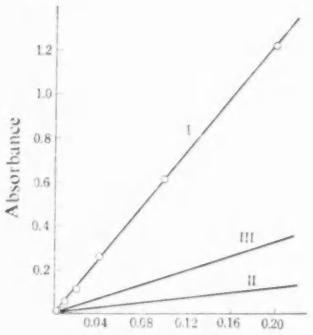

Fig. 3. Standard curves.

I The present method
II Molybdenum blue method (940 mμ)
III Simple phosphomolybdate extraction method (245 mμ)

Washing of the Extract.—This treatment is indispensable for removing the contamination of unbound moybdate which otherwise gives a higher apparent value at the final spectrophotometry. To check this point, samples containing 0.50 μg. of phosphorus and samples with

TABLE I. EFFECT OF THE WASHING ON THE BLANK VALUE AND RECOVERY OF PHOSPHORUS

Times of washing	Blank value absorbance	Recovery of 0.50 μg. of phosphorus μg.
1	0.005	0.49
1	0.001	0.51
2	0.000	0.50
2	0.001	0.50
3	0.000	0.50

TABLE II. THE INTERFERENCE OF VARIOUES IONS

Ion	Added as	Quantity mg.-element	PO_4^{3-} added μg.-P	PO_4^{3-} recovered μg.-P
AsO_4^{3-}	As_2O_5 in NaOH	0.1	0.50	0.52
GeO_3^{2-}	GeO_2 in NaOH	0.1	0.50	0.49
SiO_3^{2-}	SiO_2 in Na_2CO_3	5	0.50	0.50
Na^+	NaCl	800	0.50	0.52
K^+	KCl	500	0.50	0.50
Mg^{2+}	$MgSO_4$	400	0.50	0.50
Ca^{2+}	$Ca(NO_3)_2$	150	0.50	0.52
Fe^{3+}	$FeCl_3$	50	0.50	0.52
Al^{3+}	$Al_2(SO_4)_3$	25	0.50	0.51
Mn^{2+}	$MnSO_4$	10	0.50	0.50
Cl^-	NaCl	1200	0.50	0.52
SO_4^{2-}	$MgSO_4$	500	0.50	0.50
NO_3^-	$Ca(NO_3)_2$	100	0.50	0.52
Cu^{2+}	$CuSO_4$	1	0.50	0.49
Ag^{+}*	$AgNO_3$	1	0.50	0.48
Ba^{2+}	$BaCl_2$	1	0.50	0.50
Zn^{2+}	$ZnCl_2$	1	0.50	0.50
Cd^{2+}	$CdSO_4$	1	0.50	0.52
Hg^{2+}	$HgCl_2$	1	0.50	0.51
TiO^{2+}	TiO_2 in H_2SO_4	1	0.50	0.24
		0.1	0.50	0.47
		0.01	0.50	0.50
ZrO^{2+}	$ZrO(NO_3)_2$	1	0.50	0.52
Th^{4+}	$Th(NO_3)_4$	1	0.50	0.49
Pb^{2+}	$Pb(NO_3)_2$	1	0.50	0.50
VO_2^+	NH_4VO_3	1	0.50	0.20
		0.1	0.50	0.49
SbO^+	$K(SbO)C_4H_4O_6$	1	0.50	0.49
BiO^+	Nitrate	1	0.50	0.49
CrO_4^{2-}	K_2CrO_4	1	0.50	0.50
WO_4^{2-}	Na_2WO_4	1	0.50	0.37
		0.1	0.50	0.50
UO_2^{2+}	$UO_2(CH_3CO_2)_2$	1	0.50	0.50
SeO_3^{2-}	Na_2SeO_3	1	0.50	0.52
Co^{2+}	$CoSO_4$	1	0.50	0.50
Ni^{2+}	$NiSO_4$	1	0.50	0.51

* Sulfuric acid was used in place of hydrochloric acid for the extraction of phosphomolybdate.

* The molar extinction coefficient of molybdenum thiocyanate under the present experimental condition was determined as 1.55×10^4 l. per mol. cm. and the corresponding value of phosphate 1.85×10^5 l. per mol. cm. Thus, the atom ratio of phosphorus to molybdenum is calculated to be 1/12 within an experimental error.

no phosphorus were processed according to the procedure in which they were subjected to one to three washings. The results listed in Table I show that the blank value is already nearly zero after one washing. This points to the fact that one washing is sufficient to completely remove free molybdate from the extract. On the other hand, the phosphate value remains constant even after three washings. This shows that there is no risk for the extracted phosphomolybdate to escape through the washing.

Interference. — The interference of various ions with the present determination of phosphate was examined with the results listed in Table II.

A) An error of 5% is found only with a concentration of 100 γg. As/50 ml. for arsenate, with 100 γg. Ge/50 ml. for germanate, and with 5 mg. Si/50 ml. for silicate. B) Na^+, K^+, Mg^{2+}, Ca^{2+}, Cl^-, SO_4^{2-} and NO_3^- cause no interference up to a considerable concentration. C) Tungstate and vanadate may be partly extracted in the mixed solvent to cause a considerable interference. However, the concentration of these elements in usual natural waters is too small to consider their interference. The same thing can be said in the case of titanium. In conclusion, the present method of phosphate determination can be safely applied to usual waters with no special consideration of the interference which might be caused by co-existing elements. Examples of the application of the method to several natural waters are listed in Table III.

TABLE III. APPLICATION OF THE METHOD TO NATURAL WATERS

Description	Sample taken ml.	*P* added γg.	*P* recovered γg.
Ground water from a well on the campus of Nagoya University	5.0		0.28
	5.0	0.10	0.39
Rain (March 20, 1956; Nagoya)	200		0.77
	200	0.05	0.83
Snow (Feb. 3, 1956; Nagoya)	100		0.48
	100	0.10	0.58

Chemical Institute, Faculty of Science
Nagoya University, Chikusa-ku
Nagoya

Reduction of Organic Compounds with Urushibara Catalysts under High Pressure. VII[1]*. Feature of Various Urushibara Catalysts as Revealed in the Reduction of Benzophenone*

By Shinichi TAIRA

(Received August 22, 1960)

In the previous paper[2] of this series, catalytic reductions of ketones under high pressure with Urushibara nickel B were reported. In the present paper, reduction of benzophenone with various Urushibara catalysts under various conditions was investigated.

The preparation of the Urushibara nickel catalyst has been successively modified, and some varieties of this catalyst were reported. Each of these Urushibara nickel catalysts is prepared by digesting precipitated nickel with alkali or acid. In the original preparation[3], nickel was precipitated from nickel chloride solution with zinc dust, and digested with caustic alkali to obtain U-Ni-B. The alternative catalyst U-Ni-A[4] was prepared by digesting the precipitated nickel with acetic acid or propionic acid instead of caustic alkali. The third catalyst U-Ni-BA[1,5] was developed by modifying the preparation of U-Ni-B, using aluminum grains instead of zinc dust for precipitating nickel metal from nickel chloride solution. Each of these Urushibara nickels has been found to have a comparable activity with the Raney nickel for the hydrogenation of various organic compounds.

Now it is expected that metallic cobalt and metallic copper prepared by the same procedure as to obtain the Urushibara nickel may have

1) Part VI. I. Motoyama, This Bulletin, 33, 232 (1960).
2) K. Hata, S. Taira and T. Higase, *J. Chem. Soc. Japan, Pure Chem. Sec.* (*Nippon Kagaku Zasshi*), **78**, 186 (1957).
3) Y. Urushibara and S. Nishimura, This Bulletin, 27, 460 (1954).
4) Y. Urushibara, S. Nishimura and H. Uehara, ibid., 28, 446 (1955).
5) K. Hata, S. Taira and I. Motoyama, ibid., 31, 776 (1958).

catalytic activities for hydrogenation. Actually it was already reported[6] that Urushibara cobalt B had a property similar to Raney cobalt and was recognized to be useful for the hydrogenation of nitriles. A similar copper catalyst was also reported[7] to be prepared from copper sulfate solution and zinc dust.

In case of catalytic reduction under high pressure, the reaction velocity may be influenced by various factors, namely, the nature of the groups to be reduced, the purity of substance, the activity and quantity of catalyst, the kind of solvent, the concentration and pH value of solution, the pressure of hydrogen, the temperature of reduction, the efficiency of agitation, etc. The temperature at which the absorption of hydrogen gas begins, or the time or the quantity of catalyst required for the completion of reduction, may be regarded as a measure to determine the activity of the catalyst.

In the present experiments, reduction of benzophenone is selected as an example for determining the activities of Urushibara catalysts prepared by various methods. The time required for reducing the ketone to benzhydrol was compared with each other under a similar condition.

Experimental

Apparatus. — Reductions were carried out in a Sakashita SE-20, electro-magnetically stirring type autoclave having a capacity of 200 ml.

Materials. — Benzophenone was prepared from benzoyl chloride and benzene by the Friedel-Crafts reaction[8]. The raw product was submitted to vacuum distillation and then recrystallized twice from ethanol, b. p. 140~141°C/5 mmHg, m. p. 48°C.

General Procedure for Reduction.—The catalyst containing 1 g. of nickel, cobalt, or copper was carefully transferred with ethanol into the autoclave. Then air in the autoclave was replaced by hydrogen gas. Most operations were carried out under the following conditions: (1) benzophenone; 12.74 g. (0.07 mol.) (2) ethanol (99%); 110 ml. (3) pH; 9~11 (When Urushibara catalysts A and CA were used, 0.5 ml. of 10% sodium hydroxide solution was added.) (4) agitation; 40~50 strokes per minute (5) temperature; Since a remarkable reduction of carbonyl compounds was found to begin at about 60°C as was reported in the previous paper[2], agitation was started when the temperature in the autoclave was reached at 60°C, and it was kept between 58° and 70°C. (6) Pressures were observed at intervals of five minutes.

After the reduction was finished and the autoclave got cold, hydrogen gas was discharged and the contents were taken out with ethanol. The catalyst was filtered off and washed with ethanol. The major part of the combined solvent was distilled off and the hot residue was poured into 300 ml. of hot water with stirring. The crude benzhydrol was filtered off and dried. It was recrystallized from ligroin into colorless silky needles, m. p. 68~69°C. Yield, 90~95% of the theoretical. It did not depress the m. p. with an authentic sample.

Preparation of Catalysts.—The Urushibara nickel B[3], the Urushibara nickel A[4] and the Urushibara nickel BA[1,5] were prepared by the methods described in the references cited. Some new types of Urushibara catalysts were prepared as follows. The procedures described below are the methods for the preparation of the catalysts, each containing 1 g. of catalyst metal.

(a) Urushibara Nickel B (U-Ni-B) Prepared from Nickel Acetate.—On a boiling water bath 4.24 g. of nickel acetate ($Ni(CH_3CO_2)_2 \cdot 4H_2O$) is dissolved in 20 ml. of water. This hot solution is added at once with stirring by hand onto a hot mixture of zinc dust (10 g.) and water (10 ml.) placed in a 500 ml. beaker warmed on a boiling water bath. As a vigorous reaction takes place and the reaction mixture swells up, good agitation is required to prevent the contents running over. When the reaction subsides, 200 g. of 10% sodium hydroxide solution is cautiously added with stirring onto the reaction product (precipitated nickel). The temperature of the mixture is kept at about 50~55°C for fifteen minutes with occasional stirring. When solid matter settles down, the upper liquor is decanted. The solid is washed with two 100 ml. portions of hot water, and then with two 50 ml. portions of ethanol. In this way 8.5~10.5 g. of bulky catalyst, containing nickel (about 1 g.), zinc, zinc oxide and a very small amount of alkali, is obtained.

(b) Urushibara Cobalt B (U-Co-B). — To a hot mixture (90~100°C) of zinc dust (10 g.) and water (4 ml.) placed in a 100 ml. flask is added at once 10 ml. of hot aqueous solution (90~100°C) containing 4.04 g. of cobalt chloride ($CoCl_2 \cdot 6H_2O$) with vigorous stirring on a boiling water bath. The reaction product (precipitated cobalt) is transferred into a 300 ml. beaker and washed with 200 ml. of hot water. After 160 g. of 10% sodium hydroxide solution is added, the mixture is warmed at about 50~55°C on a water bath for fifteen minutes with occasional stirring. Then the upper liquor is decanted, and the residual solid is washed with two 100 ml. portions of hot water and then with two 50 ml. portions of ethanol. About 6.5~7 g. of catalyst, containing cobalt (about 1 g.), zinc, zinc oxide and a trace of alkali, is obtained.

(c) Urushibara Nickel CB (U-Ni-CB).—Ten milliliter of aqueous solution containing 4.04 g. of nickel chloride ($NiCl_2 \cdot 6H_2O$) is added to a mixture of zinc dust (10 g.) and water (4 ml.) placed in a 100 ml. flask. This mixture is stirred at room temperature or under cooling with water or ice until the green color of nickel ion disappears. This process requires about three to four hours. As the major part of the ion exchange reaction proceeds during the initial period, the reaction mixture may be left standing until the green color has disappeared

6) S. Saito, *J. Pharm. Soc. Japan* (*Yakugaku Zasshi*), **76**, 351 (1956).
7) Y. Urushibara, Japanese Pat., 203309.
8) Gattermann-Wieland, "Die Praxis des organischen Chemikers", Walter de Gruyter & Co., Berlin (1940), p. 340.

after stirring for an hour. When the preparation of a large quantity of precipitated nickel is required, the reaction mixture must be cooled with ice to remove the generated heat of the reaction. The slushy precipitated nickel is transferred into a 300 ml. beaker and washed with 200 ml. of cold water. After 160 g. of cold 10% sodium hydroxide solution is added, the mixture is stirred for an hour under cooling with water or ice if necessary. When the major part of solid settles down, the upper liquor is cautiously decanted, and the solid is washed with two 100 ml. portions of cold water and then with two 50 ml. portions of ethanol. About 8~11 g. of bulky catalyst, containing nickel (about 1 g.), zinc, zinc oxide and a very small quantity of alkali, is obtained.

(d) Urushibara Cobalt CB (U-Co-CB). — This catalyst is prepared from cobalt chloride by the same procedure as is described above.

(e) Urushibara Nickel A (U-Ni-A) Prepared from Nickel Acetate.—Precipitated nickel was prepared by the same procedure as is described in (a). Instead of caustic alkali, 160 ml. of 13% acetic acid is added with stirring onto the precipitated nickel. The mixture is stirred occasionally until the generation of hydrogen gas ceases and a solid comes up to the surface of the solution which is of green color. The solid is collected on a glass filter and washed with 200 ml. of hot water and then with 100 ml. of ethanol. About 0.7 g. of catalyst, containing nickel, small quantities of zinc and zinc oxide, is obtained.

(f) Urushibara Cobalt A (U-Co-A). — The precipitated cobalt prepared by the same way as is described in (b) is treated with 160 ml. of 13% acetic acid. The mixture is stirred for about five minutes until the generation of hydrogen gas ceases and a solid comes up to the surface of the solution which is rose-colored. This coloration is necessary to obtain an active catalyst. The solid is collected on a glass filter and washed with 200 ml. of hot water and then with 100 ml. of ethanol. About 1~1.2 g. of catalyst, containing cobalt (about 0.8 g.), small quantities of zinc and zinc oxide, is obtained.

(g) Urushibara Copper (U-Cu).—To a hot mixture (90~100°C) of zinc dust (10 g.) and water (5 ml.) placed in a 200 ml. flask is added at once 10 ml. of hot aqueous solution (90~100°C) containing 2.69 g. of cupric chloride ($CuCl_2 \cdot 2H_2O$) with vigorous stirring. The reaction ends at once. The upper liquor is decanted and the solid (precipitated copper) is transferred into a 300 ml. beaker and washed with 200 ml. of hot water. After the precipitated copper is treated with 160 ml. of 13% acetic acid at 70~75°C on a water bath for about thirty minutes, the upper liquor is decanted. The solid is washed with two 100 ml. portions of hot water and then with two 50 ml. portions of ethanol. About 2~2.5 g. of black catalyst, containing copper (about 1 g.) and zinc, is obtained.

(h) Urushibara Nickel CA (U-Ni-CA).—The precipitated nickel prepared by the same way as is described in (c) is transferred into a 500 ml. beaker and is carefully treated with 200 ml. of 10% acetic acid under cooling with water. After about five minutes the generation of hydrogen gas subsides and a solid comes up to the surface of the solution, which carries more deep green color than in case of Urushibara nickel A. The solid is collected on a glass filter and washed with 200 ml. of cold water and then with 100 ml. of ethanol. About 0.6~0.8 g. of fine catalyst, containing nickel (0.4~0.5 g.), small quantities of zinc and zinc oxide, is obtained.

(i) Urushibara Cobalt CA (U-Co-CA).—This catalyst is prepared from cobalt chloride by the same way as is described above, the volume of 10% acetic acid being modified to 150 ml. for the treatment of the precipitated cobalt.

(j) Urushibara Copper C (U-Cu-C).—During ten minutes 30 ml. of cold aqueous solution containing 2.69 g. of cupric chloride is added dropwise to a vigorously stirred mixture of zinc dust (10 g.) and water (10 ml.) placed in a 100 ml. flask under cooling with ice. The precipitated copper is transferred into a 300 ml. beaker and washed with 200 ml. of cold water. After the precipitated copper is treated with 160 ml. of 13% acetic acid for two hours at room temperature, the upper liquor is decanted and the residual solid is washed with two 100 ml. portions of cold water and then with two 50 ml. portions of ethanol. About 3~4 g. of black catalyst, containing copper (about 1 g.) and zinc, is obtained. Urushibara copper catalyst carries a black color before use, and it is changed in red-brown after use for reduction.

In cases of the preparations of the Urushibara catalysts B, the Urushibara copper and the Urushibara copper C, every washing is removed by decantation. In all procedures, distilled water is used for washing, and the solid must be protected from the contact with air as far as possible after the treatment of the precipitated metals with acid or alkali.

Results and Discussion

The results obtained from the reduction of benzophenone which was purified by a single vacuum distillation are summarized in Tables I and II. A series of experiments shown in Table I were carried out to examine the effect of initial pressure, and to find the difference due to the kind of nickel salt or amount of zinc dust used for preparing the catalyst. The activities of U-Ni-B and U-Co-B were also compared. As seen from Table I, the velocity of reduction was affected only slightly, if any, by the initial pressure within 30~134 kg./cm^2. Therefore the effect of the initial pressure was ignored in the following operations. The use of potassium hydroxide solution for digesting the precipitated nickel in place of sodium hydroxide solution gave the similar result (Exp. No. 14). The U-Ni-B contains a large quantities of zinc and zinc oxide aside from nickel metal. To diminish these ingredients the precipitated nickel was prepared with less amount of zinc dust and was treated with much quantities of alkaline solution (Exp. No. 15). As the catalyst thus obtained was less active and the velocity of reduction was depressed in the course of the

TABLE I. REDUCTION OF BENZOPHENONE* WITH U-Ni-B OR U-Co-B

Exp. No.	Catalyst[a]	pH	Total weight of catalyst g.[b]	Initial press. kg./cm²	Initial temp., °C	React. temp. °C	Time min.
11	U-Ni-B	10.2		40	20	58~65	95
12	U-Ni-B	11.1		134	22	58~67	95
13	U-Ni-B	8.9	6.7	30	29	58~67	95
14	U-Ni-B[c]	8.3		50	26	58~64	100
15	U-Ni-B[d]	11		50	17	59~76	165
16	U-Ni-B[e]	10.8	9.5	45.5	20	58~66	55
17	U-Ni-B[e]	11.3		35	23	58~64	55
18	U-Ni-B[e,f]	10.6	9	65	25	58~66	65
19	U-Co-B	10.1		55	26	58~68	95

* Benzophenone, purified by a single vacuum distillation, was used.
a) Each catalyst was prepared so as to contain 1 g. of nickel or cobalt.
b) The figures were obtained by weighing the dried catalysts after use for reduction.
c) The precipitated nickel was treated with 200 g. of 14% potassium hydroxide solution.
d) The precipitated nickel, obtained from nickel chloride solution with 5 g. of zinc dust, was treated with two 150 g. portions of 10% sodium hydroxide solution.
e) The precipitated nickel was prepared from nickel acetate. The other was prepared from nickel chloride.
f) The precipitated nickel was treated with 150 g. of 20% sodium hydroxide solution.

reaction, higher temperature was required to complete the reaction. This may be partly due to the big size of the particles of nickel metal and partly to the contact with an alkali for a long time. Moreover, it must be considered that the zinc and zinc oxide contaminated in the U-Ni-B may act as carrier[9]. For the reduction of benzophenone, purified by a single vacuum distillation, the U-Ni-B prepared from nickel acetate was more effective than the catalyst obtained from nickel chloride (Exp. Nos. 16, 17, 18), but this was not always true, when more carefully purified benzophenone was used. The U-Ni-B prepared from nickel acetate weighs in dry state about 8.5~10.5 g. (for 1 g. of nickel), and is about three times as bulky as the catalyst obtained from nickel chloride. Therefore, it must contain more zinc oxide (cf. micro-photograph, Fig. 1 (d)), which may act as a sort of an effective carrier in the reduction of a less purified substance.

It was already reported[10], that the catalytic reduction of a carbonyl group with Raney nickel was accelerated by a trace of alkali. For the Urushibara nickel catalyst, the effect of an alkali was quantitatively investigated in the reduction of cyclohexanone under ordinary pressure[11]. The results of the reduction of benzophenone in neutral solution with the Urushibara catalyst A and the well washed Urushibara catalyst B are shown in Table II. From these results, it is obvious that the catalytic reduction of a carbonyl group with these catalyst is desirable to operate above pH 8 (S. Nishimura reported that the excess of alkali retarded the reaction[11]).

The results tabulated in Tables III, IV, V and VI were obtained by the use of more carefully purified benzophenone, which was recrystallized twice from ethanol after vacuum distillation. The effect of purification was remarkable when the U-Ni-B was used. The U-Ni-BA was reported to be specially useful in the hydrogenation of aromatic nucleus[1,3], but it was found to be not so particularly effective for the reduction of a carbonyl group (Table III, Exp. Nos. 37, 38). It was revealed by micro-photographs that the size of the particles of the U-Ni-BA catalyst is greater than that of the other Urushibara catalysts* as shown in Fig. 1. Also the X-ray diffraction of the U-Ni-BA gives a different pattern from that of the U-Ni-A. The U-Co-BA was proved to be less active for the reduction of benzophenone, and it required higher temperature and longer time to finish the reduction than the other Urushibara catalysts (Exp. No. 39). As was already described, the U-Ni-A in neutral solution was not suitable for the reduction of a carbonyl group. But an addition of a small amount of alkali promoted remarkably the reduction and such a nickel catalyst gave better results than those obtained with the U-Ni-B (Exp. Nos. 310—313). The reason may be partly supposed to be due to the dispersability of the catalyst.

9) Y. Urushibara, S. Yamaguchi and M. Kobayashi, This Bulletin, **29**, 816 (1956).
10) M. Delépine and A. Horeau, *Bull. soc. chim. France*, [5] **4**, 31 (1937).
11) S. Nishimura, *J. Chem. Soc. Japan, Pure Chem. Sec.* (*Nippon Kagaku Zasshi*), **79**, 56 (1958).
* The size of the particles of Urushibara copper catalyst is as large as that of the U-Ni-BA.

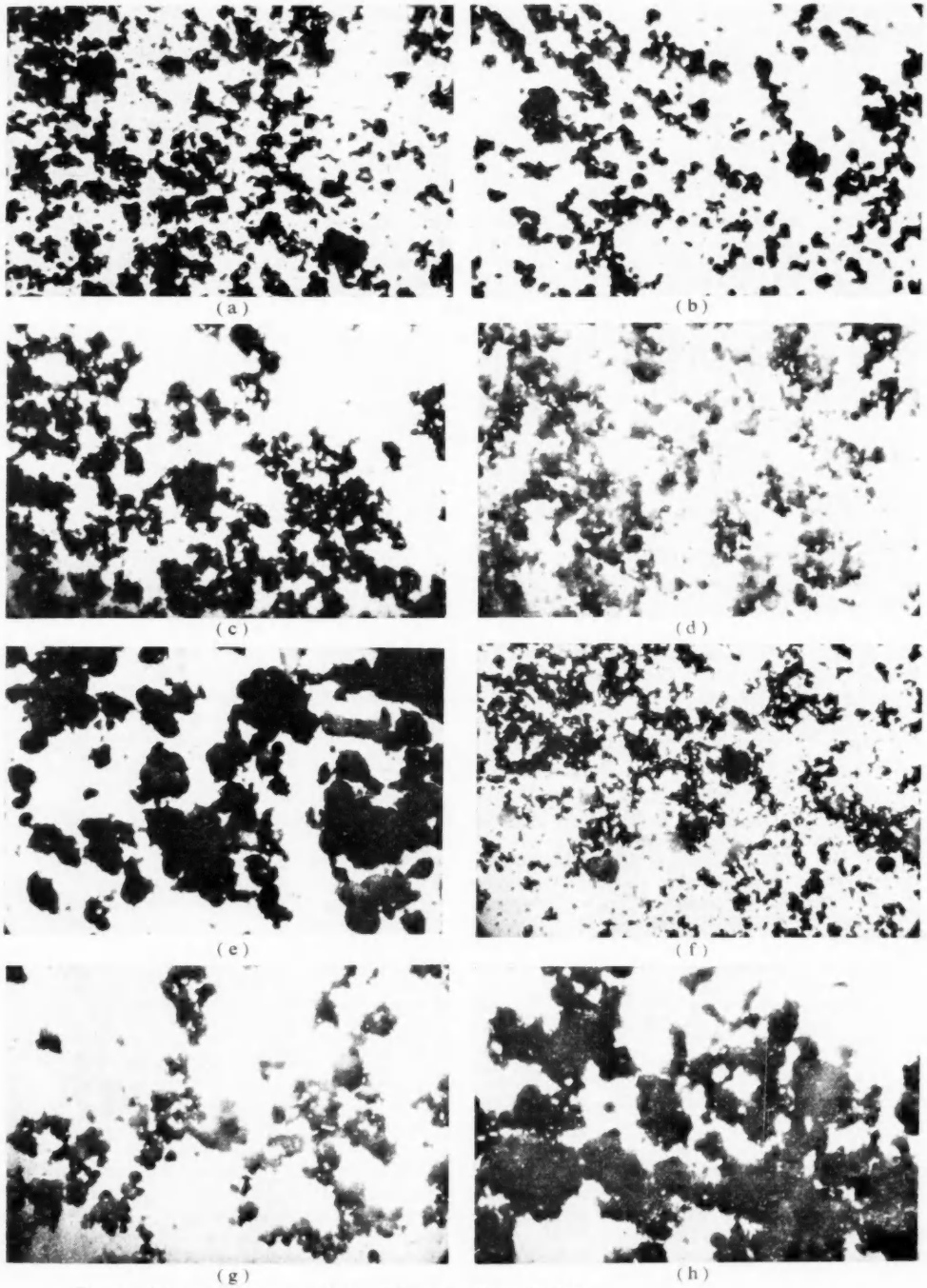

Fig. 1. Micro-photographs of Urushibara catalysts (×150).
(a) U-Ni-A (b) U-Ni-B (c) U-Ni-A (The precipitated nickel was prepared from nickel acetate.) (d) U-Ni-B (The precipitated nickel was prepared from nickel acetate.) (e) U-Ni-BA (f) U-Co-A (g) U-Co-B (h) U-Cu.

TABLE II. REDUCTION IN NEUTRAL SOLUTION

Exp. No.	Catalyst[a)]	pH	Total weight of catalyst g.[b)]	Initial press. kg./cm²	Initial temp., °C	React. temp. °C	Time min.
21	U-Ni-B[c,d)]	7.5		45	20	58～ 66	250
22	U-Co-B[d)]	7.7	6.6	55	22	58～ 66	165
23	U-Ni-A	7		55	22	58～ 64	155
24	U-Ni-A[c)]	6.8	0.7	45	18	62～102	205
25	U-Co-A	6.7		50	20	62～ 76	180

Benzophenone, purified by a single vacuum distillation, was used.

a) Each catalyst was prepared so as to contain 1 g. of nickel or cobalt.
b) The figures were obtained by weighing the dried catalysts after use for reduction.
c) The precipitated nickel was prepared from nickel acetate instead of nickel chloride.
d) The catalysts were thoroughly washed with water to remove a trace of alkali.

TABLE III. REDUCTION OF CAREFULLY PURIFIED BENZOPHENONE*

Exp. No.	Catalyst[a)]	pH	Total weight of catalyst g.[b)]	Initial press. kg./cm²	Initial temp., °C	React. temp. °C	Time min.
31	U-Ni-B	9.7	6.5	30	24	58～68	75
32	U-Ni-B	9.3	6.8	49.5	22	63～67	25
33	U-Ni-B	9.4	6.6	52.5	28	61～66	35
34	U-Ni-B[e)]	11.1	11.2	50	16	63～66	30
35	U-Co-B	10.4	7	50	15	60～69	70
36	U-Co-B	9	6.2	56	24	61～65	65
37	U-Ni-BA	10.5	1.4	50	15	60～64	45
38	U-Ni-BA	10.6	1.8	45	14	62～66	35
39	U-Co-BA	10.2	0.8	45	16	72～84	115
310	U-Ni A	10.5[d)]	1.1[e)]	52	25	60～63	10
311	U-Ni-A	10.3[d)]	1.4[e)]	46	26	59～62	8
312	U-Ni-A	10.1[d)]	1.4[e)]	48.5	20	59～63	6
313	U-Ni-A	10[d)]	1.3[e)]	46	29	60～62	12
314	U-Ni-A[e)]	10.4[d)]	0.7	45	24	59～66	60
315	U-Co-A	10.1[d)]	1[e)]	45	22	61～66	45
316	U-Co-A	10.4[d)]	1.2[e)]	49.5	25	59～65	50

* Benzophenone, purified by a single vacuum distillation and then recrystallized twice from ethanol, was used.

a) Each catalyst was prepared so as to contain 1 g. of nickel or cobalt.
b) The figures were obtained by weighing the dried catalysts after use for reduction.
c) The precipitated nickel was prepared from nickel acetate. The other was prepared from nickel chloride.
d) 0.5 ml. of 10% sodium hydroxide solution was added.
e) The quantities of nickel or cobalt were about 0.75～0.85 g.

TABLE IV. REDUCTION WITH THE U-Ni-A OF LOW ACTIVITY

Exp. No.	Weight of cat., g.[a)]	pH[b)]	Weight of sample, g.	Volume of ethanol ml.	Initial press. kg./cm²	Initial temp. °C	React. temp. °C	Time min.
41	1	10.7	12.74	110	45	16	60～ 66	30
42	2	10	12.74	110	40	22	62～ 66	10
43	1	10.1	12.74	55	32	20	60～ 68	10
44	1	10.2	25.48	110	60	14	61～ 66	20
45	1	10.2	12.74	110	50	20	97～100[c)]	7
46	1	10.5	12.74	55	45	18	98～108[c)]	4

Benzophenone, purified by a single vacuum distillation and then recrystallized twice from ethanol, was used.

a) The figures are weight of nickel metal to be included in catalysts.
b) 0.5 ml. of 10% sodium hydroxide solution was added.
c) The time for heating the autoclave before starting agitation was equal to those of the other experiments.

Table V. Reduction with Urushibara catalysts C

Exp. No.	Catalyst[a]	pH	Total weight of catalyst g.[b]	Initial press. kg./cm²	Initial temp., °C	React. temp. °C	Time min.
51	U-Ni-CB[c]		5.7	34.5	16	62~65	35
52	U-Ni-CB[c]	10.2	11.5	56	22	60~62	20
53	U-Ni-CB[d]	10.7	8.8	60	25	60~66	15
54	U-Ni-CB[d]	10	9.6	50	22	68~70	10
55	U-Ni-CA[e]	10.1[e]	0.55	40	14	66~70	15
56	U-Ni-CA[e]	10.5[e]	0.55	42	13	62~66	10
57	U-Ni-CA[e]	10.3[e]	0.7	50	17	63~65	20
58	U-Ni-CA[e]	10[e]	0.7	50	20	60~63	15
59	U-Ni-CA[e]	10[e]		60	26	61~65	10
510	U-Ni-CA[d]	10.2[e]	0.6	52.5	20	62~64	10
511	U-Ni-CA[d]	9.8[e]	0.5	42.5	24	58~60	30
512	U-Ni-CA[d]	10[e]		55	24	62~66	15
513	U-Co-CB[e]	10.5	8.5	60	20	60~62	35
514	U-Co-CB[e]	10.5	7.8	40	23	59~60	35
515	U-Co-CB[d]	10.6	3.4[f]	60	20	62~66	35
516	U-Co-CB[d]	10.2	3.2[f]	52	28	60~66	35
517	U-Co-CA[e]	10.7[e]	1.1	55	22	60~64	30
518	U-Co-CA[d]	10.6[e]	1.4	55.5	23	60~62	60[g]
519	U-Co-CA[e]	10.4[e]	1.4	37	22	59~62	80[g]

Benzophenone, purified by a single vacuum distillation and then recrystallized twice from ethanol, was used.

a) Each catalyst was prepared so as to contain 1 g. of nickel or cobalt.
b) The figures were obtained by weighing the dried catalysts after use for reduction.
c) The precipitated metal was prepared at room temperature.
d) The precipitated metal was prepared under cooling with ice.
e) 0.5 ml. of 10% sodium hydroxide solution was added.
f) The precipitated cobalt was digested for 1.5 hr. under cooling with ice.
g) The major part of the catalyst proved to be deposited on the flange of copper packing after the reduction was finished. The reason was not clear, but the magnetic nature of this catalyst might be different from the other catalysts.

Table VI. Reduction with Urushibara copper catalyst

Exp. No.	Catalyst[a]	pH[b]	Total weight of catalyst g.[c]	Initial press. kg./cm²	Initial temp., °C	React. temp. °C	Time min.
61	U-Cu	10	2.2	40	16	100~118	40
62	U-Cu	9.5	2.4	53	24	110~120	65
63	U-Cu-C	10.3	4.2	50	28	110	10
64	U-Cu-C		2.8	52.5	22	120~121	15

Benzophenone, purified by a single vacuum distillation and then recrystallized twice from ethanol, was used.

As a solvent 55 ml. of ethanol was used.

a) Each catalyst was prepared so as to contain 1 g. of copper.
b) 0.5 ml. of 10% sodium hydroxide solution was added.
c) The figures were obtained by weighing the dried catalyst after use for reduction.

As the apparent bulk of the U-Ni-A is much smaller than that of the U-Ni-B, the fine particles of the former may be easily dispersed into a solution by the up and down agitation employed in these experiments. However, the U-Ni-A prepared from nickel acetate was less active than the U-Ni-B prepared from the same salt (Exp. No. 314), and the reason is obscure. In alkaline solution the U-Co-A also gave better results than those obtained with the U-Co-B (Exp. Nos. 315, 316).

Reaction temperature, concentration of solution and quantity of catalyst are naturally expected to exert some influences on the rate of reduction. As a catalyst with high activity is not suitable for the purpose of this series of experiments, the U-Ni-A, which was specially prepared to have a lower activity, was used.

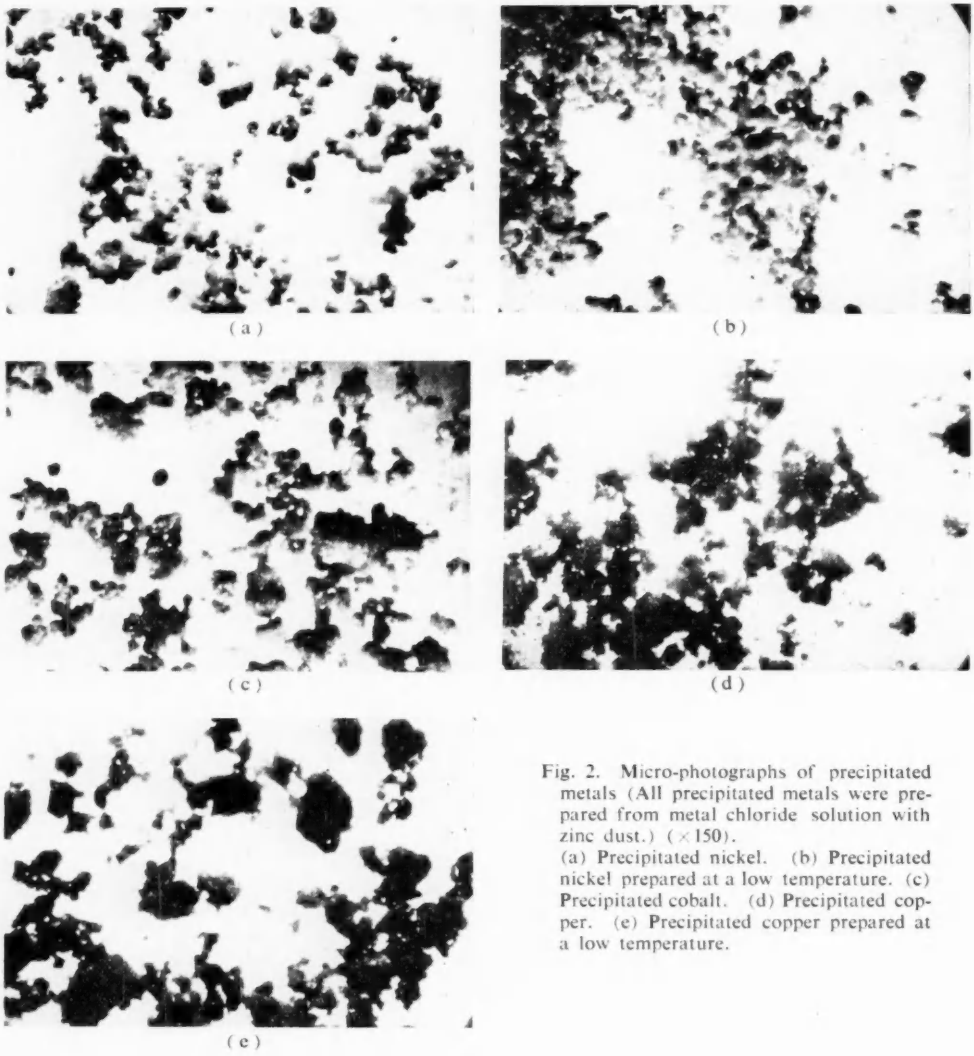

Fig. 2. Micro-photographs of precipitated metals (All precipitated metals were prepared from metal chloride solution with zinc dust.) (×150).
(a) Precipitated nickel. (b) Precipitated nickel prepared at a low temperature. (c) Precipitated cobalt. (d) Precipitated copper. (e) Precipitated copper prepared at a low temperature.

The results are listed in Table IV. To obtain a highly active U-Ni-A, the treatment of the precipitated nickel with diluted acetic acid should be continued until the solution acquires the green color of nickel ion. The U-Ni-A, used for these experiments, was prepared by interrupting the digestion before the solution was colored. The activity of this catalyst was considerably lower than that of the ordinary U-Ni-A. As shown in Table IV, the increment of either the concentration of solution or the amount of catalyst exerts a similar favorable effect on the reduction of benzophenone.

The first step of the preparation of Urushibara catalyst is to obtain precipitated metal by an ion exchange reaction. The so-called precipitated metal may consist of particles of metallic zinc covered with proper metal to be used as a catalyst, admixed with a quantity of zinc dust and zinc compounds. It can be said that the former is a true precipitated metal. Supposing that the size of the particles of a catalyst are decided mainly by those of the precipitated metal, it is necessary to prepare the fine particles of the precipitated metal for making the particles of catalyst to be fine. When a definite weight of zinc dust is used for preparing a definite weight of catalyst, the size of the particles of the precipitated metal may be decided by the size of the particles of

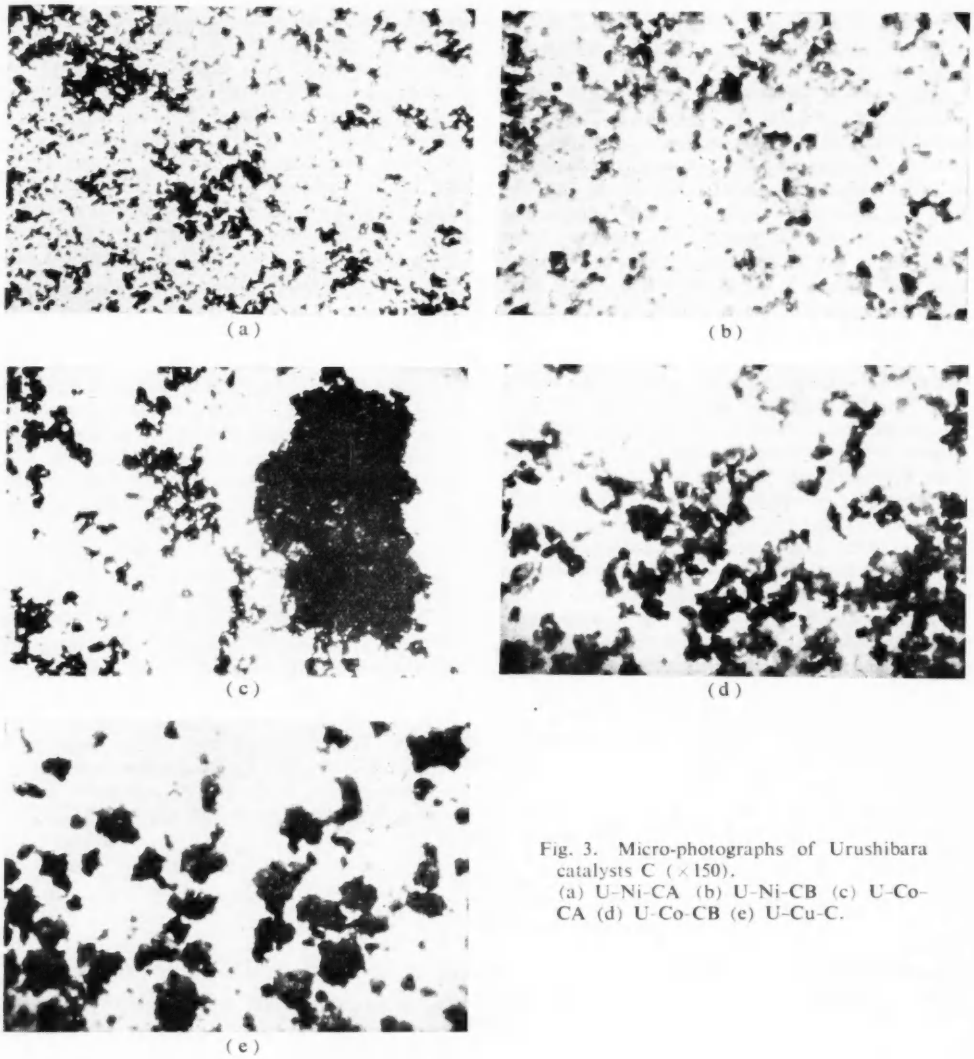

Fig. 3. Micro-photographs of Urushibara catalysts C (×150).
(a) U-Ni-CA (b) U-Ni-CB (c) U-Co-CA (d) U-Co-CB (e) U-Cu-C.

zinc dust and the rate of the ion exchange reaction. The rate of the ion exchange reaction may be affected by several factors, such as the difference of the standard electrode potential between zinc and the metal used to form a catalyst, the fineness of zinc dust, the concentration of the solution of metal chloride, the temperature and the efficiency of agitation when the precipitated metal is prepared. Of the above-mentioned factors, the size of the particles of zinc dust is difficult to change, so far as a commercially available product is used. The difference of the standard electrode potential is almost constant, and the improvement of the efficiency of agitation is limited to some extent. If the concentration of the solution of metal chloride is definite, only the temperature at which the ion exchange reaction is carried out can be freely varied. At a low temperature the ion exchange reaction occurs very slowly, and the influence of the efficiency of agitation can be minimized. Consequently, the metal may uniformly separate out on the surface of the particles of zinc dust and then fine particles of catalyst may be obtained (cf. micro-photographs, shown in Fig. 2).

Urushibara catalysts, thus prepared at a low temperature as described in the experimental part, are temporarily named Urushibara catalysts C and the abbreviations, such as U-Ni-CB,

U-Ni-CA, etc., are used. The results obtained with these catalysts are shown in Table V.

With the U-Ni-CB, better results were obtained than with the U-Ni-B. The dried U-Ni-CB is somewhat heavier in weight and more bulky than the U-Ni-B. The appearance of the U-Ni-CB resembles that of the U-Ni-B prepared from nickel acetate. A microphotograph (Fig. 3) shows that the size of the particles of this catalyst are somewhat smaller than that of the U-Ni-B, and that much zinc oxide remains undissolved. The U-Ni-CA was also proved to be effective, but somewhat longer time was necessary with this catalyst to finish the reduction than with the U-Ni-A. It is partly explained by the fact that the weight of the U-Ni-CA is about a half of that of the U-Ni-A. In the same manner, the U-Co-CB and the U-Co-CA were found to be superior to the corresponding ordinary cobalt catalyst.

To obtain a highly active Urushibara catalyst it has been claimed that the ion exchange reaction to obtain the precipitated metal should be carried out in a short time at a high temperature. Nevertheless, it was proved as mentioned above that the precipitated metal prepared in a long time at a low temperature gives an excellent catalyst. The X-ray diffraction of the U-Ni-CA gives a somewhat different pattern from that of the U-Ni-A, and it will be reported in another paper.

In Table VI the results obtained with copper catalyst are shown. As the precipitated copper does not react with 10% sodium hydroxide solution, only acid is a suitable reagent for treating the precipitated copper. The copper catalyst being considered not so active as a nickel catalyst for catalytic reduction, the condition of reduction was decided in consideration of the results obtained in Table IV. The results shown in Table VI are similar to those obtained with Raney copper[12]. Again, the U-Cu-C gave better results than those obtained with the ordinary U-Cu.

Summary

High pressure reduction of benzophenone was examined with various Urushibara catalysts under various conditions. The purity of benzophenone, the concentration and pH of a solution, reaction temperature and quantity of the catalyst exerted considerable effects on the rate of reduction. Effective Urushibara catalysts were prepared from the precipitated metals which were obtained from the metal chlorides and zinc dust at a low temperature.

The author wishes to express his gratitude to Professor K. Hata for his helpful suggestions and encouragement throughout this work.

Department of Chemistry
Faculty of Science
Tokyo Metropolitan University
Setagaya, Tokyo

12) L. Faucounau, *Bull. soc. chim. France*, [5] **4**, 58 (1937).

Formation of Cyclohexano[c]1, 2, 5-oxadiazole from 1, 2-Cyclohexanedione Dioxime. An Attempted Beckmann Rearrangement with Thionyl Chloride in Liquid Sulfur Dioxide[1,2]

By Niichiro TOKURA, Ritsuro TADA and Kunio YOKOYAMA

(Received July 20, 1960)

It has already been shown by the present authors[2,3] and also by other writers[4] that the direction of the migratory aptitude in the Beckmann rearrangement was often changed by the circumstances, by the reagents or for other reasons. A transannular rearrangement was observed when 1, 6-cyclodecanedione dioxime was subjected to the rearrangement with thionyl chloride in place of sulfur trioxide in liquid sulfur dioxide[3].

1) The Beckmann rearrangement in liquid sulfur dioxide. Part VII.

2) Part VI: R. Tada, Y. Masubuchi and N. Tokura, This Bulletin, in press.

3) N. Tokura, R. Tada and K. Suzuki, ibid., **32**, 654 (1959).

4) Y. Yukawa, "Jikken Kagaku Koza", Vol. 18, Maruzen, Tokyo (1958), p. 426; A. D. McLaren and R. E. Schat, *J. Org. Chem.*, **14**, 254 (1959); R. F. Brown, N. M. van Gulick and G. H. Schmid, *J. Am. Chem. Soc.*, **77**, 1094 (1955); R. Huisgen, J. Witte and I. Ugi, *Ber.*, **90**, 1844 (1957).

Tada, Masubuchi and Tokura[2] carried out the Beckmann rearrangement of the geometrical isomers of cyclohexyl phenyl ketoximes in liquid sulfur dioxide without any appreciable difference of the migratory aptitude by a variety of reagents at −70°C.

The Beckmann rearrangements of 1,2-diketone dioximes have scarcely been reported at all, but those of 1,2-diketone monoximes have been examined extensively to yield nitriles and carboxylic acid as the result of cleavage[5,6] of the dione monoximes. A number of trials of the Beckmann rearrangement on benzil dioximes have been reported since the turn of the last century[7-9] but the result were subjects of controversy[10] and the presence of geometrical isomers in the dioxime led the direction of the rearrangement to various products, for example, 3,5-diphenyl-1,2,4-oxadiazole, oxanilide and so on, among which the derivation of the 1,2,4-oxadiazole was ascribed to the Beckmann rearrangement of one of the two oximino groups, followed by dehydration. The reagents used were phosphorus pentachloride, phosphorus pentoxide, phosphoryl chloride and sulfuric acid. Of the three isomers, only the γ-isomer was reported to yield oxanilide, a product of the double Beckmann rearrangement, whereas the α- and β-isomers gave the diphenyl-1,2,4-oxadiazole. Recently, Conley and Mikulski[6] have obtained the same oxadiazole with polyphosphoric acid as the reagent.

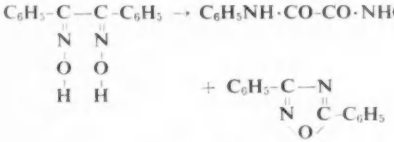

Chart 1.

The present paper describes the experiments which have been undertaken to throw light upon the nature and the migratory tendency of 1,2-cyclohexanedione dioxime in sulfur dioxide. The preparation of the 1,2-cyclohexane dioxime has been reported in a number of papers, of which the method of Belcher, Hoyle and West[11] has been adopted. This method, consisting in the oximation of 2-bromocyclohexanone (Ia), is essentially similar to that of Tokura and Oda[12] which was published earlier in 1943 and uses 2-chlorocyclohexane (Ib) as the starting material. The former method is however more convenient for laboratory work. To our regret, however, neither method was satisfactory enough to be a standard method of preparation owing to the formation of many resinous matters and unavoidable fluctuation in the yields.

1,2-Cyclohexanedione dioxime (II) was obtained in yields of 10~34% as crystals of m.p. 185~186°C (literature[11], 186~187°C), from which it was impossible further to separate the possible isomers by repeated crystallization or by repeated precipitation. Since the various reagents examined on this material have given no symptom of the geometrical isomers which will be reported in the following paper, the problem of the possible isomers was shelved in this project.

In this light of such a consideration, it is interesting to examine the direction of the Beckmann rearrangement, but contrary to expectation, the rearrangement was not caused by thionyl chloride in liquid sulfur dioxide. When thionyl chloride was used as the reagent, a low melting material III, m.p. 26°C, was obtained in a yield of 70% by ether extraction of the residue obtained on evaporation of sulfur dioxide from the reaction mixture. Although the elementary analysis was consistent with the anhydride of the dioxime II, there still remained another possibility of the presence of isomeric matters such as those produced by single and/or double rearrangement followed by dehydration. As cited above, benzil dioxime gave in such a case 3,4-diphenyl-1,2,4-oxadiazole and oxanilide, products of single and double rearrangement, respectively.

If the anhydride was formed by a simple dehydration without rearrangement, the structure must be a 1,2,5-oxadiazole derivative A, and not a 1,2,4-oxadiazole derivative B.

(A) (B)

The I.R. spectrum of III showed the characteristic absorption of a 1,2,5-oxadiazole (furazan)[13] at 1630 and 1588 cm^{-1}. This substance was very stable and resisted hydrolysis on refluxing with concentrated hydrochloric acid for 5 hr., with aqueous 25% caustic soda for 6.5 hr., with aqueous 40% sulfuric acid for 7 hr. and

5) D. Murakami and N. Tokura, This Bulletin, 31, 1044 (1958).
6) J. Conley and F. A. Mikulski, *J. Org. Chem.*, 24, 97 (1959).
7) K. Awers and V. Meyer, *Ber.*, 21, 810 (1888).
8) E. Beckmann and A. Koster, *Ann.*, 274, 18 (1893).
9) A. Günther, *Ber.*, 21, 517 (1888); *Ann.*, 257, 46 (1889).
10) J. Meisenheimer and W. Lamparter, *Ber.*, 57, 276 (1924).
11) R. Belcher, W. Hoyle and T. S. West, *J. Chem. Soc.*, 1958, 2743.
12) N. Tokura and R. Oda, *Sci. Papers Inst. Phys. Chem. Research (Tokyo)*, 22, 8501 (1943).
13) R. J. Gaughran et al., *J. Am. Chem. Soc.*, 76, 2233 (1954).

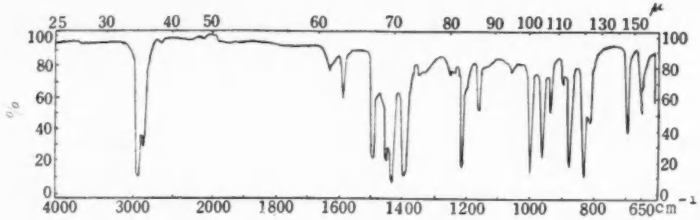

Fig. 1. I.R. spectrum of III.

heating with concentrated sulfuric acid for 5 hr. on a steam bath. Oxidation with chromic anhydride in acetic acid or with ozone in 50% acetic acid and reduction with tin and hydrochloric acid were all ended in the recovery of the starting compound. The compound underwent an oxidation only with potassium permanganate in dilute sulfuric acid to yield a dicarboxylic acid, $C_6H_6O_6N_2$, m.p. 147~148°C (decomp.), which showed no coloration with a nickel salt and is assigned to the structure of IVa. Another possible structure IVb is ruled out because the cleavage of this sort may be more difficult than the cleavage to afford IVa.

The exhaustive oxidation of the compound with the same oxidant gave a dicarboxylc acid, m.p. 178°C (decomp.), 1, 2, 5-oxadiazole-3, 4-dicarboxylic acid (V), (literature[14], m.p. 178°C), the structure being proved as V by elementary analysis and mixed melting point.

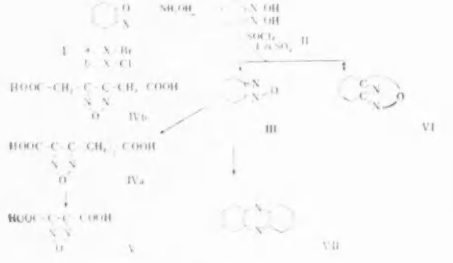

Chart 2.

Another evidence of structure III as the anhydride of the unrearranged dioxime was attained by reduction with sodium in ethanol. The use of lithium aluminum hydride was avoided because of the possible rearrangement[15] by this reagent. The reduction of III gave a basic compound, the analysis and the melting point corresponding to octahydrophenazine, $C_{12}H_{16}N_2$ (VII), m.p. 108~109°C, which was prepared by Wallach[17a], by Baumgarten and Bower[17b] and by Smith[16]. Wallach[17a] prepared the compound VII from II by reduction with zinc and alkali and a structure of decahydrophenazine was assigned, but recently[17b] it was found to be octahydrophenazine.

It was reported as early as in 1886 that 3, 4-diphenyl-1, 2, 5-oxadiazole[18] was synthesized from benzil dioxime by the reaction with potassium ferricyanide. The present authors have deviced a method of synthesis of compound III in a low yield by refluxing II in aqueous 10% sodium hydroxide. The coincidence of the melting point and the mixed melting point, and the I.R. spectra of the two materials confirmed the structure III unequivocally.

Thionyl chloride is one of the most powerful reagents to effect the Beckmann rearrangement. The failure of the rearrangement of II with thionyl chloride in liquid sulfur dioxide in contrast to benzil dioxime suggests some meaning. Benzil dioxime has presumably a coplanar structure favorable for a Beckmann rearrangement at least in one moiety of the molecule, whereas cyclohexanedione dioxime will prefer dehydration rather than a Beckmann rearrangement since it is sterically more restricted than benzil dioxime to build an intermediate azilinium cation[19] (aza-cyclopropenyl cation). In addition, the formation of the intermediate cation of benzil dioxime may be facilitated by the presence of phenyl ring participation in the rearrangement.

Gillis[20] recently reported that a cyclic sulfite derived from tetramethylene glycol and thionyl chloride gave tetrahydrofuran without stopping at the stage of a cyclic sulfone via the Bissinger rearrangement[21]. The formation of the anhydride III may likely proceed through cyclic sulfite IIa and sulfone IIIb (Chart 3).

14) L. Wolff, *Ber.*, **28**, 69 (1895); A. Quilico and M. Freri, *Gaz. chim. Ital.* **76**, 3 (1946), *Chem. Abstr.*, **41**, 382d (1947).
15) A. T. Blomquist, B. F. Hallam and A. D. Josey, *J. Am. Chem. Soc.*, **81**, 678 (1959).
16) P. A. S. Smith, ibid., **70**, 323 (1948).
17) a. A. Wallach, *Ann.*, **437**, 177 (1924); b. H. E. Baumgarten and F. A. Bower, *J. Am. Chem. Soc.*, **76**, 4561 (1954).
18) R. Koreff, *Ber.*, **19**, 176 (1886).
19) R. Huisgen, J. Witte and I. Ugi, *Ber.*, **90**, 1844 (1957).
20) R. G. Gillis, *J. Org. Chem.*, **25**, 651 (1960).
21) W. E. Bissinger, F. E. King and C. W. Hamilton, *J. Am. Chem. Soc.*, **70**, 3940 (1948).

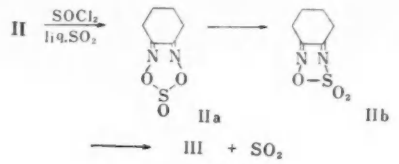

Chart 3.

A variety of products have also been obtained as the results of the attempted Beckmann rearrangement with some other reagents. The results will be reported elsewhere in near future.

Experimental

Material.—Commercial sulfur dioxide was dried with concentrated sulfuric acid and distilled. A commercial thionyl chloride was redistilled.

Apparatus and General Procedure.—The procedure and manipulation for the Beckmann rearrangement were essentially the same as described earlier[1,2].

1,2-Cyclohexanedione Dioxime (II).—To a refluxed mixture of hydroxylamine hydrochloride (227 g.), sodium acetate (45 g.), methanol (400 ml.) and water (460 ml.) was added 128 g. of 2-bromocyclohexanone (Ia) gradually. After the mixture was refluxed for 45 min., it was condensed and diluted with water. The crystals were recrystallized from water, m. p. 186~187°C. Yield, 31 g. (34%).

Found: N, 19.66. Calcd. for $C_6H_{10}O_2N_2$: N, 19.71%.

Reaction of II will Thionyl Chloride in Liquid Sulfur Dioxide.—A mixture of the dioxime II (7.1 g.), thionyl chloride (13.0 g.) and 150 ml. of liquid sulfur dioxide was allowed to stand for an hour at room temperature. The solution was then poured into ice water, sulfur dioxide was evaporated and the residue was extracted with ether. The ether solution was washed with water, dried and condensed to give 5 g. (70%) of colorless crystals III, m. p. 26°C (recrystallized from ethanol), b. p. 99~101.5°C (13 mmHg). The substance was later identified as cyclohexano[c]1,2,5-oxadiazole.

Found: C, 58.19; H, 6.16; N, 22.10. Calcd. for $C_6H_8ON_2$: C, 58.05; H, 6.50; N, 22.57%. Mol. wt. Found: 139.5 (benzene). Calcd.: 124.

I. R. ν_{max}^{liq} 1588(m) (C=N-), and 2960(s), 2880(s) (CH_2=), cm^{-1}, U. V. λ_{max}^{MeOH} 220 mμ (log ε = 3.56). No significant amount of any other material was found in the residual solution after the ether extraction.

Synthesis of III with Alkali.—With 20 ml. of 10% aqueous sodium hydroxide, 3 g. of II was refluxed for 1.5 hr. The reaction mixture was extracted with ether. After the distillation of the ether, a small quantity of crystals was obtained as the residue. This was recrystallized from ethanol, m. p. 25.5~26.0°C, b. p. 180~196°C (18 mmHg), 0.3 g. (10%). This material showed no depression of melting point when mixed with III from II and thionyl chloride and gave an I. R. spectrum completely identical with that given by the specimen obtained from II and thionyl chloride.

Oxidation of III with Potassium Permanganate.—To 10 ml. of 10% aqueous solution of sulfuric acid was added 1.5 g. of III and the mixture was stirred and heated on a water bath. About 2.0 g. of potassium permanganate was added to the mixture bit by bit till the permanent red color remained. The precipitate of manganese dioxide was dissolved by introducing sulfur dioxide gas, and the mixture was extracted with ether, and the extract was condensed to give 1.3 g. (86.7%) of colorless fine crystals IVa, m. p. 147~148°C (decomp.) (from acetone-ligroin), IVa was soluble in hot water, alkali, alcohol and acetone, but insoluble in benzene.

Structure of 4-ethyl-1,2,5-oxadiazole-3,2'-dicarboxylic acid (IVa) was assigned.

Found: C, 38.08; H, 3.62; N, 14.78. Calcd. for $C_6H_6O_5N_2$: C, 38.72; H, 3.25; N, 15.02%. Acid value, Found: 628. Calcd. for 2-COOH: 617.0. I. R. ν_{max}^{KBr} 3400~3540 (-OH) and 1695 (C=O) cm^{-1}. White precipitates with Ag^+ and Ba^{2+} ions. No red coloration with Ni^{2+}.

Exhaustive Oxidation of IVa.—A mixture of 0.5 g. of IVa, 1.0 g. of potassium permanganate and 10 ml. of 10% sulfuric acid was stirred and warmed for two days on a water bath. The precipitate of manganese dioxide was dissolved by passing sulfur dioxide gas. Extraction of the mixture with ether followed by condensing the ether solution yielded 0.1 g. of fine crystals V, m. p. 178°C (decomp.). (repeated recrystallization from alcohol.)

Found: N, 17.78. Calcd. for $C_4H_2O_5N_2$: N, 17.72%.

V was mixed with an authentic specimen of 1,2,5-oxadiazole-3,4-dicarboxylic acid prepared by the method of Wallach[17a] to show no melting point depression.

Reduction of III with Sodium and Ethanol.—To a solution of 2.0 g. of III in 100 ml. of ethanol was added 5 g. of metallic sodium with stirring. The mixture was further refluxed for 1.5 hr. and then a half of the ethanol was evaporated. The residual mixture was acidified with concentrated hydrochloric acid and was extracted with ether. Evaporation of the ether extract gave 0.4 g. of a product which was identified as the starting material III. The residual solution was again made alkaline with soda ash and the mixture was again extracted with ether. Evaporation of the ether extract gave colorless needles VII contaminated with a brown resinous matter. The needles sublimed at 60~80°C (15 mmHg). The needles were repeatedly recrystallized from ethanol to m. p. 108~109°C. Picrate, yellow needles, m. p. 155°C (decomp.).

Base: Found: C, 75.89; H, 8.10; N, 14.46. Calcd. for $C_{12}H_{16}N_2$: C, 76.55; H, 8.57; N, 14.88%. Picrate: Found: N, 16.83. Calcd. for $C_{18}H_{19}N_5O_7$: N, 16.78%.

The material VII was proved to be octahydrophenazine by admixing with an authentic sample prepared by reduction of II by the method of Wallach. No depression of the melting point[17a] was observed.

Summary

An attempted Beckmann rearrangement of 1, 2-cyclohexanedione dioxime with thionyl chloride in liquid sulfur dioxide resulted in the formation of cyclohexano[*c*]1, 2, 5-oxadiazole in 70% yield. The structure of the oxadiazole was established by oxidation, reduction, and synthesis. The reason why the condensation was predominant over the rearrangement was discussed in comparison with the case of benzil dioxime.

The authors are indebted to the Befu Chemical Industries Co., for the donation of liquid sulfur dioxide.

Research Institute of
Non-Aqueous Solutions
Tohoku University
Sendai

A Synthesis of an Octahydrophenanthrene Derivative[1]

By Takeshi MATSUMOTO and Akira SUZUKI

(Received August 22, 1960)

In the previous paper[2] synthesis of 2-methoxy-5-hydroxy-1-naphthylacetic acid and unsuccessful attempts to prepare therefrom 1, 2, 3, 4-tetrahydro-2-oxo-5-methoxy-1-naphthyl acetate (IIIb) were described. This paper reports a successful synthesis of the acetate IIIb from 5-methoxy-2-tetralone (I) and of a hydrophenanthrene derivative IX, a promising intermediate in the synthesis of certain diterpenoid skeletons, from IIIb.

The monoalkylation of β-tetralones had been in general difficult to achieve by direct alkylation since they tend to undergo partial or exclusive dialkylation[3]. However, the difficulty was recently overcome by the ingeneous procedure of Stork[4], which is concerned with alkylation of enamine derivatives of ketones with alkyl halides. In this study, the Stork method was adopted. The reaction of 5-methoxy-2-tetralone with pyrrolidine in boiling benzene afforded a previously undescribed enamine II, m. p. 78.5~79.5°C, in almost quantitative yield. II was then alkylated in benzene with ethyl bromoacetate and the intermediary ammonium salt was hydrolysed with water. Ethyl 1, 2, 3, 4-tetrahydro-2-oxo-5-methoxy-1-naphthyl acetate (IIIb), thus obtained in 74% yield, is a viscous liquid, boiling at 150~151°C (0.05 mmHg). Piperidine enamine of the methoxytetralone, on being treated in the same way, afforded a poor yield of IIIb. Hydrolysis of the ester IIIb with aqueous sodium hydroxide gave the acid IIIa, m. p. 172~173°C.

In hope of preparing a tricyclic $\alpha\beta$-unsaturated ketone V, the authors next examined the reaction of IIIb with 1-(*N*, *N*-diethylamino)-butan-3-one methiodide in benzene in the presence of potassium ethoxide. After chromatography on acid alumina, there could be isolated from the reaction mixture a compound $C_{19}H_{24}O_5$, m. p. 134~135°C, as the main product. The infrared spectrum (Fig. 1; nujol mull) of this compound exhibited absorption bands at 3400 (broad; OH), 1700 (six-membered ring ketone) 1735 and 1175 cm^{-1} (ester). The authors supposed at this stage that they had ketol IV in hand. In several instances, the Robinson annelation reaction has been shown[5] to lead to intermediary ketol of type IV, which affords $\alpha\beta$-unsaturated ketone of type V by a β-elimination process. On treatment with isopropenyl acetate in the presence of *p*-toluenesulfonic acid, the ketol IV afforded an acetate

1) Approaches to the Synthesis of Diterpenoid Alkaloid Models, Part III. A portion of Ph. D. Dissertation (Hokkaido University) of Akira Suzuki. Read in part before the 12th Annual Meeting of the Chemical Society of Japan, Kyoto, April, 1959 and outlined in part in the preliminary communication; T. Matsumoto and A. Suzuki, This Bulletin, **33**, 862 (1960).

2) T. Matsumoto and A. Suzuki, ibid., **32**, 1283 (1959).

3) J. W. Cornforth, R. H. Cornforth and R. Robinson, *J. Chem. Soc.*, **1942**, 689; C. A. Grob and W. Jundt, *Helv. Chim. Acta*, **31**, 1691 (1948); J. W. Cornforth and R. Robinson, *J. Chem. Soc.*, **1946**, 676; J. D. Chanely, *J. Am. Chem. Soc.*, **70**, 244 (1948); M. D. Soffer, R. A. Stewart, J. C. Cavagnol, H. E. Gellerson and E. A. Bowler, ibid., **72**, 3704 (1950); G. Stork, ibid., **73**, 4748 (1951).

4) G. Stork, R. Terrell and J. Szmuszkovicz, ibid., **76**, 2024 (1954); E. D. Bergmann and R. Ikan, ibid., **78**, 1482 (1956); S. Hunig, E. Benzing and E. Lucke, *Ber.*, **90**, 2833 (1957).

5) C. Mannich, W. Koch and F. Borkowsky, ibid., **70**, 355 (1937); P. Wieland, H. Neberwasser, G. Anner and K. Misscher, *Helv. Chim. Acta*, **36**, 1231 (1953); C. Georgian, *Chem. & Ind.*, **1954**, 930; J. Colonge, J. Dreux and J. P. Kehlstadt, *Bull. soc. chim. France*, **1954**, 1404; G. Stork, ibid., **1955**, 256; F. J. McQuillin, *J. Chem. Soc.*, **1955**, 528; R. Howe and F. J. McQuillin, ibid., **1955**, 2423; W. S. Johnson, J. Ackerman. J. F. Eastham and H. A. Dewalt, Jr., *J. Am. Chem. Soc.*, **78**, 6302 (1956).

having a m. p. 97.5~98.5°C. Contrary to expectation, attempted pyrolytic elimination of acetic acid from the acetate to the $\alpha\beta$-unsaturated ketone did not occur, even though the reaction temperature was raised to 300°C.

Eventually, through the aid of N. M. R. spectroscopy, the ketol was shown to be actually a bridged ring compound VI. The N. M. R.

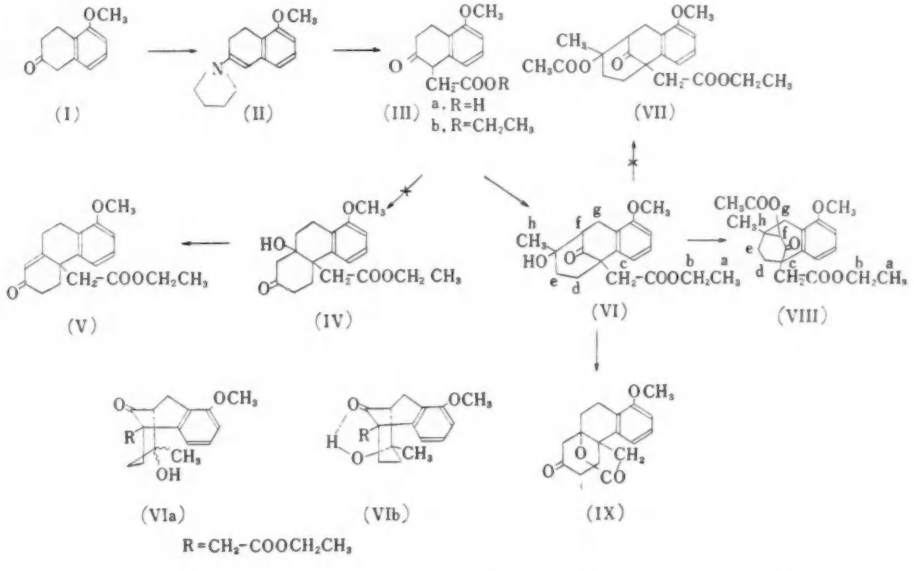

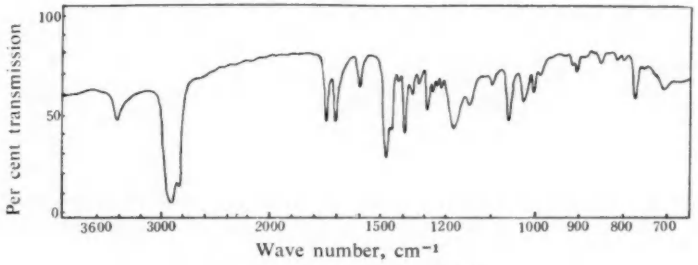

Fig. 1. Infrared spectrum of VI.

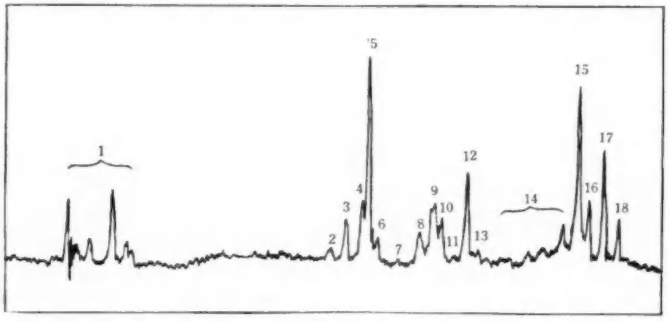

Fig. 2. N. M. R. spectrum of VI in $CDCl_3$

TABLE I. ASSIGNMENTS OF THE N. M. R. SPECTRUM OF VI

Peak number in Fig. 2	Chemical shift c. p. s. (stand. benzene)	Proton type	Number of protons	
			Calcd. for VI	Obs. from peak area
1	−21	Aromatic H	3	3.0
2, 3, 4, 6	100	b-H	2	2.5
5	105	O-CH_3	3	2.9
8, 9, 10	136	f, g-H and OH	4	3.5
12	151	c-H	2	1.7
15	203	h-H	3	3.4
16, 17, 18	215	a-H	3	3.0
14 and others		d, e-H		

spectrum[6] of the ketol (Fig. 2) showed one sharp maximum at a high applied magnetic field, characteristic of proton resonance for the

group (203 c. p. s.; standard, benzene). This observation is clearly incompatible with structure IV, and the spectrum is completely accounted for in terms of structure VI (see Table I). A formula such as VIII and Xa would also explain the resonance line at 203 c. p. s., but would not give any explanation for the other lines. The formation of a bridged ketol system similar to VI through the Robinson annelation-reaction was first disclosed only quite recently by Johnson and his coworkers[7].

In order to elucidate the conformation the authors further examined the O-H stretching absorption band of the ketol in the 3300 cm^{-1} region. The spectrum was measured in 0.0046 M[8] tetrachloroethylene solution[9] and as indicated in Fig. 3, was found to exhibit two bands at 3430 and 3590 cm^{-1}. The latter band corresponds to the vibration of aliphatic free OH group[10] while the former band may be attributed to OH group bonded to the carbonyl oxygen atom[11]. In structure VIa, in which the cyclohexanone ring takes a boat form, the hydroxyl group, be it either axial or equatorial, is unable to form an intramolecular hydrogen bond[12].

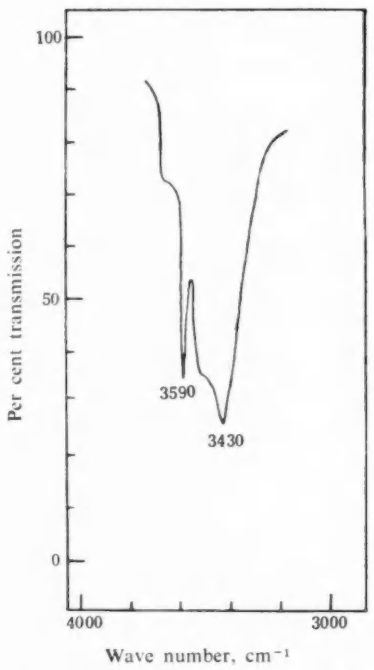

Fig. 3. ν O-H absorption of VI in tetrachloroethylene (0.0046 M).

The conformation VIb with chair cyclohexanone ring and axial OH group is the only one in which the formation of an intramolecular hydrogen bond is possible.

6) The N. M. R. spectra were taken on a Varian 40 MC instrument at the University of Illinois through the courtesy of Drs. Ben Shoulder and Masaji Ohno, to both of whom the authors are pleased to express their sincere thanks.

7) W. S. Johnson, J. J. Korst, R. A. Clement and J. Dutta, *J. Am. Chem. Soc.*, **82**, 614 (1960).

8) At this dilution the association of the solute molecule is negligible. N. D. Coggeshall, *J. Chem. Phys.*, **18**, 978 (1958); F. A. Smith and E. C. Creitz, *J. Research Natl. Bur. Standards*, **46**, 145 (1951).

9) The infrared spectrum was taken with a Hilger H 800 infrared spectrophotometer with calcium fluoride optics. The authors wish to express their gratitude to Assistant Professor Sanjuro Matsushita and Miss Hisako Nakato of the Physical Chemistry Laboratory for the infrared spectral measurement. For the absence of interaction between hydroxyl group of solute and π-electrons of tetrachloroethylene, see L. L. Ingraham, J. Corse, G. F. Bailey and F. Stitt, *J. Am. Chem. Soc.*, **74**, 2297 (1952).

10) L. J. Bellamy, "The Infrared Spectra of Complex Molecules", Methuen and Co., Ltd., London (1958), p. 96.

11) In general, an intramolecularly bonded OH group exhibits a sharp band. The rather broad absorption band at 3430 cm^{-1} might be caused by the overlapping of the absorption due to intramolecular hydrogen bond between the OH group and the ethoxy carbonyl oxygen atom (see formula VIb) and or by the rotatory isomerism of the hydroxyl group. For the latter effect, see R. Piccolini and S. Winstein, *Tetrahedron Letters*, No. 13, 4 (1959); M. Kahn, N. Lüttke and R. Mecke, *Z. anal. Chem.*, **170**, 106 (1959).

12) For example, L. Hunter, W. Klyne's "Progress in Stereochemistry", Vol. 1, Butterworths Scientific Publications, London (1954), p. 223.

TABLE II. ASSIGNMENTS OF THE N. M. R. OF VIII

Peak number in Fig. 5	Chemical shift c. p. s. (stand. benzene)	Proton type	Number of protons	
			Calcd. for VIII	Obs. from peak area
1	−22	Aromatic H	3	3.0
2, 3, 4, 6	100	b-H	2	2.2
5	104	O-CH_3	3	2.9
8	129	g-H	2	1.8
9	138	c-H	2	1.7
11	178	$COCH_3$	3	3.8*
13	190	h-H	3	3.1
15, 16, 17	212	a-H	3	3.0
10, 12, 14 and others		d and e-H		

* Absorption due to d and e-H may be overlapped.

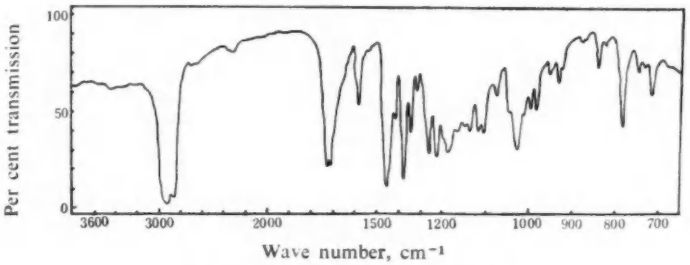

Fig. 4. Infrared spectrum of VIII.

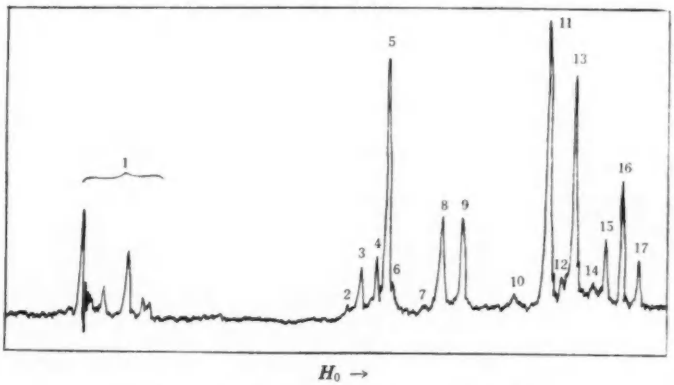

Fig. 5. N. M. R. spectrum of VIII in $CDCl_3$.

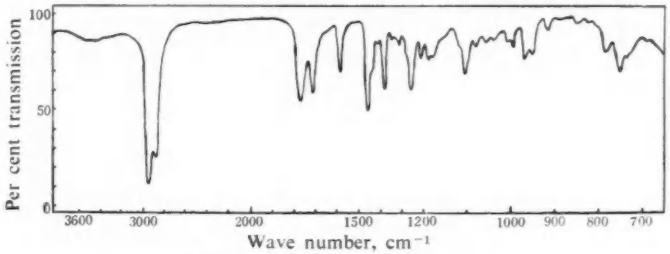

Fig. 6. Infrared spectrum of IX.

Next, examination was made of the structure of the acetylation product with m. p. 98.5°C (vide supra). The infrared spectrum (Fig. 4) of the acetate showed complete absence of hydroxyl function and presence of the following groups: saturated ester (1730 and 1175 cm^{-1}), acetate (1730 and 1230 cm^{-1}) and six-membered cyclic ketone (1715 cm^{-1}). Therefore a structural formula VII may be considered for this compound. Invalidity of this structure was however concluded from the N. M. R. spectrum, which is depicted in Fig. 5. The paramagnetic shift of the peak due to presence of CH_3-$\overset{|}{C}$- protons to 190 c. p. s., disappearance of the peak at 151 c. p. s. due to $-\overset{|}{C}-CH_2-CO_2$ protons and appearance of a new peak at 138 c. p. s. suggest a fundamental change in the framework of VI. The acetate may then be expressed by VIII, since an attack of proton upon the hydroxyl function of compound VIc would result in the formation of structure VIIIa through the well known 1, 2-shift as follows:

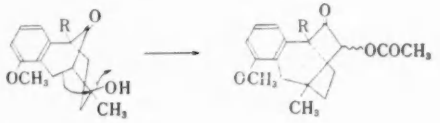

(VIc) (VIIIa)

R=$CH_2-COOCH_2CH_3$

This structure is consistent with the N. M. R. spectrum; the interpretation of the spectrum in terms of formula VIII is summarized in Table II. The structure also explains the stability of the acetate to pyrolitic treatment, since in formula VIII elimination of an element of acetic acid would be impossible. Further, convincing evidences in favor of the formula VIII were provided by positive reactions with triphenyltetrazolium chloride and with the Tollens' reagent. On the basis of these findings the structure of the acetate may be concluded to be VIII[13].

Contrary to the case of acid treatment described above, treatment of VI with dilute aqueous alkali or with sodium ethoxide in ethanol, followed by acidification gave rize to a product $C_{17}H_{18}O_4$, to which a hydrophenanthrene structure IX was assigned on the basis of infrared (Fig. 6) and N. M. R. spectra. Although the product was amorphous and could not be crystallized by chromatography or by any other means, it was regarded homogeneous enough on the basis of the behavior in chromatography and of infrared spectrum. The infrared absorption spectrum showed complete absence of the hydroxyl group and presence of six-membered cyclic ketone (1720 cm^{-1}) and γ-lactone (1770 cm^{-1}). The formation of γ-lactone is impossible from the above mentioned skeletons VI and VIII and is possible only from the structure containing the hydrophenanthrene skeleton IX. The correctness of structure IX is further substantiated by the elemental analysis and by the N. M. R. spectrum. In the spectrum[14], the sharp maximum at high magnetic field characteristic for $-\overset{|}{C}-CH_3$ protons could not be recognized. This type of conversion from skeletons VI to IX by alkaline reagent has been recently described by Johnson and coworkers[7]. The authors were thus able to obtain an intermediate IX which seems to be promising for the synthesis of a certain diterpenoid skeleton.

Experimental[15]

Preparation of Pyrrolidine Enamine (II). — A solution of 4.3 g. (0.0244 mol.) of 5-methoxy-2-tetralone, which was prepared from 2, 5-dimethoxynaphthalene by the procedure of Cornforth and Robinson[16], and 3.5 g. (0.0488 mol.) of freshly distilled pyrrolidine in 40 ml. of dry benzene was refluxed on a water bath while water, distilled off as an azeotropic mixture with benzene, was separated with a Dean-Stark type apparatus[17]. The condensation reaction was completed after 3 hr. After removal of the solvent and excess pyrrolidine, the residue afforded a distillation under reduced pressure

13) In the preliminary report[1] a formula Xb was suggested as the structure of the acetate. The formation of the spirocyclic compound was explained through a reverse aldol condensation and a subsequent aldol condensation of an intermediary diketone XI. Peaks at 129 and 138 c. p. s. were interpreted to be attributable to f and g protons, although in general these four protons constitute an ABCD system and a rather simple absorption pattern as in Fig. 5 is not to be expected except in special cases.

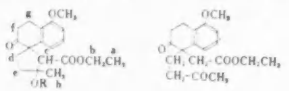

(X) (XI)

a. R=H
b. R=$COCH_3$

14) The spectrum was taken on a Varian 40 MC instrument at Tohoku University. The authors are very grateful to Professor Genjiro Hazato and his coworkers for the measurement.

15) All melting and boiling points are uncorrected. Unless otherwise specified, infrared spectra were taken in nujol mull on a Koken model DS-301 infrared spectrophotometer with sodium chloride optics. Ultraviolet spectra were measured in 95% ethanol or methanol solutions by means of a Beckmann model DK-2 spectrophotometer. The authors are indebted to Miss Noriko Fujino for microanalysis.

16) J. W. Cornforth and R. Robinson, *J. Chem. Soc.*, **1949**, 1861.

17) E. W. Dean and D. D. Stark, *Ind. Eng. Chem.*, **12**, 486 (1920); S. Natelson and S. Gottfried, *Org. Syntheses*, **23**, 37 (1943).

5.35 g. (95.5%) of a product, boiling at 159~160°C (0.09 mmHg). The enamine derivative II was a pale yellow viscous liquid, which crystallized on being allowed to stand. Recrystallization from petroleum ether yielded colorless prisms, m. p. 78.5~79.5°C.

ν_{max}^{nujol} [18] 1610, 1590 and 1565 cm^{-1}.

λ_{max}^{MeOH} [18] 243 (ε 13800) and 315 mμ (ε 19300).

Found: C, 78.48; H, 8.21. Calcd. for $C_{15}H_{19}ON$: C, 78.56; H, 8.35%.

Piperidine enamine of 5-methoxy-2-tetralone was obtained under the same condition. The condensation of 5 g. (0.0284 mol.) of the tetralone with 5 g. (0.0588 mol.) of the amine in 30 ml. of dry benzene was complete in 3 hr.; yield 4.6 g. (67%), b. p. 135~140°C (0.001 mmHg).

Found: C, 79.16; H, 8.54. Calcd. for $C_{16}H_{21}ON$: C, 78.97; H, 8.70%.

Ethyl 1,2,3,4-Tetrahydro-2-oxo-5-methoxy-1-naphthyl Acetate (IIIb).—At room temperature and during 45 min., 3.9 g. of ethyl bromoacetate in 5 ml. of benzene was added to a solution of 5.3 g. of 3,4-dihydro-2-(*N*-pyrrolidyl)-5-methoxy naphthalene (II) in 10 ml. of benzene. After refluxing for 3 hr. on a water bath (ca. 70°C), the solution was cooled to room temperature and 20 ml. of water was added.

The whole was vigorously stirred for one hour at room temperature and the organic layer was separated; the water layer was extracted twice with benzene. The combined organic layer was washed with water, dried over anhydrous sodium sulfate and distilled under reduced pressure; b. p. 150~151°C (0.05 mmHg.), colorless viscous liquid, yield 4.5 g. (74%).

ν_{max}^{film} 1725 (ketonic carbonyl) and 1735 cm^{-1} (ester carbonyl).

Found: C, 68.36; H, 6.59. Calcd. for $C_{15}H_{18}O_4$: C, 68.68; H, 6.92%.

The keto ester IIIb was also prepared from the piperidine enamine derivative by the same procedure. The yield, however, was lower than the above case; there was obtained 2 g. (41%) of IIIb from 4.5 g. of the piperidine enamine and 3.1 g. of ethyl bromoacetate.

Hydrolysis of the Ethyl Ester IIIb.—A mixture of 300 mg. of IIIb, 3 ml. of 60% sodium hydroxide and 3 ml. of ethanol was heated on a water bath for one hour. The solution was then diluted with 5 ml. of water, acidified with 6 N hydrochloric acid and extracted with ethyl acetate three times. The combined extracts were washed with water and dried over anhydrous sodium sulfate. Removal of the solvent in vacuo left an oily pale brown residue, from which on trituration with ether, a crystalline material was obtained. For analysis the product was recrystallized from benzene to afford colorless prisms, m. p. 172~173°C.

ν_{max}^{nujol} 1695 (carboxylic carbonyl) and 1710 cm^{-1} (ketonic carbonyl).

λ_{max}^{MeOH} 271 (ε 2200) and 278 mμ (ε 2220).

Found: C, 66.77; H, 6.00. Calcd. for $C_{13}H_{14}O_4$: C, 66.65; H, 6.02%.

Condensation of IIIb with 1-(*N*, *N*-Diethylamino)-butan-3-one Methiodide. — Diethylaminobutanone (4.2 g.), prepared according to the Wilds and Shunk method[19] was swirled gently in a 200 ml. flask and cooled with ice during the addition of methyl iodide (4.2 g) in portions for 15 min. The swirling was regulated, so as to obtain crystalline methiodide as an even coating on the walls of the flask. When no more liquid remained, the flask was kept in ice for one hour. A solution of the keto ester IIIb (7 g.) in dry thiophen-free benzene (40 ml.) was added, air was expelled from the flask by dry nitrogen, and a solution of potassium (1.7 g.) in absolute ethanol (25 ml.) was added with ice cooling during 5 min. Swirling was continued until the methiodide had all dissolved (about one hour) and was replaced by a precipitate of potassium iodide. After it had been kept in ice for another hour, the mixture was heated gently for 30 min. An excess of 3 N sulfuric acid was then added and the nitrogen gas was stopped. After addition of enough water (60 ml.) to dissolve the potassium sulfate the benzene layer was separated and the aqueous layer extracted three times with ether. The united extracts were washed with water, cleared with a little sodium sulfate, and concentrated in vacuo to leave 3.5 g. of an oil which was chromatographed through a column of acid-washed alumina[20] (50 g.) packed and washed with benzene. The portions eluted with benzene-chloroform (volume ratio 1:1, 450 ml.) and with chloroform only (400 ml.) were viscous oils and gave no crystalline products. The fraction obtained by elution to a total of 450 ml. of ethanol, contained 1.8 g. (20.3%) of a solid, m. p. 124~130°C; recrystallization from ligroin yielded a pure sample of the bridged ring ketol VI as colorless prisms, m. p. 134~135°C.

λ_{max}^{MeOH} 271 (ε 1410) and 278 mμ (ε 1310).

Found: C, 68.44; H, 7.10. Calcd. for $C_{19}H_{24}O_5$: C, 68.65; H, 7.28%.

The 2,4-dinitrophenylhydrazone of VI was crystallized from ethanol as orange needles and had m. p. 260°C (decomp.).

Found: C, 58.61; H, 5.43. Calcd. for $C_{25}H_{28}O_8N_4$: C, 58.58; H, 5.51%.

Acetylation of the Ketol VI.—A mixture of 300 mg. of VI, 6 mg. of *p*-toluenesulfonic acid and 3 ml. of isopropenyl acetate (Eastman) was heated on a water bath for 4 hr. After the acid was neutralized with a few drops of pyridine, the solution was concentrated in vacuo to leave a pale yellow brown oil, which on trituration with petroleum benzine completely crystallized; yield 300 mg. (89%), m. p. 77~85°C. Upon recrystallization from petroleum benzine, it formed colorless plates, m. p. 97.5~98.5°C.

Found: C, 67.10; H, 6.94. Calcd. for $C_{21}H_{26}O_6$: C, 67.36; H, 7.00%.

Alkali Treatment of the Ketol VI.—A mixture consisting of 300 mg. of VI, 35 mg. of sodium and 5 ml. of ethanol was refluxed on a water bath for 4 hr. and was then acidified with glacial acetic acid. After removal of most of the ethanol, the residue

18) For the characteristic frequencies of enamine, see G. Opitz, H. Hellmann and H. W. Schubert, *Ann.*, **623**, 112 (1959).

19) A. L. Wilds and C. H. Shunk, *J. Am. Chem. Soc.*, **65**, 471 (1943).

20) E. Lederer and M. Lederer. "Chromatography", Elsevier Publishing Company, Amsterdam (1954), p. 22.

was diluted with water and extracted with chloroform three times. The united extracts were washed with an aqueous solution saturated with sodium chloride, dried over anhydrous sodium sulfate and then concentrated in vacuo. There remained a pale brown oil which was chromatographed on acid-washed alumina[20] (ca. 30 g.) packed and washed with benzene. One hundred and six fractions were collected as in the following table.

Fraction No.	Eluant	Residue
1— 15	Benzene-chloroform (1 : 1); 150 ml.	Colorless oil 24 mg.
16— 36	The same; 200ml.	Nil.
37— 46	Benzene-chloroform (1 : 2); 100 ml.	Colorless oil 8 mg.
47— 51	Benzene-chloroform (1 : 2); 100 ml.	Nil.
52— 61	Benzene-chloroform (1 : 3); 100 ml.	Colorless oil 10 mg.
62— 71	The same; 100ml.	Pale orange oil 7 mg.
72— 91	Chloroform, 200 ml.	Nil.
92— 96	Chloroform-ethanol (1 : 1); 50 ml.	Colorless oil 8 mg.
97—101	The same; 50 ml.	Colorless oil 120 mg.
102—106	The same; 50 ml.	Colorless oil 10 mg.

Treatment of the fractions numbered 97 through 101 with ether-petroleum ether yielded an amorphous product which could not be turned into a crystalline substance by any means. The substance was however submitted to elemental, infrared and N. M. R. analysis.

Found: C, 70.64; H, 6.45. Calcd. for $C_{17}H_{18}O_4$: C, 71.31; H, 6.34%.

Infrared absorption spectrum is reproduced in Fig. 6.

Summary

Ethyl 1, 2, 3, 4-tetrahydro-2-oxo-5-methoxy-1-naphthyl acetate (IIIb) has been synthesized. Condensation of IIIb with 1-diethylaminobutan-3-one methiodide afforded an anomalous product VI. Treatment of VI with isopropenyl acetate in the presence of *p*-toluenesulfonic acid gave rise to an acetate VIII, while on treatment with alkali and then with acid, a hydrophenanthrene lactone IX was obtained.

Department of Chemistry
Faculty of Science
Hokkaido University
Sapporo

Über die Kupfer-salze der ω-Aminosäure I. Zur Kenntnis des Kupfer-Glycins

Von Ken-ichi TOMITA

(Eingegangen am 23. Juli, 1960)

Für die Kristallanalyse der Kupfer-Komplexe von ω-Aminosäuren haben wir den Kupfer-Glycin-Komplex als erste Stufe der Versuchsmaterialien ausgewählt und einige physikalisch-chemischen Versuche mit diesem Material unternommen, weil das Glycin einerseits die einfachste ω-Aminosäure und andererseits die einfachste α-Aminosäure ist.

Wenn das Cu-Ion mit verschiedenen ω-Aminosäuren einen Komplex bildet, ist es strukturchemisch sehr interessant zu sehen welche Rolle das Cu-Ion bei dieser Komplexbildung spielt und welche räumliche Konfiguration die um Cu-Ion koordinierte Gruppe hat. Überdies ist es weit bekannt, daß Kupfersalze der ω-Aminosäuren so häufig Kristallwasser enthält (z. B., daß Kupfer-salze von β-Alanin, Isoserin und γ-Aminobuttersäure jeder für sich sechs, drei und zwei Kristallwassermoleküle haben). Deshalb ist es von Bedeutung für Chemiker zu wissen wie das Kristallwassermolekül auf den Prozess der Kristallbildung und der geometrischen Anordnung der um das Cu-Ion koordinierten Atome wirkt.

Bei der Kristallstrukturbestimmung der ω-Aminosäuren selbst ist es uns auch sehr wichtig festzustellen, ob die "Schwer-atom" Methode in der röntgenographischen Kristallanalyse auch für die Kupfer-salze der ω-Aminosäuren gültig ist.

Neben dieser strukturchemischen Wichtigkeit gibt es auch noch andere biochemischen Gründe, warum wir die Kupfer-salze der ω-Aminosäuren als Versuchsmaterie gewählt haben: die verschiedenen ω-Aminosäuren wurden neuerdings in der Natur entdeckt und ihre physiologisch-chemischen Bedeutungen werden

mit grossem Interesse verfolgt. Ausserdem ist die Funktion der Cu-Ionen in den Tierkörpern sehr wichtig. Einige Beispiele dafür seien hier aufgeführt.

1) In dem Blut der Mollusken und Arthropoden findet sich Hämocyanin, welches aus einem Cu-Ion und dem Porphyrin bestehendes Farbstoffprotein ist.
2) Ferner gibt es unter den Metallproteiden einige Oxydationsenzyme mit einem Cu-Ion, z. B., Tyrosinase, Polyphenoloxydase und Ascorbinsäure-oxydase[1].
3) Wie aus der Bakteriologie bekannt, fördert das Cu-Ion die bakteriziden Wirkungen des N-haltigen Heilmittels, Isonicotinsäure-hydrazid (INH) gegen den Tuberkelbazillus[2].

Darstellung des Kupfer-Glycins

Wenn man, wie bei der gewöhnlichen Darstellung[3] der Kupfersalze, eine wässerige Lösung von Glycin mit überschüssigem, gereinigtem Kupferhydroxyd im Wasserbad etwa 1 Stunde erhitzt und filtriert, so bekommt man eine tiefblaue Lösung. Um verschiedene Kristallisationen aus dieser Lösung zu erhalten, werden Ammonium-hydroxyd, Kohlensäure oder Methanol addiert; beim nachherigen Einengen des tiefblauen Filtrates scheidet sich daraus der Kupfer-Komplex entweder als tiefblauer, aus langer Nadel bestehender Kristall (Kristall I) oder als hellblauer pulveriger Kristall (Kristall II) ab.

a) Kristall I; tiefblaue, lange Nadel, die sich bei 213°C (unkorr.) zu verkohlen beginnt und sich bei 228°C unter Gasentwicklung zersetzt. Dieser Komplex enthält 1 Molekül Kristallwasser, das bei etwa 120°C nach 32 stündigem Erhitzen entweicht. Die Analyse gibt das folgende Resultat.
Gef. Cu, 28.12; C, 20.01; H, 4.39; N, 12.19; H_2O, 7.78. Ber. für $Cu(C_2H_4NO_2)_2-H_2O$(Mol. Gew. 229.54): Cu, 27.68; C, 20.91; H, 4.39; N, 12.19; H_2O, 7.84%.

b) Kristall II; hellblauer, pulveriger Kristall, der sich bei 222~225°C unter Gasentwicklung zersetzt. Aus den folgenden Analysendaten geht hervor, dass dieser Komplex 2 Moleküle Kristallwasser enthält, das nach 12 stündigem Erhitzen bei etwa 120°C grösstenteils entweicht. Gef. Cu, 27.67; C, 18.22; H, 4.36; N, 11.81; H_2O, 13.99. Ber. für $Cu(C_2H_4NO_2)_2+2H_2O$ (Mol. Gew. 247.54): Cu, 25.66; C, 19.39; H, 4.84; N, 11.31; H_2O, 14.54%.

Aus obiger Mikroanalyse bestätigt man dass das Kupfer-Glycin zwei Hydrate, nämlich Mono- und Di-hydrat, hat.

Differential-thermoanalyse des Kupfer-Glycins

Um die Kristallwassermenge von Kristall I und II auf andere Weise zu bestimmen, wurde die Entwässerungswärme beobachtet, die in einem gewissen Verhältnis zur Kristallwassermenge steht.

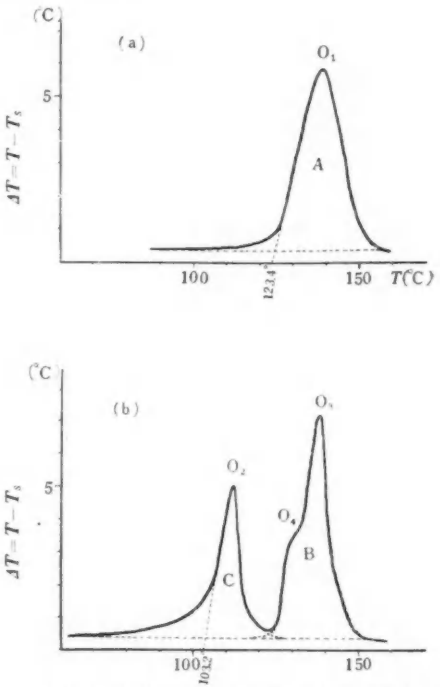

Abb. 1. Differential-thermoanalyse (DTA)-Kurven.
(a) Kupfer-Glycin-Monohydrat (Kristall I)
(b) Kupfer-Glycin-Dihydrat (Kristall II)
T: Temperatur von Normalsubstanz (Al_2O_3)
T_s: Temperatur von Versuchssubstanz.

Das Entweichen des Kristallwassers lässt sich leicht mit Hilfe der Differential-thermoanalyse (DTA) nachweisen und das Resultat wird in Abb. 1 gezeigt. Dabei gebrauchten wir Al_2O_3 als Normalsubstanz[4]. Bei dynamischem Erhitzen (z. B., 7.5°C/Min.) setzt die Reaktion für Kristall I bei $T=100$°C ein, durchläuft ein Maximum (O_1 in Abb. 1(a)) bei etwa $T=138$°C und klingt dann ab. Dieser endotherme Effekt wird durch die Entwässerung des 1 Molekülkristallwassers verursacht, welche durch die Messung der Verlustmenge von Kristallwasser nach der endothermen Reaktion bestätigt wird (Ber. 7.8%, Gef. 8.2%). Für Kristall II werden drei endotherme Reaktionen beobachtet, wie in Abb. 1(b) gezeigt, indem das erste Maximum

1) B. J. Ralph, *Rev. Pure and Appl. Chem.*, **4**, 85 (1954).
2) E. Sorkin, W. Roth und H. Erlenmeyer, *Helv. Chim. Acta*, **35**, 1736 (1952); J. Cymerman-Craig, G. N. Vaughan und D. Willis, *Nature*, **177**, 480 (1956).
3) E. Abderhalden und E. Schnitzler, *Z. physik. Chem.*, **163**, 96 (1927).
4) Über den automatischen Messungsapparat der Differential-thermoanalyse hat Herr H. Suga von unserem Institut eine baldige Veröffentlichung vorgesehen.

O_2 (Temperaturbereich von 80°C bis 120°C) durch die Bildung von Monohydrat (Verlustmenge: Ber. 6.5%, Gef. 7.8%) und das zweite Maximum O_3 durch das Entweichen von übrigem 1 Molekül-kristallwasser (Verlustmenge: Ber. 7.8%, Gef. 7.8%) verursacht wird.

Das Verhältnis der Entwässerungswärmemenge zwischen Kristall I und II wird wie dasselbe der Fläche zwischen Null-linie und DTA-Kurve beurteilt: d. h., das Verhältnis der Flächen zwischen A und B (Abb. 1(a) und 1(b)) ist ungefähr 1:1, dagegen ist das der Fläche zwischen A und C (Abb. 1(a) und 1(b)) ungefähr 1:0.58.

Daraus läßt sich ersehen, daß das erste Kristallwassermolekül von Kristall II leichter entwässert wird als das zweite Kristallwassermolekül von Kristall II. Die zwei Kristallwassermoleküle des Kupfer-Glycin-Dihydrates (Kristall II) unterscheiden sich voneinander durch ihre Verbindungsweise.

Es unterliegt also keinem Zweifel, daß es in Kupfer-Glycin-Komplexen zwei Hydrate gibt, nämlich Mono- und Di-hydrat.

Wie in Abb. 1 ersichtlich ist, ist die Entwässerungstemperatur für Kristall I (Maximum O_1) 123.4°C, und für Maximum O_2 des Kristall II 103.2°C. Für Maximum O_3 des Kristall II

TABELLE I. BEUGUNGSWINKEL UND NETZEBENENABSTÄNDE

Kristall I vor Entwässerung		Kristall I und II nach Entwässerung		Kristall II vor Entwässerung	
2θ	d, Å	2θ	d, Å	2θ	d, Å
10°30′	8,42	10°15′	8,62	12°00′	7,37
13 10	6,72	13 30	6,65	18 00	4,92
15 30	5,71	20 10	4,40	18 25	4,82
16 25	5,39	20 25	4,35	19 20	4,59
17 40	5,02	22 30	3,95	21 35	4,11
18 20	4,84	25 50	3,44	22 35	3,93
19 00	4,67	26 30	3,36	23 00	3,86
20 10	4,40	27 10	3,28	24 50	3,58
21 10	4,20	28 25	3,14	26 05	3,41
23 10	3,84	30 45	2,90	29 45	3,00
23 45	3,74	31 15	2,86	30 35	2,92
24 40	3,61	32 20	2,77	31 10	2,87
25 35	3,48	33 30	2,67	34 30	2,60
28 05	3,18	33 50	2,65	35 30	2,53
29 10	3,06	34 50	2,57	37 25	2,40
31 00	2,88	35 40	2,52	39 10	2,30
31 35	2,83	36 15	2,48	40 15	2,24
33 10	2,70	37 00	2,43	41 10	2,19
33 50	2,65	38 20	2,35	41 25	2,18
35 45	2,51	40 00	2,25	41 55	2,15
36 20	2,47	40 15	2,24	42 20	2,13
37 40	2,39	40 45	2,21	43 50	2,06
38 05	2,36	41 15	2,19	44 30	2,03
39 00	2,31	42 20	2,13	45 55	1,97
39 55	2,26	42 55	2,11	47 00	1,93
40 45	2,21	44 05	2,05	48 45	1,87
42 55	2,11	45 00	2,01	49 15	1,85
43 30	2,08	46 35	1,95	50 30	1,81
44 00	2,06	48 45	1,87	51 35	1,77
44 40	2,03	50 10	1,82	52 40	1,74
45 30	1,99	51 55	1,76	53 35	1,71
46 30	1,95	52 55	1,73	56 50	1,62
47 20	1,92	53 30	1,71	57 25	1,60
47 40	1,91	54 20	1,69		
48 40	1,87	55 55	1,64		
49 20	1,85				
51 00	1,79				
52 55	1,73				
53 30	1,71				

können wir aber die genaue Entwässerungstemperatur nicht festlegen, weil es noch ein anderes flaches Maximum O_1 zwischen 125°C und 130°C gibt, das vielleicht irgendeine Umwandlung im Kristall anzeigt.

Röntgenographische Untersuchungen des Kupfer-Glycins nach Debye-Scherrer'scher Pulver-Methode

Von den röntgenographischen Untersuchungen der Kristalle I und II, und ihrer kristallwasserfreien Materie mußten wir uns auf die Debye-Scherrer'sche Pulver-Methode beschränken, weil es sehr schwierig war, einen Einkristall von Kristall II mit geeigneter Grösse zu bekommen. Bei dieser Untersuchung wurde die gewöhnliche zylindrische Kamera (Kameraradius: 50.6 mm) angewandt. Die Versuchsmaterien (Kristalle I und II) wurden

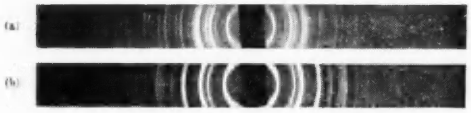

Abb. 2.

(a) Kupfer-Glycin-Monohydrat
(b) Kupfer-Glycin-Dihydrat

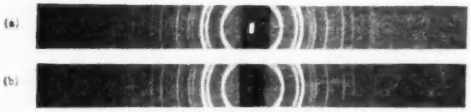

Abb. 3.

(a) Nach Entwässerung des Kristallwassers von Kupfer-Glycin-Monohydrat
(b) Nach Entwässerung des Kristallwassers von Kupfer-Glycin-Dihydrat

in die Glaskapillaren gepackt und nach Debye-Scherrer'scher Methode aufgenommen (Abb. 2). Nach etwa halb-stündigem Erhitzen bei 150°C im Vakuum wurden die Substanzen in diesen Kapillaren entwässert, sofort eingeschlossen und wieder photographiert. Abb. 3 zeigt die Debye-Scherrer'schen Aufnahmen nach Entzug des Kristallwassers.

Bei der Anwendung Norelco Diffraktometers (North American Philips Gesellschaft) wurden auch die Pulver-Diagramme von Kristallen I und II vor und nach Entwässerung erhalten und davon wurden die Beugungswinkel (2θ) und die Netzebenenabstände (d) jeder Reflexion festgesetzt (Tabelle I).

Aus den obigen experimentalen Ergebnissen können die folgenden Schlussfolgerungen gezogen werden.

1) Die Kristallstrukturen der Kristalle I und II unterscheiden sich voneinander.
2) Bei der Entweichung des Kristallwassers zeigen die Debye-Scherrer'sche Aufnahmen von Kristallen I und II eine vollkommene Übereinstimmung, d. h., Kristalle I und II haben nach Entzug des Kristallwassers die gleiche Kristallstruktur.
3) Bei der Benutzung von Tabelle I und Hull-Davey-Harrington'schen Kurven[5] wurde vorausgesehen, daß Kristall I vor Entwässerung zu dem rhombischen System gehört, während Kristall II vor Entwässerung und Kristalle I und II nach Entzug des Kristallwassers nicht zu den vier Systemen (isometrischen, tetragonalen, hexagonalen, und rhombischen Systemen) gehören.

Infrarotspektroskopische Untersuchungen des Kupfer-Glycins

Die Spektren wurden mittels eines Hilger H-800 Doppelstrahlspektrophotometers mit Kochsalz-optik bei Zimmertemperatur (23°C) untersucht. Die in Nujol (Messungsbereich von 650 cm^{-1} bis 2000 cm^{-1}) oder Daifloil (Messungsbereich von 1500 cm^{-1} bis 4500 cm^{-1}) suspendierten Substanzen von Kristallen I und II wurden benutzt (Abb. 4). Die Wellenzahlen jeder spektralen Lage von Kristallen I und II sind in der ersten und dritten Reihe von Tabelle II wiedergegeben.

Von S. Mizushima et al.[6] wurden infrarotspektroskopische Untersuchungen des Kupfer-

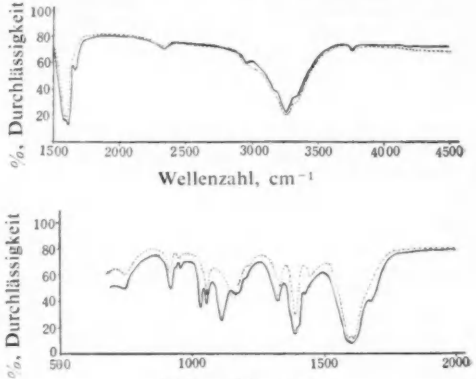

Abb 4. Infrarotabsorptionsspektren des Kupfer-Glycins.
——: Kupfer-Glycin-Monohydrat (Kristall I).
------: Kupfer-Glycin-Dihydrat (Kristall II).

5) J. C. Bell und A. E. Austin, „Battelle Indexing Charts for Diffraction Patterns of Tetragonal, Hexagonal and Orthorhombic Crystals", Battelle Memorial Institute, Columbus 1, Ohio, U. S. A.
6) D. N. Sen, S. Mizushima, C. Curran und J. V. Quagliano, *J. Am. Chem. Soc.*, **77**, 211 (1955).

TABELLE II.

Kupfer-Glycin-Monohydrat (Kristall I) Wellenzahl cm^{-1}	Zuordnung nach K. Nakamura	Kupfer-Glycin-Dihydrat (Kristall II) Wellenzahl cm^{-1}
745	COO-Scherenschwingung.	745
924	*sym.* C-N-Valenzschwingung +	917
935	CH_2-Schaukelschwingung.	—
959		948
1036	*antisym.* C-N-Valenzschwingung +	—
1057	NH_2-Torsionsschwingung.	1059
1118	NH_2-Nickschwingung	—
—		1152
1167		—
1179	CH_2-Torsionsschwingung.	—
1194		1201
1323	CH_2-Nickschwingung.	1319
—		1333
1391	*sym.* COO-Valenzschwingung.	1391
1403		—
1424	CH_2-Scherenschwingung.	1435
1580		—
1592	*antisym.* COO-Valenzschwingung +	1590
1605	NH_2-Scherenschwingung.	1610
1672	Scherenschwingung von Kristallwasser.	—
2325		2325
2935		2935
—		2980
3165		3165
3254		3254
3320		3300
3754		3754

Glycin-Monohydrates und Nickel-Glycin-Dihydrates durchgeführt. Ihre Messergebnisse über das Kupfer-Glycin-Monohydrat stimmen mit unserem Ergebnis des Kristall I überein.

K. Nakamura[7] hat neulich die Isotopenverschiebungen der Infrarotspektren des Kupfer-Glycin-Monohydrates beim Substituieren des Wasserstoffs von Kristallwassermolekül und den CH_2- und NH_2-Gruppen des Glycinmoleküls durch das Deuterium untersucht und er hat die genauen Zuordnungen über jede Spektren ausgeführt, die in der zweiten Reihe von Tabelle II gezeigt werden.

Die Infrarotabsorptionsspektren von Kristall II sind etwas anders als Kristall I (vgl. Abb. 4 und Tabelle II).

Die infrarotspektroskopischen Unterschiede von Kristallen I und II beruhen, im allgemeinen gesagt, auf den Unterschieden der beiden Kristallsysteme, der Symmetrieeigenschaften von beiden Molekülen, der Zahlen des Kristallwassermoleküls, usw.

Ausgegangen nur von dem Unterschied der geometrischen Konfiguration von Molekül, d. h., cis und trans Konfiguration[8], muß sich deutlich dieser Unterschied in dem Band von symmetrischer COO-Valenzschwingung (Bereich: 1300 $\sim$1420 cm^{-1}) und in den Bändern von NH_2-Schaukelschwingung und COO-Deformationsschwingung (Bereich: 400$\sim$700 cm^{-1}, und diese Bänder können mit KBr-optik beobachtet werden) zeigen.

Bei der Benutzung unserer Messergebnisse über das Spektrum der symmetrischen COO-Valenzschwingung können wir den Unterschied der geometrischen Konfiguration von Kristallen I und II betrachten. Wenn das Kupfer-Glycin-Molekül eine cis oder trans Konfiguration hat, so gibt es folgende vier symmetrische COO-Valenzschwingungen:

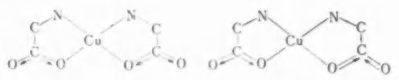

(I) (II)

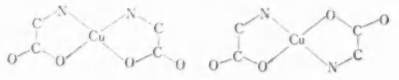

(cis) (trans)

7) K. Nakamura, *J. Chem. Soc. Japan, Pure Chem. Sec.* (*Nippon Kagaku Zasshi*), (in der Presse).

8) In diesem Fall bedeuten die cis und trans Konfigurationen den folgenden geometrischen Anordnungsunterschied der um zentrales Cu-Atom eben koordinierten N und O von zwei Glycin-Molekülen:

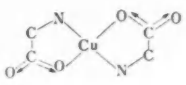

(III)

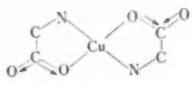

(IV)

Während dabei (I), (II) und (IV) alle ultrarotaktiv sind, ist aber (III) ultrarot-inaktiv. Es zeigt, dass der Kristall mit cis Konfiguration zwei symmetrische COO-Valenzschwingungen hat, während der Kristall mit trans Konfiguration nur einen Band hat.

Benutzt man diese Annahme auf Kristall I und II, so zeigt Kristall I zwei Spektren von symmetrischer COO-Valenzchwingung bei 1391 cm^{-1} und 1403 cm^{-1}, während bei Kristall II nur ein Spektrum bei 1391 cm^{-1} beobachtet wird. Demnach vermuten wir, dass Kristall I eine cis Konfiguration und Kristall II eine trans Konfiguration hat.

Rosenberg[9] hat schon beobachtet, dass der Unterschied zwischen cis und trans Konfiguration von Metall-Komplexen der verschiedenen Aminosäuren in den Infrarotabsorptionsspektren bei der Temperatur von flüssiger Luft (−170°C)in den Gebieten von 3μ und 6μ(NH_2-Valenzschwingungsband und antisymmetrischer COO-Valenzschwingungsband) erscheint. Aus unseren Messergebnissen konnten wir aber den Unterschied zwischen cis und trans Konfiguration in dieser Gebieten nicht feststellen, weil unsere Beobachtung nur bei Zimmertemperatur durchgeführt wurde und der gebrauchte Apparat kein genügendes Auflösungsvermögen hat, um die Differenz der Zahl der Spektren und die Verschiebung der Wellenzahl von cis und trans Konfigurationen in diesen breiten Bändern zu bestimmen.

Schluss

Aus der obigen physikalisch-chemischen Untersuchung können wir die folgenden Schlüsse ziehen:

1) Bei Zimmertemperatur hat das Kupfer-Glycin zwei Hydrate, nämlich Mono- und Di-hydrat. Von diesen beiden ist das Kupfer-Glycin-Dihydrat (Kristall II), worüber bis heute keine Mitteilung erschien, ein neu gefundenes Hydrat.
2) Mit Hilfe der Differential-thermoanalyse findet sich, dass das Kupfer-Glycin-Monohydrat (Kristall I) eine endothermische Reaktion wegen der Entwässerung eines Kristallwassermoleküls zeigt, während die endothermischen Reaktionen des Kupfer-Glycin-Dihydrates (Kristalls II) drei Maxima haben, zwei davon durch die Entwässerungen von zwei Kristallwassermolekülen entstehen, und ein übriges Maximum vielleicht wegen irgendeiner Umwandlung im Kristall vorkommt. Die Entwässerungstemperaturen sind 123.4°C für Kristall I und 103.2°C für erstes Maximum von Kristall II, aber wir können die genauen Entwässerungstemperaturen für die zweite und dritte Maxima von Kristall II wegen der Überlappung der zwei Maxima nicht feststellen. Aus Kristall II wird das erste Kristallwassermolekül leichter entwässert als das zweite Kristallwassermolekül.
3) Das Kristallsystem des Kupfer-Glycin-Monohydrates (Kristalls I) gehört vor Entwässerung zu dem rhombischen System, das Kristallsystem des Kupfer-Glycin-Dihydrates (Kristalls II) ist aber vor Entzug des Kristallwassers noch nicht feststellbar. Nach Entwässerung haben diese beiden Kristalle die gleiche Kristallstruktur miteinander.
4) Von der infrarotspektroskopischen Untersuchung können wir vermuten, dass das Kupfer-Glycin-Monohydrat (Kristall I) eine cis Konfiguration hat, und das Kupfer-Glycin-Dihydrat (Kristall II) eine trans Konfiguration hat.
5) Aus der Tatsache des gleichzeitigen Entstehens zwei verschiedener Kristalle (Kristalle I und II) aus wässeriger Lösung wird vorausgesehen, dass die Differenz der freien Energie beider Hydrate also sehr klein ist und in wässeriger Lösung die zweierlei Komplexmoleküle (mit cis Konfiguration einerseits, und mit trans Konfiguration andererseits) vermutlich existieren.

Es scheint uns, dass die Strukturbestimmung dieser zwei Hydrate nicht nur zur Erweiterung der Kenntnis des geometrischen Verbindungszustandes des Glycin-Moleküls im Kristall, sondern auch zur Kenntnis der Wirkungsarten des Kristallwassermoleküls sehr wünschenswert ist.

Herrn Professor Dr. I. Nitta danke ich herzlichst für mannigfache Anregungen und seine Unterstützung bei der Durchführung dieser Arbeit, insbesondere für seine freundlichen Diskussionen. Mein Dank gilt auch Dr. Y. Sasada für seine hilfreichen Ratschläge bei der Durchführung dieser Arbeit. Zu danken habe ich ferner Dr. H. Suga für seine freundliche Mitwirkung bei Benutzung des Messungsapparates der Differential-thermoanalyse und den Herren T. Shiba, T. Inui und

9) A. Rosenberg, *Acta Chem. Scand.*, **10**, 840 (1956).

M. Okumiya und Fräulein K. Koike für ihre Messungen von Mikroanalyse und Infrarotspektren.

Chemisches Institut
Naturwissenschaftliche Fakultät
Universität Osaka
Kita-ku, Osaka

Über die Kupfer-salze der ω-Aminosäure. II. Über die Kristallstruktur des Kupfer-Glycin-Monohydrates

Von Ken-ichi TOMITA und Isamu NITTA

(Eingegangen am 23 Juli, 1960)

Wie schon in Teil I gesagt[1], hat das Kupfer-Glycin zwei Hydrate, Mono- und Di-hydrat, die sich durch die Kristallstruktur unterscheiden. Während diese beiden Kristallstrukturen durch die röntgenographischen Untersuchungen bestimmt werden können, wurde zunächst das Kupfer-Glycin-Monohydrat (Kristall I in Teil I) als Strukturbestimmungsmaterie genommen, weil ein reiner Einkristall von Kupfer-Glycin-Dihydrat (Kristall II in Teil I) schwer zu bekommen war.

Vor kurzem erschien eine Mitteilung von Stosick[2,3], dass sowohl Nickel-Glycin-Dihydrat als auch Kupfer-*dl*-α-Aminobuttersäure eine plane trans Konfiguration haben. Schon vorher haben wir durch unsere infrarotspektroskopischen Untersuchungen[1] vermutet, daß das Kupfer-Glycin-Monohydrat eine plane cis Kofiguration und das Kupfer-Glycin-Dihydrat eine plane trans Konfiguration hat.

Im Anschluss daran haben wir die Kristallanalyse von Kupfer-Glycin-Monohydrat mit der röntgenographischen Methode unternommen, das Verhalten des Kristallfeldes um das zentrale Metallatom zu untersuchen, deren Ergebnisse im folgenden mitgeteilt werden.

Experimentelles

Bei der gewöhnlichen Darstellungsmethode, wie schon in Teil I gesagt[1], konnte man der Kristall von Kupfer-Glycin-Monohydrat erhalten; die Grösse der angewandten Kristallnadeln bei der röntgenographischen Untersuchung ist ungefähr 0.2 mm × 0.2 mm × 0.6 mm. Mittelst der Oszillationsmethode, wobei die mit dünner Ni-Folie filtrierte CuK_α-Strahlung ($\lambda_{CuK\alpha}=1.542$ Å) gebraucht wurde, konnten die Gitterkonstanten dieses Kristalls wie folgt ausgemessen werden.

$$a=10.78\pm0.01\text{ Å}$$

$$b=5.208\pm0.004\text{ Å}$$

$$c=13.47\pm0.02\text{ Å}$$

Dabei wurden die genauen Werte der Gitterkonstanten nach der folgenden Methode bestimmt.

Bei der Benutzung des Norelco-Diffraktometers (von North American Philips Gesellschaft geliefert) haben wir zuerst die Beugungswinkel $2\theta_0$ von acht Reflexionen des pulverigen Silikon-Kristalls (normale Materie) beobachtet. Von dem Diagram des Winkels $2\theta_0$ versus $\Delta(2\theta)=2\theta_s-2\theta_0$, wobei Winkel θ_s den normalen Wert der Reflexion des Silikons (nach der Tabelle von Norelco-Gebrauchsanleitung) zeigt, wurde der Nullpunkt-fehler des Norelco-Diffraktometers mit der Methode der kleinsten Quadrate korrigiert. Zunächst wurden die Bragg-Winkel von acht Reflexionen des Kupfer-Glycin-Monohydrates beobachtet, die in dem Gebiet $10°<2\theta_0<20°$ erschienen, und nach der Berichtigung des Nullpunkt-fehlers, wie oben gesagt, wurden die genauen Werte der Gitterkonstanten mit der Methode der kleinsten Quadrate festgestellt.

Die Dichte dieses Kristalls beträgt nach einer Messung mittels der Schwebemethode (Äthylen-Dibromid/Benzol-Gemisch) bei 15°C 1.998 g/cc. Aus diesem Wert kann man annehmen, daß vier Moleküle von der Formel $Cu(C_2H_4NO_2)_2{\cdot}H_2O$ in jedem Zellinhalt vorhanden sind (Die röntgenographishe Dichte dieses Kristalls beträgt 2.016 g/cc).

Die Auswertung der Weissenberg- und Sauter-Aufnahmen ergab folgende Auslöschungsgesetze:

(hkl) in allen Ordnungen vorhanden,
($h00$), ($0k0$) und ($00l$) jeder für sich nur mit $h=2n$, $k=2n$ und $l=2n$ vorhanden.

Diese Auslöschungen kommen nur in der Raumgruppe D_2^4-$P2_12_12_1$ vor.

Mittels Äquator-Weissenberg-Aufnahmen um [010], [100] und Schwenkaufnahme um [001] mit CuK_α-Strahlung (Ni-Folie) werden die Intensitäten nach der „multiple-film method" aus vier Filmen im Vergleich zu einer Intensitätsskala geschätzt, und das Verhältnis der relativen Intensitäten von stärkster Reflexion zu schwächster Reflexion war ungefähr 3000 : 1 für ($h0l$) Zone, 1800 : 1 für ($0kl$) Zone, und 120 : 1 für ($hk0$) Zone. Unberücksichtigt

1) K. Tomita, Diese Zeitschrift, **34**, 280 (1961).
2) A. J. Stosick, *J. Am. Chem. Soc.*, **67**, 365 (1945).
3) A. J. Stosick, ebenda **67**, 362 (1945).

der Absorption und Extinktion wurden die Lorentz-Polarizationsfaktoren und die $(\sin\theta/\lambda)$-Werte für die einzelnen Reflexe mit der gewöhnlichen Weise ermittelt. Die totalen Zahlen der unabhängigen Äquator-Reflexionen, die in der Ausbreitungskugel enthalten sind, sind 190 für [010]-Projektion, 92 für [100]-Projektion und 74 für [001]-Projektion, während die beobachteten Zahlen jeder für sich 170, 75 und 26 sind.

Strukturbestimmung

Es wurde eine Pattersonprojektion nach [010] gerechnet, die in Abb. 1 wiedergegeben ist. Eine „zugespitzte" („sharpened")[4] Synthese unter Verwendung „unitärer" Atomformamplituden wurde ausgeführt. Berücksichtigt man

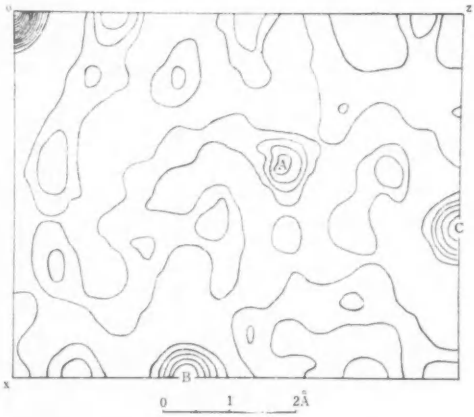

Abb. 1. „Zugespitzte" Pattersonprojektion nach [010].

die Raumgruppe und die Zahl der Formeleinheiten in der Elementarzelle von diesem Kristall, können alle Metallatome (Cu-Atome) eine allgemeine Lage in der Elementarzelle einnehmen. Aus den Maxima A, B und C in der Pattersonprojektion nach [010] kann aber der x- und z-Parameter des Kupferatoms leicht gefunden werden.

Raumgruppe D_2^1 $P2_12_12_1$ hat kein symmetrisches Zentrum im Kristall. Wird für jede Projektion dabei der Anfangspunkt auf der 2_1-Achse aufgewährt, so steht dieser Anfangspunkt auf symmetrischem Zentrum in Projektion. Dann wurde eine vorläufige Fouriersynthese mit 87 $(h0l)$-Reflexen gerechnet (Abb. 2), und die Vorzeichen jedes Reflexes wurden von der mit Parameterswert des Cu-Atoms gerechneten Strukturfaktoren geführt. (Von den gebrauchten 87 Reflexen veränderten im

4) H. Lipson und W. Cochran, „The Determination of Crystal Structures", G. Bell & Sons, London (1953), S. 170.

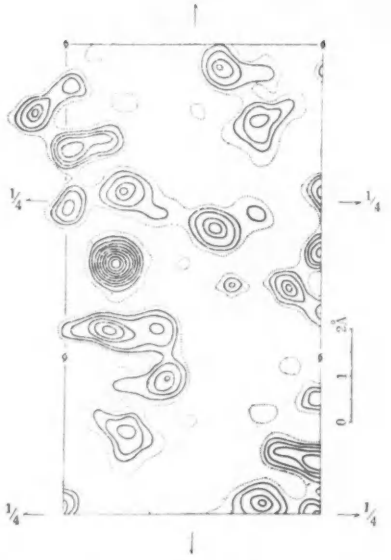

Abb. 2. Erste Fourierprojektion nach [010]. Es wurde die für die Kupferlagen berechneten Vorzeichen eingesetzt (Methode des schweren Atoms).

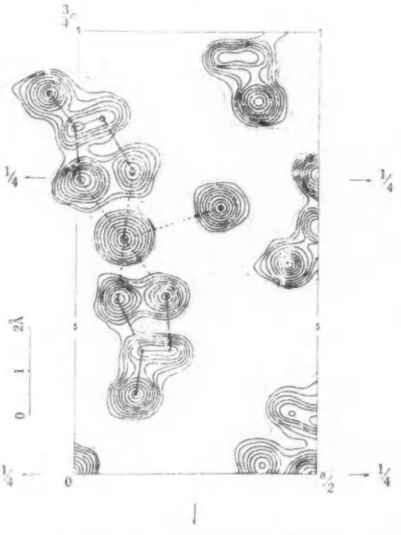

Abb. 3. Elektronendichteprojektion nach [010]. Das punktierte Niveau der Kurven geht durch $2\,e/Å^2$ und die Kurven gleicher Elektronendichte liegen um $1\,e/Å^2$ auseinander, ausgenommen in den Kupfermaxima, wo die Äquidistanz $5\,e/Å^2$ beträgt.

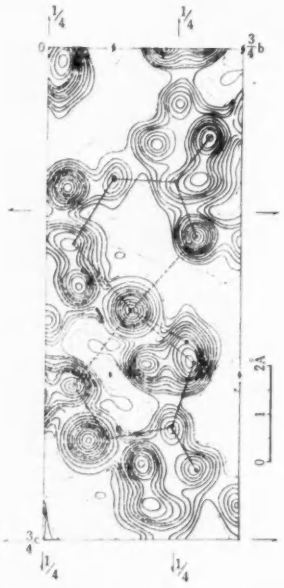

Abb. 4. Elektronendichteprojektion nach [100]. Das punktierte niedrigste Niveau der Kurven liegt bei $3\,e/\text{Å}^2$ und die Kurven gleicher Elektronendichte sind in Abständen von $1\,e/\text{Å}^2$ gezeichnet, von den Cu-Maxima abgesehen, wo diese Äquidistanz fünfmal grösser ist.

Vergleich zu den endgültigen F_c-Werten nur 7 Reflexe die Vorzeichen.)

Zur Berechnung der Strukturamplituden wurde die Atomstreukurve für Cu nach Berghuis et al.[5] gebraucht, die mit der genauen Berechnungsmethode gefunden wurde und im Vergleich zu den Werten von „Internationalen Tabellen„[6] bei weitem die besseren Werte zeigt. Für C, N und O benutzen wir die Atomstreukurven nach McWeeny[7].

Der y-Parameterswert des Kupferatoms kann auch mit der Pattersonsynthese nach [100] in gleicher Weise wie mit derselben nach [010] leicht gefunden werden. Die Parameterswerte von anderen leichten Atomen wurden schrittweise mit Fouriersynthese und sukzessiver Näherung („trial-and-error" method) gefunden und verfeinert, wie in Tabelle I gezeigt. Der Abbruchsfehler von Parameterswerten wurde im Vergleich von F_0- und F_c-Synthesen nach [010] und [100] korrigiert; dabei sind die Zahl und Vorzeichen der Reflexe von F_0- und F_c-Synthesen selbstverständlich gleich, und die Lagen der Maxima (Atome) von F_0- und F_c-Synthesen wurden nach Booth-Methode[8] gerechnet. Die letzten absoluten Fourierprojektionen nach [010] und [100] zeigen sich in Abb. 3 und 4, während die letzte absolute Fourierprojektion nach [001] nicht gezeigt wurde. Die isotropischen B-Werte nach [010], [100] und [001] betragen jeder für sich 3.0, 2.8 und 2.5. Werden die nicht beobachteten Reflexe berücksichtigt, so beträgt der Zuverlässigkeitsfaktor ($R=\Sigma||F_0|-|F_c||/\Sigma|F_0|$) 0.16 für [010]-Projektion und 0.17 für [100]-Projektion. Für [001]-Projektion wurde $R=0.17$ gerechnet; dabei wurden die aus dem Projektionen nach [010] und [100] gefundenen Parameterswerte und die beobachtbaren Reflexe benutzt. Die mit diesen endgültigen Parameterswerten (Tabelle I) berechneten F_c und die beobachteten F_0 sind graphisch in Abb.

TABELLE I. PARAMETER

Atomart	x/a	y/b	z/c
Cu	0.102	0.339	0.400
N^{I}	0.185	0.110	0.302
N^{II}	0.129	0.113	0.516
O_1^{I}	0.083	0.572	0.290
O_2^{I}	0.119	0.620	0.131
O_1^{II}	0.016	0.572	0.490
O_2^{II}	−0.064	0.582	0.648
O_3	0.292	0.538	0.450
C_1^{I}	0.191	0.252	0.210
C_2^{I}	0.126	0.494	0.211
C_1^{II}	0.058	0.233	0.598
C_2^{II}	0.004	0.487	0.578

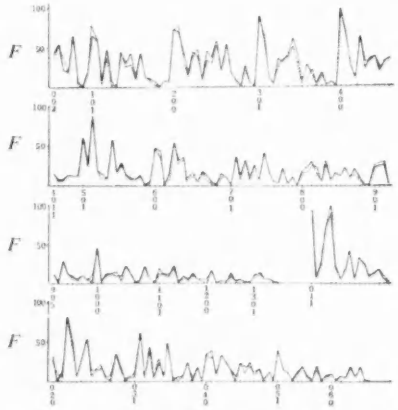

Abb. 5. Vergleich der beobachteten und berechneten F-Werte.
(——: F_0, – – – –: F_c)

5) J. Berghuis, I. M. Haanappel, M. Potters, B. O. Loopstra, C. H. MacGillavry und A. L. Veenendaal, *Acta Cryst.*, **8**, 478 (1955).

6) „Internationale Tabellen zur Bestimmung von Kristallstrukturen", Bornträger, Berlin (1935).

7) R. McWeeny, *Acta Cryst.*, **4**, 513 (1951).

8) A. D. Booth, "Fourier Technique in X-ray Organic Structure Analysis", Cambridge at the University Press (1948), S. 62.

5 zusammengestellt, wobei sich die F_c auf vier Formeleinheiten in der Elementarzelle beziehen.

Zur Bestätigung der gefundenen Parameter wurde für jedes Atom und jede Bindungslänge noch mittlere Fehler nach Cruickshank[9] wie folgt gerechnet:

$\sigma(x) \fallingdotseq 0.005$ Å, $\sigma(y) \fallingdotseq 0.006$ Å,
$\sigma(z) \fallingdotseq 0.006$ Å für Cu,
$\sigma(x) \fallingdotseq 0.030$ Å, $\sigma(y) \fallingdotseq 0.025$ Å,
$\sigma(z) \fallingdotseq 0.030$ Å für N,
$\sigma(x) \fallingdotseq 0.025$ Å, $\sigma(y) \fallingdotseq 0.027$ Å,
$\sigma(z) \fallingdotseq 0.029$ Å für O,
$\sigma(x) \fallingdotseq 0.034$ Å, $\sigma(y) \fallingdotseq 0.043$ Å,
$\sigma(z) \fallingdotseq 0.043$ Å für C,

für Bindungslänge;

$\sigma(r) \fallingdotseq 0.03$ Å für Cu—N,
$\sigma(r) \fallingdotseq 0.03$ Å für Cu—O,
$\sigma(r) \fallingdotseq 0.06$ Å für N—C,
$\sigma(r) \fallingdotseq 0.06$ Å für C—C,
$\sigma(r) \fallingdotseq 0.05$ Å für C—O,
$\sigma(r) \fallingdotseq 0.04$ Å für O—O,
$\sigma(r) \fallingdotseq 0.04$ Å für N—O.

Beschreibung der Struktur und Diskussion

Die Projektionen der Atomschwerpunkte nach [010] und [001] sind jeder für sich in Abb. 6 und 7 wiedergegeben. Die interatomaren Abstände und Bindungswinkel werden auch in Abb. 6 und 7 gezeigt.

Wie schon in Abb. 6 und 7 deutlich gezeigt, haben die um das zentrale Metallatom (Cu-Atom) koordinierten vier Atome der zwei Glycin-Molekülen (d. h., O_1^I, O_1^{II}, N^I und N^{II}) in Beziehung auf dem zentralen Metallatom eine plane cis Konfiguration; das Kupfer-Glycin-Monohydrat hat eine andere Kristallstruktur als wie in Nickel-Glycin-Dihydrat, das eine plane trans Konfiguration hat.

Um das zentrale Metallatom wurde ein entstellter Oktaeder mit sechs Atomen, d. h., O_1^I, O_1^{II}, N^I, N^{II}, O_3 (ein Sauerstoffatom von Kristallwassermolekül) und O_2^I (ein Sauerstoffatom der COO-Gruppe von einem anderen Salz, welches mit 2_1-Achse zu dem zentralen Metallatom koordiniert wird) gebildet. In diesem entstellten Oktaeder gibt es eine intramolekulare Wasserstoffbindung zwischen N^{II} und O_3 und damit wird O_3 Atom nach einem Glycin-Molekül (II) mehr oder weniger gezogen.

Von den infrarotspektroskopischen Untersuchungen haben schon Mizushima et al.[10] folgendes geschlossen: das Kupfer-Glycin-Monohydrat (Kristall I) hat wie Nickel-Glycin-Dihydrat eine plane trans Konfiguration, die mit *sp* Hybridisation geradlinig gebildet ist, und die Bindung zwischen COO-Gruppe von zwei Glycin-Molekülen und ein zentrales Metallatom (Cu-Atom) ist wesentlich eine Ionenbindung. Das Resultat unserer röntgenographischen Kristallanalyse stimmt aber nicht gänzlich mit ihrer Schlussfolgerung überein: das Kupfer-Glycin-Monohydrat hat eine um das zentrale Metallatom gebundene plane cis Konfiguration und deshalb können wir die Bindung zwischen der COO-Gruppe und dem zentralen Metallatom mit sp Hybridisation nicht anerkennen. Es scheint uns, dass diese, um das zentrale Metallatom gebildeten Bindungen auf dsp^2 oder d^2sp^3 Hybridisation beruhen, so daß ein planes Quadrat mit O_1^I, O_1^{II}, N^I und N^{II} gebildet wird.

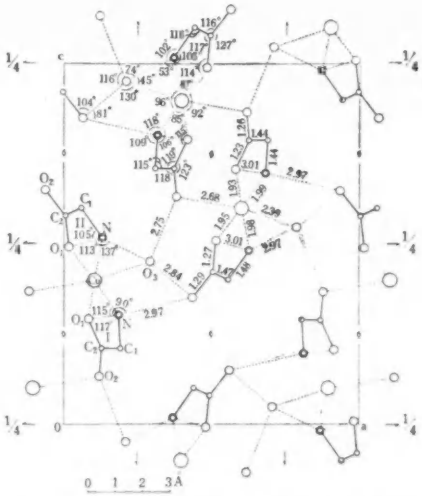

Abb. 6. Schematische Projektion der Atomschwerpunkte nach [010].

Die interatomaren Abstände von Cu—O_3 und Cu—O_2^I weichen miteinander über die Grenze von mittlerem Fehler ab: dieser Unterschied wird vielleicht auf den folgenden Ursachen basieren, nämlich auf den Unterschied der molekularen Anordnungsweisen, der Ioneneigenschaften und der Zahlen der Wasserstoffbindung von O_3 und O_2^I, die jedes Sauerstoffatom (O_3 und O_2^I) bilden kann.

Wenn die Bildung von Cu—O_1^I (oder Cu—O_1^{II}) wesentlich den Ionencharakter hat, soll sich diese Bindungslänge zwischen Cu und O_1^I (oder O_1^{II}) im Vergleich zu der Kovalenzbindungslänge ziemlich verändern. Bis heute ist

9) D. W. J. Cruickshank, *Acta Cryst.*, **2**, 65 (1949).

10) D. N. Sen, S. Mizushima, C. Curran und J. V. Quagliano, *J. Am. Chem. Soc.*, **77**, 211 (1955).

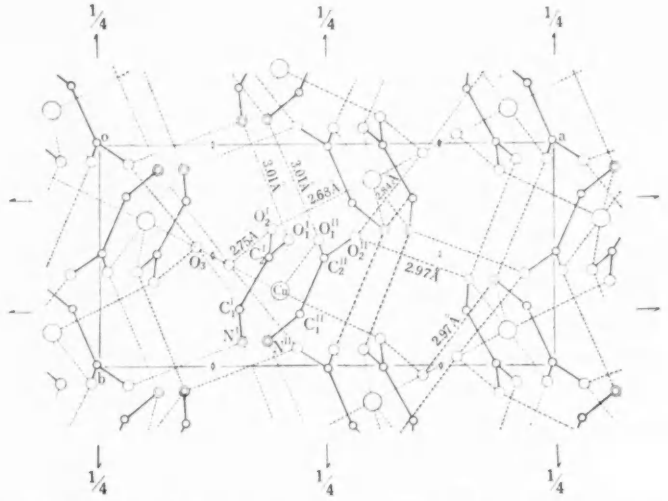

Abb. 7. Schematische Projektion der Atomschwerpunkte nach [001].

das genaue Resultat über den Ionenradius von Cu^{2+}-Ion noch nicht veröffentlicht geworden[11], und es ist undenkbar, dass das Cu^{2+}-Ion die vollkommende Kugel-Konfiguration hat, wenn sich das Cu^{2+}-Ion mit anderen Atomen im Kristall verbindet. Damit ist es unmöglich, den Unterschied zwischen Ionen- und Kovalenzradius über die Bindung von Cu—O_1^I (oder Cu—O_1^{II}) zu vergleichen und die Menge des Ionencharakters von Cu—O_1^I (oder Cu—O_1^{II}) Bindung zu bestimmen.

Werden auch die Verbindungsweise berücksichtigt, müssen sich die interatomaren Abstände von Cu—O_1^I (oder Cu—O_1^{II}) und Cu—N^I (oder Cu—N^{II}) sichtbar voneinander verändern, weil das Cu-Atom einerseits mit Stickstoffatom eine Kovalenzbindung oder Koordinationsbindung bildet und andererseits mit Sauerstoffatom von COO-Gruppe zum Teil eine Ionenbindung und zum Teil eine Kovalenzbindung bildet. Wir konnten aber den Unterschied von diesen beiden Bindungslängen nicht erklären, weil der Unterschied von beiden beobachteten Abständen weniger als die Grenze von einem mittlerem Fehler war.

Wie in Abb. 6 und 7 gezeigt, formiert der zentrale Cu-Atom mit O_2^I von einem anderem Molekül die Cu—O_2^I-Bindung und das Molekül von Kupfer-Glycin-Monohydrat bildet mit der 2_1-Operation die unendliche spiralförmige Konfiguration nach der *c*-Achse, wobei zwei N—H···O Wasserstoffbindungen (N^I—H···O_1^I und N^{II}—H···O_1^{II}) die Bindungskraft nach der *c*-Richtung verstärken. Die intermolekularen Bindungskräfte nach *a*- und *b*-Richtungen werden mit verschiedenen Wasserstoffbindungen (N—H···O und O—H···O) zusammengesetzt.

Während dem, das Kupfer-Glycin-Monohydrat eine plane cis Konfiguration hat, was von uns festgestellt worden ist, können wir aber noch nicht bestätigen, welche Kristallstruktur das Kupfer-Glycin-Dihydrat hat. Obgleich wir den Schluss gezogen haben, daß das Kupfer-Glycin-Dihydrat (Kristall II von Teil I) der Analogie der Kristallstruktur des Nickel-Glycin-Dihydrates nach und aus dem Resultat der infrarotspektroskopischen Untersuchung von Teil I eine plane trans Konfiguration mit zwei N und zwei O von Glycin-Molekülen hat, kann man aber nicht bestimmen, ob die zwei Kristallwassermoleküle einander mit gleicher Bindungsweise zu dem zentralen Metallatom koordinieren oder nicht. Wie aus DTA-Kurve von Teil I festgestellt, entwässert sich ein Kristallwassermolekül (Maximum O_2 in Abb. 1 von Teil I) leichter als ein anderes Kristallwassermolekül (Maximum O_3 in Abb. 1 von Teil I), so daß die Bindungsweise von beiden Kristallwassermolekülen nicht gleich ist: d. h., in dem Fall des Kupfer-Glycin-Dihydrates (Kristall II von Teil I) ist es also undenkbar, daß die zwei Kristallwassermoleküle mit der gleichen Bindungsweise koordiniert sind. Aus den Tatsachen, daß die Entwässerungswärme von Maximum O_1 (von Kupfer-Glycin-Monohydrat) in DTA-Kurve mit derselben von

11) V. M. Goldschmidt, *Nature*, **157**, 192 (1949).

Maximum O_3 (von Kupfer-Glycin-Dihydrat) ungefähr gleich ist und die beiden Entwässerungstemperaturen voneinander ähnlich sind, kann man vermuten, daß das eine Kristallwassermolekül des Kupfer-Glycin-Dihydrates in seiner Bindungsweise dem Kristallwassermolekül des Kupfer-Glycin-Monohydrates ähnlich ist und das ein übriges Kristallwassermolekül des Kupfer-Glycin-Dihydrates mit einer anderen schwächeren Bindungskraft gebunden ist.

In Teil I haben wir schon bestimmt, daß das Kupfer-Glycin-Monohydrat (Kristall I von Teil I) und das Kupfer-Glycin-Dihydrat (Kristall II von Teil I) nach Entweichung des Kristallwassers eine vollkommen gleiche Kristallstruktur zeigt. Die Kristallstrukturen dieses Anhydrates und des Dihydrates sind noch nicht festgestellt. Berücksichtigt man aber das Resultat der DTA-Kurve von Teil I, so kann man vermuten, daß nach Entwässerung von erstem Wassermolekül der Kristall II eine Umwandlung von planer trans Konfiguration nach planer cis Konfiguration beginnt und nach dem Durchgang von Maximum O_1 in DTA-Kurve eine plane cis Konfiguration hat, so daß die Kristalle I und II bei dem Zustand von Anhydrat eine gleiche Kristallstruktur haben.

Herrn Professor Dr. T. Watanabe danken wir herzlichst für mannigfache Anregungen bei der Durchführung dieser Arbeit. Sei auch dabei Herrn Dr. Y. Sasada für seinen hilfreichen Rat gedankt.

Chemisches Institut
Naturwissenschaftlche Fakultät
Universität Osaka
Kita-ku, Osaka

SHORT COMMUNICATIONS

Electron Spin Resonance and Electronic Absorption Spectra of the Radical Anions of Pyridine and Acridine

By Keiji KUWATA, Teiichiro OGAWA and Kozo HIROTA

(Received December 20, 1960)

Recently a number of radical anions of aromatic hydrocarbons have been studied[1-3] extensively and their electronic structures have been elucidated to some extent. As for anions of conjugated heterocyclic compounds, however, the phenazine anion was the only one studied hitherto[4]. It seems to be interesting, therefore, to study the electronic structures of anions of heterocyclic compounds, giving special attention to hyperfine interaction between unpaired electron spins and nuclear moments of heteroatoms, and to compare the results with those of aromatic hydrocarbons. In the present communication a study on the anions of pyridine and acridine is reported briefly. The method of preparation of the anions was the same as reported in the previous paper[3]; that

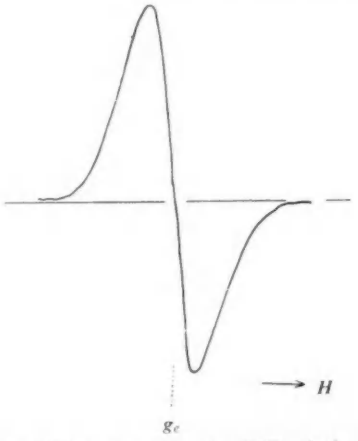

Fig. 1. ESR spectrum of the THF solution of the adduct of pyridine with sodium (H_{msl} = 10 gauss).

1) D. E. Paul, D. Lipkin and S. I. Weissman *J. Am. Chem. Soc.*, **78**, 116 (1956); T. R. Tuttle, Jr. and S. I. Weissman, ibid., **80**, 5342 (1958).
2) G. J. Hoijtinks and W. P. Wiyland, *Molecular Physics*, **1**, 231 (1958).
3) K. Morigaki, K. Kuwata and K. Hirota, This Bulletin, **33**, 952, 958 (1960); K. Kuwata, K. Morigaki and K. Hirota, ibid., **32**, 895 (1959).
4) Y. Fellion and J. Uebersfeld, *J. Arch. Sci.*, Geneve, **10**, 95 (1957); cf. D. J. E. Ingram, "Free Radicals as Studied by Electron Spin Resonance", Butterworths Scientific Publication, London (1955), p. 167.

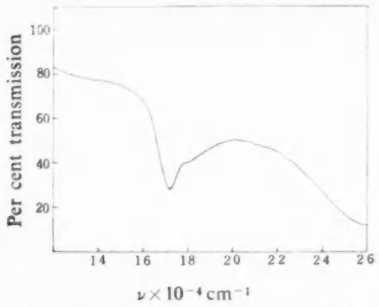

Fig. 2. Absorption spectrum for the THF solution of the adduct of pyridine with sodium.

is to say, all the procedures were carried out in an extremely evacuated system.

On heating pyridine with metallic sodium in tetrahydrofuran solution, a brownish yellow solution was obtained after evolution of a definite amount of gas[5]. This solution exhibited an ESR spectrum of a broad singlet as shown in Fig. 1. On continuing the procedure a red solution was obtained. Its absorption spectrum in the visible region is shown in Fig. 2, and the ESR spectrum obtained in this reaction stage was the same as that obtained in the early stage.

In the case of acridine a red solution of diamagnetic adduct was formed at the early stage of the reaction with sodium. The color of the solution changed to blue on heating it with sodium, and the ESR spectrum of a broad singlet was observed, the *g*-facter and the line width (H_{msl}) of which were 2.003 and 13 gauss, respectively.

In the previous investigation on the reaction of pyridine with alkali metals[6], formation of "sodium bipyridyl" was proposed on the basis of the results of chemical analysis of its decomposition product. However, according to our experiment described above, it is highly probable that radical anions of pyridine and also of acridine were formed.

Further studies will be published elsewhere.

The authors wish to express their sincere thanks to Professor M. Nakagawa of Osaka University for his helpful discussions.

Department of Chemistry
Faculty of Science
Osaka University
Kita-ku, Osaka

5) In the case of dimethoxyethane solution, a main part of the gas evolved was methane which may be formed from decomposition of the solvent.
6) B. Emmert, *Ber.*, **50**, 31 (1917).

Selectivity in Radiation-Induced Crosslinking and Scission of Polyvinyl Alcohol (PVA)

By Yutaka Hirano and Ayao Amemiya

(Received December 17, 1960)

The chemical structure of radiation-induced crosslinking of PVA irradiated in aqueous solution was supposed to be of 1, 2-glycol type and/or α-oxy ketone type[1].

We studied the mechanism of scission and/or crosslinking of irradiated PVA. The samples were either dry or swollen with water, when irradiated.

We found a certain selectivity in scission and crosslinking in PVA. The samples were exposed to radiation from a cobalt-60 gamma source in air or in vacuo up to 10^8 rad. at several temperatures and intensities.

We observed the influence of oxidation by periodic acid (HIO_4) upon the limiting viscosity number of irradiated PVA and, in particular, its variation with radiation dose.

In our experiments, the limiting viscosity number of PVA decreased with the increase in radiation dose. As shown in Fig. 1, there is a difference in the results between dry samples and swollen ones.

It should be noted that the limiting viscosity number after oxidation of dry samples is quite independent of radiation dose and agrees with the value of the sample, oxidized but not irradiated. But swollen samples show a different behavior of the limiting viscosity number after oxidation which definitely increases with radiation dose.

These results are inconsistent with the assumption of random scission and crosslinking, on which current theories[2,3] are based.

We are forced to conclude as follows: Only special types of bonds such as of 1, 2-glycol type which exists initially in usual samples[4], can be fractured selectively in either dry or swollen samples. Also, bonds formed by crosslinking in dry samples are definitely of the special types that are susceptible to oxidation by periodic acid. But in swollen samples we have at least two kinds of bonds formed by crosslinking, one susceptible and one not susceptible to oxidation.

1) M. Matsumoto and A. Danno, *Large Radiation Source in Industry*, Vol. I, p. 331. Conference Proceedings, Warsaw, September 1959.
2) O. Saito, *J. Phys. Soc. Japan*, **13**, 198, 1451, 1465 (1958).
3) A. Charlesby, *Proc. Roy. Soc.*, **A222**, 542 (1954), **A224**, 120 (1954).
4) P. J. Flory and F. S. Leutner, *J. Polymer Sci.*, **3**, 880 (1948).

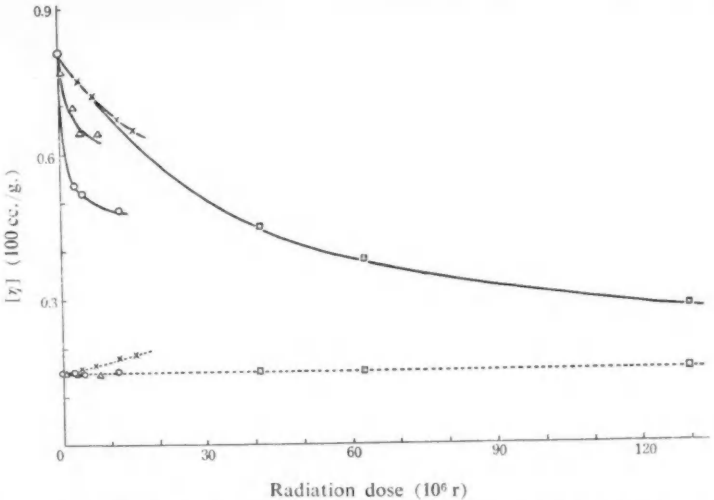

Fig. 1. The changes in the limiting viscosity number of irradiated PVA before and after oxidation by HIO_4 plotted against radiation dose: Full lines show the results before oxidation and dotted lines after oxidation by HIO_4.

△ Dry powder, irradiated in air at 95°C and 1×10^5 r/hr. and aged for 9 months.
○ Dry powder, irradiated in air at room temperature and 3×10^4 r/hr. and aged for 1.9 years.
□ Dry powder, irradiated in vacuo at room temperature and 2.9×10^4 r./hr. and aged for 1.1 years.
× Monofilament containing 6.7% water by weight, irradiated in air at room temperature and 4×10^4 r/hr.

Detailed results will be presented in a forthcoming paper.

Department of Applied Physics
Faculty of Engineering
the University of Tokyo
Hongo, Tokyo

A Method for Estimation of the Hydration Numbers of Ions in Ion Exchange Resins

By Hitoshi Ohtaki, Kôzô Gonda and Hidetake Kakihana

(Received December 16, 1960)

A method for estimation of the hydration numbers of ions in ion exchange resins is proposed on the basis of the measurement of the amount of the solvent adsorbed isopiestically on the resin. The sulfonated cation exchange resins, Dowex 50-X4 (4% DVB resin), Diaion SK (8% DVB), Dowex 50-X16 (16% DVB) and Diaion SK-X24 (24% DVB) of sodium form, were used in mesh sizes of 50 to 200. They were dried at 50°C in vacuo. The resins were placed in the small dishes of stainless steel and were contacted with the solvent vapor under the pressure of about 3 mmHg. Ethanol-water and dioxane-water mixtures were used as the solvent systems. The concentrations of the organic solvents were in the range of 0 to 99.6% (v/v). The equilibrium of each isopiestic experiment had been attained in three days in a thermostat at 25 ±0.5°C.

The total amount of solvents adsorbed on the resin was determined gravimetrically. The solvent composition on the resin was determined by the following ways: in the ethanol-water system the solvents adsorbed on the resin were eluted with water and the amount of ethanol in the eluate was measured colorimetrically[1]. In the dioxane-water system, the solvents on the resin were distilled completely

1) B. Lange, "Kolorimetrische Analyse", Verlag Chemie, Weinheim (1956), p. 334.

and the refractive index of the distilled solution was measured.

The distribution coefficient of the solvents, K_o^w, is defined as

$$K_o^w = \frac{\bar{m}_w \cdot m_o}{\bar{m}_o \cdot m_w} \quad (1)$$

where $\bar{m}$ and m denote the concentrations of the solvents in the resin and the solution phases, respectively, and subscripts w and o represent water and the organic solvent.

The distribution of the solvents between the resin and the solution phases is thermodynamically given as follows*:

$$\ln \frac{\bar{a}_w \cdot a_o}{a_o \cdot a_w} = \frac{\pi}{RT}(\bar{v}_o - \bar{v}_w) \quad (2)$$

where $\bar{a}$ and a denote the activities of the solvents in the resin and the solution phases, respectively, and $\bar{v}$ is the partial molal volume of the solvent in the resin phase. π is the swelling pressure of the resin.

It may be considered that the solvent adsorbed on the resin is devided to two different parts: the one I is the solvents solvating to the functional groups (sulfonic acid groups) and their counter ions (sodium ions), another II is the solvents condensed on the exchange sites which become solvophilic by the solvation of the exchange groups. The fact that the resin particles without functional groups do not adsorb the solvent shows that the solvent is not adsorbed on the resin skeleton. We assume that only water molecules can solvate to the ions even in the considerably high concentration of the organic solvent in the solution phase (probably up to about 80%).

From these considerations Eq. 1 may be rewritten as follows:

$$K_o^w = \frac{(\bar{m}_{w_I} + \bar{m}_{w_{II}})}{\bar{m}_{o_{II}}} \cdot \frac{m_o}{m_w} \quad (3)$$

where subscripts I and II denote part I and part II described above.

Being different from the case in which the resin is derectly dipped in the solvents, it is observed that the resin scarcely swells in the equilibrium with the solvent vapor. From this observation, we assume that π in Eq. 2 is very small, or

$$\frac{\pi}{RT}(\bar{v}_o - \bar{v}_w) \simeq 0 \quad (4)$$

As the water molecules solvated to the functional groups are fixed and hardly move, the fugacities of the solvents in the resin phase which is equilibrated with the vapor phase may be proportional to the molar fractions of the solvents in part II. It is assumed that the activities of the solvents in the solution phase are proportional to their molar fractions, the following equation is derived from Eqs. 2 and 4:

$$\ln \frac{\bar{a}_{w_{I\text{-}II}} \cdot a_o}{a_{o_{II}} \cdot a_w} \simeq \ln \frac{\bar{N}_{w_{II}} \cdot N_o}{\bar{N}_{o_{II}} \cdot N_w} = \ln \frac{\bar{m}_{w_{II}} \cdot m_o}{\bar{m}_{o_{II}} \cdot m_w} \simeq 0 \quad (5)$$

where $\bar{N}$ and N denote the molar fractions of the solvents in the resin and the solution phases, respectively, and hence

$$\frac{\bar{m}_{w_{II}}}{\bar{m}_{o_{II}}} \simeq \frac{m_w}{m_o} \quad (6)$$

Applying Eqs. 3 and 6, the hydration number per one functional group and its counter ion (sodium ion), H, is calculated readily by the following equation:

$$H = \frac{(1-m_o)W_o}{1000\,EM_w m_o}(K_o^w - 1) \quad (7)$$

where W_o is the weight of the organic solvent adsorbed on the resin (gram), E denotes the exchange capacity (meq.) of the resin used, M_w is the molecular weight of water and m_o represents the concentration of the organic solvent given in the scale of weight percentage.

In Fig. 1 the hydration numbers are plotted against the concentrations of ethanol for the variously cross-linked resins. The similar results can be obtained in the dioxane-water system.

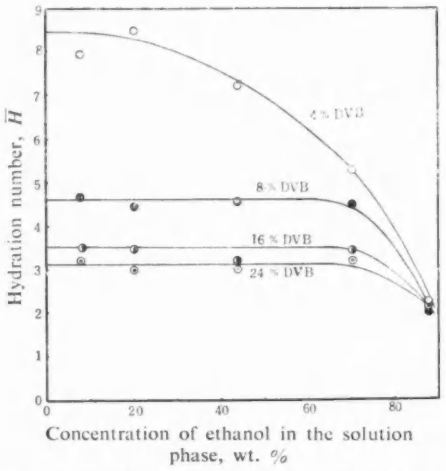

Fig. 1. Hydration number per one functional group and its counter ion (sodium ion) of the cross-linked sulfonic acid resins in the various concentrations of ethanol.

* Cf. H. Kakihana, H. Ohtaki and T. Nomura, *Bull. Tokyo Inst. Tech., Series-B*, No. 1, 1 (1960); H. Kakihana, T. Nomura and H. Ohtaki, ibid., No. 1, 14 (1960).

The numbers extrapolated to zero concentration of the organic solvents may correspond to the hydration numbers of the ions on the ion exchange resins equilibrated with the saturated water vapor. The values of the numbers are listed in Table I. The agreement of the results obtained in the cases of ethanol-water and dioxane-water systems is satisfactory.

TABLE I. HYDRATION NUMBERS, $\bar{H}$, EXTRAPOLATED TO ZERO CONCENTRATION OF THE ORGANIC SOLVENTS

Resins	Ethanol-water	Dioxane-water	Mean
4% DVB resin	8.3	8.4	8.4
8% DVB resin	4.6	4.5	4.6
16% DVB resin	3.5	3.7	3.6
24% DVB resin	3.1	3.0	3.1

Tokyo Institute of Technology
Meguro-ku, Tokyo

The Crystal Structure of $[Cr(NH_3)_6]\,[CuCl_5]$*

By Masayasu MORI, Yoshihiko SAITO** and Tokunosuké WATANABE

(Received December 9, 1960)

Unstable halogen complexes of heavy metals sometimes exist in more than two forms having considerably different chemical constitutions and structures. Thus bromothallates(III) are found with compositions, $KTlBr_4 \cdot 2H_2O$, $Rb \cdot TlBr_4 \cdot H_2O$ and $CsTlBr_4$. These complexes have the octahedral, pyramidal and square configurations[1]. The interatomic distances Tl–Br in these complexes are considerably different from that found in a more stable complex, $[Co(NH_3)_6]\,[TlBr_6]$[2].

Such variety in ionic species is also found in the case of chlorocuprates, but the information seems much less satisfactory. A pentachlorocuprate(II) of hexamminechromium(III), $[Cr(NH_3)_6]\,[CuCl_5]$ has recently been prepared[3]. It occurred to the present authors that the crystal analysis of this compound would give a useful guide to the structural chemistry of chlorocuprates(II).

Weissenberg photographs for the equatorial, the first and fourth layer lines, and oscillation photographs were prepared using $CuK\alpha$ (λ = 1.5418 Å) radiation. From these data, it was concluded that the crystals belong to the cubic system, and the systematic reflections were characteristic only for O_h^5-Fd3c. The exact reflection angles of several ($hk0$) reflections for $CuK\alpha_1$ radiation (λ = 1.5405 Å) were determined by means of a GM counter X-ray defractometer which was calibrated with a standard microcrystalline plate of metallic silicon (a = 5.4301 Å). From these values the unit cube edge was determined to be a = 22.265 ±0.01 Å. There are 32 formula units in each unit cell, the calculated density being 1.901 g. cm^{-3}, in good agreement with the observed value, 1.892 g. cm^{-3}. The relative intensities of reflections were visually estimated with a calibrated standard, and the Lorentz and polarization corrections were made using Cochran's chart[4].

There are 32 Cu, 32 Cr, 160 Cl and 192 N atoms in the unit cell. The observed intensities were best accounted for when these atoms are placed in the following equivalent positions:

32 Cu: (b) 1/4, 1/4, 1/4, etc.,
32 Cr: (c) 0, 0, 0, etc.,
64 Cl: (e) u, u, u, (u = 0.190), etc.,
96 Cl: (g) 1/4, v, −v, (v = 0.075), etc.,
192 N: (h) x, y, z, (x = 0.070, y = 0.050, z = −0.030), etc.

The parameters were obtained by the trial and error method, by comparing the calculated and observed structure factors, F_c and F_o at the each stage. At the final stage, corrections were made for extinction and the anomalous dispersion of copper and chromium atoms. The atomic coordinates given above, combined with the overall temperature factor, B = 2.5, gave for the equatorial ($hk0$) Weissenberg data a reliability factor, R = 0.136. The intensities of the unobserved reflections were taken equal to zero in this comparison. For 333 (hkl) reflections up to l = 8 the R value was 0.190 (in this case the unobserved reflections were excluded).

According to the above atomic coordinates, the crystal is composed of octahedral complex ion, $[Cr(NH_3)_6]^{3+}$ and trigonal bipyramidal complex ion, $[CuCl_5]^{3-}$ arranged the sodium chloride type. Because of the symmetry requirement, however, the unit cube edges are twice as much of a simple sodium chloride

* Presented at the Symposium on Coordination Chemistry, Sendai, September 1960.

** Present Address: Institute for Solid State Physics, the University of Tokyo, Shinryudo-cho, Azabu, Minato-ku, Tokyo.

1) T. Watanabe, Y. Saito, R. Shiono and M. Atoji, *Structure Repts.* **11**, 393 (1947–8).
2) T. Watanabe, M. Atoji and C. Okazaki, *Acta Cryst.* **3**, 405 (1950).
3) M. Mori, This Bulletin, **33**, 985 (1960).
4) J. Cochran, *J. Sci. Instr.*, **25**, 253 (1948).

arrangement. The threefold axis of the $[CuCl_5]^{3-}$ ion lies on the body diagonal of the cube cell, in accordance with the point symmetry of the Cu position, D_3–32. This structure of the $[CuCl_5]^{3-}$ ion is quite a new one, most chlorocomplexes of copper(II) being distorted octahedra. The only exception is the structure of $[CuCl_4]^{2-}$ ion in Cs_2CuCl_4 or its bromine analogue, in which case $[CuCl_4]^{2-}$ ion can be taken to be a flattened tetrahedron or a twisted square[5,6].

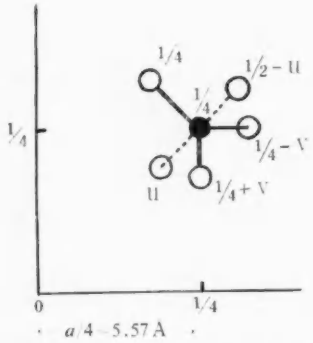

Fig. 1. The structure of $[CuCl_5]^{3-}$ with Cu at 1/4, 1/4, 1/4 (the figure refers to the z coordinate).

The important characteristic of the trigonal bipyramidal structure of $[CuCl_5]^{3-}$ found in the present research is that the distance between the copper atom and the two chlorine atoms on the threefold axis (2.32 Å) is of the same order of magnitude as the distance between the copper atom and the three chlorine atoms at the corner of the triangle (2.35 Å) (Fig. 1). This is in a clear contrast to much greater distances (2.8~3.0 Å) between copper and chlorine atoms on the fourfold or nearly four fold axis found in many distorted octahedral chlorocomplexes.

The authors wish to express their sincere thanks to Dr. Yozo Chatani of Osaka University for the cooperation in preparing Weissenberg photographs.

Institute of Polytechnics
Osaka City University
Kita-ku, Osaka
(M. M.)

Faculty of Science, Osaka University
Kita-ku, Osaka
(T. W.)
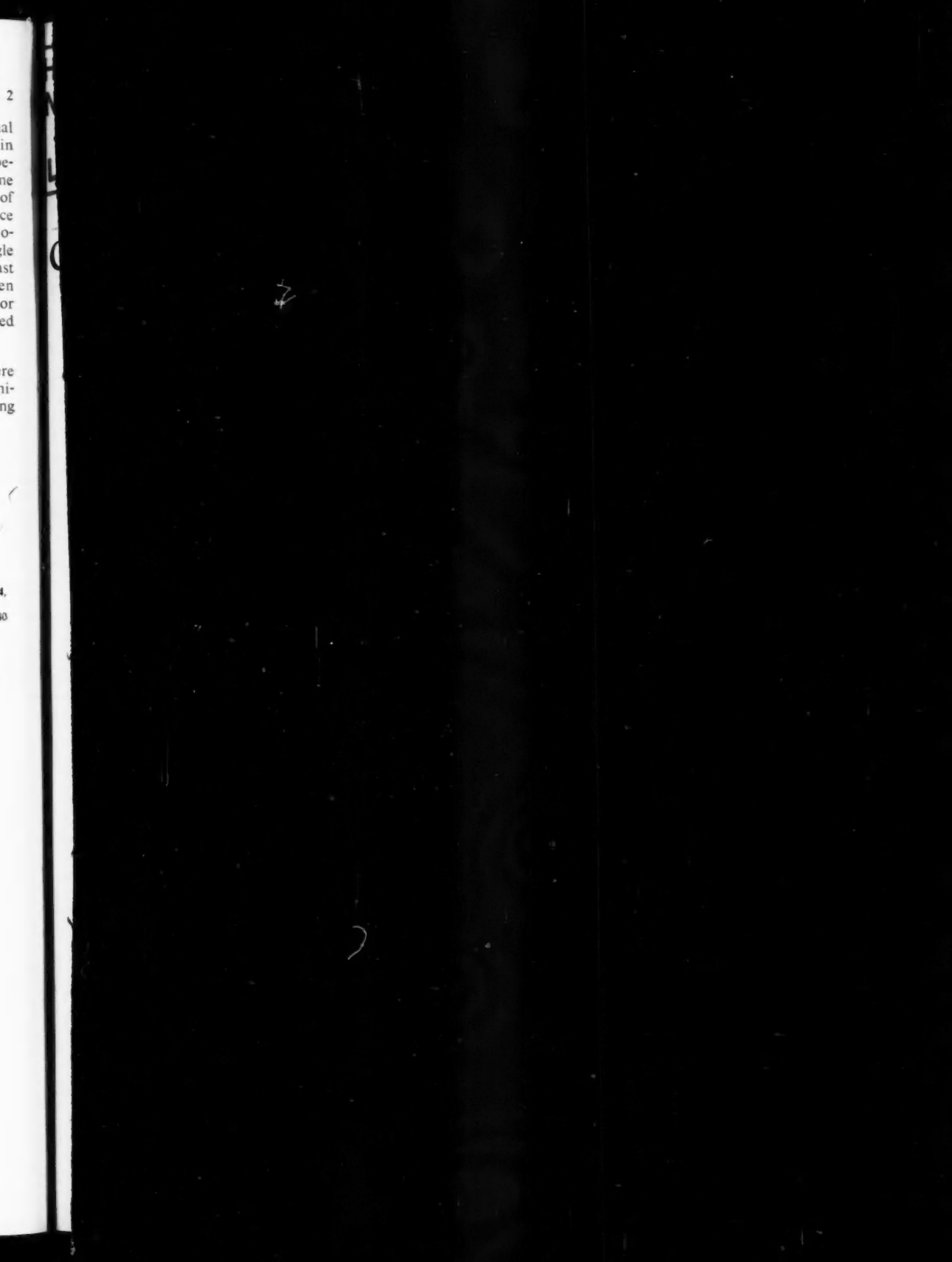
5) L. Helmholz and R. F. Kruh, *J. Am. Chem. Soc.*, **74**, 1176 (1952).
6) B. Morosin and E. C. Lingafelter, *Acta Cryst.*, **13**, 80 (1960).